Long-Term Pavement Performance (LTPP) Data Analysis Support: National Pooled Fund Study TPF-5(013)

Effects of Multiple Freeze Cycles and Deep Frost Penetration on Pavement Performance and Cost

PUBLICATION NO. FHWA-HRT-06-121

NOVEMBER 2006

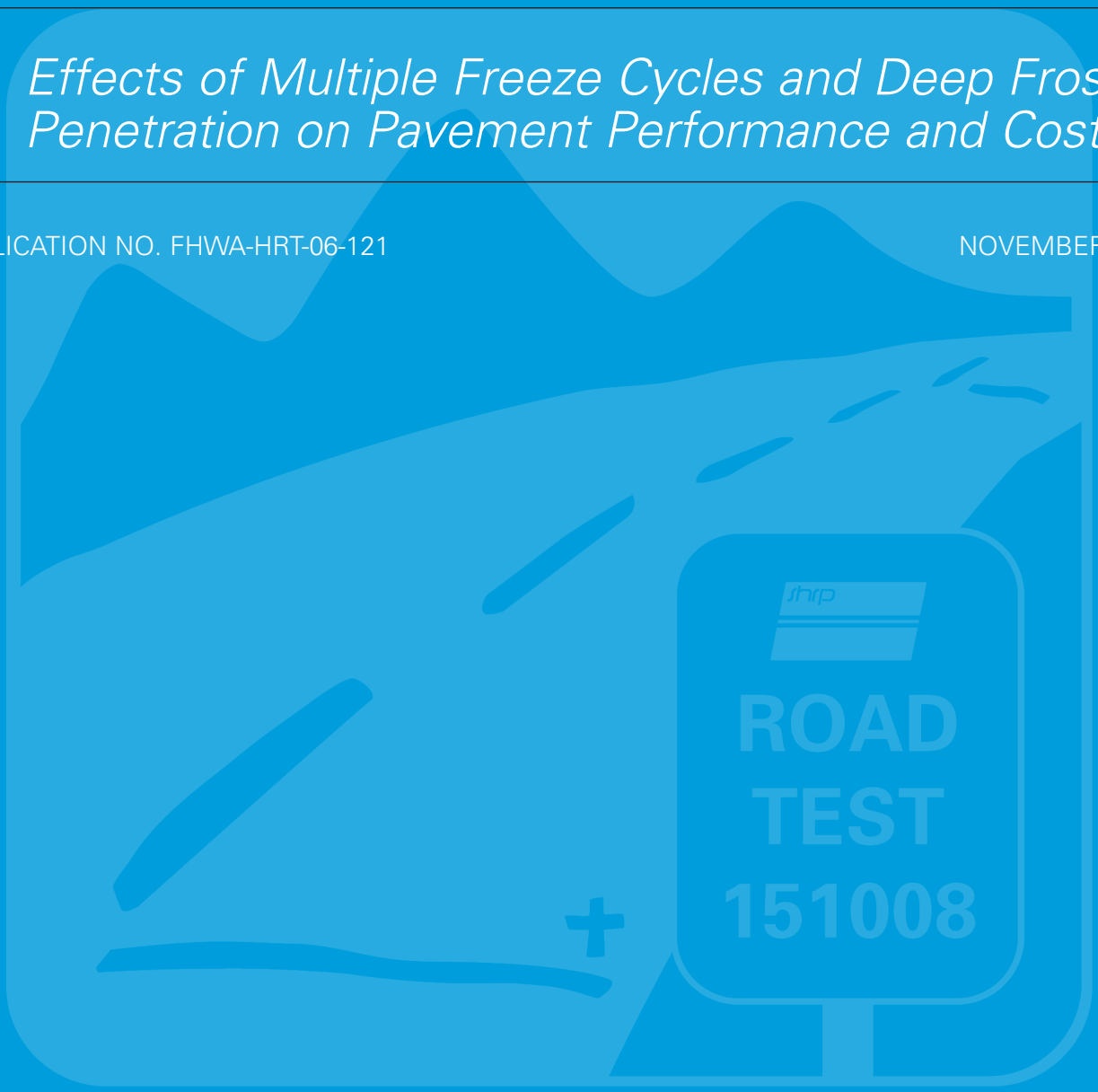

U.S. Department of Transportation
Federal Highway Administration

Research, Development, and Technology
Turner-Fairbank Highway Research Center
6300 Georgetown Pike
McLean, VA 22101-2296

LTPP

Foreword

Understanding deterioration of pavements exposed to climates with multiple freeze-thaw cycles as compared to climates with sustained deep-frost penetration is important to State Highway Agencies (SHAs) across the country. Consideration must also be given to differential performances between pavements in these freezing climates and those in nonfreezing areas. This report documents a study conducted to evaluate pavement deterioration in various environmental settings. In addition, it documents local adaptations currently in use to mitigate frost-related damage along with the cost differences associated with constructing and maintaining pavements in the various climates. Performance models developed from the Long-Term Pavement Performance (LTPP) database were used to predict and compare performance in various environments. As demonstrated in the report, the prediction models are also an important tool in the calibration process outlined in the National Cooperative Highway Research Program (NCHRP) *Guide for Mechanistic-Empirical Design of New and rehabilitated Pavement Structures* as well as in pavement management applications for SHAs with limited quantities of regional performance data.

Gary L. Henderson
Director, Office of Infrastructure
Research and Development

Notice

This document is disseminated under the sponsorship of the U.S. Department of Transportation in the interest of information exchange. The U.S. Government assumes no liability for its contents or use thereof. This report does not constitute a standard, specification, or regulation.

The U.S. Government does not endorse products or manufacturers. Trade and manufacturers' names appear in this report only because they are considered essential to the object of the document.

Quality Assurance Statement

The Federal Highway Administration (FHWA) provides high-quality information to serve Government, industry, and the public in a manner that promotes public understanding. Standards and policies are used to ensure and maximize the quality, objectivity, utility, and integrity of its information. FHWA periodically reviews quality issues and adjusts its programs and processes to ensure continuous quality improvement.

1. Report No. FHWA-HRT-06-121	2. Government Accession No.	3. Recipient's Catalog No.	
4. Title and Subtitle Long-Term Pavement Performance (LTPP) Data Analysis Support: National Pooled Fund Study TPF-5(013) *Effects of Multiple Freeze Cycles and Deep Frost Penetration on Pavement Performance and Cost*		5. Report Date November 2006 6. Performing Organization Code	
7. Author(s) N. Jackson and J. Puccinelli		8. Performing Organization Report No. 123210-8	
9. Performing Organization Name and Address Nichols Consulting Engineers 1885 South Arlington Avenue Suite 111 Reno, NV 89509-3370		10. Work Unit No. (TRAIS) 11. Contract or Grant No. DTFH61-02-D-00139	
12. Sponsoring Agency Name and Address Office of Infrastructure R&D Federal Highway Administration 6300 Georgetown Pike McLean, VA 22101-2296		13. Type of Report and Period Covered Final Report March 2003 to May 2006 14. Sponsoring Agency Code	
15. Supplementary Notes Contracting Officer's Technical Representative (COTR): Larry Wiser, Long-Term Pavement Performance Team, HRDI-13			
16. Abstract The objectives of this study are to: (1) quantify the effects of frost penetration on pavement performance in climates with deep sustained frost as compared to environments with multiple freeze-thaw cycles, (2) investigate the effect that local adaptations have on mitigating frost penetration damage, and (3) estimate the associated cost of constructing and maintaining pavements in freezing climates. The approach consisted of modeling various pavement performance measures using both climatic and nonclimatic input variables and performance data collected as part of the Long-Term Pavement Performance program. Five climatic scenarios are defined in terms of climatic input variables for the models. Predicted performance measures are presented for each of the climatic scenarios and compared at a 95 percent confidence interval to determine statistically significant performance differences. Participating pooled fund States (PFS) were queried as to standard specifications, standard designs, average life expectancies, and construction costs specific to each State Highway Agency (SHA). This data along with information acquired through literature review of SHA standard practices is summarized with consideration given to the mitigation of frost-related damage. Life cycle cost analysis for each climatic scenario using predicted performance to determine average life and average agency construction costs for standard pavement sections is also discussed and compared. The use of the performance models for local calibration as required in the National Cooperative Highway Research Program *Guide for Mechanistic-Empirical Design of New and Rehabilitated Pavemen Structures* is explored along with the possible application of the performance models in pavement management systems.			
17. Key Words Frost, freeze-thaw, LTPP, life cycle cost analysis, performance modeling, climate, M-E pavement design guide, pavement management system, AC, PCC		18. Distribution Statement No restrictions. This document is available to the public through the National Technical Information Service, Springfield, VA 22161.	
19. Security Classification (of this report) Unclassified	20. Security Classification (of this page) Unclassified	21. No. of Pages 262	22. Price

SI* (MODERN METRIC) CONVERSION FACTORS

APPROXIMATE CONVERSIONS TO SI UNITS

Symbol	When You Know	Multiply By	To Find	Symbol
		LENGTH		
in	inches	25.4	millimeters	mm
ft	feet	0.305	meters	m
yd	yards	0.914	meters	m
mi	miles	1.61	kilometers	km
		AREA		
in^2	square inches	645.2	square millimeters	mm^2
ft^2	square feet	0.093	square meters	m^2
yd^2	square yard	0.836	square meters	m^2
ac	acres	0.405	hectares	ha
mi^2	square miles	2.59	square kilometers	km^2
		VOLUME		
fl oz	fluid ounces	29.57	milliliters	mL
gal	gallons	3.785	liters	L
ft^3	cubic feet	0.028	cubic meters	m^3
yd^3	cubic yards	0.765	cubic meters	m^3
		NOTE: volumes greater than 1000 L shall be shown in m^3		
		MASS		
oz	ounces	28.35	grams	g
lb	pounds	0.454	kilograms	kg
T	short tons (2000 lb)	0.907	megagrams (or "metric ton")	Mg (or "t")
		TEMPERATURE (exact degrees)		
^oF	Fahrenheit	5 (F-32)/9 or (F-32)/1.8	Celsius	^oC
		ILLUMINATION		
fc	foot-candles	10.76	lux	lx
fl	foot-Lamberts	3.426	candela/m^2	cd/m^2
		FORCE and PRESSURE or STRESS		
lbf	poundforce	4.45	newtons	N
lbf/in^2	poundforce per square inch	6.89	kilopascals	kPa

APPROXIMATE CONVERSIONS FROM SI UNITS

Symbol	When You Know	Multiply By	To Find	Symbol
		LENGTH		
mm	millimeters	0.039	inches	in
m	meters	3.28	feet	ft
m	meters	1.09	yards	yd
km	kilometers	0.621	miles	mi
		AREA		
mm^2	square millimeters	0.0016	square inches	in^2
m^2	square meters	10.764	square feet	ft^2
m^2	square meters	1.195	square yards	yd^2
ha	hectares	2.47	acres	ac
km^2	square kilometers	0.386	square miles	mi^2
		VOLUME		
mL	milliliters	0.034	fluid ounces	fl oz
L	liters	0.264	gallons	gal
m^3	cubic meters	35.314	cubic feet	ft^3
m^3	cubic meters	1.307	cubic yards	yd^3
		MASS		
g	grams	0.035	ounces	oz
kg	kilograms	2.202	pounds	lb
Mg (or "t")	megagrams (or "metric ton")	1.103	short tons (2000 lb)	T
		TEMPERATURE (exact degrees)		
^oC	Celsius	1.8C+32	Fahrenheit	^oF
		ILLUMINATION		
lx	lux	0.0929	foot-candles	fc
cd/m^2	candela/m^2	0.2919	foot-Lamberts	fl
		FORCE and PRESSURE or STRESS		
N	newtons	0.225	poundforce	lbf
kPa	kilopascals	0.145	poundforce per square inch	lbf/in^2

*SI is the symbol for the International System of Units. Appropriate rounding should be made to comply with Section 4 of ASTM E380.
(Revised March 2003)

TABLE OF CONTENTS

LIST OF FIGURES

LIST OF TABLES

List of Acronyms

AASHTO	American Association of State Highway and Transportation Officials
AASHO	American Association of State Highway Officials
AC	Asphalt concrete
ACTHICK	Asphalt layer thickness
AIRI	Absolute international roughness index
ATB	Asphalt-treated base
BASE	Base material type
BC	Block cracking
CB	Corner breaking
CI	Annual cooling index
COTR	Contracting officer's technical representative
CRCP	Continuously reinforced concrete pavement
CSM	Chemically stabilized material
D	Slab thickness
DGAB	Dense graded-aggregate base
DIRI	Change in international roughness index
EALF	Equivalent axle load factor
ESAL	Equivalent single axle load
FC	Fatigue cracking
FHWA	Federal Highway Administration
FI	Annual freezing index
FLT	Accumulation of faulting
FTC	Freeze-thaw cycle
FWPC	Combined LWP and FC
GLM	General linear model
GPS	General Pavement Study
HMA	Hot-mix asphalt
HMAC	Hot-mix asphalt concrete
IMS	Information management system
IRI	International roughness index
JPCP	Jointed plain concrete pavement
JRCP	Jointed reinforced concrete pavement
LC	Longitudinal cracking
L.A. wear values	Los Angeles wear values
LCCA	Life cycle cost analysis
LEDT	Logarithm of ESAL divided by depth
LESN	Logarithm of ESAL divided by structural number
LTPP	Long-Term Pavement Performance (program)
LWP	Longitudinal wheelpath cracking
MBE	Modified Berggren equation
M-E	Mechanistic-empirical
MIRI	Initial recorded international roughness index values

Mn/ROAD	Minnesota Road Research Project
M_r	Resilient modulus
NCHRP	National Cooperative Highway Research Program
NONBIT	Nonbituminous-treated base
NYSDOT	New York State Department of Transportation
PATB	Permeable asphalt-treated base
PCC	Portland cement concrete
PCCP	Portland cement concrete pavement
PCI	Pavement condition index
PFS	Pooled fund States
PG	Performance grade
PMS	Pavement management systems
PRECIP	Annual precipitation data
PUMP	Pumping/water bleeding
RMSE	Root mean squared error
RTM	Road testing machine
RUT	Rut depth index value
SAS®	SAS software
SG	Subgrade material type
SHA	State Highway Agency
SHRP	Strategic Highway Research Program
SMP	Seasonal monitoring program
SN	Structural number
SPS	Specific Pavement Studies
TDR	Time domain reflectometry
TC	Transverse cracking
TSR	Tensile strength ratio
WSDOT	Washington State Department of Transportation

EXECUTIVE SUMMARY

Pavements subjected to frost effects have different service lives than do similar pavements with no exposure to frost; however, limited national research is available quantifying the effect frost has on pavement performance let alone the costs resulting from reduced service life. This study provides some insight into pavement performance and service life, considering conditions of both deep-frost and moderate-frost depth with multiple freeze-thaw cycles (FTC).

The study included a review of all available relevant literature to provide guidance and to support the project work. Literature directly related to this investigation was quite limited, with most of the literature regarding frost effects dealing with quantifying the change in material properties and performance characterization on particular projects. In addition, relatively limited information was found on modeling pavement performance in frost areas using Long-Term Pavement Performance (LTPP) data. State Highway Agency (SHA) Web sites were also reviewed to accumulate reports documenting studies of frost mitigation techniques.

To study pavement performance in the various frost settings, models were developed using multivariate regression analysis. LTPP data from General Pavement Study (GPS) projects 1, 2, 3, and 6 as well as Specific Pavement Study (SPS) experiments 1, 2, and 8 were used to generate the models. Data from more than 520 test sections were used in developing the prediction models for flexible pavements, while approximately 270 test sections were used for rigid pavement modeling. More than 20 models were developed to represent the rate of pavement deterioration with age unique to environmental regions. Of these, nine models were selected that were determined to best predict basic pavement trends with time. A summary of these nine models can be found in Table 1.

Using the models presented above, statistical comparisons of pavement performance were made for the following five climatic region scenarios:

- Deep-freeze, wet (low FTC).
- Moderate-freeze, wet (high FTC).
- No-freeze, wet.
- Deep-freeze, dry (low FTC).
- Moderate-freeze, dry (high FTC).

All of the models (with the exception of flexible pavement roughness) predicted significantly different performance, at 95 percent confidence, between two or more of the climatic scenarios.

Table 1. List of models and basic logistic and regression statistics.

Model	Pavement	Model Type	Logistic Cutoff Probability	Percent Correct	R-Squared	Number of Observations
Roughness	Flexible	Regression (shifted)	NA	NA	0.78	4544
Roughness	Rigid	Regression	NA	NA	0.78	2652
Rut Depth	Flexible	Regression	NA	NA	0.45	1966
Faulting	Rigid	Regression	NA	NA	0.47	1384
Fatigue and Wheelpath Cracking	Flexible-deduct	Logistic	0.7	72.6	NA	1977
		Regression	NA	NA	0.63	1486
Fatigue and Wheelpath Cracking	Flexible-percent	Logistic	0.7	72.6	NA	1977
		Regression	NA	NA	0.49	1481
Transverse Cracking	Flexible	Logistic	0.7	78.4	NA	1920
		Regression	NA	NA	0.71	1077
Longitudinal Cracking	Rigid	Logistic	0.55	63.5	NA	475
		Regression	NA	NA	0.38	240
Transverse Cracking	Rigid	Logistic	0.6	63.5	NA	489
		Regression	NA	NA	0.54	228

To gain an understanding of state design practices, a questionnaire was developed and sent to the pooled fund State participants. Basic information on standard roadway sections including structural design for given scenarios, standard specifications, and test procedures were requested.

Responses to the survey revealed that there is a large variation in the roadway section for similar design situations. However, most of the States in the study experiencing deep frost did include a construction specification requiring additional surfacing or the replacement of frost-susceptible soils with frost-free surfacing for a depth of 1 to 2 meters (m) (3 to 6 feet (ft)).

Agency responses also revealed that the use of Superpave mix design procedures has, to a large extent, eliminated local adaptations in mix designs and specifications that might have provided improved performance in areas of deep frost penetration or numerous FTCs, or both. The Superpave® mix design procedure does not differentiate between mix designs where pavements will be exposed to numerous FTCs and those that will experience little or no FTCs. Because many SHAs are in the process of adopting the Superpave binder specifications as well as the mix design procedures, local adaptations as far as mix designs and specifications were not found that would indicate improved pavement performance in areas with either deep frost penetration or numerous FTCs.

An additional objective of the study involved evaluating the costs associated with performance differences in the various environments. Life cycle cost analysis (LCCA)

was used to evaluate pavement costs in the various climatic settings because it produces comparable results (i.e., equivalent uniform annual costs). Comparisons were made using both deterministic and probabilistic methods of LCCA.

Standard flexible pavement sections were developed based on the 1993 *AASHTO Guide for Design of Pavement Structures* design procedures[1] and using input variables from the questionnaire. A cost comparison was performed using this standard section for all environmental zones; therefore, the initial and rehabilitation costs were constant for all regions. Cost differences were the result of changes in treatment timing because of performance variations between the regions. Predictions from the models were used to determine treatment timing for each climatic scenario.

To account for local adaptations used to mitigate damage associated with freezing and thawing climates, an additional cost evaluation was performed in which the initial costs of the deep- and moderate-freeze regions included extra frost-free material (i.e., unbound base) to obtain a pavement structure with a total depth of 1 m (3 ft). Based on responses from the participating Agencies, this is a typical frost-free depth for many SHAs experiencing 1 to 1.5 m (3 to 4 ft) of frost penetration. The initial construction costs for the no-freeze region did not include additional base material.

Using the standard section for all regions resulted in costs that were not significantly different for the five climatic scenarios. When the cost of additional surfacing was considered, the life cycle costs in the no-freeze region were significantly lower than in the deep- and moderate-freeze regions.

Consideration was given to the use of the developed performance models in the implementation of mechanistic-empirical (M-E) design procedures. The National Cooperative Highway Research Program (NCHRP) *Guide for Mechanistic-Empirical Design of New and Rehabilitated Pavement Structures*,[2] Project 1-37A final report, was developed using damage models that represent average pavement damage trends for the entire United States. The models developed in this project can be used to predict average rutting or fatigue cracking trends for a specific regional or statewide environment. In turn, these estimates can be used in the iteration and verification process described in the NCHRP 1-37A *Guide* designprocedure to determine if modified calibration factors are required in the design program for the specific environment. An example of how to use the models from this study to provide regional calibration is described in the report.

The models developed for this project will also be useful in pavement management applications. The pavement distress trend models developed in this study can be used to provide general pavement deterioration trends for a specific environment. These trends can be used to develop a family of curves for use in a pavement management system (PMS) where an SHA or local agency does not have sufficient data to develop those curves.

1. INTRODUCTION

It is well recognized that pavements subjected to frost effects have different service lives as compared to similar pavements that are not subjected to frost effects. However, there is a need to better understand the failure mechanisms (particularly the impact of multiple FTCs as compared to deep frost penetration) and how they are mitigated by various compensatory strategies implemented throughout the pavement community. Observably, deep frost penetration and extensive frost-thaw cycles have a pronounced effect on the service pavements provide. There has been very limited research on quantifying the effect frost has on pavement performance, as well as on the cost of that effect on reduced service life and the additional costs to maintain those pavements in serviceable condition. This study will help provide some insight into the total cost of frost action as it applies to pavement performance and service life, considering both deep-frost conditions and moderate-frost conditions with multiple FTCs.

Following is a list of project's research objectives:

- Quantify the effect of seasonal frost penetration on the rate of loss of pavement performance for environments where deep, sustained frost penetration occurs, and for environments where multiple shallow FTCs occur.
- Establish the extent to which local adaptations of materials standards and pavement thickness designs have compensated for or mitigated the effect of seasonal frost penetration.
- Determine financial effects associated with freeze-thaw mitigation in the construction and rehabilitation of pavements.

In addition to the objectives listed above, the use of the models developed for the project in PMS applications and NCHRP 1-37A *Guide* design procedures was explored.

This study was structured with two phases. The first phase consisted of six tasks that essentially confirmed that the project could be accomplished with the data available. Phase 2 consisted of an analysis of the data collected. Work conducted in phase 1, and the resulting findings were used to tailor analysis conducted in phase 2.

2. BACKGROUND

In phase 1 a literature review was conducted to provide guidance and support to the work on this project. The available literature directly related to this investigation was quite limited. While most of the literature regarding frost effects deals with quantifying the change in material properties and performance characterization on particular projects, studies have been conducted on modeling pavement performance using LTPP data. The literature review is included in appendix A.

As part of phase 1, the contractor was asked to complete the following task:

> *Identify the specific LTPP data to be used in the analysis, acquire the data, and process it as necessary to create the analysis database to be used in subsequent analysis.*

The analysis database was first developed to evaluate the potential of using only data from Seasonal Monitoring Program (SMP) test sections for the study. This evaluation showed that including additional test sections beyond SMP sites would increase the dataset to better represent the large number of variables and lead to improved results. With the approval from Federal Highway Administration (FHWA) and the pooled fund States (PFS) panel, the sample set was expanded to include GPS-1 and GPS-6 experiments for phase 1 analysis. The analysis database was expanded for phase 2, which included accumulating additional variables, combining data that had been segregated into environmental zones for phase 1, and thoroughly reviewing the data. Chapter 3 contains a more detailed discussion of the database development.

Based on phase 1 findings, it was evident that the available data could support the study, and that performance differences did exist. Because the analysis dataset required additional data, it was proposed that it be expanded to include not only GPS-1 and GPS-6 sites, but also GPS-2, SPS-1, and SPS-8 projects for an investigation of AC sections for phase 2. Similarly, GPS-3, SPS-2, and SPS-8 test sections were proposed to model PCC pavements. The analysis datasets for phase 2 were designed to combine the data into a more comprehensive form where the environmental factors could be fully addressed in a statistical analysis. This approach was presented to, and accepted by, the PFS panel.

Another consideration from the phase 1 study was the use of frost depths, information that is collected only at SMP sites. The database could not be expanded from SMP sites without using a substitute for frost depths. The annual freezing index (FI) was shown to correlate quite well to frost depths, and it was subsequently used in both the phase 1 and phase 2 studies to represent relative freezing conditions. A complete analysis of these findings is reported in chapter 3

An investigation of the interaction between FTCs and FI found that moderate- and deep-freeze zones experience approximately the same number of annual freeze cycles; therefore, the initial assumption that each was mutually exclusive, that the moderate-freeze zone would experience multiple FTCs while sections in the deep-freeze zone would experience few cycles, is not

confirmed by the data. Consideration of this finding in phase 2 analysis was essential to making performance comparisons, described in chapter 5.

An initial trend analysis was conducted to determine if the rate of deterioration varied between environmental settings. Linear regression was performed on the preliminary dataset and differences in performance were observed; however, because of the large spread of data, most differences would not likely be statistically significant at the 95-percent confidence interval. Moreover, simple linear regression does not consider the large amount of independent variables that contribute to pavement performance. Considering this, a more complex investigation (consisting of multivariate regression analysis) was initiated in phase 2.

A preliminary cost investigation was performed to determine the amount of cost data available for future analysis. Sufficient amounts of cost data were found to be available to make cost comparisons between States in different frost conditions; however, the unit descriptions were not consistent among the agencies. Therefore, phase 2 work consisted of determining standard roadway sections and identifying unit descriptions that were consistent. This was accomplished through inquiries with each SHA.

3. DEVELOPMENT OF ANALYSIS DATASET

In the initial work on this project, the data analysis team specifically developed SMP site data as called for in the task order. The task order clearly identified SMP sites to be the basis of this project. Task 3 had the following requirement:

> *Make a comparison of performance data from the LTPP Seasonal Monitoring Program (SMP) sites that are located in the southern reaches of the wet-freeze zone or the northern reaches of the wet no-freeze zone versus those sites that are further north in the wet-freeze zone.*

The task order also stated:

> *Initial trend analysis studies should determine whether the SMP data support the contention that the rate of accumulation of pavement distress is greater (more rapid) in climatic zones where there are a large number of annual freeze-thaw cycles versus deep frost penetration.*

It is assumed that the intent of using SMP data for this study was to make use of frost depth measurements taken at the sites, which were based on resistivity, temperature, and moisture data. SMP sites are the only source of actual frost penetration measurements in the LTPP database.

Tables 2, 3, and 4 list all SMP sites in the wet freeze, wet no-freeze, and dry freeze zones, respectively. Included in the tables are the experiment designations of each section, which are based on the type of pavement structure as defined in the *Long Term Pavement Performance Information Management System Pavement Performance Database User Guide*.[(3)] Table 5 summarizes the number of SMP test sections in each climatic zone separated by experiment type.

The number of test sites listed in table 5 includes all SMP sites. The actual number of potential sites for use in this study is more limited when considering only the following factor:

> *…sites that are located in the southern reaches of the wet-freeze zone or the northern reaches of the wet no-freeze zone versus those sites that are farther north in the wet freeze zone.*

There are GPS-1 sites in the wet no-freeze zone that could potentially be included in the "northern reaches of the wet no-freeze zone." Combining these sites with the nine GPS-1 sites in the wet freeze zone provides a total of 13 test sections in the wet freeze zone to analyze. Six of the SPS sites could also be used; however, these SPS projects were constructed relatively recently and many have not yet developed a clear damage trend.

Table 2. Wet freeze SMP sites.

State	State Code	SHRP ID	Experiment
CT	09	1803	GPS-1
IN	18	3002	GPS-3
KS	20	4054	GPS-4
ME	23	1026	GPS-1 (and GPS-6B)
MD	24	1634	GPS-2
MA	25	1002	GPS-1
MN	27	1018	GPS-1
MN	27	1028	GPS-1
MN	27	4040	GPS-4
MN	27	6251	GPS-1
NE	31	3018	GPS-3
NH	33	1001	GPS-1
NY	36	4018	GPS-4
OK	40	4165	GPS-2
PA	42	1606	GPS-4
VT	50	1002	GPS-1
MB	83	3802	GPS-3
ON	87	1622	GPS-1
PQ	89	3015	GPS-3
DE	10	0102	SPS-1
NE	31	0114	SPS-1
NY	36	0801	SPS-8 (AC)
OH	39	0204	SPS-2

Note: GPS-1 AC over granular base
GPS-2 AC over bound base
GPS-3 JPCP
GPS-4 JRCP
GPS-6 AC overlay over existing AC
SPS-1 AC
SPS-2 PCC
SPS-8 Environmental (AC and PCC)

Table 3. Wet no-freeze SMP sites.

State	State Code	SHRP ID	Experiment
GA	13	1005	GPS-1
GA	13	1031	GPS-1
GA	13	3019	GPS-3
MS	28	1016	GPS-2
MS	28	1802	GPS-2
NC	37	1028	GPS-1
TX	48	1060	GPS-1
TX	48	1068	GPS-1
TX	48	1077	GPS-1
TX	48	1122	GPS-1
TX	48	3739	GPS-1
TX	48	4142	GPS-4
TX	48	4143	GPS-4
WA	53	3813	GPS-3
AL	01	0101	SPS-1
AL	01	0102	SPS-1
NC	37	0201	SPS-2
NC	37	0205	SPS-2
NC	37	0208	SPS-2
NC	37	0212	SPS-2
VA	51	0113	SPS-1
VA	51	0114	SPS-1

Table 4. Dry freeze SMP sites.

State	State Code	SHRP ID	Experiment
CO	08	1053	GPS-1
ID	16	1010	GPS-1
ID	16	3023	GPS-3
MT	30	8129	GPS-1
SD	46	9187	GPS-1
UT	49	1001	GPS-1
UT	49	3011	GPS-3
WY	56	1007	GPS-1
MB	83	1801	GPS-1
SK	90	6045	GPS-1 (and GPS-6B)
MT	30	0114	SPS-1
NV	32	0101	SPS-1
NV	32	0204	SPS-2
SD	46	0804	SPS-8 (AC)

Table 5. Number of pavement types in SMP sites.

Experiment	Wet Freeze	Wet No-Freeze	Dry Freeze	Total
GPS-1	9	9	8	25
GPS-2	2	2	0	4
GPS-3	4	2	2	8
GPS-4	3	2	0	5
GPS-6	1	0	1	2
SPS-1	2	4	2	8
SPS-2	1	4	1	6
SPS-8	1	0	1	2

The number of test sections must be compared with the number of variables that can contribute to pavement performance. Task 3 calls for the consultant to conduct a trend analysis in which the rates of distress accumulation will be analyzed considering the following factors:

- Number and duration of partial thaw events.
- Tradeoff between material qualities.
- Availability of moisture beneath the pavement.
- Severity of frost penetration.

In addition, task 5 asks the contractor to quantify the effect on pavement performance based on the analysis of the following factors:

- Pavement types (rigid, flexible).
- Climatic data (rainfall, FI, and thawing index from temperature data).
- Frost depth (temperature sensors and resistivity data).
- Deflection data (stresses and strains calculated from layer material properties).
- Performance data (distress and permanent deformation).
- Soils and material properties.
- Traffic data.

From these lists, a total of nine variables were incorporated into the dataset:

- Rainfall.
- FI.
- Thawing index.
- Annual cooling index (CI) (added by consultant to indicate heat loading).
- Frost depth.
- Pavement structure (either structural number (SN) or deflection data).

- Subgrade properties.
- Pavement layer material properties.
- Traffic data.

Nineteen potential AC pavements and eleven potential PCC pavements do not compare well against the nine potential variables. For a reasonable statistical analysis, there should be a larger number of sites for each independent variable. Assuming a desired minimum of 10 to 20 sites for each independent variable, 90 to 180 sites would be desirable to meet the needs of this project.

In addition, evaluation was performed to determine the actual number of SMP sites that were available with reasonable performance data. For the AC pavement sites, 9 sites of the 19 noted above had reasonably deterioration trends. At most, 15 sites could be included in the analysis equating to 8 sites in the deep-freeze environment, 4 sites in the moderate-freeze environment, and 3 sites in the no-freeze environment. With this breakdown, there are more independent variables than sites in either environment. This further illustrated the necessity to use additional LTPP test sections.

The important question facing the analysis team was: "Could the objectives be met by expanding beyond the SMP sites?" As will be explained in the following paragraphs, the answer was a resounding "Yes."

Table 6 lists only the 23 reported SMP sites with measured, nonzero, frost depths. The actual measured frost depths vary from one measurement to four. The two frost depths reported in this table are the largest (representing the coldest year) and smallest (representing the warmest year) annual maximum frost depth over the monitoring period, which was—at most—4 years. One of the challenges when dealing with annual frost depths is that the actual frost depth can vary markedly from year to year. Simply stated, the frost depth is as changeable as the weather, and the severity of the winter weather can change drastically from one year to the next. As can be seen in table 6, frost depths vary between 25 percent and 50 percent from year to year. In the event that only one measurement was taken, the same value was reported in the table for both the maximum and minimum year. Where the minimum measured value is shown as zero, then two or more measurements were taken with 1 year receiving no frost penetration. The most noticeable variation in frost measurements is section 364018, which indicates 2.09 m (6.86 ft) of frost 1 year and no frost another year.

In actuality, using a limited number of frost measurements is not a good design practice because of its variability. The maximum frost depth measured during one of the more severe winters is often used for design values. For example, the Washington State Department of Transportation (WSDOT) has used frost measurements taken in 1950, which was a very severe winter, as its basis for the part of the pavement design that accounts for frost.[4]

Table 6. SMP sites with measured frost depths.

State Code	SHRP ID	Pavement Type	Average FI Degree-Celsius days	Average FTC	Maximum Frost Depth m (ft)	Minimum Frost Depth m (ft)
42	1606	JRCP	353.8	91.3	0.415 (1.4)	0 (0)
31	0114	AC	409.8	105.1	0.865 (2.8)	0.665 (2.2)
36	0801	AC	436.9	86.6	0.835 (2.7)	0 (0)
25	1002	AC	437.8	117.9	0.76 (2.5)	0 (0)
31	3018	JPCP	478.8	117.8	1.22 (4.0)	0 (0)
56	1007	AC	545.8	140.4	0.945 (3.1)	0.515 (1.7)
30	8129	AC	579.7	151.8	1.025 (3.4)	0.82 (2.7)
36	4018	JRCP	583.6	113.0	2.095 (6.9)	0 (0)
16	1010	AC	665.2	135.9	0.76 (2.5)	0.61 (2.0)
30	0114	AC	687.8	113.7	1.004 (3.3)	1.004 (3.3)
46	9187	AC	757.1	117.0	1.465 (4.8)	1.115 (3.7)
50	1002	AC	786.0	98.2	0.79 (2.6)	0.63 (2.1)
23	1026	AC	827.6	115.1	1.77 (5.8)	1.00 (3.3)
46	0804	AC	977.9	107.2	1.435 (4.7)	0.875 (2.9)
87	1622	AC	1080.8	102.5	1.23 (4.0)	1.03 (3.4)
27	1018	AC	1108.3	92.9	2.13 (7.0)	1.865 (6.1)
89	3015	JPCP	1227.6	84.4	1.38 (4.5)	0.97 (3.2)
27	4040	JRCP	1347.8	90.7	2.21 (7.3)	2.01 (6.6)
27	1028	AC	1387.7	87.0	2.38 (7.8)	2.38 (7.8)
27	6251	AC	1484.9	88.5	2.25 (7.4)	1.895 (6.2)
83	1801	AC	1732.9	88.9	1.975 (6.5)	1.16 (3.8)
83	3802	JPCP	1862.8	79.9	2.31 (7.6)	1.71 (5.6)
90	6405	AC	1863.3	83.3	2.05 (6.7)	2 (6.3)

There has been a considerable amount of work relating frost depth to FI. A detailed description in estimating frost depths based on soil properties and FI is covered in some detail in the *WSDOT Pavement Guide for Design, Evaluation and Rehabilitation, Volume 2, Pavement Notes*.[4] In Minnesota, it was found that using a similar approach with modification in the standard n-factors, thermal conductivity, and mean annual soil temperature, the majority of the calculated depths fell within ±13.3 percent of the depths measured.[5]

There is clearly a relationship between FI and frost depth. As shown in figure 1, graphing the measured frost depth for the SMP sites and the FI for the same sites shows a reasonable trend between measured frost depth and the average FI from the virtual weather station for each site. The trend line developed by using a linear least squares regression approach indicates that the frost depth equals 0.0014 times the average FI.

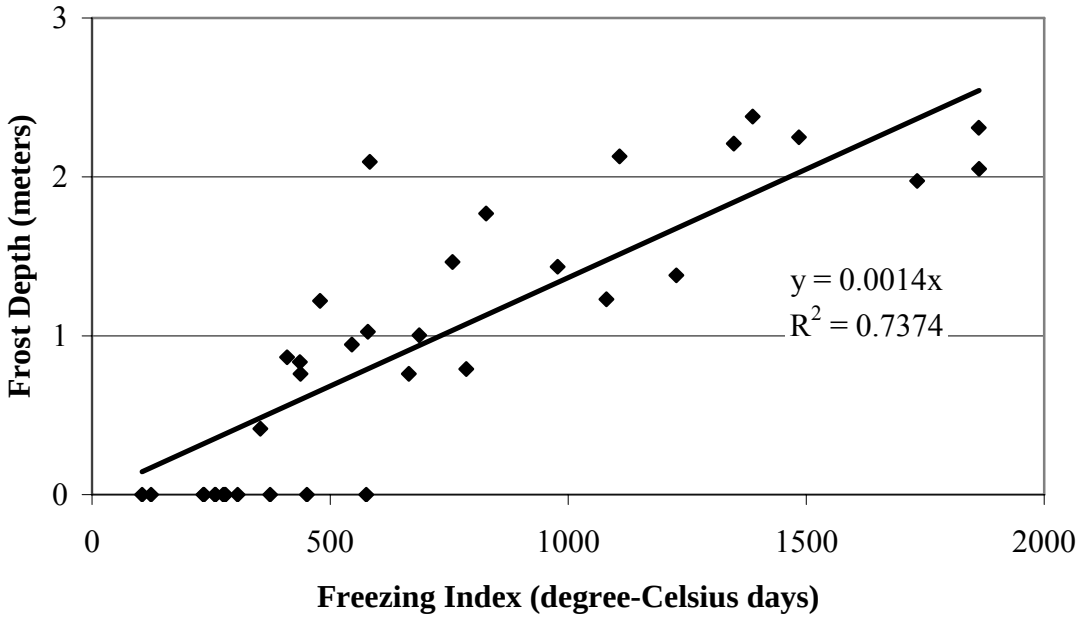

Figure 1. Graph. Plot of measured maximum frost depth to FI.

The regression data indicated that this trend line fits the data with an R-squared (coefficient of determination) of 0.74, which is quite good using such widespread national data. In the context of this study, this correlation is acceptable because the FI would be used only to compare the frost conditions at each site. The approximate frost condition will provide enough information to account for frost exposure in the pavement performance models.

Considering the variability in measured frost depths over only a few years, it could be argued that estimating the average frost depth based on almost 20 years of FI measurements would relate better to 15 to 25 years of pavement performance than four or fewer isolated frost measurements.

For these reasons, the analysis team proposed to expand the study to include non-SMP, GPS, and SPS sites using the FI as an indicator of actual frost depth. This approach was included in the work plan for phase 2 of the study, which was approved by the PFS Technical Advisory Committee and the FHWA LTPP Data Analysis contracting officer's technical representative (COTR). Therefore, the analysis team expanded the dataset to include LTPP experiments listed in table 7. Complete details on each experiment can be found in the *Long Term Pavement Performance Information Management System Pavement Performance Database User Guide*.[(3)]

Table 7. LTPP experiments included in the analysis dataset.

Pavement Type	LTPP Experiment	Description
Flexible	GPS-1	Asphalt concrete pavement (ACP) on granular base
Flexible	GPS-2	ACP pavement on bound base
Flexible	GPS-6	ACP overlay of existing ACP
Flexible	SPS-1	Strategic study of structural factors for ACP
Flexible	SPS-8	Study of environmental effects in the absence of heavy loads
Rigid	GPS-3	Jointed plain concrete pavement (JPCP)
Rigid	SPS-2	Strategic study of structural factors for rigid pavements
Rigid	SPS-8	Study of environmental effects in the absence of heavy loads

DATABASE STRUCTURE AND CONTENT

All databases developed for use in this study were created in Microsoft Access 2000© format to be consistent with the format of the LTPP Information Management System (IMS) Data Release 17.0 (version 2004.01). Some of the necessary tables were imported from the data release without requiring modification; other tables were created or imported from the data release and modified to aid in the data extraction process. Queries were then developed to acquire the desired data in the proper format as well as to perform calculations.

The task order proposal request for this project outlined the following factors to be considered in the analysis:

- Pavement types (rigid, flexible).
- Climatic data (rainfall, FI, and thawing index from temperature data).
- Frost depth (temperature sensors and resistivity data).
- Deflection data (stresses and strains calculated from layer material properties).
- Performance data (distress and permanent deformation).
- Soils and material properties.
- Traffic data.

To evaluate the effect of frost penetration and FTCs on pavement performance, other contributing factors, listed above, had to be taken into consideration. There are two methods that can be used to address this. The first is to separate the dataset into groups of similar test sections (i.e., structural properties) under similar conditions in terms of climate, materials, and traffic. In turn, regression analysis would be performed on each of the groupings. Considering the number of variables that need to be accounted for, the data would be separated into a large number of groups to explain all of the combinations of interest. The primary disadvantage to this method is that the results can be confounded by the grouping method used. In addition, each regression is based on a smaller subset of the entire dataset making the models less robust.

The other alternative is to perform regression analysis on the entire dataset and include all of the factors as explanatory variables within the model. This allows the contribution of each factor to be explained independently in the model. Comparisons of predicted performance can be made by keeping all inputs constant except for the factors of interest for the study (i.e., climatic variables). This approach was adopted for modeling performance in this study; therefore, each of the factors listed previously was incorporated into the datasets and used as explanatory variables in the models. The following paragraphs contain descriptions of each explanatory variable as well as the performance measures selected for evaluation.

Pavement Types

Separate datasets were developed for each pavement type. To account for the performance of flexible pavements, test sections classified as SPS-1, SPS-8, GPS-1, GPS-2, and GPS-6 experiments were included in the study. Only test sections constructed with jointed plain concrete pavement were considered for use in the rigid pavement dataset (SPS-2, SPS-8, and GPS-3 experiments). These experiments provide test sections that have various structures and are exposed to a wide array of climatic and traffic conditions.

It should be noted than some test sections received rehabilitation during LTPP monitoring. This resulted in test sections changing experiment designation; therefore, one test section may be included in two experiments. Data collected both before and after the rehabilitation were included in the dataset (with different experiment designations).

The experiment classification was included as an explanatory variable (labeled as EXP) in the models to account for possible differences in performance between the experiment types. For example, GPS-6 test sections have been overlaid while the other flexible experiments have not.

Climatic Data and Frost Depth

Precipitation, CI, FTCs, longitude, latitude, and elevation were included in the datasets to account for climatic effects. As discussed in previous sections, the FI was used to provide a relative comparison of frost depth conditions at each location.

Annual FI and annual number of FTCs were obtained directly from the virtual weather station table (CLM_VWS_TEMP_ANNUAL). Operating weather stations are not available at every test section; therefore, virtual weather stations were created by extrapolating climatic data from up to five nearby weather stations. This gives an estimation of the actual weather conditions at the location of the test section. To obtain values that are representative over the performance life of the pavement section, annual averages were computed for all years available, which is at least 20 years of data.

Annual cooling index (CI) was not directly available from the LTPP data release, and it was computed for each year with temperature values in the CLM_VWS_TEMP_ANNUAL table. Like FI and FTC, the values used in the analysis dataset were annual averages from at least 20 years of data. The equation to calculate CI is shown in equation 1.

$$Cooling\ Index = \sum (\overline{T} - 18.33) \quad if\ \overline{T} > 18.33 \tag{1}$$

where

$\overline{T}$ = mean daily temperature (°C) from virtual weather stations

Cooling Index = cooling index (°C - days)

Annual precipitation data (PRECIP) also was obtained from virtual weather station data in the CLM_VWS_PRECIP_ANNUAL table. The data used in the analysis dataset were the annual average of values in the table for each section, which consist of least 20 years of data.

Collectively, these four factors describe the relevant climatic conditions for this study. FI has been closely correlated to depth of frost penetration. Because actual frost depth measurements were not taken at the test sections, FI was used as a surrogate to frost depth. FI and FTC are the primary factors investigated in the analysis, and they describe the cold portion of the climatic spectrum. On the other hand, CI offers information regarding the warmer portion of the climate. Two sites with approximately the same winter weather conditions (similar FI values) could have drastically different summer conditions, which are indicated by CI. For example, test sections 361001 (located in New York) and 851801 (located in Newfoundland) both exhibit similar winter conditions. The FI for both sections is 505 degree-Celsius days, and the FTC is 90 and 100 for test sections 361001 and 851801, respectively. However, there is a large difference in CI. Newfoundland experiences a much milder summer with a CI of 25 degree-Celsius days, while the summer in New York is considerably warmer, exhibiting a CI of approximately 300 degree-Celsius days. This difference in summer conditions could contribute to variant performance and must be considered when comparing performance trends.

Geographic parameters of longitude, latitude, and elevation were incorporated in the dataset, but their contribution to pavement performance was found to be insignificant. These data were queried from the INV_ID or SPS_ID tables, depending on the experiment.

Performance Data

In addition to strain values discussed previously, accumulated surface distress, change in roughness with age, absolute roughness, rut depth (flexible pavements), and faulting (rigid pavements) were all used as performance measures.

Pavement performance is a function of pavement age. As such, pavement age was calculated and coupled with the performance measures in the dataset. Depending on the experiment type, either the date of original construction or date of rehabilitation was extracted from the LTPP database. Details on the extracted data can be found in table 8. Data collection dates were subtracted from the established construction/rehabilitation dates to establish pavement age. A new construction/rehabilitation date was generated for each new rehabilitation activity. Subsequent data collection dates were subtracted from the new reference age. Performance could then be predicted as a function of pavement age.

Table 8. Sources of construction and rehabilitation dates.

LTPP Experiment	LTPP Database Table
GPS-1, -2, and -3	INV_ID
SPS-1, -2, and -8	SPS_ID
GPS-6	INV_MAJOR_IMP or RHB_IMP

Only distress data collected using manual techniques were used in this study. Data collected using photographic/automated techniques were not included. Research that has been conducted by Rada et al.[6] evaluating the variability of LTPP distress data collection found that the overall variability of distress collected manually is lower than that collected by photographic methods. In addition, the apparent bias of data collected by photographic techniques was much higher than that collected manually. The study found a reasonable correlation between the two methods; however, manual data collection tended to yield higher amounts of distress than the photographic techniques. Considering these findings, only manual data collection was included in the study to eliminate variability introduced when data from multiple techniques are used. The study also concluded that total distress quantities exhibit less bias and variability than each severity level independently. The recorded amounts of distress at each severity level were summed. Different methods were used to combine severity levels for each dataset, each of which is explained subsequently.

The LTPP pavement distress identification procedures characterize the various distress categories in terms of the type of the distress, the severity of the distress (i.e., low, moderate, and high severity), and the amount of the distress (area, length, number of occurrences).

There are two primary alternatives available to represent measured distress accumulation with pavement age for performance modeling. The first option would be to represent the accumulation of distress over time for the three levels of severity separately. This would add a very high level of complexity to the process and segment an already limited amount of distress measurements. Studies have shown that there is greater variability in classification of severity level for a distress type than that associated with distress type identification.[6] Modeling each severity level independently would compound this variability. To counter this, the quantities of all three severity levels could be summed (without weighting factors) for each distress type, which would reduce the variation apparent between severity levels. For example, a survey consisting of 3 m^2 of low severity, 5 m^2 of moderate severity, and 2 m^2 of high severity fatigue would be treated as 10 m^2 of fatigue for regression development. The disadvantage of this approach is that it eliminates the resolution gained by collecting pavement distress measurements in terms of severity levels.

Pavement distress measurements have historically been collected in terms of low, moderate, and high severity levels,[7] which where developed for implementation into pavement management systems. The pavement distress measurements were initially compiled as a composite index where the measurements of several distress types and severity levels were combined into a single index[8] such as the Pavement Condition Index (PCI) used in the Micro PAVER™ PMS system. More recently, the distress measurements have been compiled as a unique pavement distress

index where the severity levels of a single distress type are combined to produce a specific distress index.[9] The distress index is usually expressed as 100 minus the sum of the deduct points, where separate deduct points are computed for the amount of distress in each severity level for a specific distress type.

It is important to that that most SHAs use different pavement distress indices based to some extent on the specific pavement management system they have adopted, and a wide range of systems are in use throughout the United States. One of the predominant pavement condition deduct systems for unique pavement distress indices was used in this study to represent the change in flexible pavement distress with time.[10]

For the surface distress values of flexible pavements, all three severity levels for each distress type were combined through the use of deduct curves developed for the South Dakota Department of Transportation[10] to obtain a deduct value for each distress. The equations for these curves can be found in equations 2 through 4. Figure 2 provides a graphical representation of the low, moderate, and high severity deduct equations. The deduct values for the three severity levels were summed for each distress type and used in the regression analysis (i.e., equation 5).

$$D_L = 3.4082 * P_L^{0.514} \quad (2)$$

$$D_M = 4.4575 * P_M^{0.6107} \quad (3)$$

$$D_H = 5.2064 * P_H^{0.6956} \quad (4)$$

$$D_T = D_L + D_M + D_H \quad (5)$$

where:

D_L = low severity deduct value

D_M = moderate severity deduct value

D_H = high severity deduct value

D_T = total deduct value

P_L = recorded percentage of low severity distress

P_M = recorded percentage of moderate severity distress

P_H = recorded percentage of high severity distress

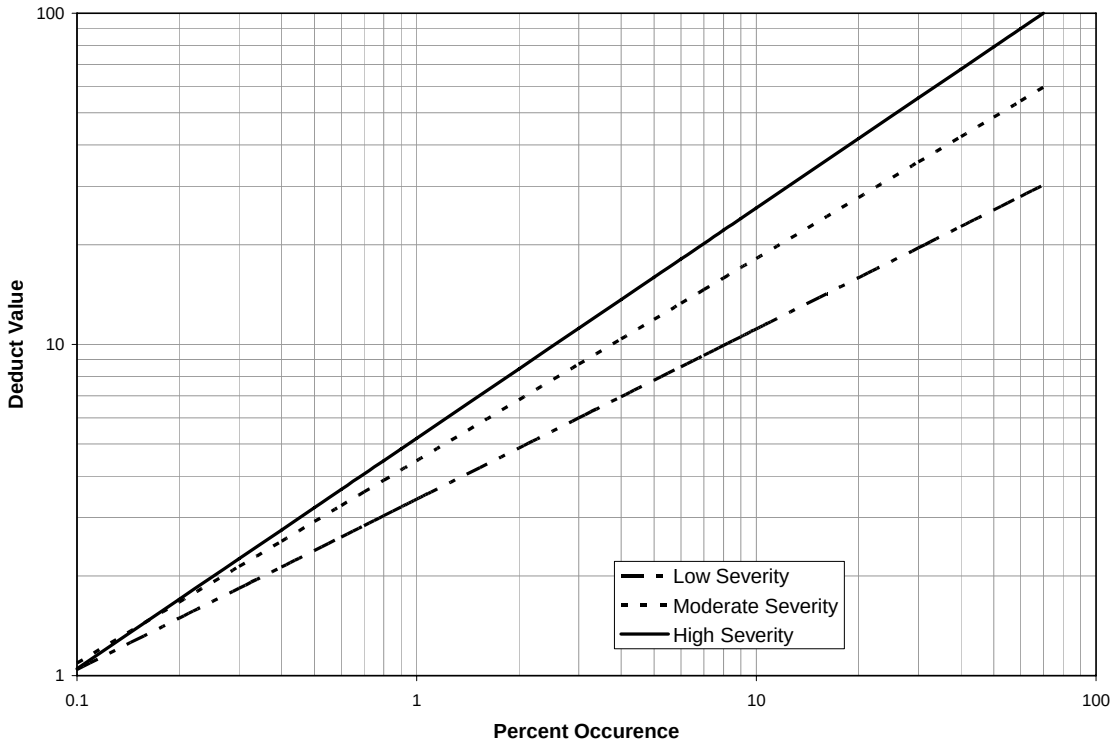

Figure 2. Graph. Individual distress deduct curves.

Fatigue cracking (FC), block cracking (BC), longitudinal wheelpath cracking (LWP), and transverse cracking (TC) were considered in the study. All distress data for the flexible dataset were queried from the MON_DIS_AC_REV table. Because LWP often progresses to FC, the two distress types were combined (FWPC). LWP was converted from a linear unit to a unit of area to be consistent with FC. This was done by applying a standard width of 0.3 m (1 ft) to the recorded length of LWP. All severities of LWP were considered as low severity to compute deduct values that would be combined with the FC.

The recorded amounts of distress were converted into percentages (based on the total length or area of the test section). This was done to account for test sections with different lengths in the dataset. Percentages for FC and FWPC were determined based on the area of one wheelpath in the test section. The width of the wheelpath was assumed to be 1 m (3 ft). For BC, percentages by total area were used in the deduct equations, while the percentage of TC was based on the total length of the section.

It has been observed by various researchers, as well as the regional support contractors, that there is considerable variability in the rating of longitudinal wheelpath cracking and low severity fatigue cracking. A study by Rada, et al.[(6)] observed that compensatory differences exist among fatigue and longitudinal wheelpath cracking. That is, a reduction in one of these distress types

generally coincides with an increase in the other type. For example, fatigue and longitudinal cracking values from section 080501 can be found in table 9. There is a reduction in fatigue cracking between 1996 and 1998 that is accompanied by an increase in longitudinal wheelpath cracking. The opposite is true between 1998 and 1999.

Table 9. Fatigue and longitudinal wheelpath cracking for LTPP section 080501.

Date	Total Fatigue Cracking (m^2 (ft^2))	Total Longitudinal Wheelpath Cracking (m (ft))
26-Oct-94	0 (0)	3.3 (10.8)
12-Apr-96	114.7 (1234.6)	0 (0)
31-Jul-98	19.9 (214.2)	180.3 (591.5)
01-Sep-99	128.4 (1382.1)	2.9 (9.5)

In addition, in the beginning stages fatigue cracking generally appears as longitudinal cracking in the wheelpath (and is rated as such by surveyors). Over time, with repeated traffic loading, this cracking develops patterns indicative of fatigue; therefore, longitudinal wheelpath cracking values diminish as fatigue values increase. An example of this can be found in table 10. The longitudinal wheelpath cracking reduces with age as the fatigue cracking increases at section 068153 because the longitudinal cracking is progressing to fatigue cracking. Modeling these two distress types independently would result in significant variation within the regression.

Table 10. Fatigue and longitudinal wheelpath cracking for LTPP section 068153.

Date	Total Fatigue Cracking (m^2 (ft^2))	Total Longitudinal Wheelpath Cracking (m (ft))
25-Nov-91	3.7 (39.8)	86.6 (932.1)
27-Jul-94	35.9 (386.4)	53.3 (573.7)
27-Jul-95	247 (2658.7)	0 (0)

For these reasons, fatigue and longitudinal cracking were combined. The combination provides a better indication of the damage in the wheelpaths because it is less variable and more consistent over time. This has improved the developed models.

The format of distress data collected on rigid pavements does not match the required format used in the established deduct curves;[8] therefore, the severity levels were summed for each distress type. This total distress was then normalized based on the size of the test section in the same manner as the flexible sections. For example, the sum of all three severities of longitudinal cracking were summed and divided by the total area of the section. Distress data were extracted

from the MON_DIS_JPCC_REV table. Rigid distress types evaluated were longitudinal cracking (LC), transverse cracking (TC), corner breaking (CB), and pumping/water bleeding (PUMP). Pavement roughness was computed by averaging international roughness index (IRI) values from all runs available for each survey date and test section in the MON_PROFILE_MASTER table. Two forms of IRI were incorporated in the dataset for model development: change in IRI (DIRI) and absolute IRI (AIRI).

Many factors, such as construction techniques, existing geometrics, and material quality contribute to the roughness of newly constructed or rehabilitated pavements. In turn, initial pavement roughness significantly affects the accumulation of roughness as the pavement ages. To negate this variability from the models used to make performance comparisons in different climatic regions, DIRI values were computed based on initial roughness values. Roughness data at the completion of construction were not available for the test sections; therefore, the first recorded roughness value was used as the initial value. Subsequent measurements were subtracted from this value. The initial roughness value was also included in the dataset for reference. Using test section 481094 as an example, the first roughness measurement—average IRI of 0.875 meters per kilometer (m/km) (55.5 inches per mile (inches/mi))—was performed in March 1990, equating to a pavement age of approximately 14 years. Successive testing performed in September 1997 resulted in an average IRI of 0.963 m/km (61.1 inches/mi). The DIRI value reported in the dataset was 0.088 m/km (5.6 inches/mi) at age 21.

Alternatively, recorded IRI values in absolute terms (AIRI) were established as performance measures. However, to account for postconstruction variability, the MIRI and the age at which they were recorded (MIRI_AGE) were incorporated as explanatory variables in the regression analysis.

The air temperature recorded during profile data collection was also included as an explanatory variable for the roughness models in the rigid dataset. Temperature variations throughout the day cause warping and curling that can contribute to variations in roughness values.

Data from MON_T_PROF_INDEX_SECTION were queried to obtain rut depth information for the flexible dataset. This table contains computed rutting index parameters calculated from transverse profile information. The lane-width wire line rut index, which calculates the maximum rut depth (in each wheelpath) based on a wire line reference, was selected for use in this study. The reference is defined as a straight line between peak elevation points for each half of the lane.[3] Each time rutting was measured, rut depth values for both wheelpaths were averaged and incorporated into the analysis dataset (RUT).

Faulting values were extracted from MON_DIS_JPCC_FAULT_SECT for the rigid dataset. The values used for the study were average values of all faulting recorded at the transverse joints. The faulting measurements were taken in the outside wheelpath.

Soils and Material Properties

Multiple explanatory variables were included to account for the contribution of soils and material properties on pavement performance, and they consisted of: base material type (BASE); subgrade material type (SG); structural number (SN) for flexible pavements; asphalt layer thickness (ACTHICK) for flexible pavements; and slab thickness (D) for rigid pavements.

Materials classifications for base layers were grouped into six categories. Information from the TST_LO5B table was used to obtain material codes for base layers (i.e., layer description=5). Data in the TST_LO5B table are the most representative information in the LTPP IMS Pavement Performance Database regarding pavement layering because it is derived primarily from laboratory test results. Table 11 lists each BASE category as well as the material codes used to define the category. Complete details on material code classifications can be found in Operational Guide No. SHRP-LTPP-OG-004.[(11)] Each test section was assigned a base type category as an explanatory variable. Each of the BASE categories established have significantly different characteristics (i.e., drainage, strength/in-situ moisture relationships), which directly effect the rate at which pavements deteriorate. In some cases multiple base layers existed in the pavement structure. Guidelines were established and they are provided in table 12 to assign BASE categories for these situations.

Similarly, material code classifications of subgrade layers (layer description=7) were extracted from TST_LO5B and grouped into three categories. Test sections with material codes between 100 and 178 were assigned a FINE subgrade type. All of these material codes correspond to material that has at least 50 percent passing the 0.075 millimeters (mm) (No. 200) sieve. Subgrade layers consisting of materials codes 200 to 267 were categorized as a COARSE subgrade. These material codes represent soils with less than 50 percent passing the 0.075 mm (No. 200) sieve. The third subgrade type established for this study was labeled ROCK/STONE and includes "naturally formed solid mineral matter occurring in large masses, and naturally or crushed angular particles of rock."[(11)]

The type of subgrade material can make a large contribution to the performance of pavement structures. Fine-grained materials become very weak with excess moisture, and are susceptible to frost heave.

For flexible pavements, structural capacity is most commonly defined in terms of SN. Methods detailed in SHRP-LTPP Technical Memorandum AU-167[(12)] were used to calculate SN values. The memo defines structural coefficients for each combination of material classification code and layer description. This coefficient was used in conjunction with layer thickness to obtain structural number. The method does not incorporate drainage coefficients to adjust structural capacity. Both material classification codes and layer thicknesses were extracted from the TST_LO5B table. If either the material classification code or the layer thickness was unavailable or unreasonable, data from agency project records, which are located in rehabilitation (RHB_LAYER) and inventory (INV_LAYER) tables, were used.

For rigid pavements, SN is not a valid parameter, and is replaced by slab thickness in design procedures.[13] As such, D was included as an explanatory variable in the dataset. Thickness values were extracted from the TST_LO5B table for surface layers (layer description=3).

Table 11. Material code classifications for each BASE type category.

BASE Category	BASE Description	Material Code	Material Code Description
DGAB	Unbound Base	302	Gravel (uncrushed)
		303	Crushed stone
		304	Crushed gravel
		305	Crushed slag
		306	Sand
		307	Soil-aggregate mixture (predominantly fine-grained)
		308	Soil-aggregate mixture (predominantly coarse-grained)
		309	Fine-grained soils
ATB	Asphalt Treated Base	319	Hot mix asphalt concrete (HMAC)
		320	Sand asphalt
		321	Asphalt treated mixture
		322	Dense graded, hot laid, central plant mix
		323	Dense graded, cold laid, central plant mix
		324	Dense graded, hot laid, mixed in-place
		328	Recycled asphalt concrete, plant mix, hot laid
		329	Recycled asphalt concrete, plant mix, cold laid
		330	Recycled asphalt concrete, mixed in-place
PATB	Permeable Asphalt Treated Base	325	Open graded, hot laid, central plant mix
		326	Open graded, cold laid, central plant mix
		327	Open graded, cold laid, mixed in-place
NONBIT	Nonbituminous Treated Base	331	Cement aggregate mixture
		332	Econocrete
		333	Cement-treated soil
		335-360	Includes treated soils (e.g., lime, calcium chloride)
LCB	Lean Concrete Base	334	Lean concrete
NONE	No Base	N/A	No layer description=5-inch layer structure

Table 12. BASE types assigned to structures with multiple base layers.

Existing Base Layer Combinations	BASE Category Assigned
ATB/DGAB	ATB
PATB/ATB	PATB
PATB/DGAB	PATB
NONBIT/DGAB	NONBIT
LCB/NONBIT	LCB
NONBIT/ATB	Sections removed from dataset (if present)
NONBIT/PATB	Sections removed from dataset (if present)
LCB/ATB	Sections removed from dataset (if present)
LCB/PATB	Sections removed from dataset (if present)

In addition, the total thickness of the AC binder course layers (layer descriptions 1, 3, and 4) was also calculated and included as an explanatory variable in the dataset. Again, data in the TST_LO5B table were used to determine these values.

To summarize all of the soil and material property variables discussed previously, TST_LO5B information from test section 481094 is provided as an example in table 13 along with structural coefficients from SHRP-LTPP Technical Memorandum AU-167.[(12)]

The material classification code for the base layer (layer description 5) is 303; therefore, the BASE category dense graded aggregate base (DGAB) was assigned to test section 481094. The subgrade explanatory variable for this section was designated as COARSE because of the material code classification of 214 for the subgrade layer. The SN calculation provided in table 12 resulted in an SN of approximately 2.01.

Last, two AC binder course layers are present in the pavement structure with thicknesses of 1.2 and 0.7 (layers 3 and 4, respectively); therefore, the ACTHICK value was computed as 1.9 for this section.

Table 13. TST_LO5B data for test section 481094.

Layer	Layer Description from TST_LO5B	Material Code from TST_LO5B	Structural Coefficient from AU-167 (a)	Layer Thickness from TST_LO5B (D) (mm (inch))	Structural Contribution (a*D)
1	7	214	0	NA	0
2	5	303	0.14	213 (8.4)	1.176
3	4	1	0.44	31 (1.2)	0.528
4	3	1	0.44	18 (0.7)	0.308
Total					2.012

Note: a= structural coefficient, D=layer thickness, a*D=structural coefficient multiplied by layer thickness

Traffic Data

Traffic data are one of the most significant factors affecting pavement performance. Equivalent single axle load (ESAL) values provide a representative value of the traffic loading experienced by a pavement structure. Equivalent axle load factor (EALF) values were computed using equations set forth in the American Association of State Highway and Transportation Officials (AASHTO) *Guide for Design of Pavement Structures*.[13] Values of SN or D, discussed previously, were inputs for the calculation of EALF. In turn, the EALF values were used to convert weight bin data from the TRF_MONITOR_AXLE_DISTRIB table to ESALs. Values were averaged over all available years in the dataset. If monitored traffic data were unavailable, data from the estimated traffic (TRF_MON_EST_ESAL) table were used. These estimations are provided by the SHA.

It is recognized by the analysis team that traffic load spectra has been introduced to represent loading conditions for design purposes; however, the tools to apply load spectra from LTPP data were not readily available at the onset of the project.

To provide an indication of the structural capacity of the pavement relative to the amount of loading experienced, a ratio of SN and logarithm of ESALs was computed. Pavement performance is highly dependent on the relationship between these two. For example, the amount of alligator cracking is directly related to both the magnitude of loading and the overall strength of the pavement structure. Therefore, the ratio could be used to determine if differences in performance are related to frost conditions or are a consequence of the improper pairing of pavement strength and loading. A similar ratio was computed for rigid pavements with the exception that SN was replaced with slab thickness. The logarithmic relationship of ESALs was applied in both ratios to reflect the processes outlined in the 1993 *AASHTO Guide for Design of Pavement Structures*.[1] The design charts in the design guide correlate accumulated damage to ESAL values using a logarithmic relationship. The SN or D values are integrated into the design equations using a linear relationship.

In addition, the functional classification for each test section was included in the roughness datasets (both absolute and change in roughness). This factor was included to account for differences in the initial smoothness of the sections due to a range of construction smoothness specifications.

TEST SECTION SELECTION

Criteria were established to select test sections to be used in the development of regression models. This was to reduce variability within the dataset and improve the resultant models.

The first condition was set forth in the statement of work for the project, which stated that performance comparisons would be made with sites that are located in:

> *...the southern reaches of the wet-freeze zone or the northern reaches of the wet no-freeze zone versus those sites that are farther north in the wet freeze zone. Contrast these findings with pavement performance in the dry freeze and wet no-freeze climatic regions.*

Therefore, only sections located in the wet freeze, wet no-freeze, and dry freeze regions were included in the analysis. While climatic differences were accounted for as explanatory variables, only data from the regions of interest for this study were included.

In addition, to limit the variability of the performance data within the dataset, the TST_LO5B table was used to identify and remove test sections with surface treatments such as slurry and chip seals. Routine applications of surface treatments significantly reduce the progression of pavement deterioration. These treatments mask the surface of the pavement, thus improving performance measures such as pavement roughness and surface distress. If these test sections would have been included in the study, additional explanatory variables would have been required to properly account for their effect.

Test sections with unavailable or questionable explanatory data were also removed from the analysis dataset. For example, the computed 1994 annual ESAL value for test section 124109 was approximately 47.8 million. This value is very unreasonable, and the average ESAL value used in the dataset was computed using all other available years except 1994.

The resultant datasets consisted of more than 520 test sections for flexible pavements and over 270 test sections for rigid pavements. Between 2,500 and 4,500 observations (depending on the performance measure) were included to develop the flexible models. The number of observations for the rigid dataset ranged from 1,400 to 2,700. The size of the dataset is adequate to properly incorporate the relatively large number of variables required in the study. In addition, the number of test sections ensures pavements exposed to a wide range of conditions are represented in the models.

4. MODEL FITTING STATISTICAL APPROACH

This section describes the overall procedure for developing regression models for each of the performance measures considered in the study. The intent of the process was to generate a model with the best prediction capability while ensuring assumptions inherent in the process were not violated. Statistical analysis was performed using SAS® software, version 9.1.3.[14]

All explanatory variables discussed in previous sections of this report were included in the initial regression analysis. These variables were both continuous (i.e., FI) and categorical (i.e., BASE) factors. Table 14 provides a summary of all variables considered in the study as well as details on the format of each parameter.

Table 14. Summary of explanatory variables.

Explanatory Variable	Parameter Type
Pavement Structure	Categorical
Freezing Index (FI)	Continuous
Freeze-Thaw Cycles (FTC)	Continuous
Cooling Index (CI)	Continuous
Annual Precipitation (PRECIP)	Continuous
Pavement Age (AGE)	Continuous
Subgrade Type (SG)	Categorical
Base Type (BASE)	Categorical
Asphalt Cement Concrete Thickness (ACTHICK)	Continuous
Slab Thickness (D)	Continuous
Traffic Loading/Structural Capacity Ration (LESN or LEDT)	Continuous

An initial investigation was performed on each of the predictor variables to gain an understanding of the range present in the dataset and the nature of the parameters to be used in the regression modeling. Graphical techniques and descriptive statistical measures were used for this evaluation. These visual techniques allowed for problems with calculations in the dataset or possible outliers to be identified. As an example, a box plot diagram is provided in figure 3, and table 15 presents a sample set of statistical parameters evaluated.

Box plots provide an excellent visual summary of many important aspects of a distribution.[15] The box plot is based on a 5-number summary that includes the median, quartiles, and extreme values. The box stretches from the lower hinge (Q1: 1st quartile) to the upper hinge (Q3: 3rd quartile) and therefore contains the middle half of the scores in the distribution. The median is shown as a line across the box. A quarter of the distribution is between this line and the top of the box and one quarter of the distribution is between this line and the bottom of the box. The plus (+) symbol in box plot represents the mean of the response within that group. The distance between Q3-Q1 is known as interquartile range (IQR). This measure is very useful in detecting

outliers in the data. Any observation falling outside Q3+1.5IQR or Q1−1.5IQR could be flagged as potential outlier. Box plots can be useful in detecting right and left skewness as well.

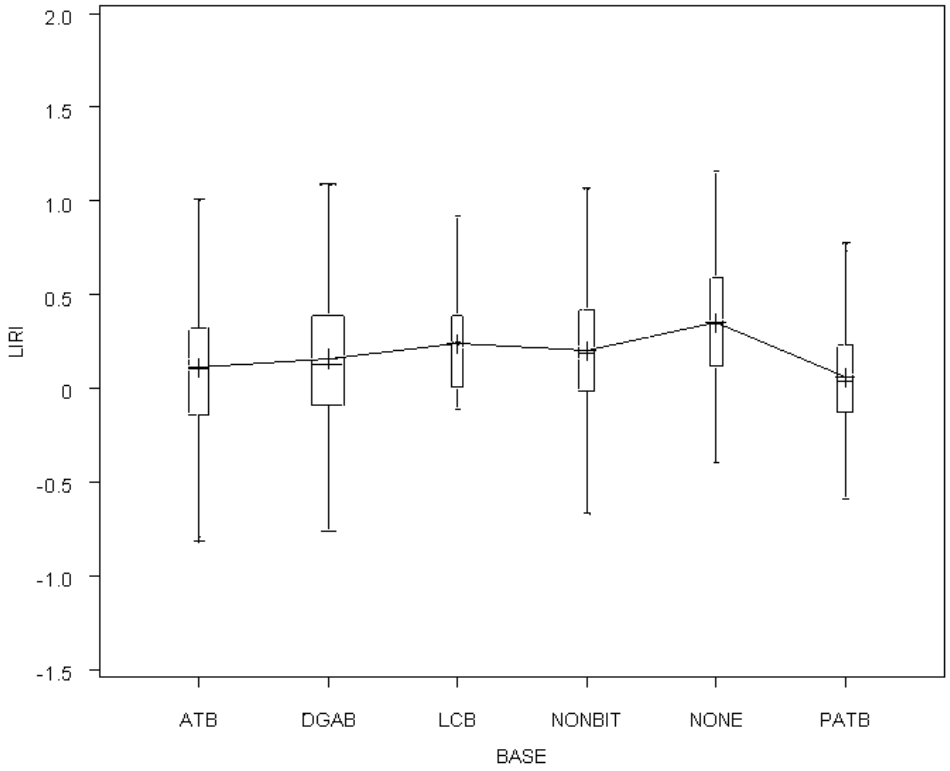

Figure 3. Graph. Sample box plot.

Table 15. Sample of statistical parameters.

Variable	N	Mean	Std Dev	Sum	Minimum	Maximum	Label
ESAL	1991	209757.0	200366.0	417627102	1.10000	1484889	ESAL
SN	1991	5.39970.0	1.92871	10751	0.60000	12.20000	SN
ACTHICK	1991	6.33305.0	2.83518	12609	1.00000	22.80000	ACTHICK
ELEV	1991	1384.0	1569.0	2755713	8.00000	7400	ELEV
LAT	1991	39.50387	6.86929	78652	18.44200	64.94800	LAT
LONG	1991	93.88745	18.13777	186930	52.86900	156.67000	LONG
FTC	1991	85.63034	40.13912	170490	0	192.00000	FTC
FI	1991	360.47850	408.44595	717713	0	2584	FI
CI	1991	644.74681	523.55940	1283691	0.10000	2506	CI
PRECIP	1991	909.58970	388.44307	1810993	187.30000	2020	PRECIP
RUT_AGE	1991	7.86801	6.87675	15665	0	31.80000	RUT_AGE
RUT	1991	5.17353	4.13532	10301	0.50000	55.00000	RUT

Partial regression effects between the response and continuous predictor variables were evaluated, which provided information regarding the independent contribution of each parameter. Figure 4 shows an example of an augmented partial residual plot.

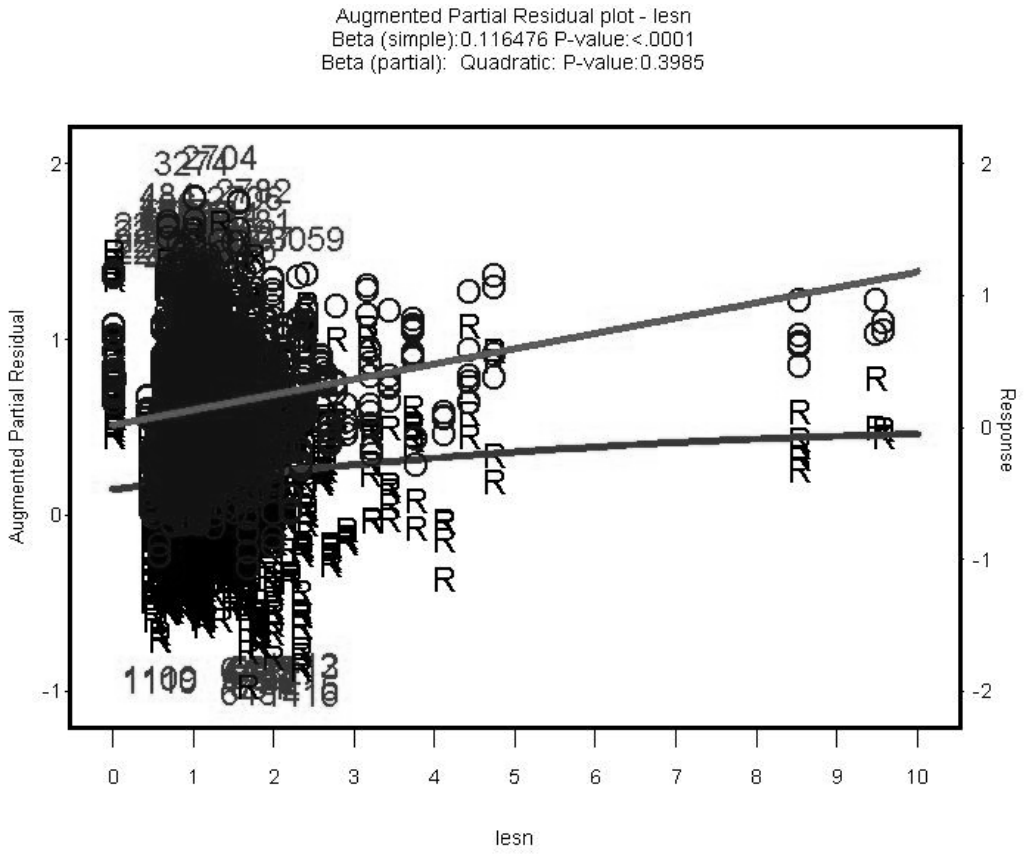

Figure 4. Scatter Plot. Sample augmented partial residual plot.

In augmented partial residual plots, both partial linear and quadratic effects of a continuous explanatory variable (equation 6) are plotted against one of the explanatory variables using symbol "R". The simple regression line (symbol "O") between the explanatory variable and the response variable is also overlaid in the same plot to show the differences between the simple and the partial effects. This augmented partial residual plot is considered very effective in detecting outliers, nonlinearity, and heteroscedasticity.[15]

$$\varepsilon_i = \beta_1 X_1 + \beta_3 X_1^2 \tag{6}$$

Where:

ε_i = residual

β_1, β_3 = coefficients

X_1 = explanatory variable

While partial regression coefficients present information on the contribution of each predictor variable after controlling for other effects in the model, correlation between variables (i.e., multicollinearity) as well as interacting effects of multiple predictor variables on the performance measure do exist and must be checked. A preliminary analysis of multicollinearity was conducted using an explanatory variable correlation matrix (table 16). In the presence of multicollinearity, the regression parameter estimates become unstable due to a large inflation of the parameter variance. Any two explanatory variables having a significantly larger correlation (>0.9) could be involved in multicollinearity and should be examined by the variance inflation factor (VIF > 10) estimate for each explanatory variable.[15] Significant interaction between any two continuous predictors or between a continuous and categorical predictor variables indicate that the performance measure is influenced by the interacting variables multiplicatively. Omitting significant interaction terms could under- or overestimate the model prediction significantly. Graphical methods were used to examine interaction between continuous and categorical parameters. Interaction plots and the P-values for the interaction terms from the full model were used to check for interaction between two continuous variables and between a continuous and a categorical variable.

Using the knowledge gained through the preliminary review, regression models were developed with all of the explanatory variables and potential interaction terms (identified in the initial review). Resulting P-values were used to determine which variables contributed significantly to the regression model. Generally, parameters with a P-value greater than 0.15 were considered insignificant because there could be more than a 15 percent chance that the regression parameter estimates could be equal to zero, and therefore, should be removed from subsequent regression iterations. In some cases, the independent contribution of an explanatory variable was insignificant, but its interaction effect with other parameters was significant. Both the independent and interacting terms were included in subsequent models when this occurred. Terms that were marginally significant were incorporated in the model only if their contribution improved the prediction capability of the model, which was achieved by iteratively developing models and evaluating adjusted R-squared, root mean squared error and AIC statistics to select the model that best predicted the observed data. All parameters within a categorical variable were included if one of the parameters was found to be significant. For example, in table 17, all BASE types were included in the model because DGAB is significant. LCB was included even though its contribution was not significant. The entire category must be accounted for in the model if one parameter was found to be significant.

As part of the model development activities, transformations were incorporated to reduce the violation of assumptions inherent in regression models. Figure 5 provides graphical results on the validity of assumptions for the AIRI model before transforming the data. As can be seen from the residual plot (upper right corner of figure 5), the shape of the plot indicates unequal error variance (signified by the diagonal orientation of the bottom boundary of data points). In addition, the normal probability plot (lower left figure) indicates non-normality in the dataset (residual points depart from the straight line). For these reasons, a natural logarithm transformation of the performance measure was performed. The results of the validity check after the transformation can be found in figure 6. As the figure indicates, both the unequal error

variance and non-normality have been reduced, thus improving the validity of assumptions in the model.

The final regression models were used to predict mean performance values, and 95 percent confidence intervals were also computed and used in making performance comparisons between the regions. These predictions were made for climatic scenarios of interest in the study. Complete details on this process are discussed in the following section of this report

Table 16. Sample of correlation matrix.

	ESAL	SN	ACTHICK	ELEV	LAT	LONG	FTC	FI	CI	PRECIP	RUT AGE	RUT
ESAL ESAL	1.00000	0.25535 <.0001	0.15887 <.0001	-0.09449 <.0001	-0.25639 <.0001	-0.03808 0.0894	-0.16282 <.0001	-0.24556 <.0001	0.22145 <.0001	0.13579 <.0001	0.03080 0.1696	0.00151 0.9462
SN SN	0.25535 <.0001	1.00000	0.43217 <.0001	0.05645 0.0118	0.06731 0.0027	-0.12238 <.0001	0.22680 <.0001	-0.05253 0.0191	-0.18038 <.0001	-0.10588 <.0001	-0.27243 <.0001	-0.15508 <.0001
ACTHICK ACTHICK	0.15887 <.0001	0.43217 <.0001	1.00000	0.01245 0.5786	0.06886 0.0021	-0.09872 <.0001	0.11020 <.0001	0.03918 0.0805	-0.14686 <.0001	0.00599 0.7895	-0.04717 0.0353	-0.02761 0.2181
ELEV ELEV	-0.09449 <.0001	0.05645 0.0118	0.01245 0.5786	1.00000	0.28208 <.0001	0.51202 <.0001	0.76208 <.0001	0.19521 <.0001	-0.43518 <.0001	-0.78481 <.0001	-0.10769 <.0001	-0.00238 0.9154
LAT LAT	-0.25639 <.0001	0.06731 0.0027	0.06886 0.0021	0.28208 <.0001	1.00000	0.25897 <.0001	0.61287 <.0001	0.76147 <.0001	-0.89240 <.0001	-0.40206 <.0001	-0.08413 0.0002	0.04866 0.0299
LONG LONG	-0.03808 0.0894	-0.12238 <.0001	-0.09872 <.0001	0.51202 <.0001	0.25897 <.0001	1.00000	0.22746 <.0001	0.17877 <.0001	-0.13525 <.0001	-0.58561 <.0001	-0.01362 0.5436	-0.02278 0.3097
FTC FTC	-0.16282 <.0001	0.22680 <.0001	0.11020 <.0001	0.76208 <.0001	0.61287 <.0001	0.22746 <.0001	1.00000	0.38152 <.0001	-0.78366 <.0001	-0.62650 <.0001	-0.18159 <.0001	0.02663 0.2349
FI FI	-0.24556 <.0001	-0.05253 0.0191	0.03918 0.0805	0.19521 <.0001	0.76147 <.0001	0.17877 <.0001	0.38152 <.0001	1.00000	-0.61977 <.0001	-0.40330 <.0001	0.05764 0.0101	0.03397 0.1297
CI CI	0.22145 <.0001	-0.18038 <.0001	-0.14686 <.0001	-0.43518 <.0001	-0.89240 <.0001	-0.13525 <.0001	-0.78366 <.0001	-0.61977 <.0001	1.00000	0.43074 <.0001	0.10822 <.0001	-0.02763 0.2179
PRECIP PRECIP	0.13579 <.0001	-0.10588 <.0001	0.00599 0.7895	-0.78481 <.0001	-0.40206 <.0001	-0.58561 <.0001	-0.62650 <.0001	-0.40330 <.0001	0.43074 <.0001	1.00000	0.13377 <.0001	0.02610 0.2443
RUT_AGE RUT_AGE	0.03080 0.1696	-0.27243 <.0001	-0.04717 0.0353	-0.10769 <.0001	-0.08413 0.0002	-0.01362 0.5436	-0.18159 <.0001	0.05764 0.0101	0.10822 <.0001	0.13377 <.0001	1.00000	0.43351 <.0001
RUT RUT	0.00151 0.9462	-0.15508 <.0001	-0.02761 0.2181	-0.00238 0.9154	0.04866 0.0299	-0.02278 0.3097	0.02663 0.2349	0.03397 0.1297	-0.02763 0.2179	0.02610 0.2443	0.43351 <.0001	1.00000

*The top number in each cell represents correlation; the bottom number denotes the P-value.

Table 17. Regression coefficients with P-value statistics.

Regression Parameter		Estimate	Standard	t Value	Pr > |t|
Intercept		−1.08	0.29	−3.79	0.0002
BASE	ATB	0.45	0.15	2.89	0.0040
BASE	DGAB	0.63	0.14	4.62	<.0001
BASE	LCB	0.93	0.92	1.02	0.3101
BASE	NONBIT	0.75	0.18	4.24	<.0001
BASE	NONE	−0.28	0.35	−0.79	0.4284
BASE	PATB	0	.	.	.
SG	COARSE	0.12	0.20	0.58	0.5618
SG	FINE	0.16	0.20	0.78	0.4346
SG		0	NA	NA	NA
EXP	G1	0.66	0.06	10.50	<.0001
EXP	G2	0.61	0.08	7.65	<.0001
EXP	G6	0.60	0.06	10.79	<.0001
EXP	S1	0.52	0.06	8.62	<.0001
EXP	S8	0	NA	NA	NA
lesn		0.77	0.13	5.84	<.0001
logrut_age		0.50	0.04	14.10	<.0001
CI		$3.4 * 10^{-4}$	$8.2 * 10^{-5}$	4.11	<.0001
FI		$1.5 * 10^{-4}$	$1.7 * 10^{-4}$	0.91	0.3649
PRECIP		$1.2 * 10^{-5}$	$6.4 * 10^{-5}$	0.19	0.8475
FTC		$3.5 * 10^{-3}$	$6.9 * 10^{-4}$	5.02	<.0001
FI*PRECIP		$3.0 * 10^{-7}$	$1.1 * 10^{-7}$	2.71	0.0068
lesn*logrut_age		$-8.4 * 10^{-2}$	$2.6 * 10^{-2}$	−3.25	0.0012
logrut_age*CI		$-1.4 * 10^{-4}$	$3.2 * 10^{-5}$	−4.44	<.0001
logrut_age*FI		$-1.4 * 10^{-5}$	$3.7 * 10^{-5}$	−0.38	0.7063
lesn*BASE	ATB	−0.44	0.16	−2.76	0.0059
lesn*BASE	DGAB	−0.54	0.14	−4.00	<.0001
lesn*BASE	LCB	−0.75	1.22	−0.61	0.5416
lesn*BASE	NONBIT	−0.66	0.15	−4.28	<.0001
lesn*BASE	NONE	0.36	0.42	0.86	0.3901
lesn*BASE	PATB	0	NA	NA	NA
FI*BASE	ATB	$-3.8 * 10^{-4}$	$1.5 * 10^{-4}$	−2.58	0.0099
FI*BASE	DGAB	$-4.2 * 10^{-4}$	$1.3 * 10^{-4}$	−3.20	0.0014
FI*BASE	LCB	$-5.2 * 10^{-3}$	$7.9 * 10^{-3}$	−0.66	0.5108
FI*BASE	NONBIT	$-1.3 * 10^{-3}$	$3.1 * 10^{-4}$	−4.35	<.0001
FI*BASE	NONE	$-4.3 * 10^{-4}$	$2.1 * 10^{-4}$	−2.07	0.0382
FI*BASE	PATB	0	NA	NA	NA

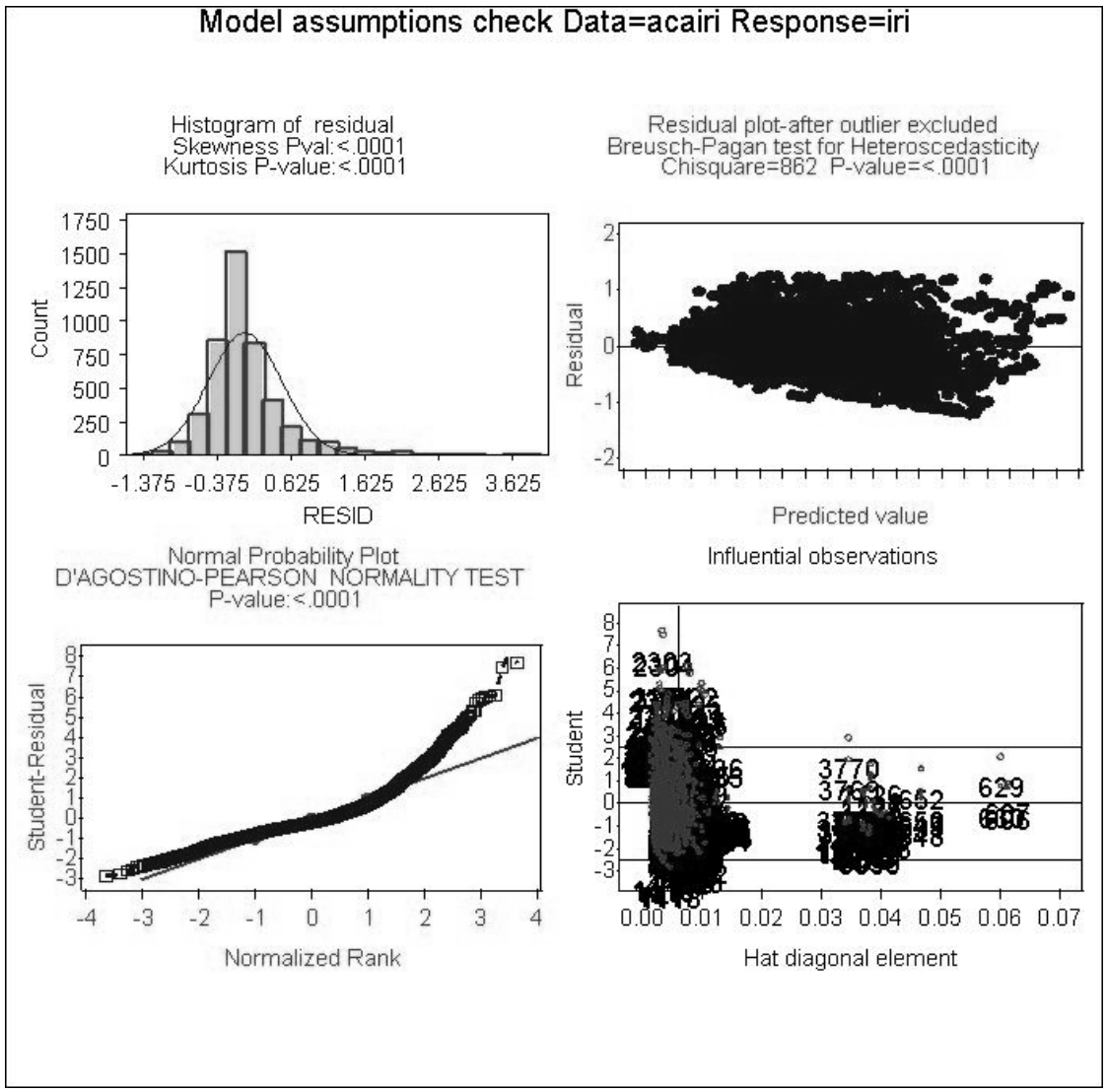

Figure 5. Graphs. Assumption validity check for absolute IRI model (before transformation).

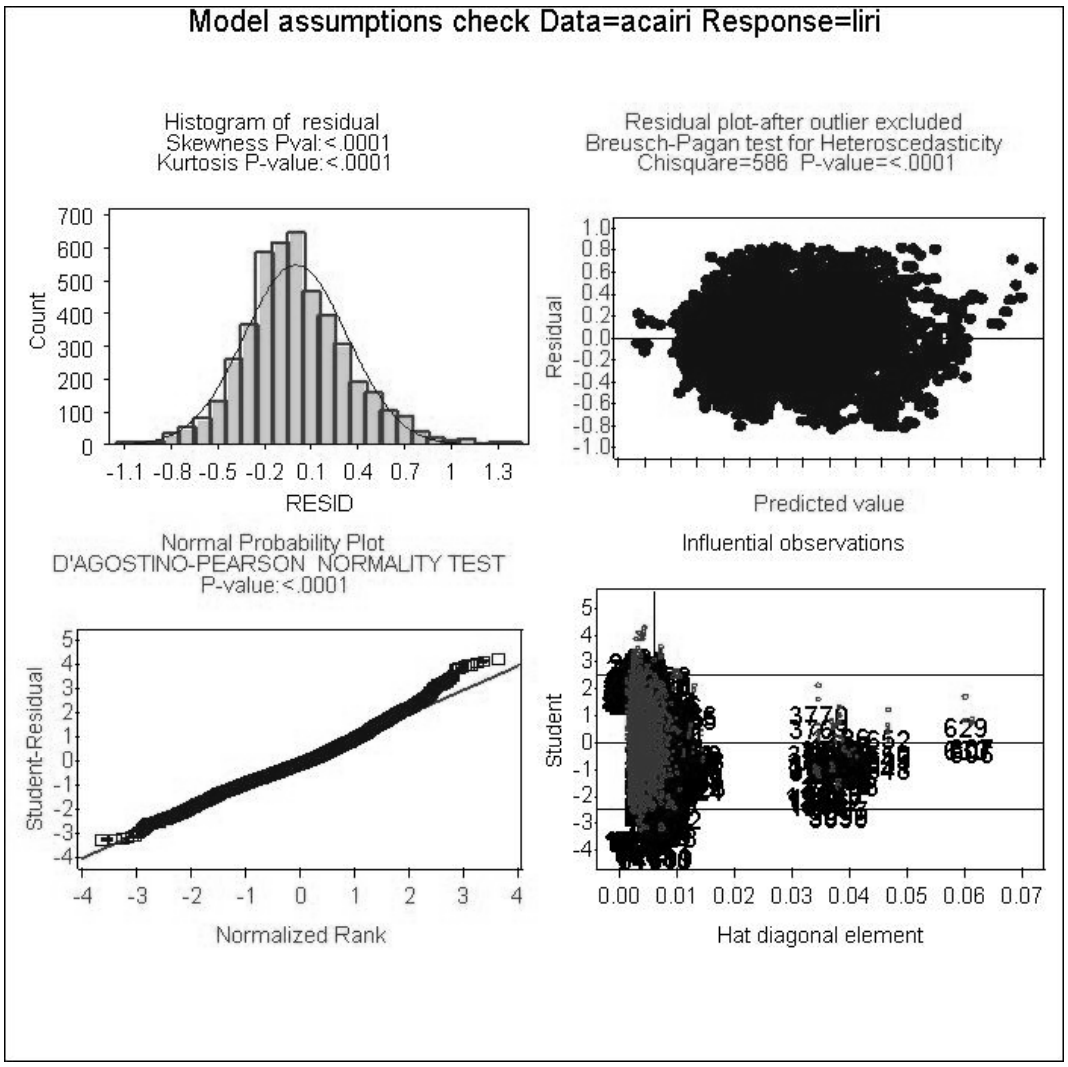

Figure 6. Graphs. Assumption validity check for absolute IRI model (after natural logarithm transformation of the performance measure).

5. PERFORMANCE MODEL DEVELOPMENT AND SELECTION

As described in the previous section, simple statistical tools such as maximum, minimum, average, and standard deviation were reviewed to identify data acquisition errors or problems with the calculations performed. Box plots, frequency graphs, and residual plots were also created to develop an understanding of the datasets and to study interaction, correlation, and the type of distribution present in the data. These tools were also used to verify whether the nature of the data violate any statistical assumptions made during the analysis. As part of this initial statistical review, the dataset was also inspected to identify and remove data collected after unrecorded pavement improvements were performed. Criteria were developed for each performance measure and applied to the dataset to flag instances of significant reductions in deterioration. Table 18 summarizes the checks used in this process.

Table 18. Criteria to warrant additional investigation of unrecorded pavement improvements.

Pavement Type	Performance Measure	Reduction Criteria that Warrant Investigation
AC	IRI	>0.4 m/km (25.4 inches/mi) reduction
AC	DISTRESS	>30% reduction in sum of key distress types[a]
AC	RUTDEPTH	>10 mm (0.4 inch) reduction
PCC	IRI	>0.4 m/km (25.4 inches/mi) reduction
PCC	DISTRESS	>30% reduction in sum of key distress types[b]
PCC	FAULTING	>2 mm (0.08 inch) reduction

[a]Deduct values of fatigue cracking, block cracking, longitudinal wheelpath cracking, longitudinal nonwheelpath cracking, transverse cracking, and patching were summed for this evaluation.
[b]Normalized quantities of corner breaks, longitudinal cracking, transverse cracking, and patching were summed for this evaluation.

Each test section flagged was thoroughly examined using all performance measures to determine if the reduction was most likely caused by an improvement to the pavement or if it could be attributed to data variability. In general, if the majority of the performance measures demonstrated a reduction in deterioration, it was concluded that an unreported pavement improvement was applied. Data collected after the improvement were removed from the dataset.

Due to the subjective nature of distress data, additional quality reviews were performed on the data to remove records where a reduction was observed in one of the distress types as a result of rater variability. For example, distress data collected at test section 181037 at pavement age equal to 10.2 years recorded a BC deduct value of 74.3 (and 0 values for TC and FWPC). The next distress survey (11.4 years) recorded a decreased BC value of 33.2; however, the values of TC and FWPC increased significantly (values of 68 and 7.5, respectively). The first surveyor rated the distress as BC while the second rater opted to rate a series of longitudinal and transverse cracks. As such, the BC data recorded at 11.4 years were removed from the dataset.

Test sections with known construction issues were also removed from the dataset. One such example is the Nevada SPS-2 project that experienced excessive cracking just after construction. These types of issues could not be accounted for in the models, and they would simply add variability to the analysis.

Upon completion of the review, work began on developing regression models. Two regression methods were considered for use in the study: the general linear model (GLM) and the robust regression model. The GLM is susceptible to extreme outlying cases that cannot be definitively determined as erroneous data. Because this project incorporates national data with many contributing factors, extreme cases do exist that cannot be established as errors, and they need to be accounted for in the model. The robust regression techniques dampen the effect of these extreme cases by applying a weighting factor based on residuals. The robust model is used to make adjustments to the GLM and validate the model using an iterative process.

Figure 7 is a plot of student residuals as a function of Hat values,[15] which is a graphical tool to evaluate observations in a dataset. The student residual is the ratio of a residual to its standard error. Large absolute values of the student residual (larger than 2.5) are an indication of outliers in the data. The Hat diagonal refers to the diagonal elements of the Hat matrix in the least squares estimation,[16] and it quantifies the leverage of each observation on the predicted value for that observation. The cluster of points located further to the right in figure 7 is a group of influential observations.

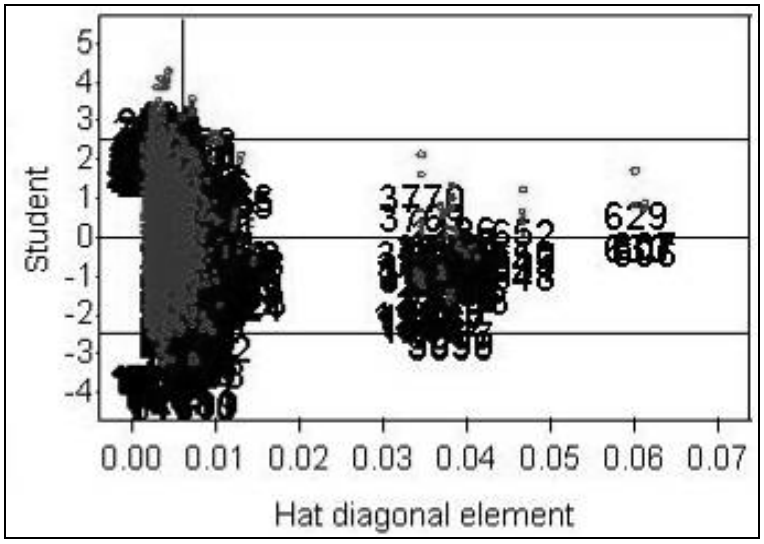

Figure 7. Scatter plot. Outlier-influential observation detection plot.

The robust method should be used if these influential observations are truly outliers or questionable data points that would negatively affect the model. On the other hand, these cases could be treated as any other with their full effect incorporated into the model (the GLM method) if they are valid data points that represent extreme conditions.

To determine which method is more appropriate and will produce the most representative model, the nature of the dataset, as well as the number of quality control checks performed on the data, must be considered. If extreme cases are expected (given the

design of the experiment) and a rigorous quality review has been performed on the data, it is highly probable that the remaining influential observations are valid, and reducing their impact on the model would bias the model's prediction capability.

For this study, data come from a national database in which some of the variables may be set to extreme limits resulting in extreme performance observations. On a small scale, the SPS-1 projects can be used to illustrate this. Each of the 12 test sections at an SPS-1 project has a different structural capacity, but all experience the same traffic loading. By experimental design, certain variables (in the case of SPS-1 projects, the ratio of traffic loading to structural capacity) would be set to the extreme ends of the spectrum. As such, extreme observations are to be expected in the dataset, and they are necessary to generate a model that reflects observed performance.

In addition, the analysis team performed considerable logical quality review on the data to identify and remove data that were believed to be erroneous. The data have also undergone the quality control process used by the LTPP team before releasing the data for public use. It is unlikely that the remaining influential observations are erroneous or unrepresentative of the dataset.

To further compare the two methodologies, two models were developed for absolute IRI of asphalt pavements. One model was developed using the robust method while the other used the GLM procedure. The predicted IRI values from the robust and GLM models versus the observed IRI values can be found in figures 8 and 9, respectively. The GLM method produces a model that has less bias than the robust model. In figure 8, the majority of the data points are clustered below the line of equality (circled in the figure). The cluster of the GLM model is more centered on the equality line compared with the robust model. This indicates that the robust method of reducing the effect of extreme observations results in a model that generally predicts values less than the observed values.

Considering the nature of the dataset, the level of quality reviews performed on the data, and the results from the previous comparison, the GLM method was chosen to develop regression models for this study.

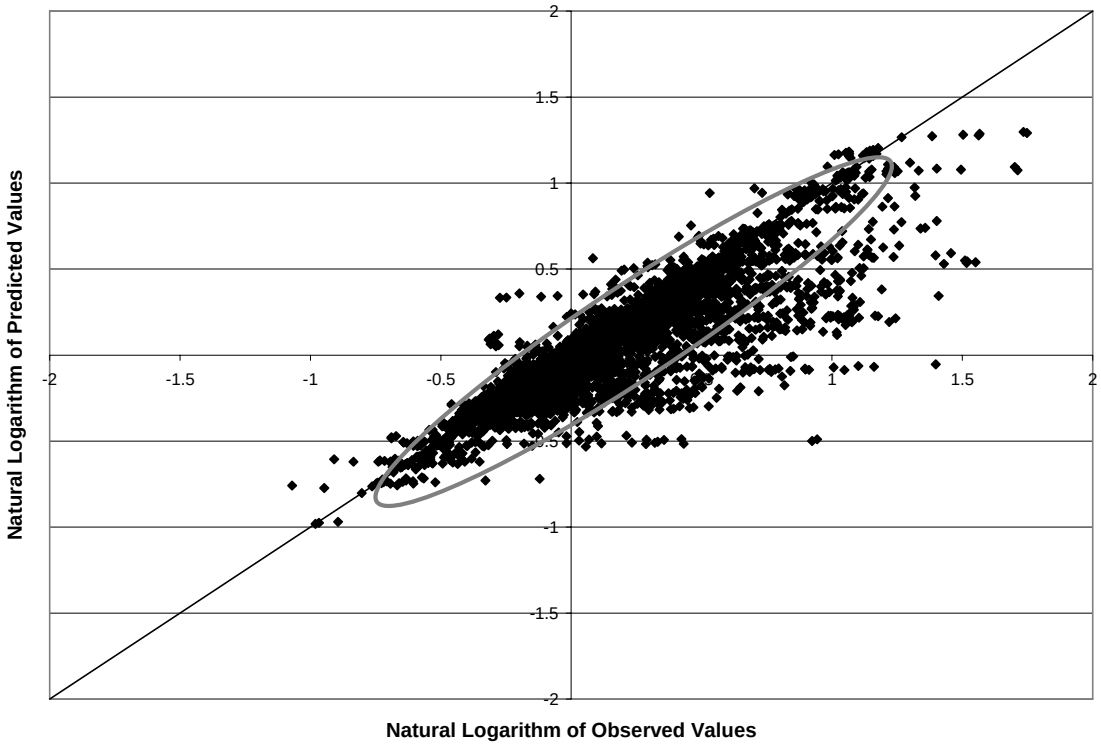

Figure 8. Scatter plot. Observed versus predicted values of absolute IRI (shifted) using the robust method.

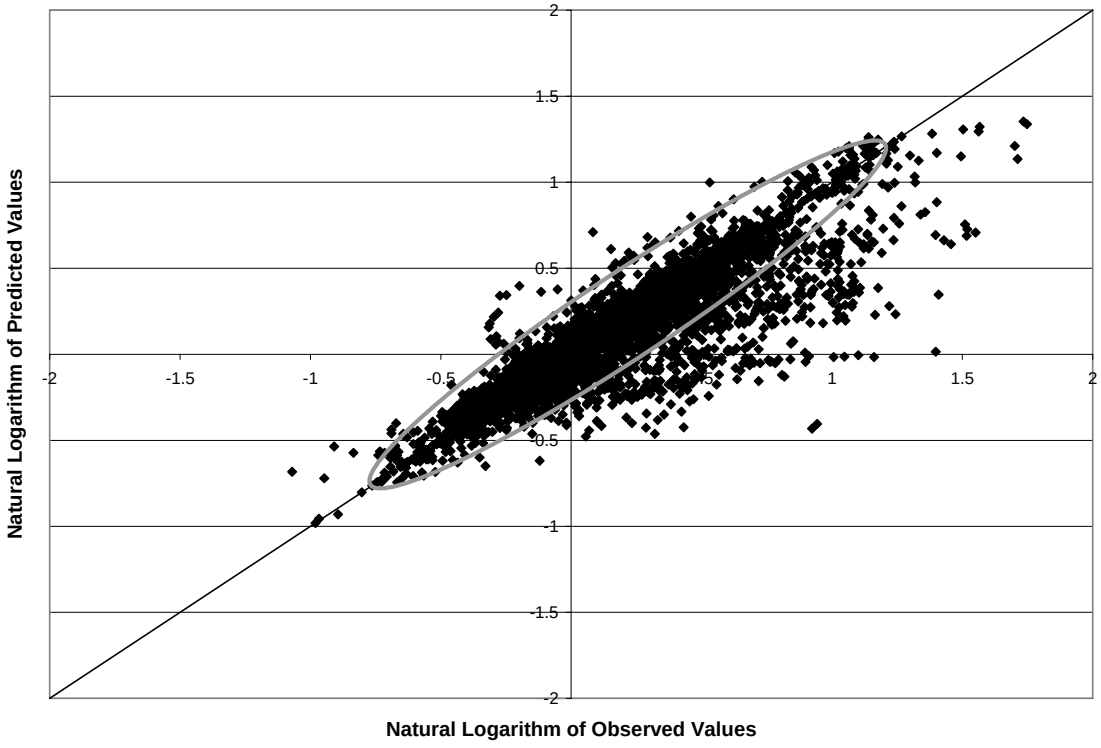

Figure 9. Scatter plot. Observed versus predicted values of absolute IRI (shifted) using the GLM method.

PAVEMENT ROUGHNESS PREDICTION MODELS

It is well known that postconstruction roughness varies from one project to the next because of differences such as construction techniques and specifications. These differences also significantly affect the progression of roughness over time, and could add variability to the model. To counter this, the analysis team investigated models to predict change in IRI as the performance measure. As described previously, change in IRI was calculated by subtracting the first LTPP measurement from each of the subsequent measurements. Through this process, it was believed that the postconstruction differences were inherent to the initial IRI measurement and would be removed from the subsequent measurements.

The resultant models, however, did not provide a good correlation with the observed dataset. The lack of fit can be partially contributed to the differences in age at which the first LTPP measurement was taken. For example, the first IRI measurement at test section 086002 was taken at an age of 21.3 years while the initial measurement at test section 100101 was taken at 1.1 years. The reference measurement used to calculate change in IRI for subsequent measurements was captured at different ages as well as at locations on the deterioration curve which was not accounted for in the model.

Based on the observations made using the change in IRI, a decision was made to develop regression models using absolute IRI. To account for the postconstruction differences in roughness, initial IRI and the age of initial IRI measurement were incorporated as explanatory variables in the model. The models for this performance measure provided a better correlation than the change in IRI measure. Figure 10 provides a graph of actual values measured at test section 307066 along with values predicted by the model. As can be seen in the graph, the model is predicting the accumulation of roughness with time fairly accurately (indicated by equivalent slopes), but the model is offset from the actual measurements. Although only one example is shown, this offset was observed in many cases and varied for each test section. These differences can be reduced or eliminated by shifting the model to predict the initial IRI at the corresponding age of initial IRI measurement. The shifted model for test section 307066 can be found in figure 11.

To further evaluate the prediction capability of the model, two scatter plots were generated using the flexible dataset. A scatter plot for the regression model (without shifting) is shown in figure 12, while the scatter plot for the shifted regression model is shown in figure 13. As can be seen from the figures, shifting the predicted values based on the initial IRI value results in an improvement in the model's accuracy.

Furthermore, the root mean squared error (RMSE) for the regression model (without shifting) was 0.18, while the shifted model exhibited a RMSE value of 0.17. RMSE is used to make relative comparisons on the "goodness of fit" between two models predicting the same performance measure (from the same dataset). Lower RMSE values are indicative of a model that represents the observed values better.

In consideration of the reasons discussed, it was determined that the shifted model provided a better representation of the observed values in the dataset, and therefore, the

shifting methodology was used to predict pavement roughness over time for flexible pavements.

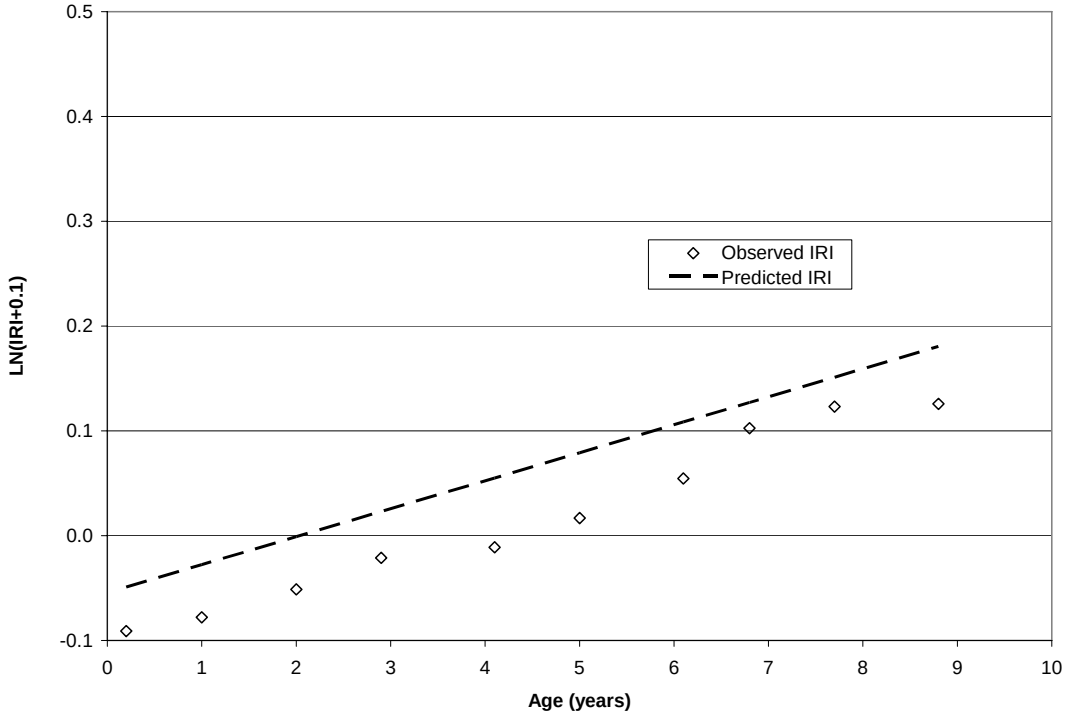

Figure 10. Graph. Example of predicted (without shifting) and observed values for test section 307066.

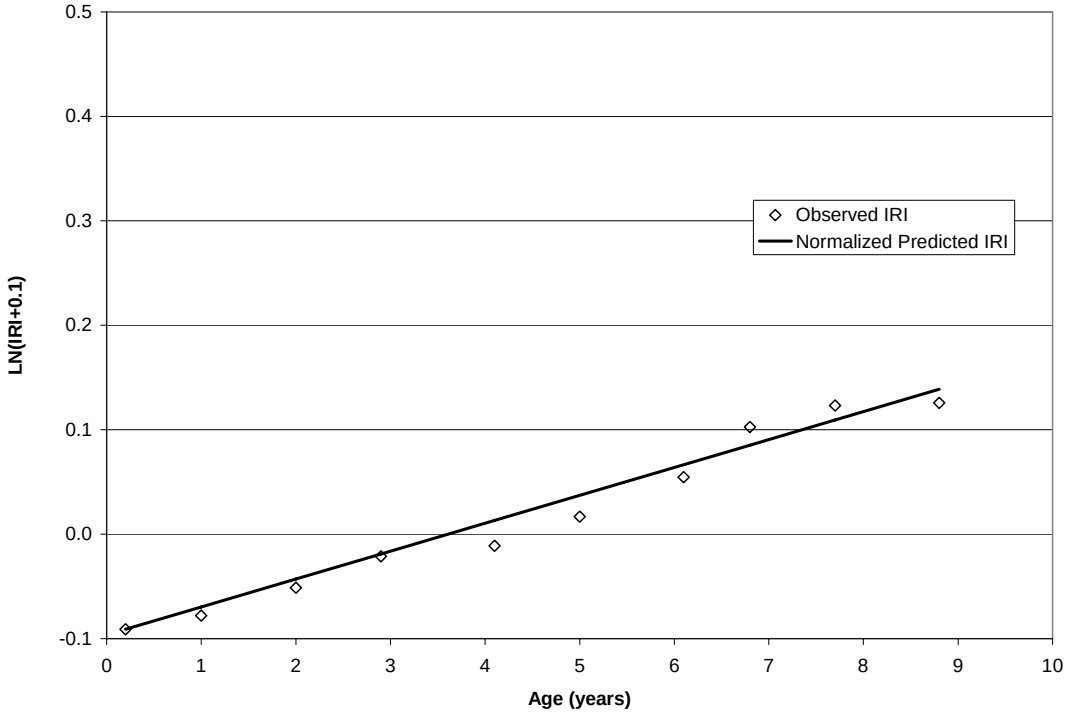

Figure 11. Graph. Example of predicted (shifted) and observed values for test section 307066.

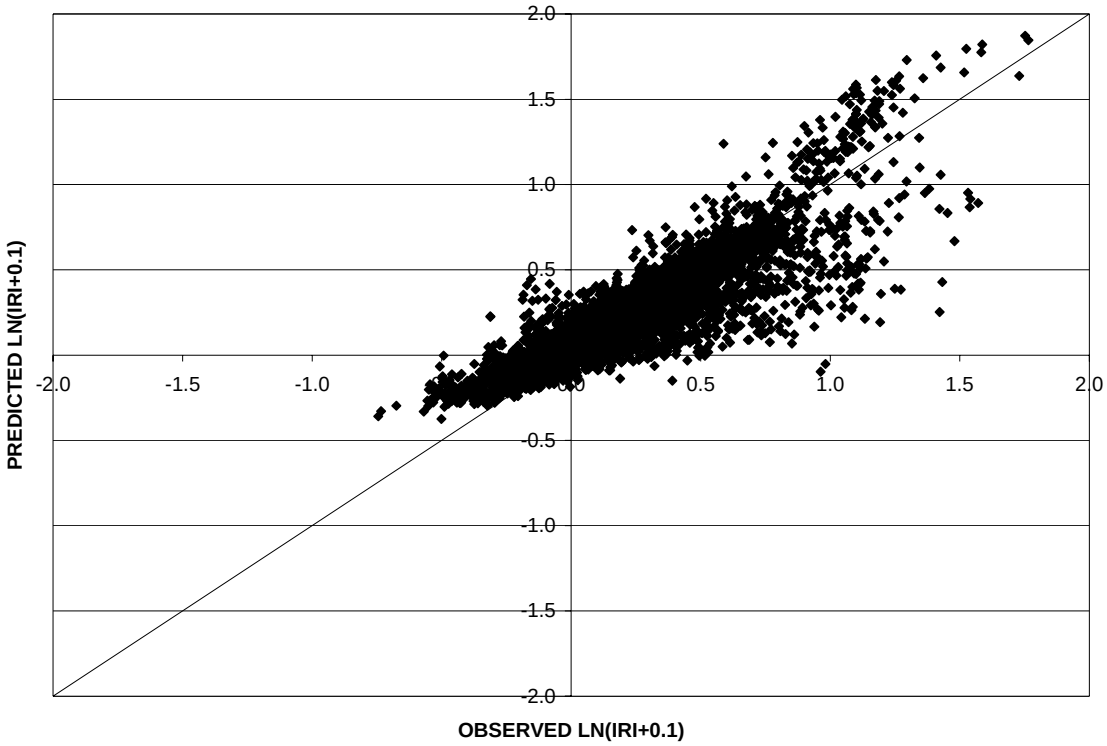

Figure 12. Scatter plot. Flexible IRI model without shifting.

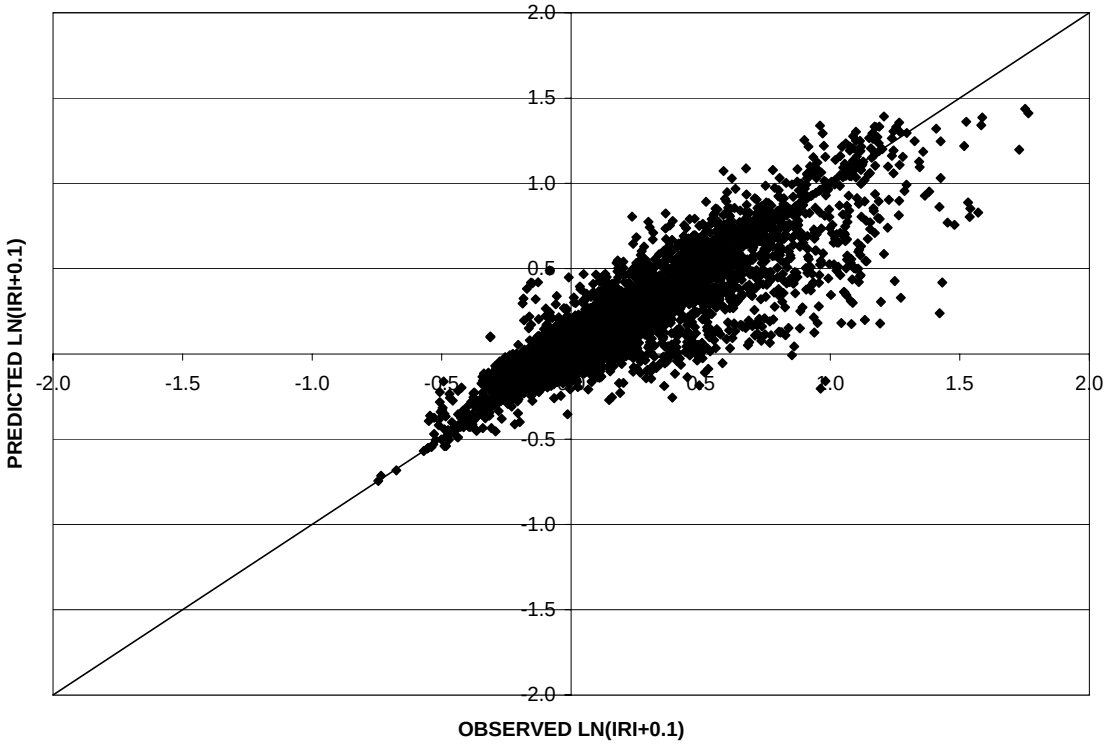

Figure 13. Scatter plot. Flexible IRI model (shifted).

The same exercise was performed for rigid pavement roughness to determine if shifting the model made an improvement on its prediction capability. Figures 14 and 15 provide scatter plots for the model (without shifting) and the shifted model, respectively. In this case, the model (without shifting) resulted in a lower RMSE value (0.14) than the shifted model (RMSE equal to 0.15). Therefore, comparisons on rigid pavements were made using the model that was not shifted.

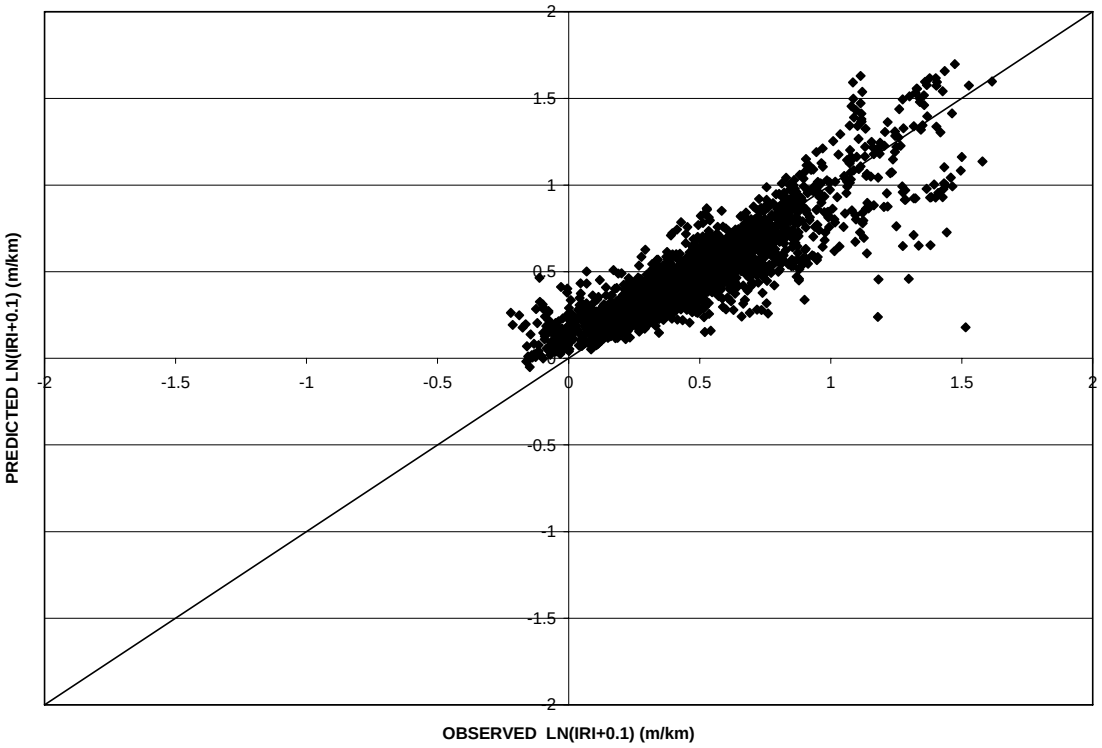

1 m/km = 5.28 ft/mi

Figure 14. Scatter plot. Rigid IRI model without shifting.

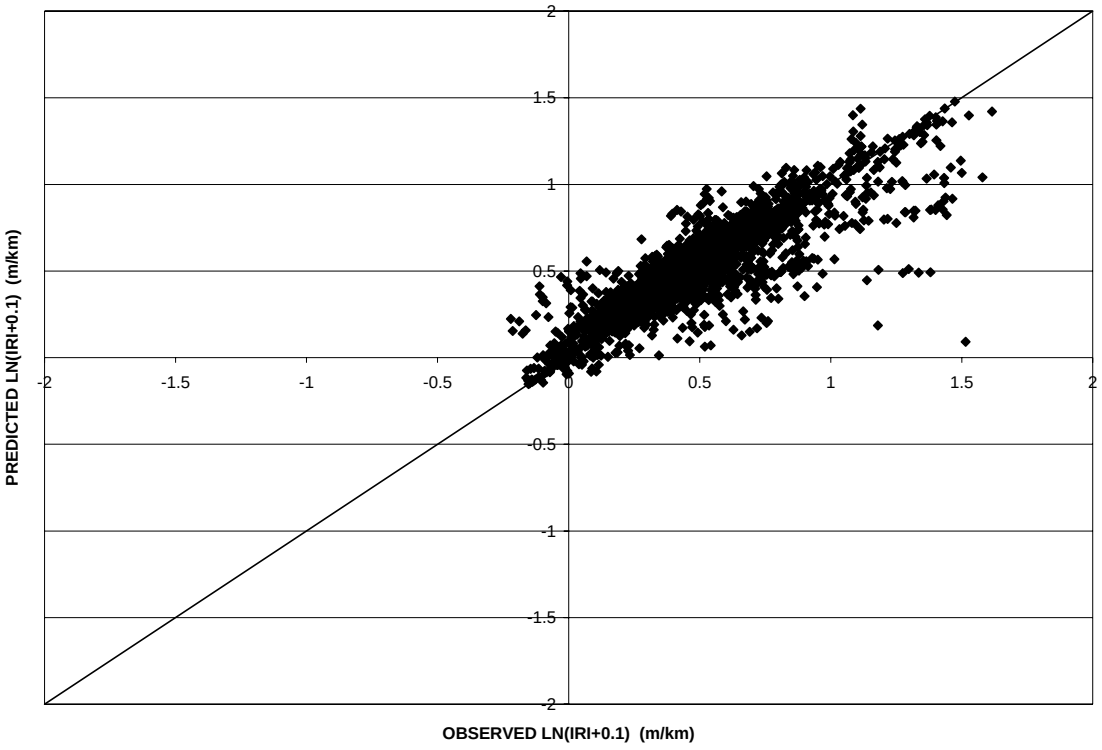

1 m/km = 5.28 ft/mi

Figure 15. Scatter plot. Rigid IRI model (shifted).

Different relationships between the performance measure, IRI, and pavement age were evaluated to ensure the model with the best prediction capability was selected for use in the environmental comparisons. Two models using different IRI-pavement age relationships were generated. The first model used a linear relationship between IRI and pavement age. Figure 16 provides a scatter plot of the predicted IRI values (shifted) versus the observed IRI values in the flexible dataset. An additional model was generated using an exponential relationship between IRI and pavement age. It is shown in figure 17 for the flexible dataset.

Using a linear relationship between IRI and age results in a model that is less biased than the exponential relationship. This is evident when comparing figures 16 and 17. In figure 16 the cluster of data points is more centered on the equality line as compared with figure 17 where the majority of the cluster falls below the line. This indicates a model that is generally predicting values less than the observed values. Further, the RMSE value for the linear model was considerably lower (0.17) than the exponential model (0.33). It is also interesting to note that the exponential model does not predict an increase in the IRI over time (as can be seen in figure 18). For these reasons, the linear relationship model was selected for consideration in the environmental comparisons. A scatter plot of predicted (shifted) versus observed values using the linear age relationship for the rigid dataset appears in figure 19.

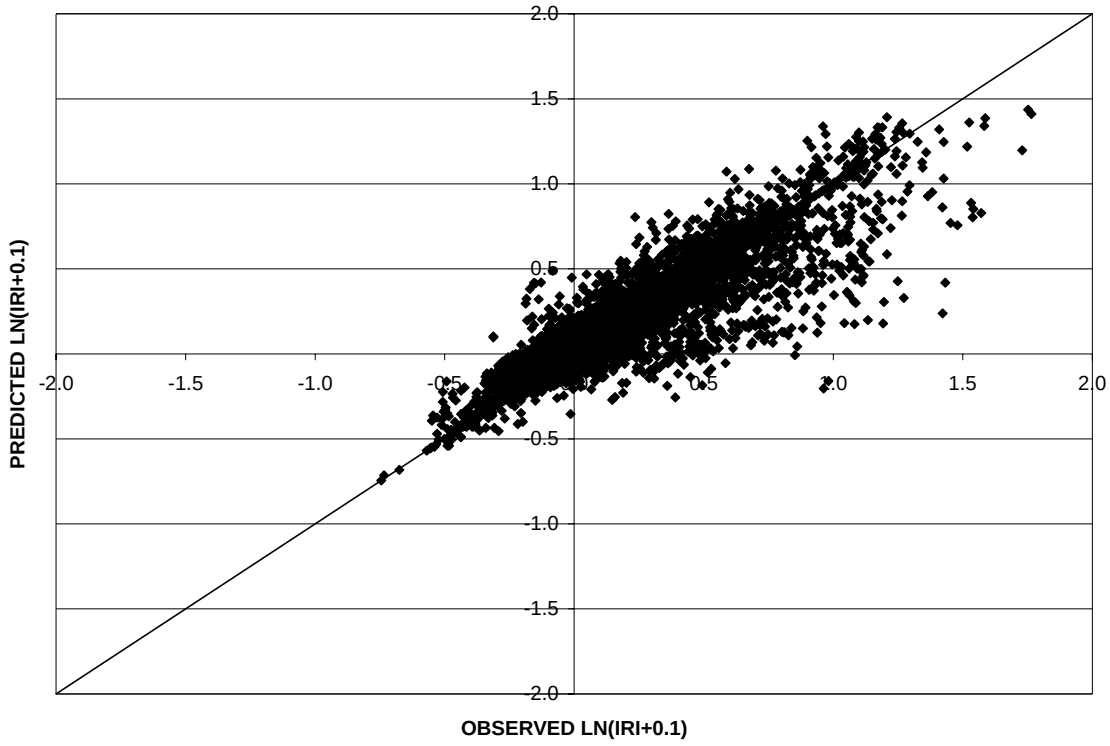

Figure 16. Scatter plot. Flexible IRI model with linear IRI-age relationship.

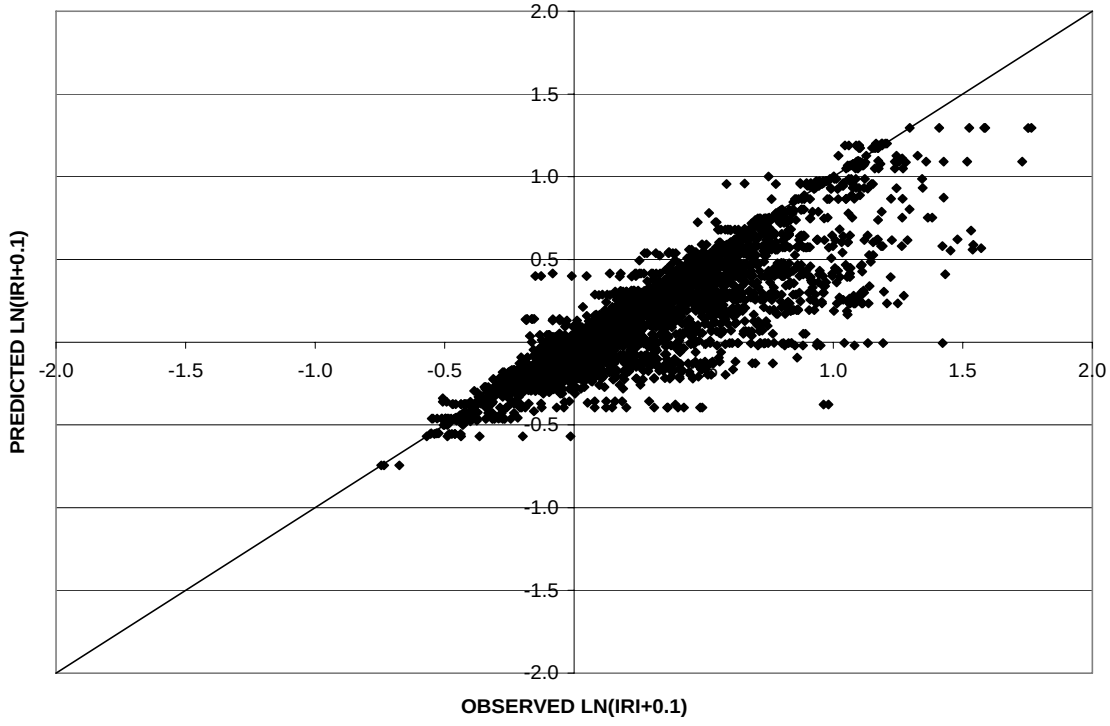

Figure 17. Scatter plot. Flexible IRI model with IRI-exponential age relationship.

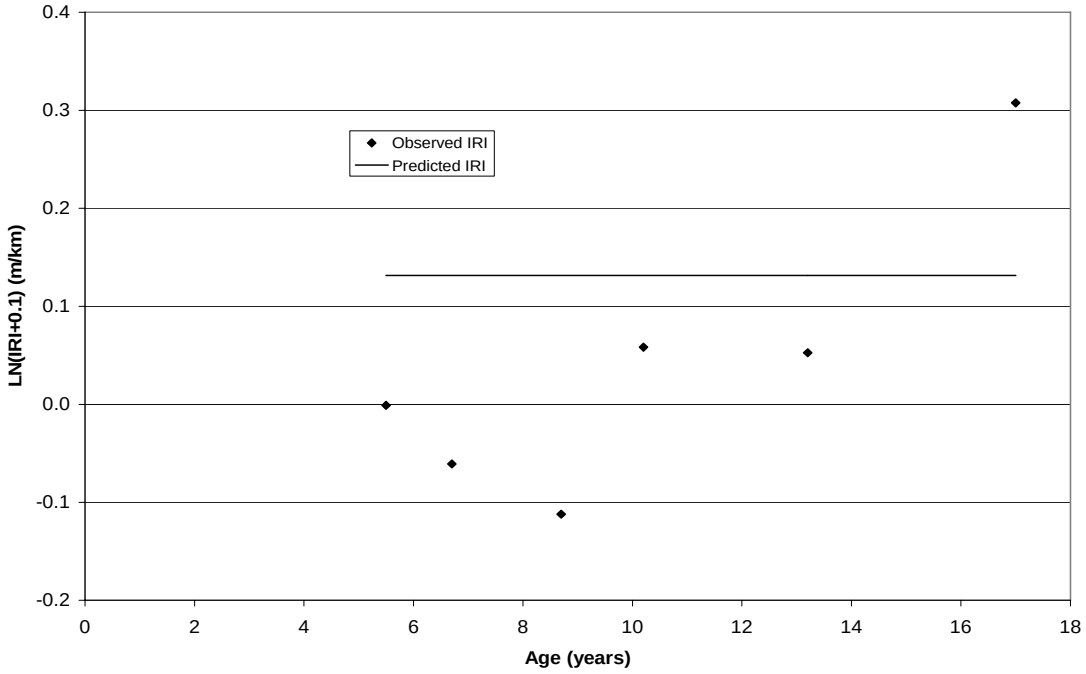

1 m/km = 5.28 ft/mi

Figure 18. Scatter plot. Actual and predicted IRI values for test section 011001 using IRI-exponential age relationship model.

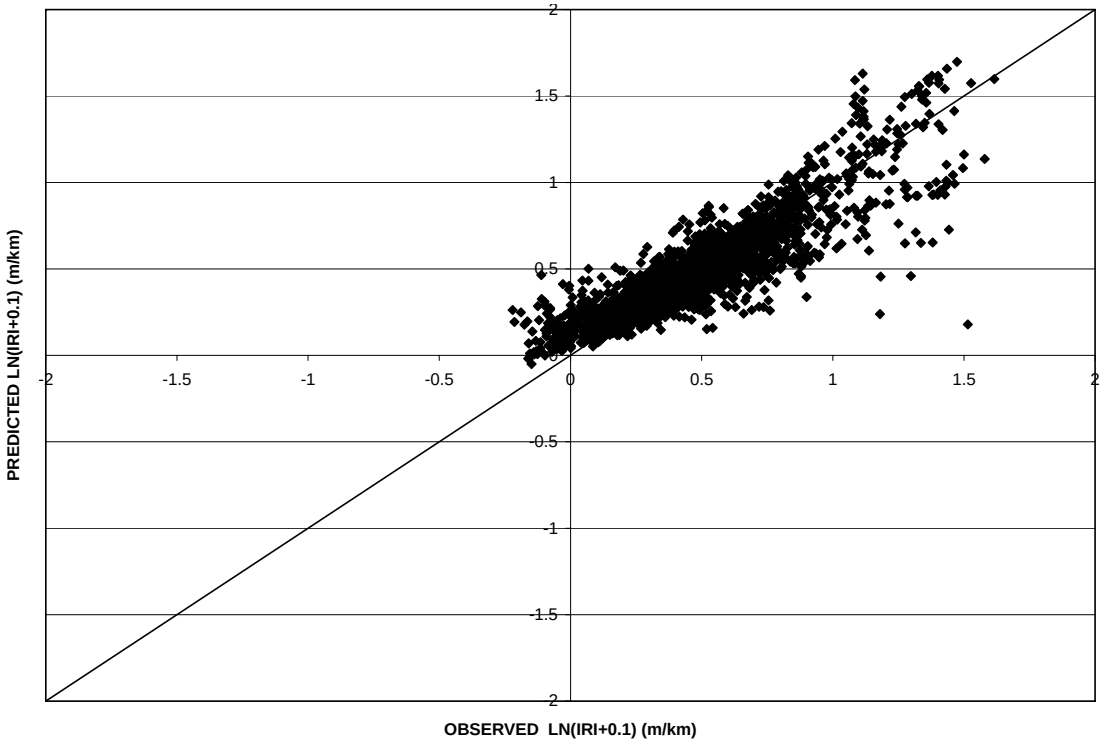

1 m/km = 5.28 ft/mi

Figure 19. Scatter Plot. Rigid IRI model with linear IRI-age relationship.

Equations representing the selected IRI models for both flexible and rigid pavements can be found in appendix B. The R-squared value for the flexible pavement IRI model (shifted) using the linear relationship between age and IRI is approximately 0.78 (P-value < 0.0001). The rigid pavement IRI model exhibited an R-squared of 0.78 (P-value < 0.0001).

RUTTING PREDICTION MODELS FOR FLEXIBLE PAVEMENTS

Two models were considered in the prediction of rut depth in flexible pavements. The first model incorporated a linear relationship between rut depth and pavement age. A scatter plot of predicted versus observed rut depth values for this model is shown in figure 20. It resulted in a RMSE value of 0.59. The second model under consideration for use in predicting rut depth incorporated a natural logarithm relationship between rut depth and pavement age. The scatter plot of predicted versus observed values can be found in figure 21 corresponding to an RMSE value of 0.55.

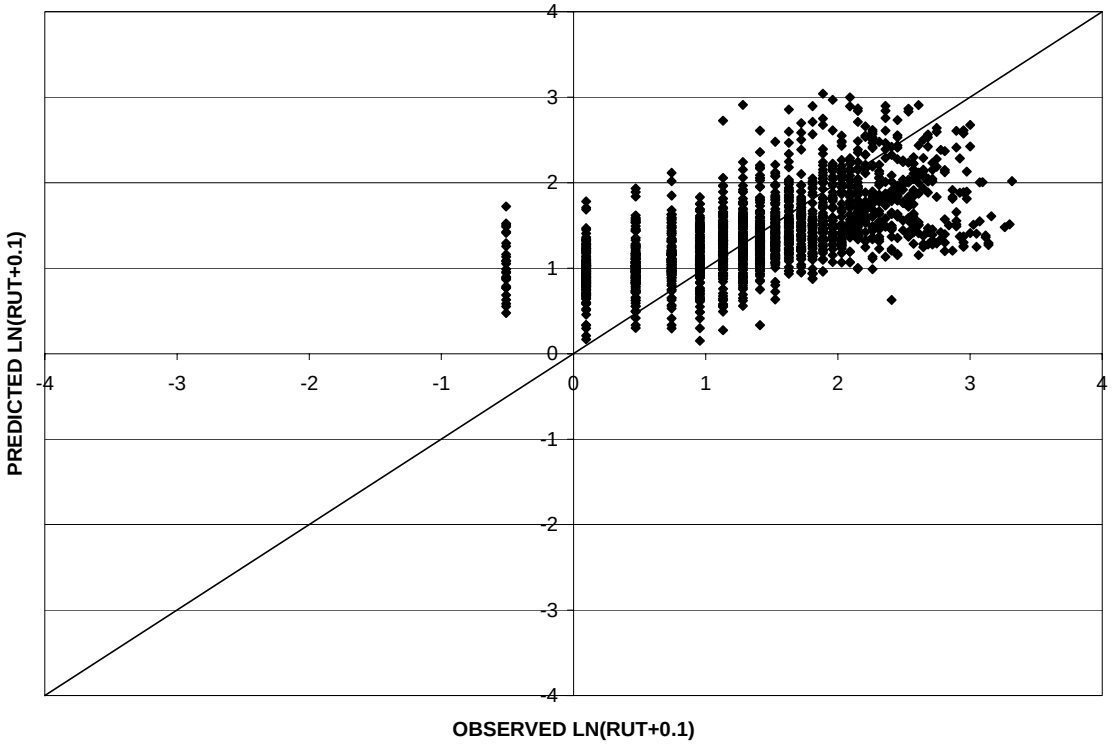

Figure 20. Scatter plot. Rut depth model with linear rut–age relationship.

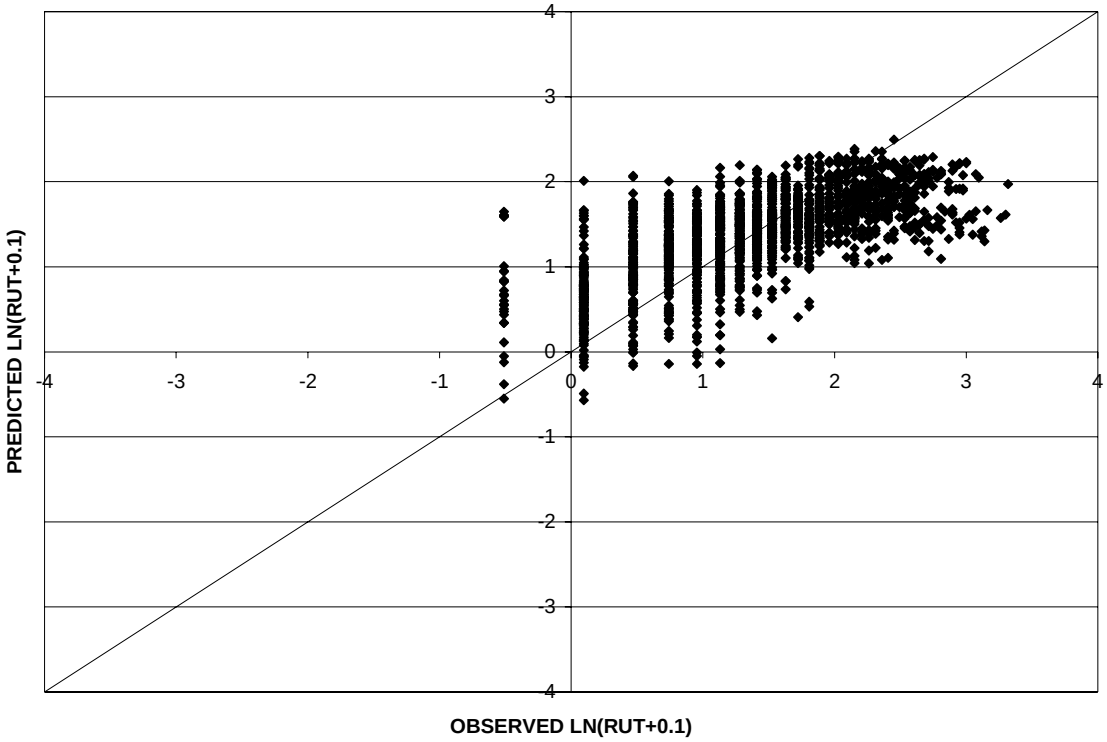

Figure 21. Scatter plot. Rut depth model with rut–natural logarithm age relationship.

The second model was selected for use in comparing rut depth performance of pavement in different environmental regions because of the improved fit of the dataset. Rutting mechanisms generally result in an increased rate of rutting in the early years of pavement life. As the pavement ages, this rate diminishes and rutting values level off (following a logarithmic relationship). Applying the logarithmic relationship in the model provides a better representation of the dataset, which is evident in the improved RMSE value. Details on this model can be found in appendix B. The adjusted R-squared value for this model was approximately 0.45 (P-value < 0.0001).

SURFACE DISTRESS PREDICTION MODELS FOR BOTH FLEXIBLE AND RIGID PAVEMENTS

To develop the flexible dataset for distress measures, all three severity levels for each distress type were combined through the use of deduct curves developed for the South Dakota Department of Transportation[10] to obtain a deduct value for each distress. The study considered FC, BC, LWP, and TC. Because LWP often progresses to FC, the two distress types were combined into FWPC). LWP was converted from a linear unit to a unit of area to be consistent with FC. This was done by applying a standard width of 0.3 m (1 ft) to the recorded length of LWP. All severities of LWP were considered as low severity to compute deduct values that would be combined with the FC.

The format of distress data collected on rigid pavements does not match the required format used in the established deduct curves;[8] therefore, the severity levels were summed for each distress type. This total distress was then normalized based on the size

of the test section in the same manner as the flexible sections. CB, LC, TC, and PUMP distress types were used in the rigid dataset.

Figure 22 provides a scatter plot of FWPC as a function of pavement age. As can be seen from the figure, there is a large amount of variability in the data, and numerous zeroes are recorded across the entire range of ages. For these reasons, regression models alone did not provide a good correlation with the measured values.

A small subset of the measured FWPC values was plotted (figure 23). Each series in the figure represents data from one test section. It appears that a substantial portion of the variability in the data can be attributed to the differences in age at which distress initiates. For example, distress initiation occurs just after construction at two of the sections, while another section does not initiate distress until age 17. There does appear to be a reasonable trend in the accumulation of distress with age after the initiation of distress.

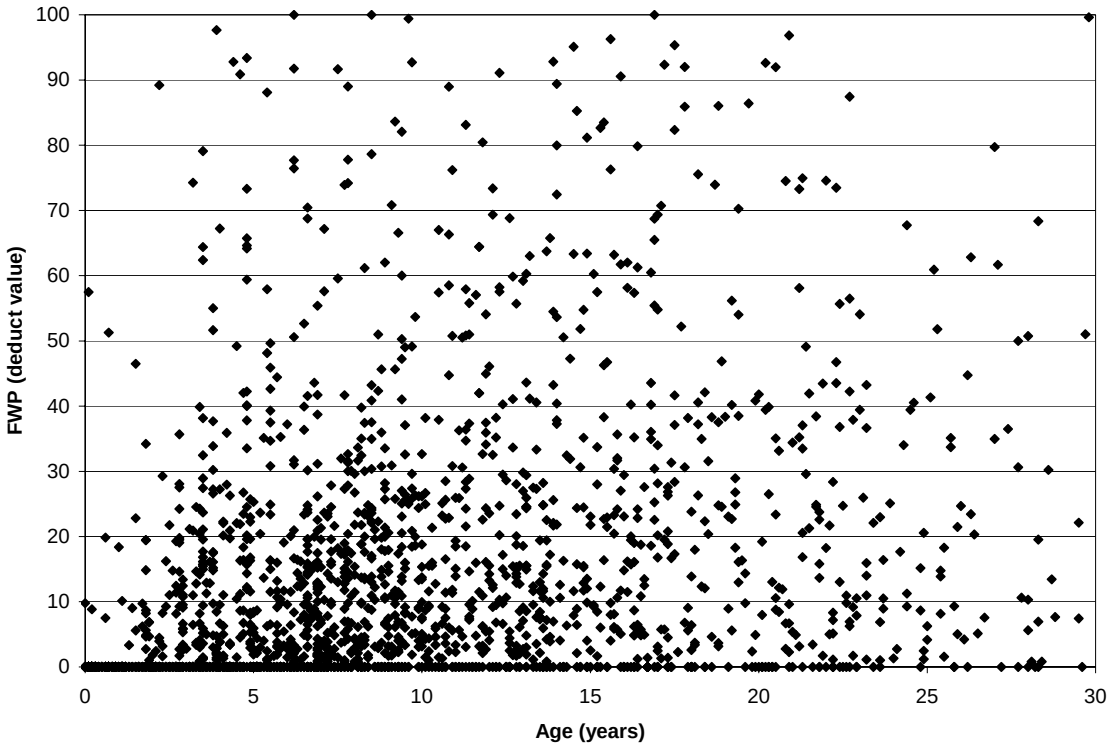

Figure 22. Scatter plot. Measured FWPC deduct values.

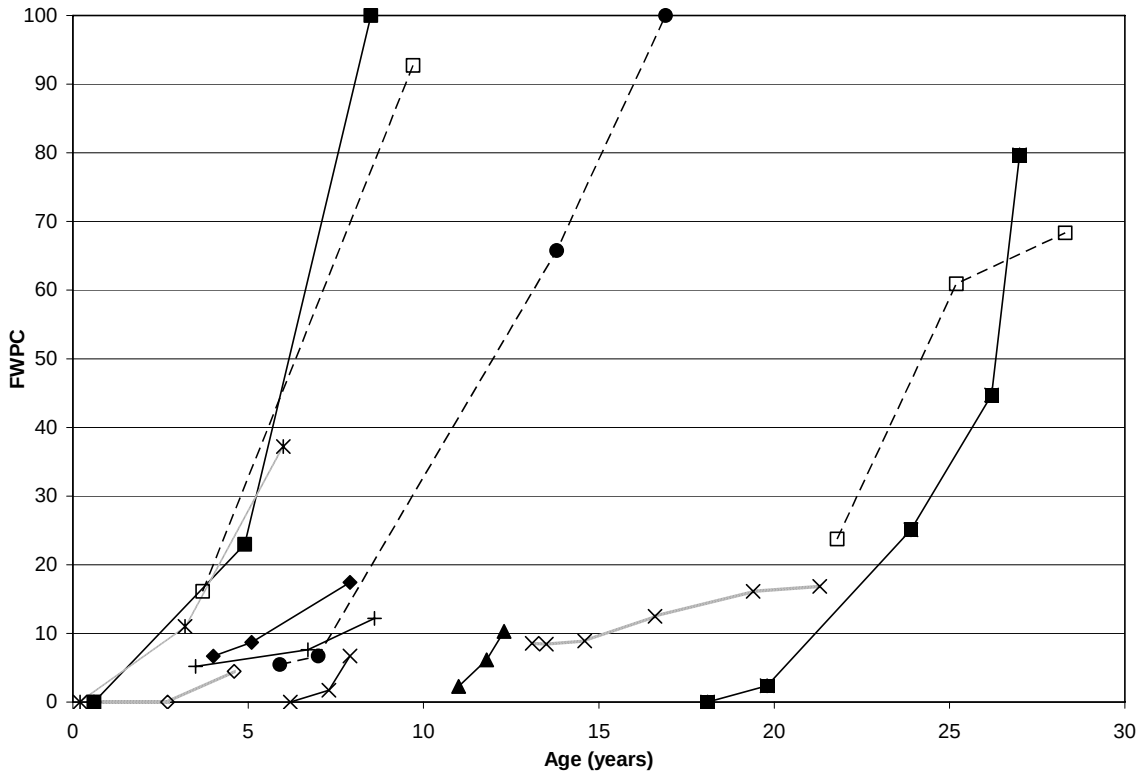

Figure 23. Graph plot. Measured FWPC values (using a subset of test sections).

Given the nature and form of the distress accumulation with age, two models were used concurrently to predict distress progression. The first model was used to predict the age at which distress initiation occurs, while the second estimated the accumulation of distress with age (after initiation).

The first model was developed using logistic analysis to predict age at which distress first appears. Logistical models predict the probability of an event occurring (e.g., distress initiation or nonzero distress value) given a set of variables including pavement age. Figure 24 shows an example of a logistic model. A cutoff probability must be established to predict an initiation age from the given model. As the cutoff probability increases, the accuracy of the model predicting events goes down, while the accuracy of predicting nonevents goes up; therefore, the selection of the cutoff probability depends on the nature of the data and the relative importance of events compared to nonevents. In the case of distress prediction, events and nonevents are of equal importance, so a cutoff value was selected that predicted each with equal accuracy. To determine the initiation age, all inputs for the logistic model are held constant (for a particular pavement section) except for pavement age, which is increased until the predicted probability is equivalent to the selected cutoff probability. This pavement age is defined as the initiation age. Table 19 is provided as an example illustrating the effect of the probability level on the accuracy of the model. The sensitivity denotes the percentage of events correctly identified, while the specificity reflects the nonevent accuracy. As the probability increases, the sensitivity decreases and the specificity increases. These two measures are approximately equal at the 0.7 probability level indicating events and nonevents, and are predicted with equal accuracy; therefore, 0.7 was established as the cutoff probability.

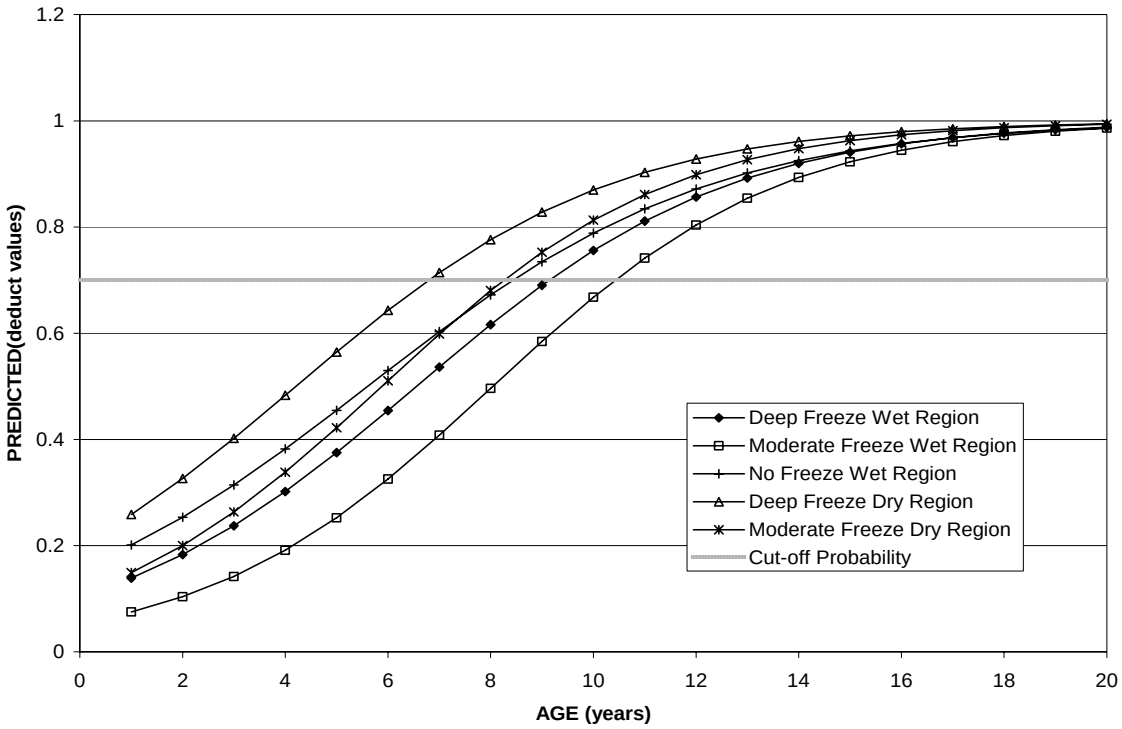

Figure 24. Graph plot. Example of logistical analysis to predict distress initiation.

Table 19. Example of probability level effect on logistic prediction.

Probability Level	Correct		Incorrect		Percentages				
	Event	Non-Event	Event	Non-Event	Correct	Sensitivity	Specificity	False POS	False NEG
0.1	1370	1	606	0	69.3	100.0	0.2	30.7	0.0
0.2	1365	60	547	5	72.1	99.6	9.9	28.6	7.7
0.3	1357	179	428	13	77.7	99.1	29.5	24.0	6.8
0.4	1326	272	335	44	80.8	96.8	44.8	20.2	13.9
0.5	1232	361	246	138	80.6	89.9	59.5	16.6	27.7
0.6	1128	429	178	242	78.8	82.3	70.7	13.6	36.1
0.7	955	480	127	415	72.6	69.7	79.1	11.7	46.4
0.8	753	517	90	617	64.2	55.0	85.2	10.7	54.4
0.9	511	556	51	859	54.0	37.3	91.6	9.1	60.7
1.0	0	607	0	1370	30.7	0.0	100.0	NA	69.3

After the crack initiation age is predicted, linear regression models were used to predict the accumulation of distress with age (after initiation). The example in figure 24 indicates that the distress initiation ranges from approximately 7 years to more than10 years for the different environmental regions.

The pavement age variable in the dataset had to be adjusted to reflect age after distress initiation to develop the regression models used to predict surface distress. Two methodologies were used to adjust pavement age depending on the timing of distress initiation relative to the pavement monitoring period.

Some of the test sections were monitored both before and after crack initiation. For these cases, crack initiation was directly determined as the maximum pavement age where a zero distress value was observed. This crack initiation age was then used to adjust the remaining pavement ages to ages after distress initiation. An example of one such test section is presented in figure 25. The crack initiation age was determined to be 2.4 years. The remaining ages were then adjusted by subtracting 2.4 years from the pavement age to obtain age after initiation.

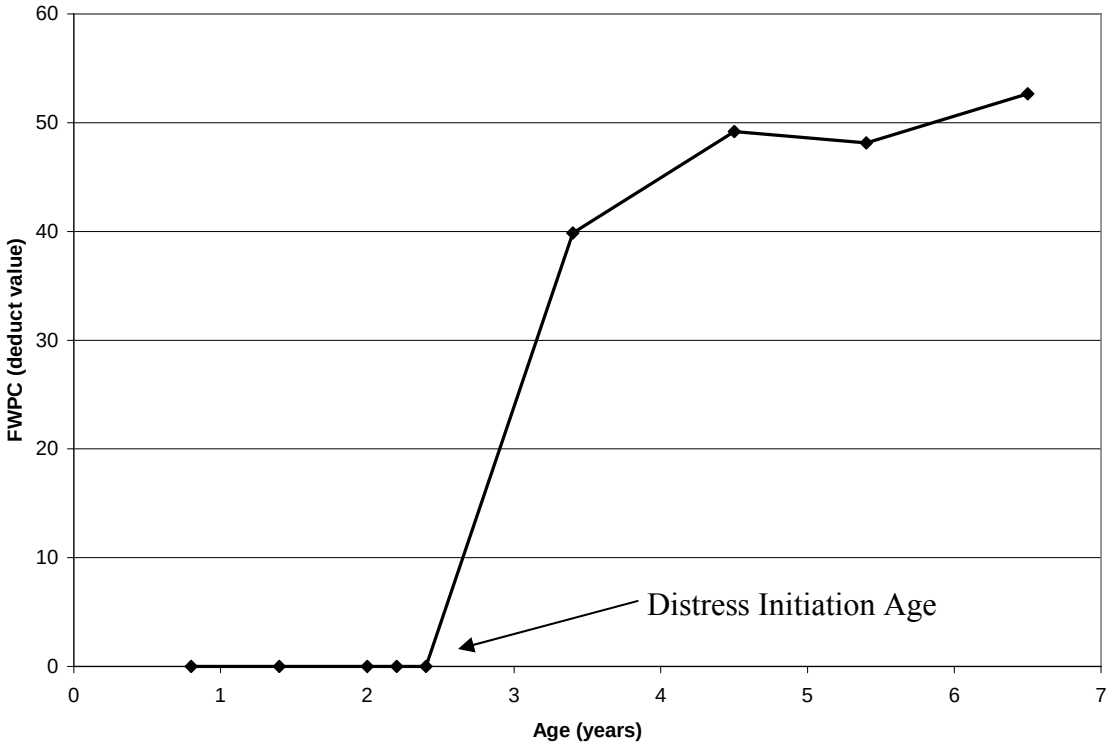

Figure 25. Graph plot. Observed FWPC deduct values for test section 100102.

For test sections that were not monitored before the distress initiation, linear regression was performed on each test section and used to determine the age at which the distress was initiated. An example of this is shown graphically in figure 26. The initiation age estimated from the regression equation was subtracted from subsequent pavement ages to get the age after initiation. The regression models were developed using only nonzero distress values (i.e., values recorded after initiation) and replacing age with these calculated adjusted age values.

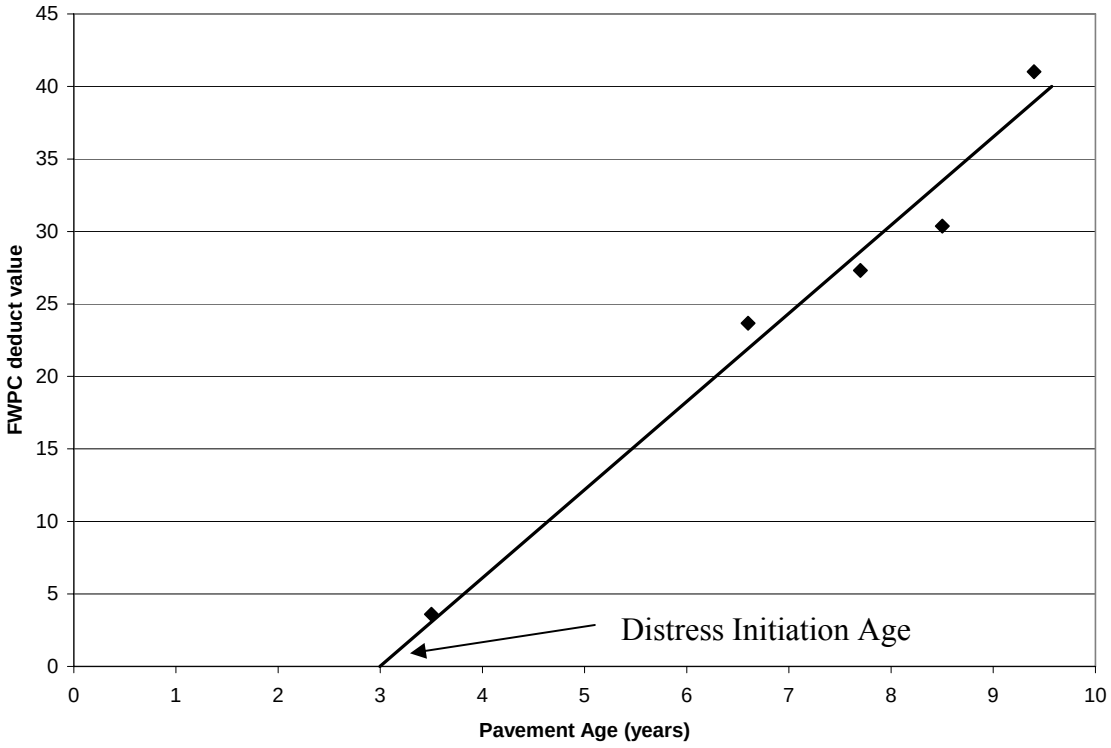

Figure 26. Graph plot. Observed FWPC deduct values for test section 050121 (with regression line).

Similar to other performance measures, multiple regression models were developed for each distress type using different distress-age relationships. These models were evaluated to select the model that predicts the observed values with the best accuracy. The first model incorporated a linear relationship between distress and pavement age while the second model was developed using a natural logarithm relationship.

Figure 27 provides a scatter plot of observed versus predicted values for the FWPC model using the logistic analysis coupled with the linear distress/pavement age regression model. Figure 28 shows a scatter plot for values generated from the regression model with the natural logarithmic relationship.

The vertical lines on the left side and the horizontal lines on the bottom of both figures indicate the error within the logistic analysis. The data points on the vertical lines (above the line of equality) are a result of the logistic analysis predicting distress initiation earlier than it was actually observed. Conversely, instances where the logistic analysis predicted crack initiation later than observed appear as data points on the horizontal line to the right of the line of equality. Although it looks as if only one of these data points falls on the line of equality, in actuality approximately 1,800 of the 2,400 points predicted using the logistic analysis were classified correctly as events or nonevents. Because the probability level of 0.7 resulted in equal sensitivity and specificity for the logistic model, it was selected as the cutoff probability. The vertical lines on the right side and the horizontal line on the top of both figures are the results of establishing a maximum allowable deduct value of 100.

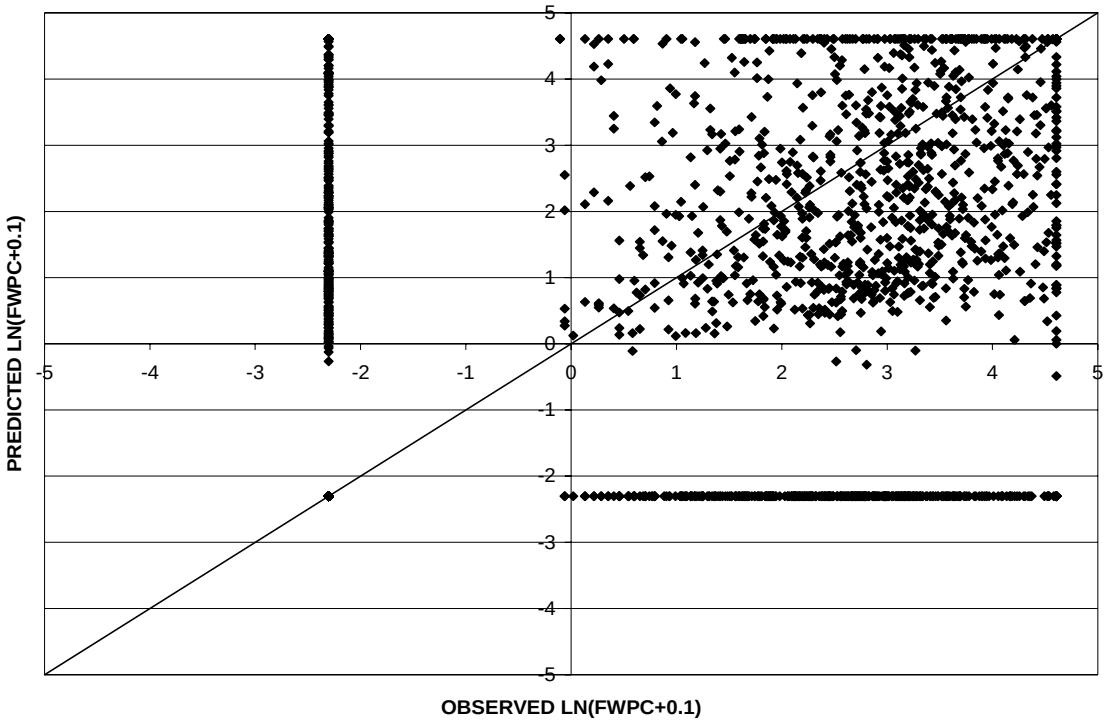

Figure 27. Scatter plot. FWPC model for flexible pavements with linear FWPC-age relationship.

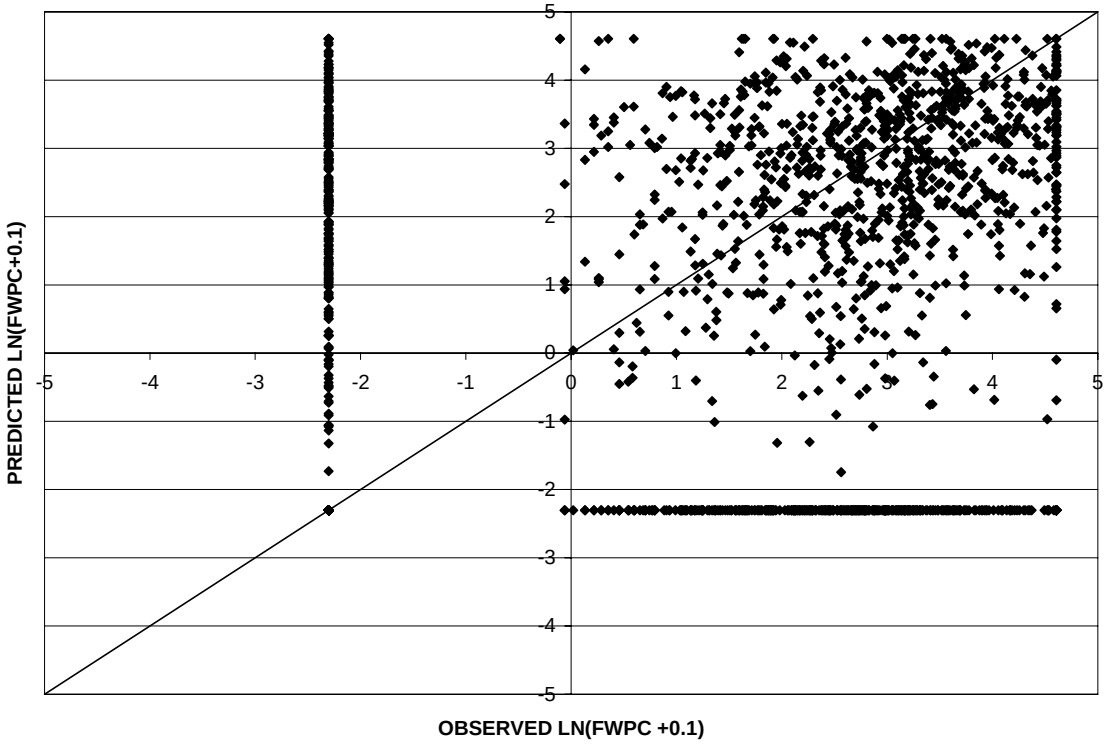

Figure 28. Scatter plot. FWPC model for flexible pavements with FWPC-natural logarithm age relationship.

In comparing the two models, the cluster of data points in figure 28 are more densely clustered around the line of equality. The linear regression model exhibits a larger RMSE value (1.85) as compared with the logarithmic regression model (1.41). In addition, the linear relationship model overpredicts a larger percentage of data points compared with the logarithmic relationship (evident in the horizontal line on the top of figure 27). For these reasons, the natural logarithmic relationship was selected for use in the environmental comparisons.

Appendix B provides details on the logistic and regression models used to predict FWPC. The R-squared value for the regression model was 0.63 (P-value < 0.0001). In addition, a regression model was developed for FWPC accumulation in terms of percentage of wheelpath area, and it was used in the description of application to mechanistic design (chapter 10). The R-squared value for this regression model was 0.49 (P-value < 0.0001).

Figures 29 and 30 provide scatter plots for TC models using linear and logarithmic relationships, respectively. To evaluate the logistic analysis, approximately 1,900 out of 2,400 records were accurately categorized as events or nonevents by the logistic model. This was achieved with a cutoff probability of 0.6. Similar to the FWPC models, the logarithmic relationship model exhibits an improved RMSE value of 1.21 as compared to a value of 1.69 for the linear model; therefore, the natural logarithmic relationship model was selected for use in the environmental comparisons.

Appendix B contains information on the TC logistic and regression models. The adjusted R-squared value for the TC regression model is approximately 0.71 (P-value < 0.0001).

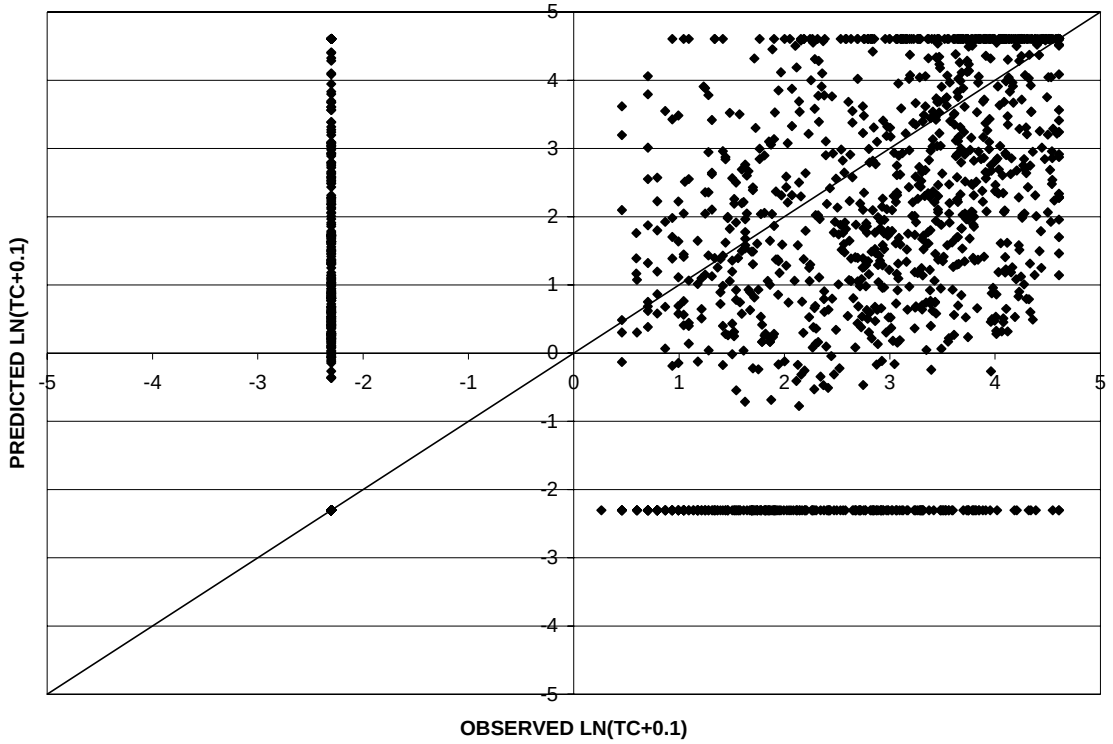

Figure 29. Scatter plot. TC model for flexible pavements with linear TC-age relationship.

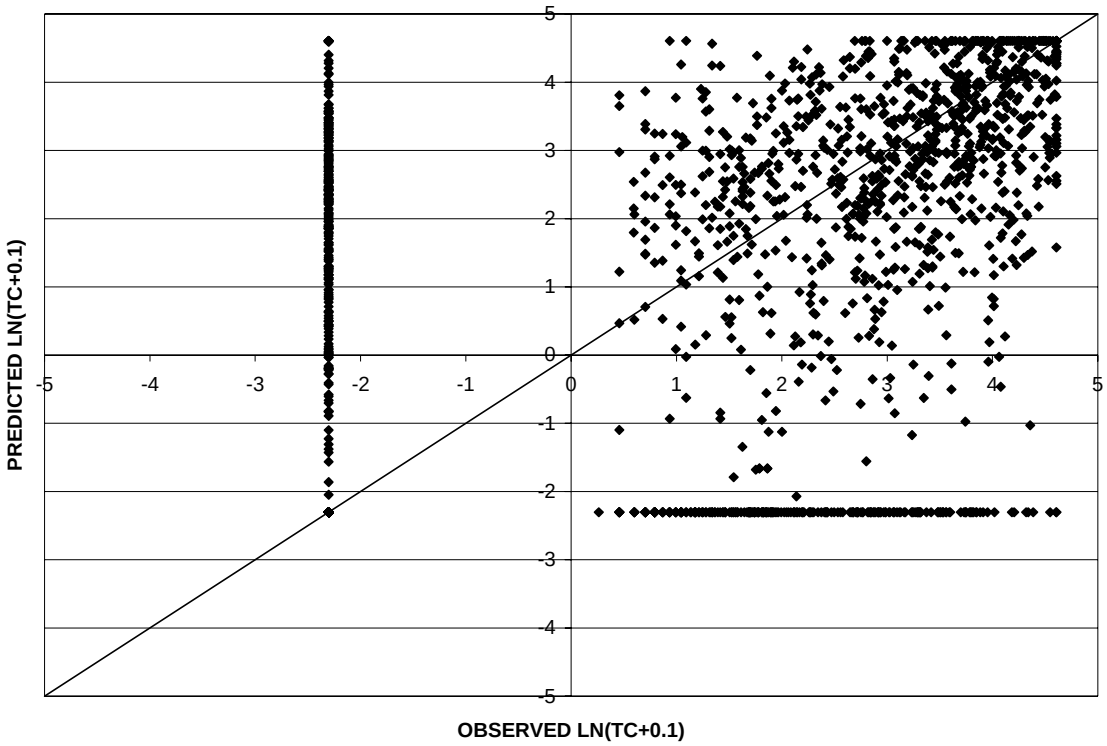

Figure 30. Scatter plot. TC model for flexible pavements with TC-natural logarithm age relationship.

Additional regression models were developed for block cracking. The regression models include a negative coefficient for pavement age. This indicates a reduction in pavement distress with increases in pavement age (under certain environmental conditions). The model's poor correlation and negative distress age relationship can be attributed to the relatively small percentage of records in the dataset with nonzero BC deduct values (approximately 90 of the 2,400). In addition, it is probable that rather variability contributed to the regression results. Due to the subjective nature of data collection, an area of distress could be rated as block cracking during one data collection visit and subsequently rated as a series of longitudinal and transverse cracking on the next survey. This would result in a reduction in block cracking quantities with age. Therefore, given these issues as well as the results of the regression model, block cracking models were not evaluated as part of the performance comparisons.

CB was modeled using data from the rigid pavements selected for use in this study. Scatter plots for the linear and logarithmic CB-age relationship models appear in figures 31 and 32, respectively.

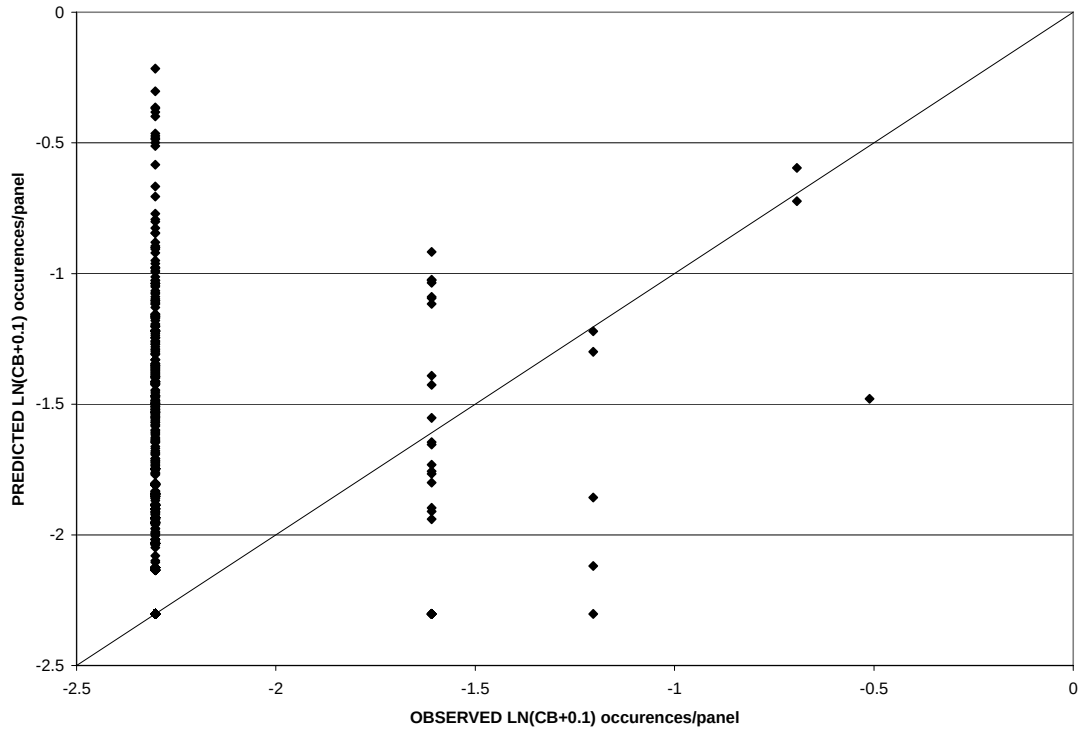

Figure 31. Scatter plot. CB model for rigid pavements with linear CB-age relationship.

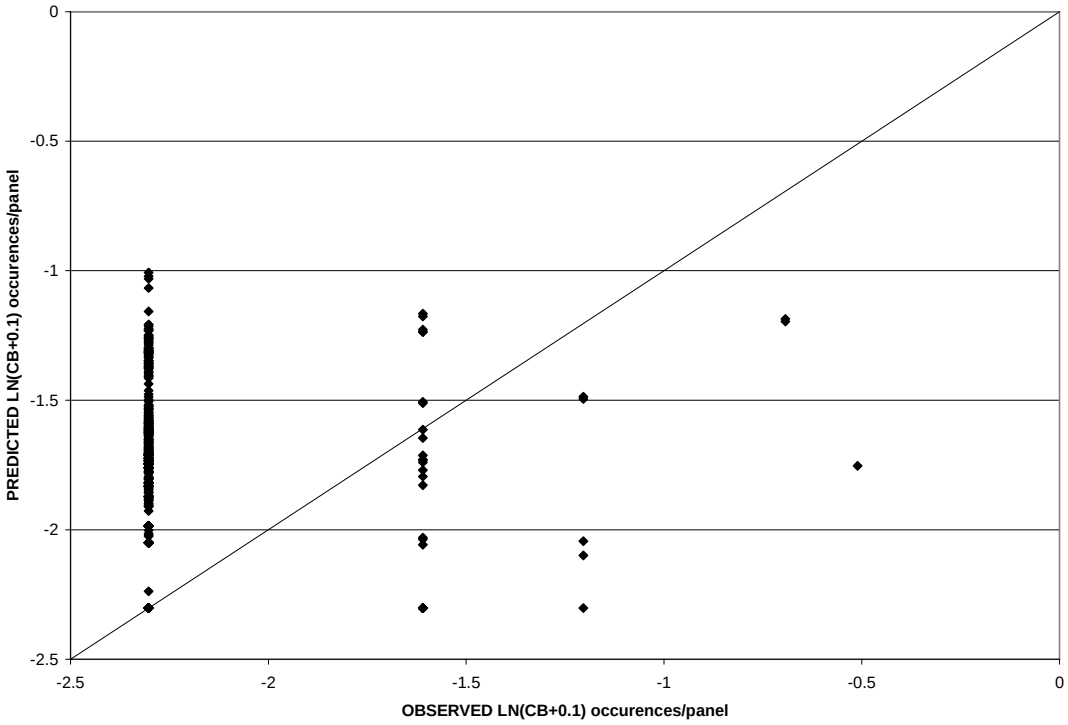

Figure 32. Scatter plot. CB model for rigid pavements with CB-natural logarithm age relationship.

As can be seen from the figures, both models provide poor correlation between predicted and observed values. This is caused, in part, by the limited number of nonzero observations in the dataset (approximately 3 percent of the records) in which the regression analysis was developed. The quantity of data points used in the regression was not large enough to account for the contribution of each explanatory variable. As such, the models developed from CB data were not used to make performance comparisons.

Additional analysis was performed on the rigid dataset to predict longitudinal cracking (LC). Consistent with the other distress performance measures, two models with different relationships between LC and pavement age were developed. Scatter plot results from the linear relationship model can be found in figure 33, while figure 34 provides similar results for the logarithmic model. The RMSE values for the linear and logarithmic relationship models were determined to be 1.49 and 1.42, respectively.

Because the model developed using the logarithmic relationship between LC and pavement age provides less variability compared with the linear relationship, it was selected for use in the performance comparison analysis. The logistic model correctly classified approximately 990 of the 1,350 records in the dataset. A cutoff probability of 0.55 was selected to determine initiation age. The regression portion of the model exhibits an R-squared value of 0.38 (P-value < 0.0001). Appendix B provides equations detailing the logistic and regression models for LC performance on rigid pavements.

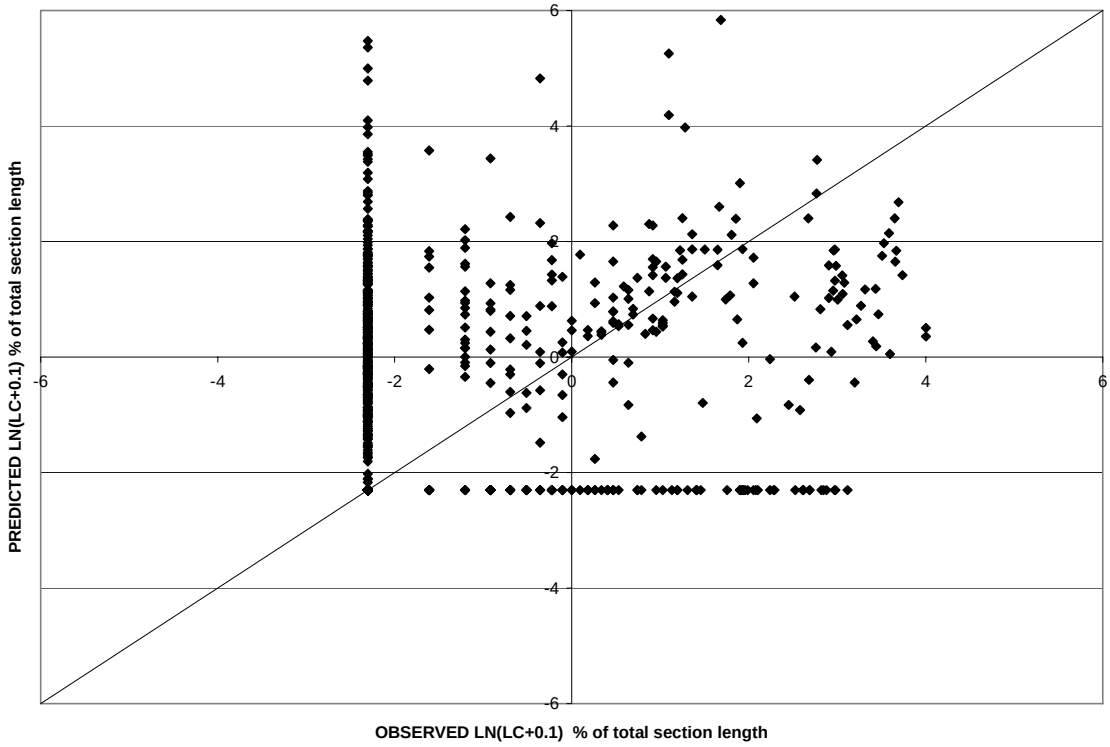

Figure 33. Scatter plot. LC model for rigid pavements with linear LC-age relationship.

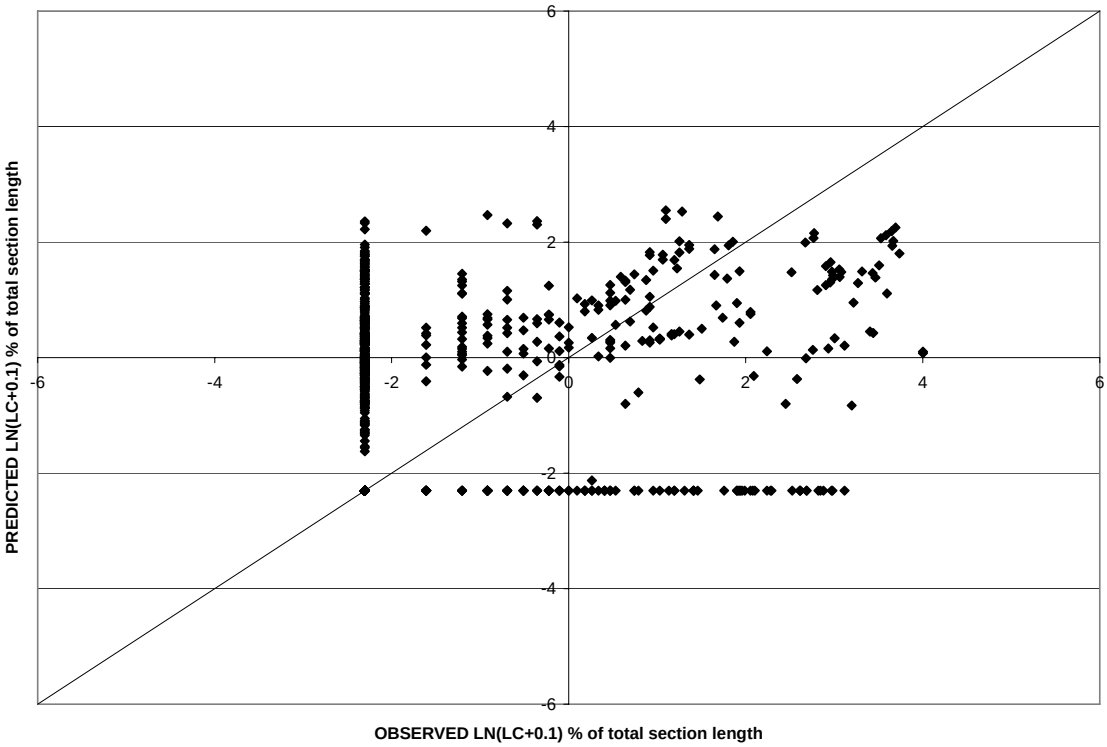

Figure 34. Scatter plot. LC model for rigid pavements with LC-natural logarithm-age relationship.

Similar analysis was performed for TC of rigid pavements. Scatter plots for each of the models is provided in figures 35 and 36. As can be seen from the graphs, the logarithmic relationship model (RMSE equals 1.17) results in a better correlation between observed and predicted values as compared with the linear model (RMSE equals 1.24). The adjusted R-squared for the regression model is 0.53 (P-value < 0.0001) and the logistic analysis correctly categorized 920 of the 1,350 records in the dataset (at the selected cutoff probability of 0.6).

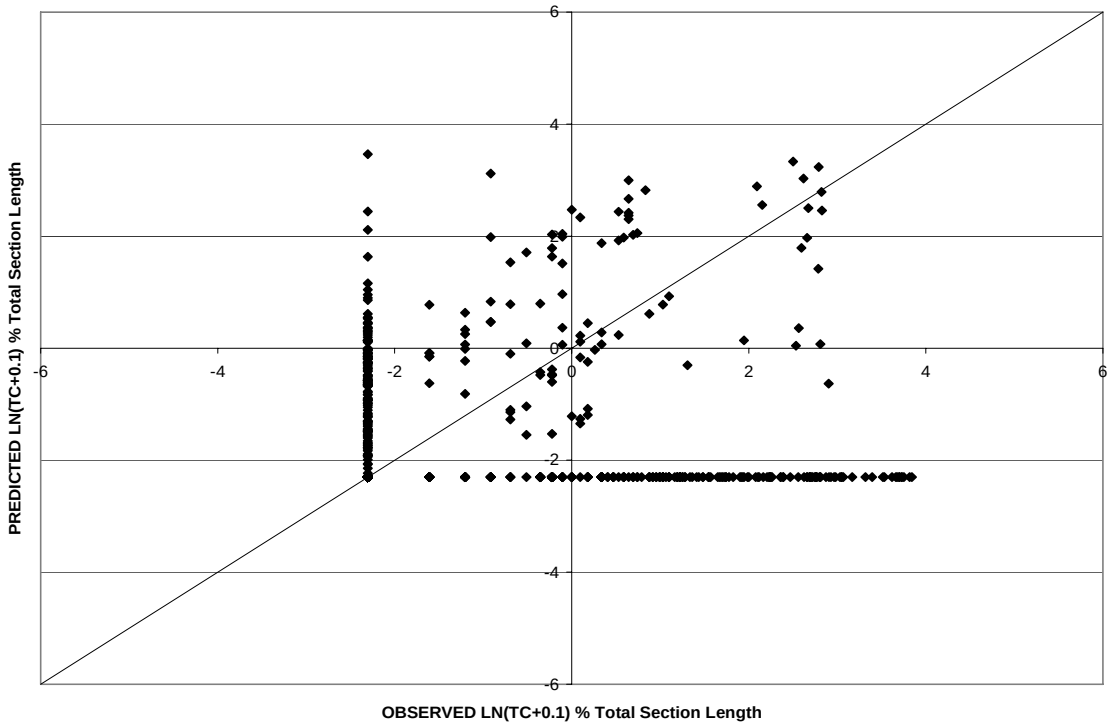

Figure 35. Scatter plot. TC model for rigid pavements with linear TC-age relationship.

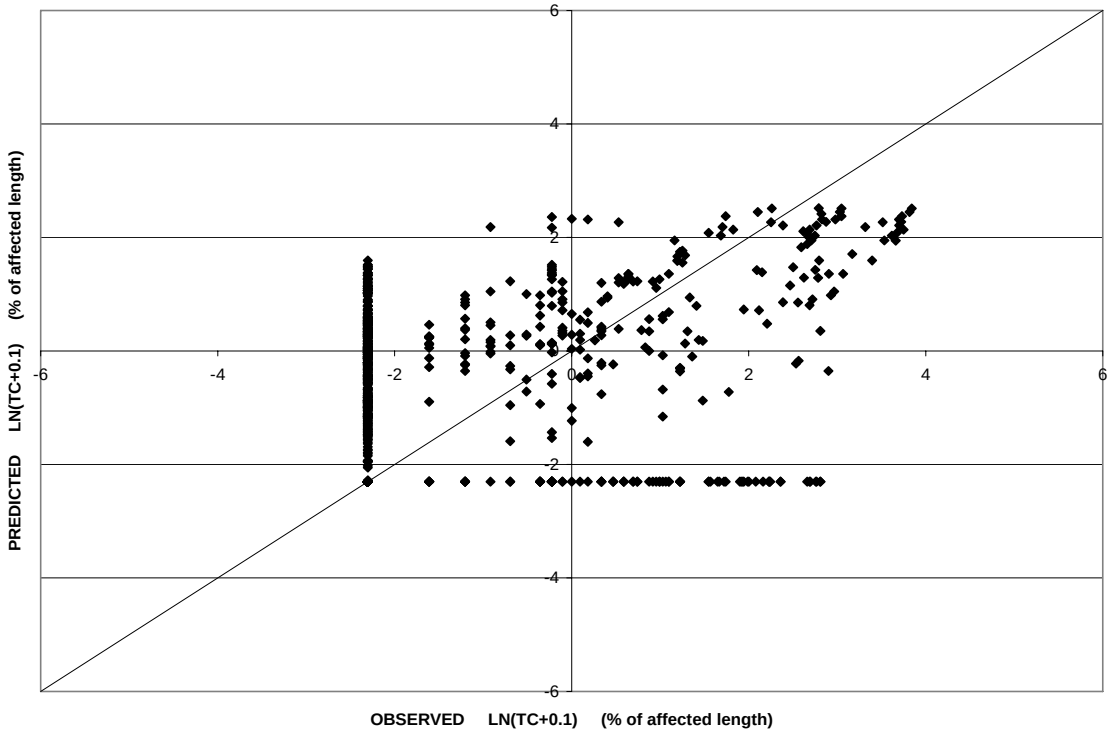

Figure 36. Scatter plot. TC model for rigid pavements with TC-natural logarithm age relationship.

Last, PUMP was modeled for the rigid pavement dataset. It should be noted that there was limited accumulation of pumping in the dataset. Approximately 110 records (8 percent) of the dataset exhibited nonzero PUMP values. The number of nonzero records is relatively small compared with the number of explanatory variables considered in the regression developed. Figure 37 provides the prediction capabilities of the model developed with a linear relationship between PUMP and pavement age. Figure 38 shows the results from the logarithmic model. Predicted values from the models do not correlate well with observed values, and therefore, they were not used to make performance comparisons.

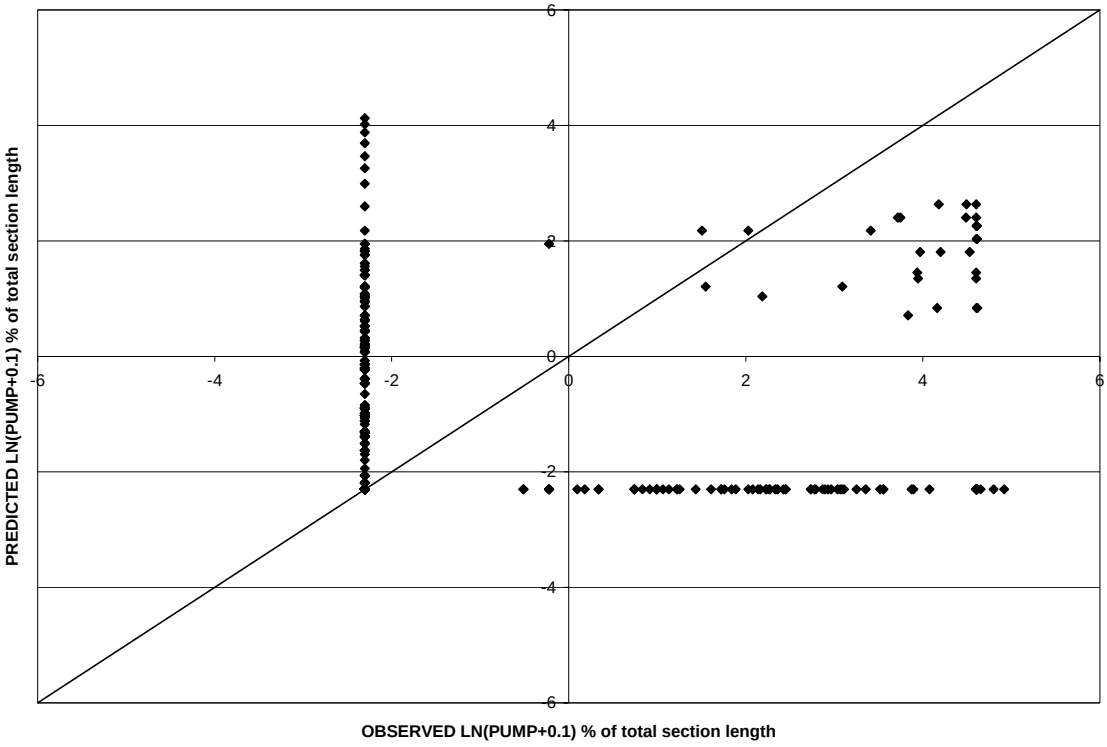

Figure 37. Scatter plot. PUMP model for rigid pavements with linear PUMP-age relationship.

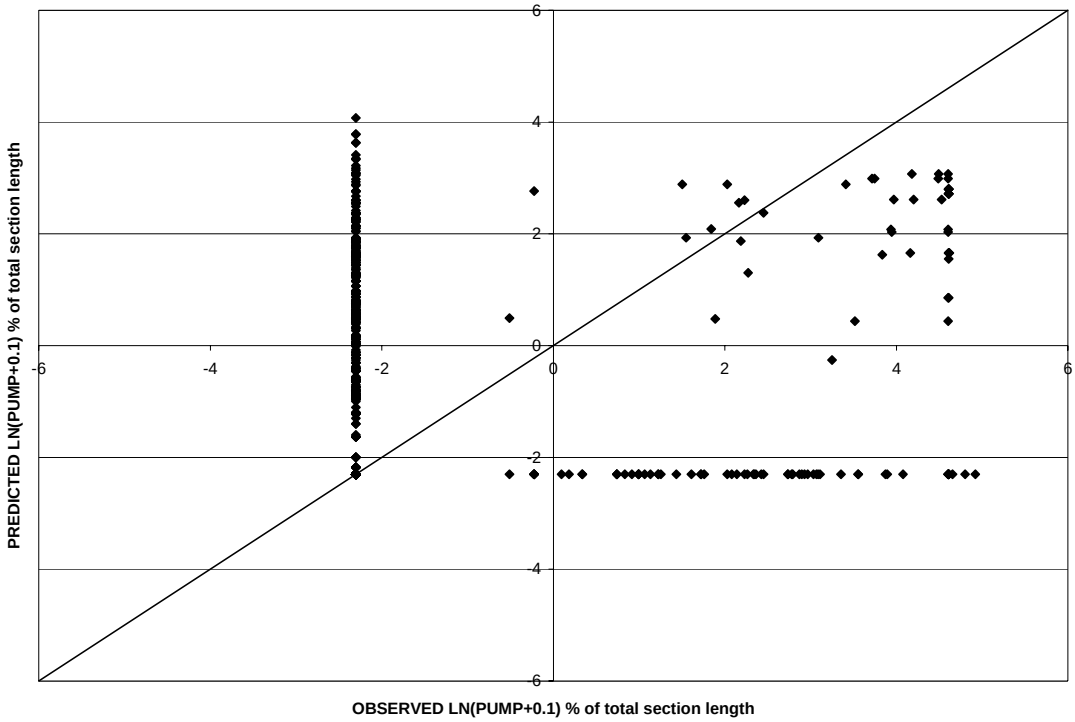

Figure 38. Scatter plot. PUMP model for rigid pavements with PUMP-natural logarithm age relations.

TRANSVERSE JOINT FAULTING PREDICTION MODELS FOR RIGID PAVEMENTS

Faulting provides an indication of the joint integrity (load transfer efficiency) as well as the condition of the underlying unbound layers. In addition, pavement roughness is directly affected by the magnitude of faulting, and performance models were developed for transverse joint faulting of rigid pavements. The average faulting value for all joints on a test section was established as the performance measure.

Two models were developed to predict the accumulation of faulting (FLT) with pavement age. The first model incorporated a linear relationship between the performance measure and pavement age; the second regression was developed with a logarithmic relationship. Figure 39 provides the scatter plot for the linear relationship model. Figure 40 represents the observed versus predicted values for the logarithmic relationship model.

The RMSE for the linear relationship model is approximately 0.37, which is an improvement over the logarithmic model (RMSE equal to 0.39). In addition, the logarithmic model predicted a decrease in accumulated faulting with an increase in pavement age in some cases. This is not logical because faulting should not improve as the pavement structure ages and is exposed to traffic loading. In consideration of this fact, as well as the improved goodness of fit, the linear relationship model was selected for use in the study.

Details regarding the model, which resulted in an adjusted R-squared value of 0.47 (P-value < 0.0001), appear in appendix B.

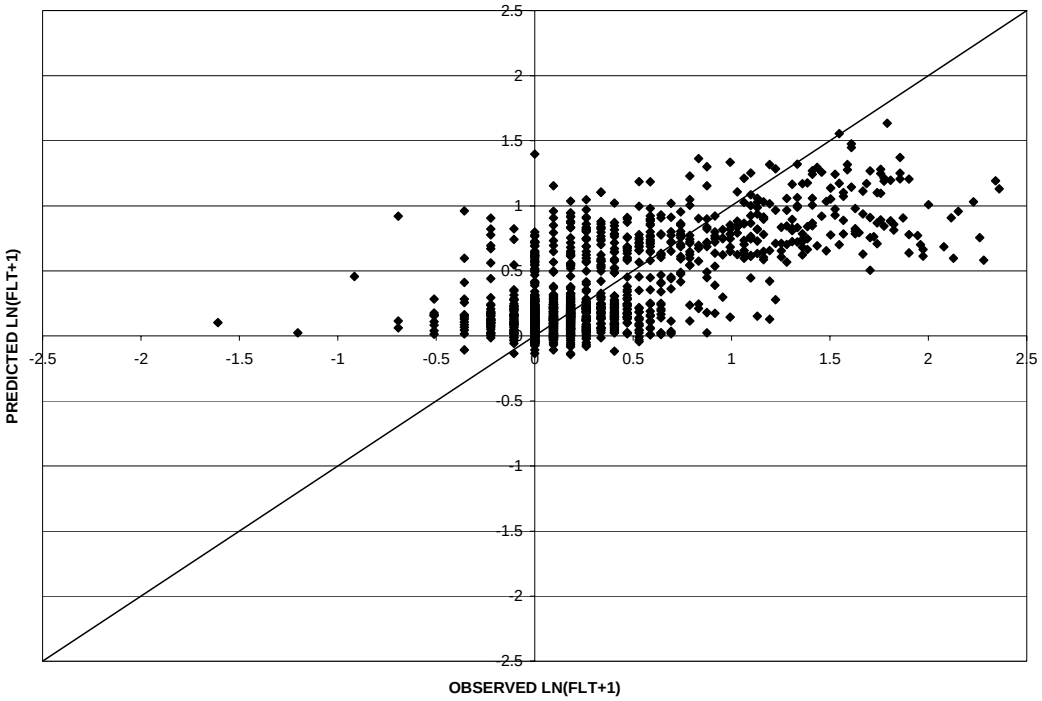

Figure 39. Scatter plot. FLT model for rigid pavements with linear FLT-age relationship.

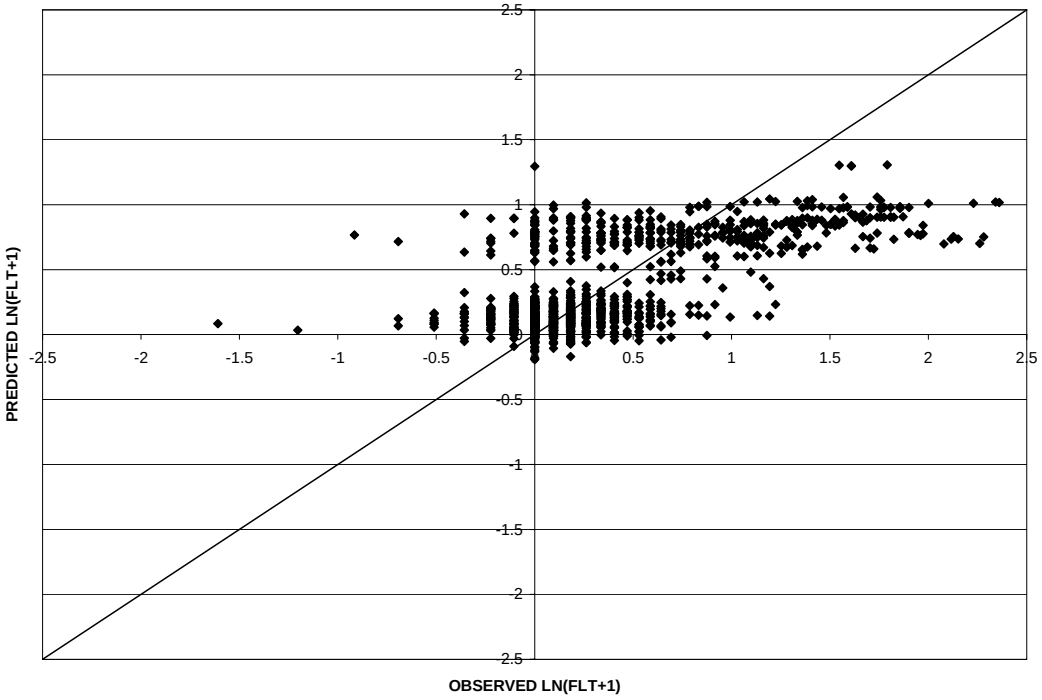

Figure 40. Scatter plot. FLT model for rigid pavements with FLT-natural logarithm age relationship.

6. ENVIRONMENTAL PERFORMANCE COMPARISONS

One of the main objectives of this study was to compare pavement performance in various climatic settings. The environmental regions of interest were loosely defined as (1) southern freeze/northern no-freeze, (2) northern freeze, and (3) southern no-freeze regions. These regions were intended to capture pavement performance in areas with moderate frost depth (with multiple FTCs), deep sustained frost depth, and very little frost depth to provide a means of comparing the effect of FTC compared with the contribution of deep frost penetration (represented by FI) on pavement deterioration. As such, the following groupings were established for this study:

- Deep-freeze, wet region.
- Deep-freeze, dry region.
- Moderate-freeze, wet region.
- Moderate-freeze, dry region.
- No-freeze, wet region.

The deep-freeze regions were established to represent typical climatic conditions of the northern freeze zones where deep sustained frost penetration was presumed to occur. The moderate-freeze regions correspond to the southern freeze/northern no-freeze zone, which implied a multiple FTC climate. The region was established to represent the southern no-freeze region where frost penetration and multiple FTCs are very minimal.

While LTPP has defined wet/dry regions in terms of annual precipitation—508 mm/year (20 inches/year) and freeze/no-freeze regions as a function of FI (83.3 degree-Celsius days), the limits of the regions listed above have not been previously established; therefore, an investigation of FI and FTC relationships was performed on the analysis dataset to define limits for each of the scenarios.

Figure 41 provides the relationship between FI and FTC based on data from all test sections evaluated in the study. The no-freeze region was limited to areas with an FI less than 50 degree-Celsius days while the moderate-freeze was defined with FI between 50 and 400 degree Celsius days. The deep-freeze region consists of locations exhibiting an FI greater than 400 degree-Celsius days. These limits were established based on the natural break points inherent in the dataset, while also considering the LTPP-defined criteria for the freeze-, no-freeze regions (i.e., the moderate-freeze region must be centered on the LTPP freeze/no-freeze cutoff and include data points in both zones). The geographic boundaries for each of the regions were used to verify that selected FI limits were logical. The geographic location of each test section is plotted in figure 42.

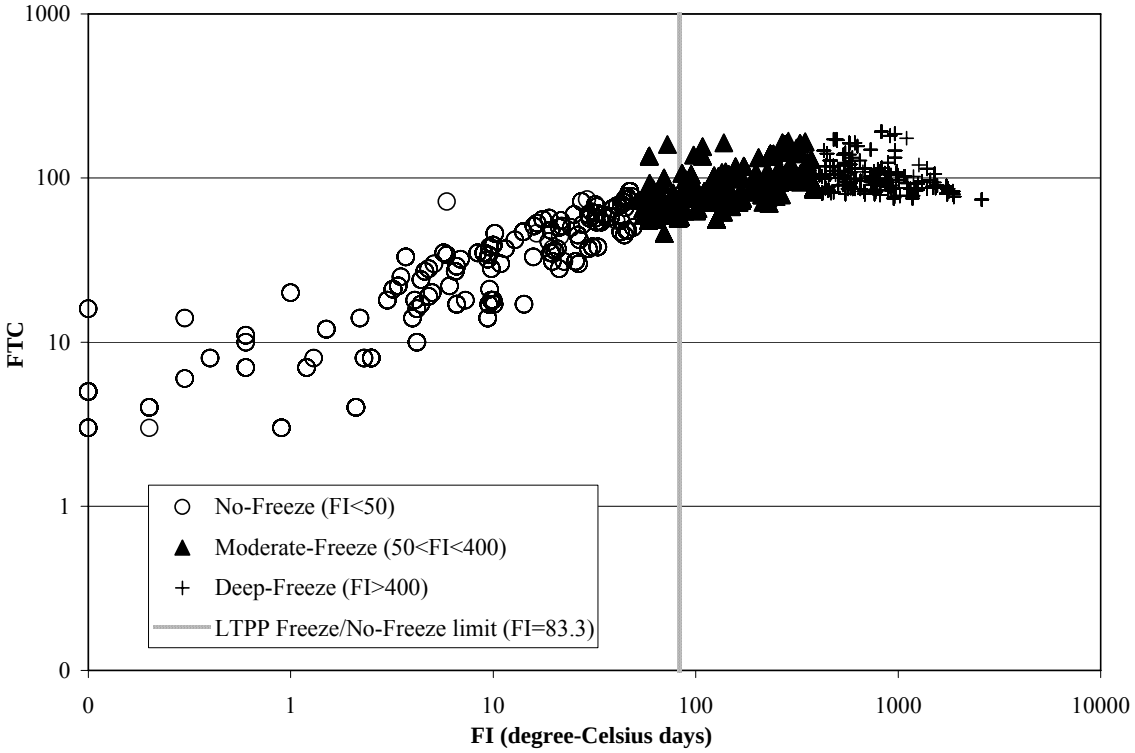

Figure 41. Scatter plot. Regional FI and FTCs values.

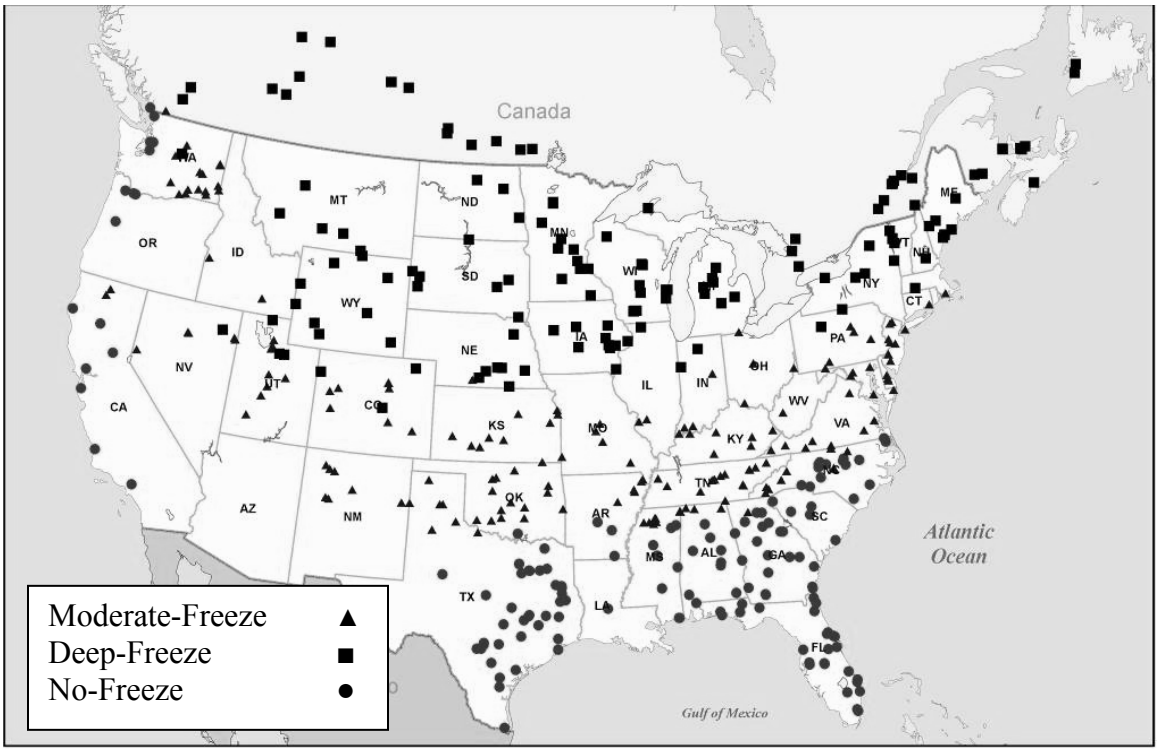

Figure 42. Map. Geographic locations of climatic regions.

The majority of test sections classified as no-freeze is located in the Southern States with a few remaining sites located along the Pacific coast of the United States. The deep-freeze region consists of sites located in Canada and the northern United States. The band of sites in the moderate-freeze region is located across the middle of the United States running from northern Texas in the south to southern Washington in the north. These geographic locations are logical and consistent with the expected climates across the continent.

It should be noted that the following statement from the Task Order Proposal Request (TOPR) description of work indicates an inference that there are fewer FTCs in the northern freeze zone as compared with the moderate-freeze zone:

> *Near the southern edge of the freeze/no-freeze zone, pavements are subjected to multiple freeze-thaw cycles each year. Farther north, pavements may be subjected to few freeze-thaw cycles, but the depth of frost penetration is generally greater.*

By inspection of figure 43, FTC values do not decrease in the deep-freeze regions (i.e., relatively high FI locations). Rather, the amount of FTC is approximately equivalent in the moderate- and deep-freeze regions; therefore, deep frost depths and multiple freeze-thaw cycles are not necessarily mutually exclusive factors and pavements do exist in areas that are classified as deep-freeze that also experience a large number of FTC.

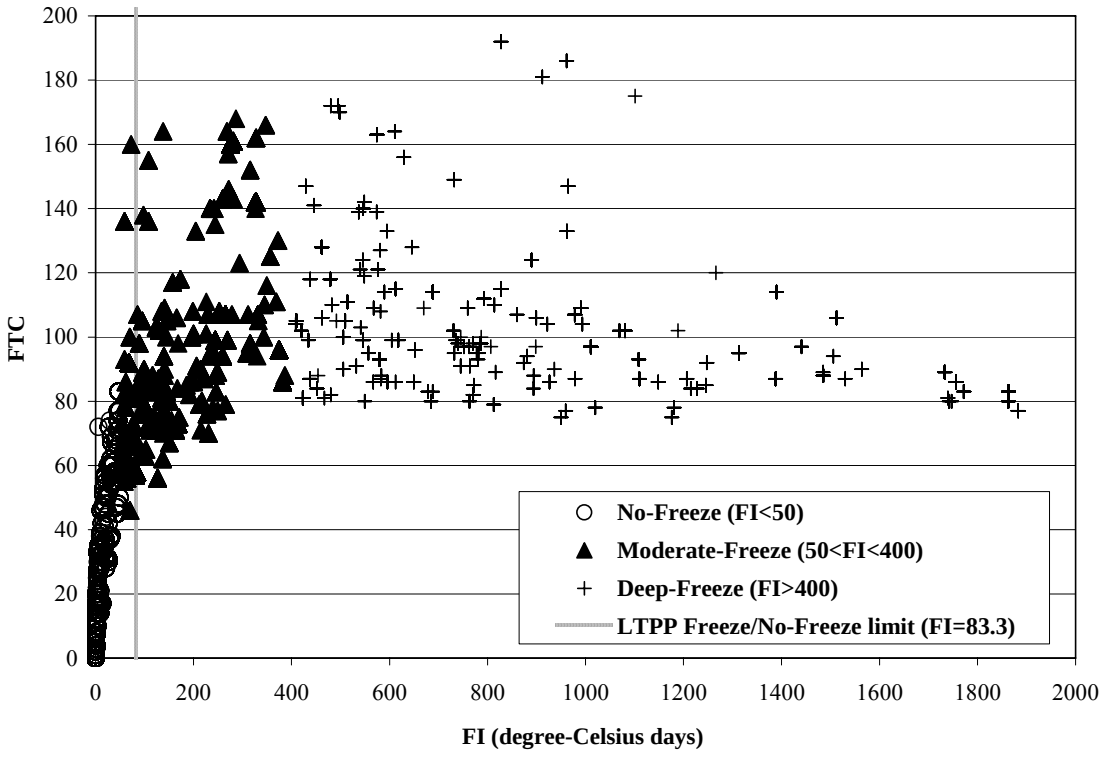

Figure 43. Scatter plot. Relationship between FI and FTCs.

The above analysis was used to define the limits of deep-freeze, moderate-freeze, and no-freeze regions based on FI. To represent these climatic scenarios in the performance models, input values for each had to be established. Tables 20 and 21 provide the explanatory variable (i.e., input) values used to represent each of the regions for flexible and rigid pavements respectively. Nonenvironmental variables such as ACTHICK and logarithm ESAL divided by structural number (LESN) were held constant for each of the regions; therefore, performance predictions were made for consistent pavement structures exposed to similar traffic loading. This allowed the climatic effects on pavement performance to be compared without confounding the results by varying other contributing factors. The values for these nonclimatic factors were selected as the median value present in the analysis dataset. The scenarios listed in tables 19 and 20 incorporate constant BASE and SG types (DGAB and FINE, respectively). Predictions made using these two layer types are presented in the following text. Performance estimates were also established for other base/subgrade combinations, and key findings from those combinations are provided in the following discussion. This includes predictions for flexible pavement structures with overlay layers as well.

Table 20. Overview of climatic scenarios for flexible pavements.

Scenarios	ACTHICK	BASE	SG	LESN	EXP	FI	FTC	PRECIP	CI
Deep-Freeze, Wet Region (low FTC)	6.5	DGAB	FINE	1.02	G1	688	80	1140	205
Moderate-Freeze, Wet Region (high FTC)	6.5	DGAB	FINE	1.02	G1	137	130	1140	645
No-Freeze, Wet Region	6.5	DGAB	FINE	1.02	G1	10	10	1140	1300
Deep-Freeze, Dry Region (low FTC)	6.5	DGAB	FINE	1.02	G1	688	80	380	205
Moderate-Freeze, Dry Region (high FTC)	6.5	DGAB	FINE	1.02	G1	137	130	380	645

Table 21. Overview of climatic scenarios for rigid pavements.

Scenarios	FC	D	BASE	SG	LEDT	EXP	FI	FTC	PRECIP	CI
Deep-Freeze, Wet Region (low FTC)	2	9.5	DGAB	FINE	0.59	S2	688	80	1140	205
Moderate-Freeze, Wet Region (high FTC)	2	9.5	DGAB	FINE	0.59	S2	137	130	1140	645
No-Freeze, Wet Region	2	9.5	DGAB	FINE	0.59	S2	10	10	1140	1300
Deep-Freeze, Dry Region (low FTC)	2	9.5	DGAB	FINE	0.59	S2	688	80	380	205
Moderate-Freeze, Dry Region (high FTC)	2	9.5	DGAB	FINE	0.59	S2	137	130	380	645

Table 22 gives process details used to select environmental values for each climatic region shown in tables 20 and 21. With the exception of FTC, the values selected for all environmental variables were the median value present in the region. For example, the median FI of all test sections in the no-freeze region (i.e., 0<FI<50) was found to be 10 degree-Celsius days. Similarly, the CI value of 205 degree-Celsius days was determined to be the median CI value present for test sections in the deep-freeze region (FI>400).

Because the aim of the study is to compare the trade-off in pavement deterioration between deep frost and multiple FTCs, the percentile used to select FTC values was different for each region. In the deep-freeze region, one of the lowest FTC values present (10th percentile) was selected while one of the highest values was identified for the moderate-freeze region (90th percentile). This approach was used to isolate the contribution of FI from FTC in the deep-freeze region and allow the contribution of FTC to be investigated in the moderate-freeze region. As a caveat, it is apparent that pavements do exist in areas with both deep-frost penetration and multiple FTCs as can be seen in figure 43.

Table 22. Details on selection of environmental variables.

Variable	Percentile Criteria	Value
Deep-Freeze (FI)	50th, deep-freeze (>400 FI)	688
Moderate-Freeze (FI)	50th, moderate-freeze (50<FI<400)	137
No-Freeze (FI)	50th, no-freeze (<50 FI)	10
Low FTC	10th, FTC values in deep-freeze (>400 FI)	80
High FTC	90th, FTC values in mod-freeze (50<FI<400)	130
No-Freeze FTC	50th, FTC values in no-freeze (<50 FI)	10
Dry (PRECIP)	50th, dry region (<508mm)	380
Wet (PRECIP)	50th, wet region (>508mm)	1140
Deep-Freeze (CI)	50th, deep-freeze (>400 FI)	205
Moderate-Freeze (CI)	50th, moderate-freeze (50<FI<400)	645
No-Freeze (CI)	50th, no-freeze (<50 FI)	1300

When making comparisons, a determination must be made as to whether performance differences in the prediction of each scenario are statistically significant. The relatively small differences in performance can be confounded by the error inherent in the models. These differences cannot be attributed solely to the contribution of climatic setting. Rather, it is likely that the variability in the model is the source of the differences. Confidence intervals were used to determine if differences in performance were statistically significant. A confidence interval of 95 percent was selected for this study.

Using a lower confidence interval (i.e., 90 percent) would possibly lead to additional significant differences between the scenarios. Scenario departures that are marginally insignificant at the 95 percent confidence interval would likely be significant at the 90 percent level. The 95 percent level was used to provide highly significant differences, and it can also indicate the significance of variant performance. One can use the

confidence intervals provided to determine which marginal differences could be significant at a lower confidence interval.

In general, performance comparisons were made at a pavement age of 20 years for flexible pavements. This timeframe allows deterioration to accumulate to a sufficient level to make performance comparisons, and it is well within the range of pavement ages in the dataset used to develop the models. Approximately 80 out of 520 test sections in the flexible dataset were monitored at ages greater than 20 years. As such, there are sufficient quantities of observed data past 20 years represented in the models, and predictions made at an age of 20 years are not extrapolations from the dataset. In addition, the objective of the analysis was to study long term differences in performance so that financial effects of climate can be evaluated through life cycle cost analysis. The 20-year basis will provide a means of accomplishing this.

Comparisons were made at 20 years for the majority of the rigid pavement performance measures as well. Approximately 50 of the 275 test sections were monitored at ages greater than 20 years. Some of the scenarios evaluated initiated surface distress at after 20-year ages. To make comparisons at a point where all scenarios have initiated distress, the reference age was changed to 25 years for both TC and LC surface distress comparisons. Even at 25 years, the observations were not based on extrapolated predictions because approximately 29 of the 275 test sections were monitored at ages greater than 25 years. This reference age was not extended to 30 years because only six test sections were monitored at greater ages, which is a relatively limited number compared to the number of explanatory variables incorporated in the models.

Because transformations were incorporated into the model development process, it is essential that comparisons were made using the transformed scale. Mean predictions and confidence intervals were established based on transformed values; therefore, comparisons must be made in the same scale used to develop the estimates to be accurate. As such, all of the following prediction and confidence interval figures use a transformed scale (i.e., natural logarithm). Results can be converted to a linear scale if the model output is used solely as a predictive tool and the confidence intervals are not used for comparison.

PAVEMENT ROUGHNESS COMPARISONS FOR FLEXIBLE PAVEMENTS

Mean pavement roughness predictions were made for each of the scenarios defined above, and they are provided in figure 44 as a function of age. These predictions were established using an initial IRI of 1 m/km (63.3 inches/mi) at a pavement age of 1 year. Mean predicted values at 20 years along with the upper and lower limits of the 95 percent confidence interval are provided in figure 45 for each climatic region.

Figure 44 makes it apparent that pavement roughness accumulates at a more rapid rate in the wet deep-freeze and dry deep-freeze regions compared to the other regions, based on mean prediction values; however, these differences are not significant at 95 percent confidence and pavement age of 20 years as indicated in figure 45. The variability in the model confounds the differences observed in the mean predictions. The same

observations can be made for all other base/subgrade combinations for both overlay and nonoverlay pavement structures.

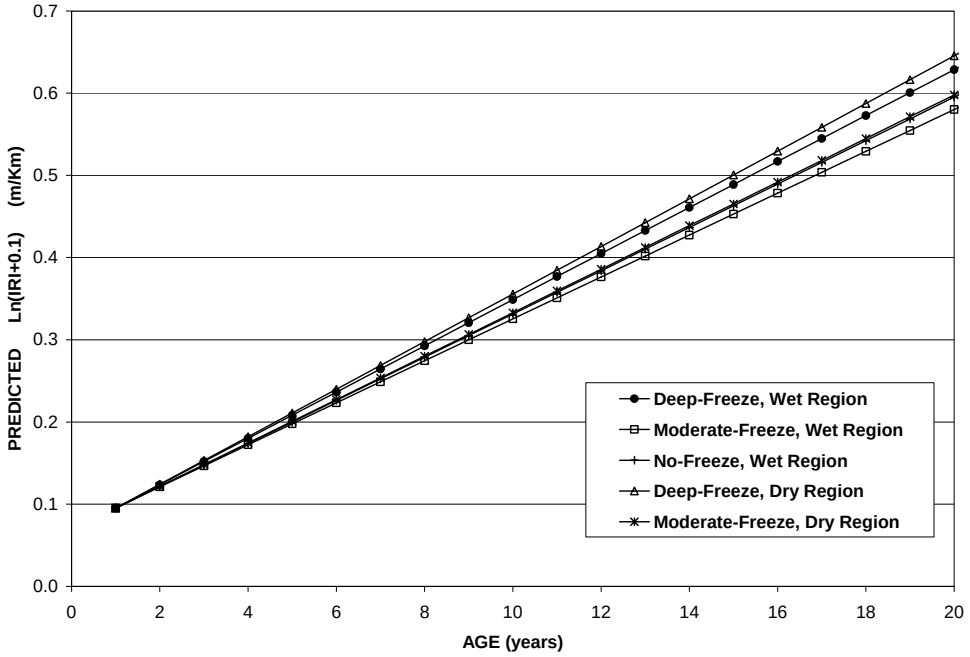

1 m/km = 5.28 ft/mi

Figure 44. Scatter chart. Mean predicted flexible pavement IRI values for each climatic region (BASE=DGAB/SG=FINE).

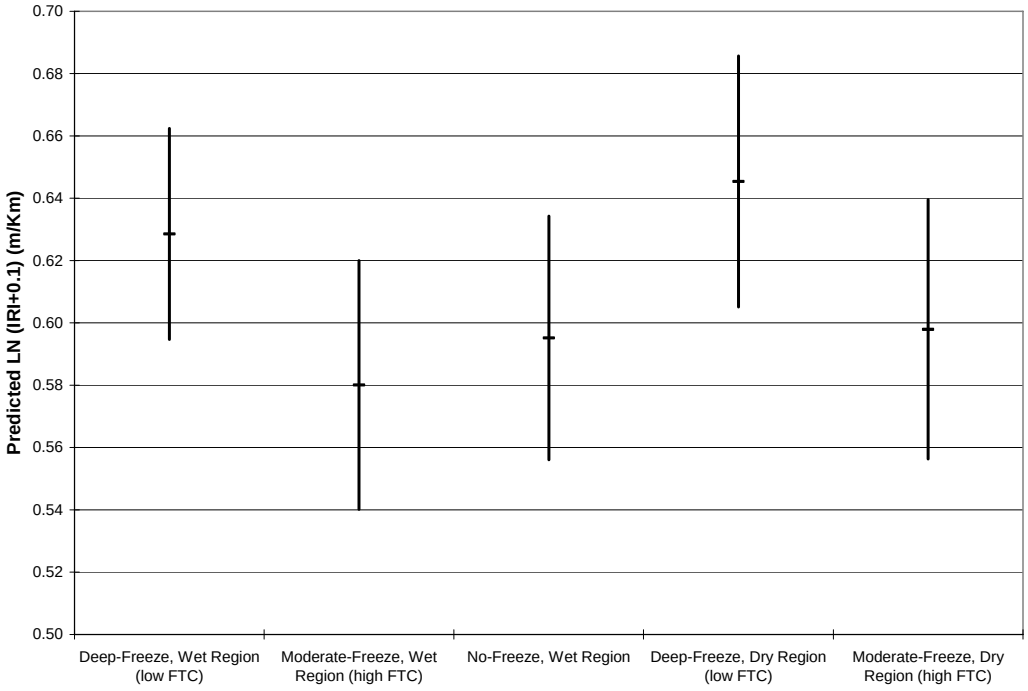

1 m/km = 5.28 ft/mi

Figure 45. Bar chart. Predicted flexible pavement IRI values at 20 years for each climatic region (BASE=DGAB/SG=FINE).

As documented by Kameyama et al.[16] considerable increases in roughness during the freezing season do exist in areas of moderate and deep frost penetration; however, the increased roughness subsides by the middle of the following summer season. Based on the results in figure 45, any adverse long-term effects on flexible pavements from these seasonal cycles observed in the freezing areas are confounded by other variability.

PAVEMENT ROUGHNESS COMPARISONS FOR RIGID PAVEMENTS

Figure 46 provides mean rigid pavement roughness predictions as a function of age for each of the scenarios listed in table 20. Performance comparisons can be made using figure 47, which provides 95-percent-confidence interval information at a pavement age of 20 years for each of scenario.

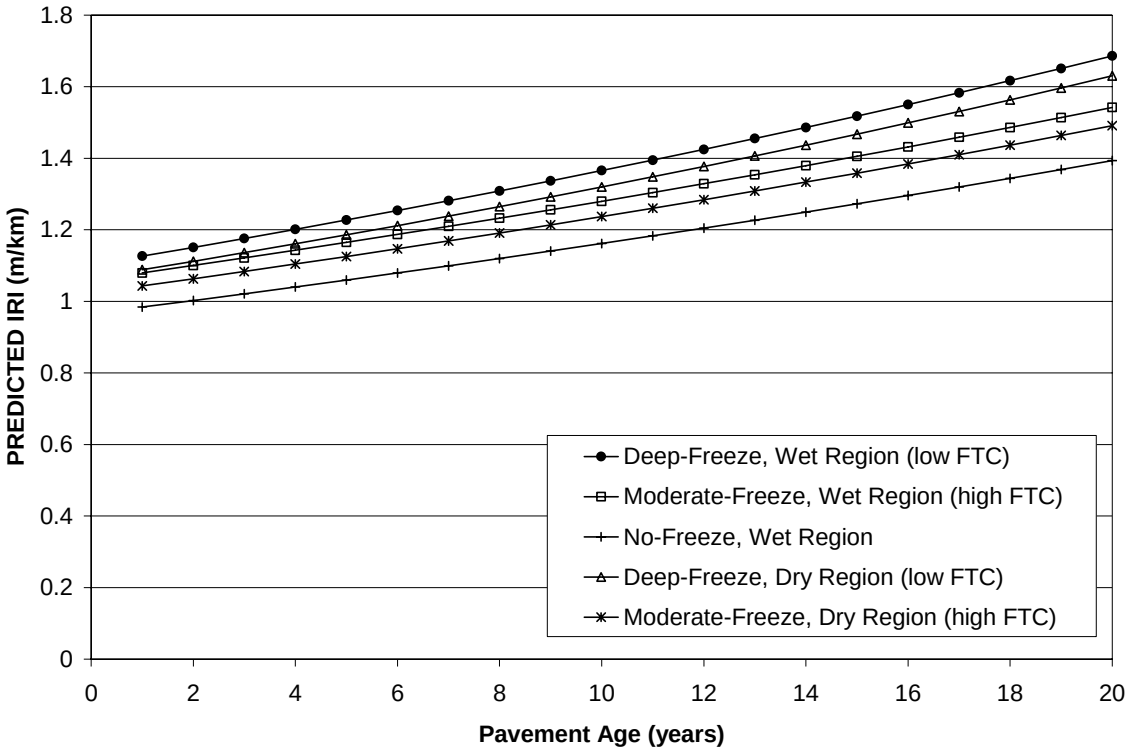

1 m/km = 5.28 ft/mi

Figure 46. Scatter graph. Mean predicted rigid pavement IRI values for each climatic region (BASE=DGAB/SG=FINE).

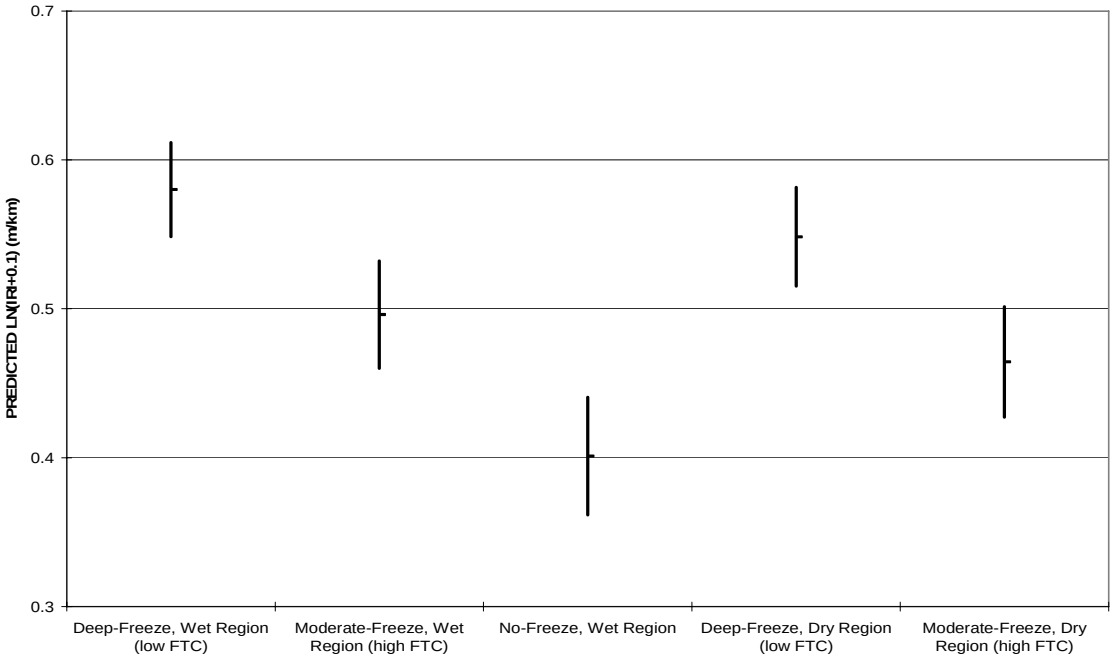

1 m/km = 5.28 ft/mi

Figure 47. Bar chart. Predicted rigid pavement IRI values at 20 years for each climatic region (BASE=DGAB/SG=FINE).

Predicted pavement roughness at 20 years in areas of deep frost penetration is significantly different than in areas experiencing multiple FTCs. This can be seen in both the dry and wet climates. The wet no-freeze region exhibits roughness values that are significantly lower than that of the moderate- and deep-freeze wet regions. Rigid pavements in relatively wet climates and in areas exposed to frost penetration accumulate roughness more rapidly than wet climates in areas with no frost.

Similarly, the same observations for other base/subgrade combinations can be made. One exception is prediction values for pavements with ROCK/STONE subgrade type. Variability with this subgrade type results in insignificant performance differences between the dry multiple freeze-thaw climate and the wet no-freeze region.

RUT DEPTH COMPARISONS FOR FLEXIBLE PAVEMENTS

Mean predictions for the progression of rut depth with pavement age can be found in figure 48 for each of the climatic regions. The 20-year confidence interval results are presented in figure 49. Both of these graphs were established for DGAB base and FINE subgrade.

The following conclusions can be drawn for figure 49: While multiple FTCs and deep sustained frost penetration do not result in changes in rutting performance in wet climates (at a 95 percent confidence interval), pavements in both of these climates accumulate larger amounts of rutting compared to the no-freeze climates; conversely, in the dry

region, multiple FTCs contribute to more rutting deterioration than both the deep-frost and no-freeze zones. The contribution of deep-frost penetration in relatively dry climates on rutting is not significantly different than that of the no-freeze wet region.

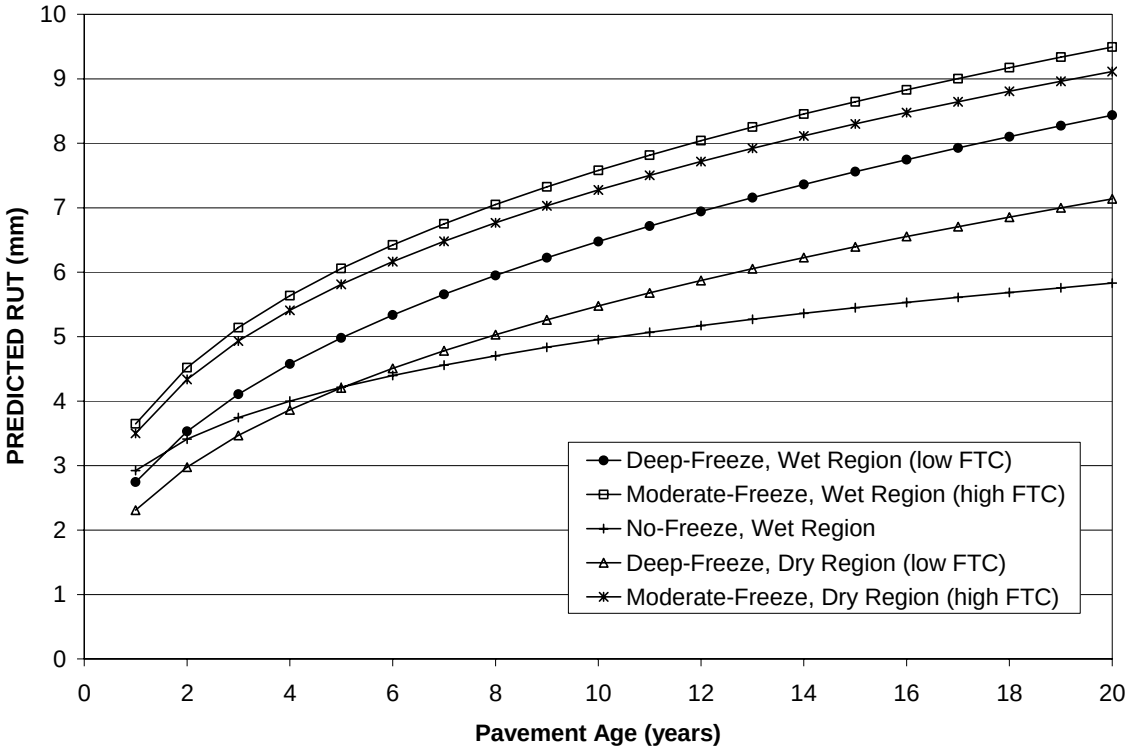

1 mm = 0.04 inch

Figure 48. Scatter graph. Mean predicted flexible pavement RUT values for each climatic region (BASE=DGAB/SG=FINE).

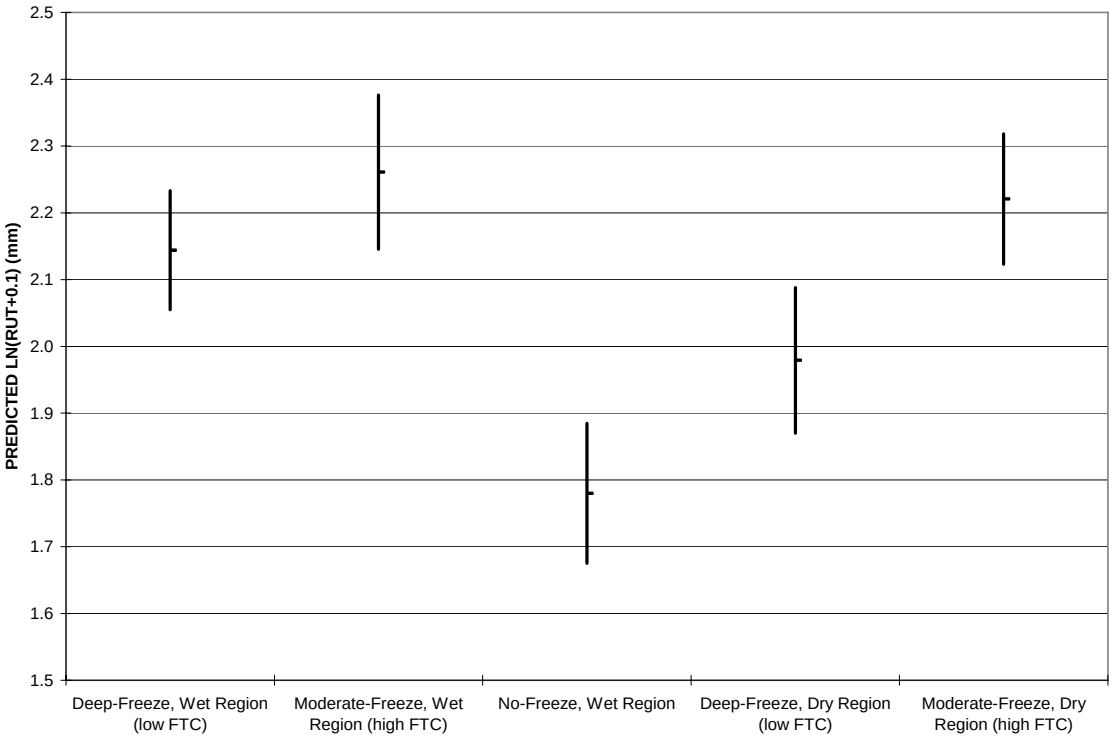

1 mm = 0.04 inch

Figure 49. Bar chart. Predicted flexible pavement RUT values at 20 years for each climatic region (BASE=DGAB/SG=FINE).

Rutting predictions for different base and subgrade combinations as well as overlay structures were also evaluated. In general, the observations discussed above for DGAB base, FINE subgrade, and nonoverlay structures can be made for other combinations. However, ROCK/STONE subgrade as well as LCB base types exhibit relatively large variability in both overlay and nonoverlay structures. This results in any performance differences between climates being statistically insignificant.

Rutting accumulation in pavements with PATB base type is not significantly different in areas exposed to deep-frost penetration and multiple FTCs (regardless of precipitation level). These accumulations are, however, significantly larger than the no-freeze wet region.

For pavements with NONBIT base, the multiple FTC climate exhibits significantly larger quantities of rutting as compared with the deep-frost penetration and no-freeze regions. Differences between the contribution of deep-frost penetration and no-freeze wet climates on rutting development are confounded by the variability in the model.

FATIGUE AND WHEELPATH CRACKING SURFACE DISTRESS COMPARISONS FOR FLEXIBLE PAVEMENTS

Mean predictions of FWPC progression for pavements with FINE subgrade and DGAB base are provided in figure 50. These predictions were generated by combining logistic analysis with regression models. As can be seen, variations in crack initiation timing as well as the rate of distress accumulation (after initiation) contribute to FWPC performance differences.

Confidence interval data for FWPC are illustrated in figure 51. The contribution of deep sustained frost significantly outweighs the effect of multiple FTCs on accumulation of FWPC. This holds true in both the wet and dry regions. The no-freeze region exhibits the largest FWPC values which, statistically speaking, are larger than FWPC predictions in areas experiencing multiple FTCs (regardless of the amount of precipitation).

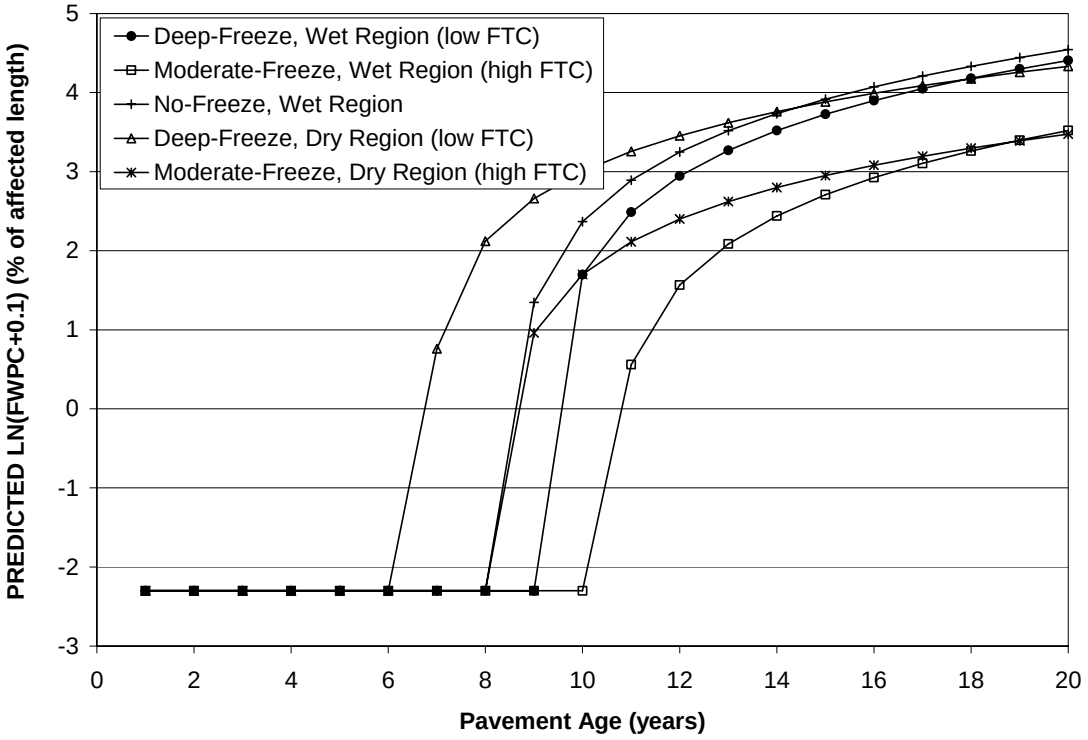

Figure 50. Chart. Mean predicted flexible pavement FWPC values for each climatic region (BASE=DGAB/SG=FINE).

The same general trends are apparent for different base/subgrade pavement structure combinations. Increased variability in some combinations results in performance differences to be less than the error band of the model. This is the case for ROCK/STONE subgrade and LCB base types in both pavement structure groups. To a lesser extent, variability for the NONE base type results in insignificant differences between the deep-frost regions and the multiple FTC climates. Predicted accumulation in

the no-freeze wet region is significantly larger than the multiple FTC climates (both precipitation levels).

TRANSVERSE CRACKING SURFACE DISTRESS COMPARISONS FOR FLEXIBLE PAVEMENTS

Figure 52 shows transverse cracking performance predictions for each climatic region in for DGAB base and FINE subgrade. Transverse cracking initiation ranges between 6 and 12 years, initiating earlier in the deep-freeze regions that experience colder minimum temperatures in the winter months. Conversely, pavements in the no-freeze regions, with mild winter temperatures, initiate transverse cracking much later.

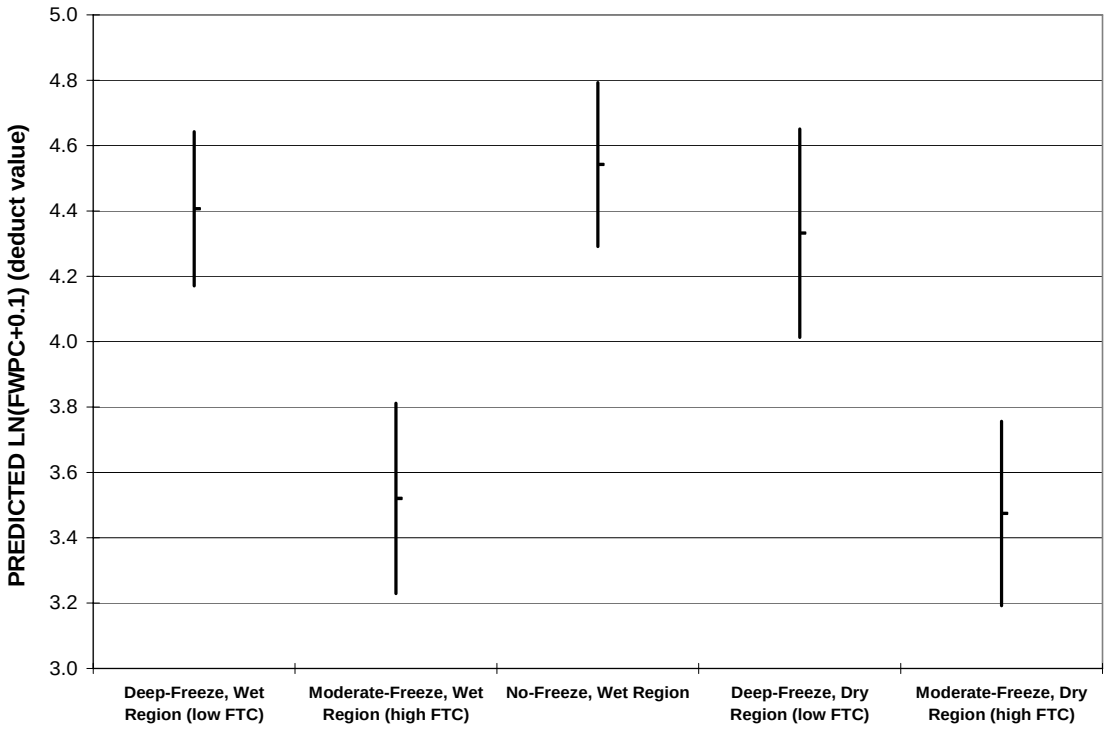

Figure 51. Bar chart. Predicted flexible pavement FWPC values at 20 years for each climatic region (BASE=DGAB/SG=FINE).

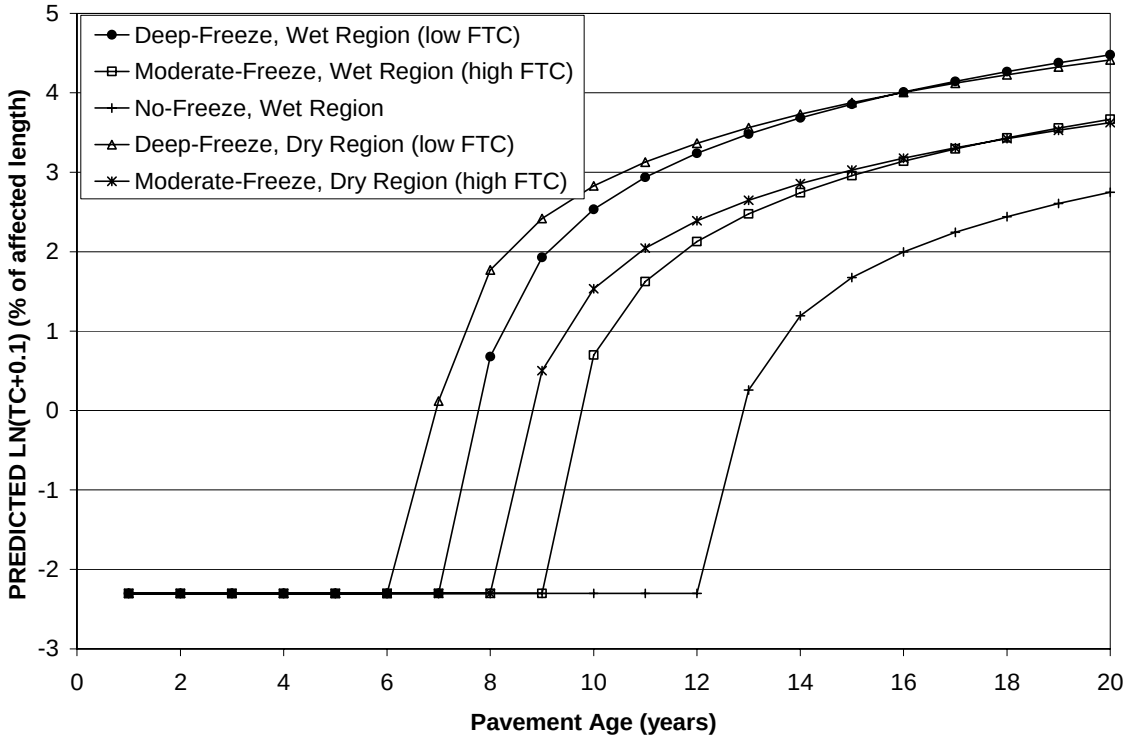

Figure 52. Scatter chart. Mean-predicted flexible pavement TC values for each climatic region (BASE=DGAB/SG=FINE)

Figure 53 provides mean TC predictions accumulated at a pavement age of 20 years along with the upper and lower limits of the confidence interval. Pavements exposed to deep sustained frost penetration exhibit quantities of transverse cracking that are significantly larger than pavements in the multiple FTC climates. In addition, pavements exposed to climatic conditions that are representative of the southern reaches of the no-freeze region accumulate less transverse cracking (at 95 percent confidence) compared to areas with both deep sustained frost and multiple FTCs.

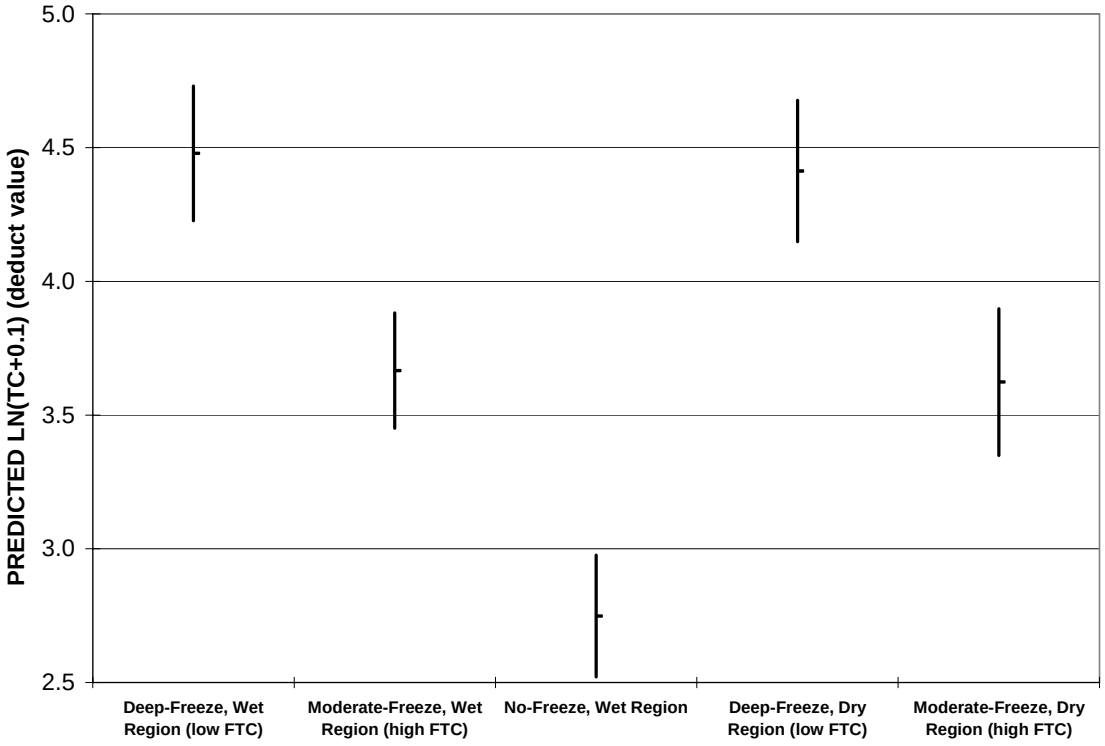

Figure 53. Bar chart. Predicted flexible pavement TC values at 20 years for each climatic region (BASE=DGAB/SG=FINE).

Changes in subgrade, base, and pavement structure types do alter the absolute magnitude of predicted TC. In some cases, the predicted TC deduct value reaches the equivalent of 100 on a natural logarithmic scale at a pavement age less than 20 years. Because the model is predicted natural logarithm of TC plus 0.1, a deduct value of 100 corresponds to the natural logarithm of 100.1 or 4.606. For example, if the predicted TC value for both of the deep-freeze regions reaches this maximum at age 16 while the other climatic scenarios do not reach the maximum value within 20 years, comparing confidence intervals at age 20 for this case would not account for the regions that reached the maximum value 4 years earlier. The deep-freeze regions were capped at 4.606 for those 4 years, while the other regions accumulated additional quantities of TC. To counter this, confidence intervals for all regions would be compared at the earliest age that one region reached the maximum value. For this example, age 16 would be used to make comparisons.

In general terms, comparisons between the various climatic scenarios are similar to those made for DGAB base, FINE subgrade, and nonoverlay pavement structure types. Key exceptions are noted below:

- Predictions for pavements with ROCK/STONE subgrade type are relatively variable and performance differences for these cases are confounded by the error within the model. This is also the case for LCB base types.

- For permeable asphalt-treated base (PATB) and no-base (NONE) base types (nonoverlay structures), deep frost (in both wet and dry climates) contributes to significantly larger accumulations of TC as compared with the multiple FTC climates and the no-freeze wet region. There is no significant difference between the multiple freeze-thaw climates and the no-freeze wet region. This is also true for overlay structures with DGAB/FINE, PATB/FINE, PATB/COARSE, ATB/FINE, NONBIT/FINE, NONBIT/COARSE, NONE/FINE, and NONE/COARSE combinations.
- TC predictions on overlay pavement structures exhibit distress initiation at earlier pavement ages as compared with nonoverlay pavement structures. This is likely caused by cracking in the existing pavement layers reflecting through the overlay layers.
- The observations in transverse cracking initiation as well as accumulation at 20 years are logical in consideration of the driving mechanism of this distress type. Transverse cracking is largely a result of tensile stress that accrues as the pavement contracts as a result of low temperatures. Propagation occurs when the tensile stress exceeds the tensile strength of the asphalt mixture. In addition, the tensile strength of the mixture diminishes with each low temperature cycle. FI represents the duration and severity of the freezing season with higher values of the FI correlating to a longer duration or colder winter, or both (both of which contribute to transverse cracking propagation). Therefore, larger quantities of transverse cracking are expected in areas with a relatively high FI.

LONGITUDINAL CRACKING SURFACE DISTRESS COMPARISONS FOR RIGID PAVEMENTS

As mentioned previously, comparisons of rigid surface distress predictions were made at 25 years because of crack initiation ages greater than 20 years. Figure 54 presents the mean predicted LC values for each climatic scenario. As can be seen, distress initiation occurred at 25 years in the wet no-freeze region. Figure 55 provides the confidence intervals at 25 years.

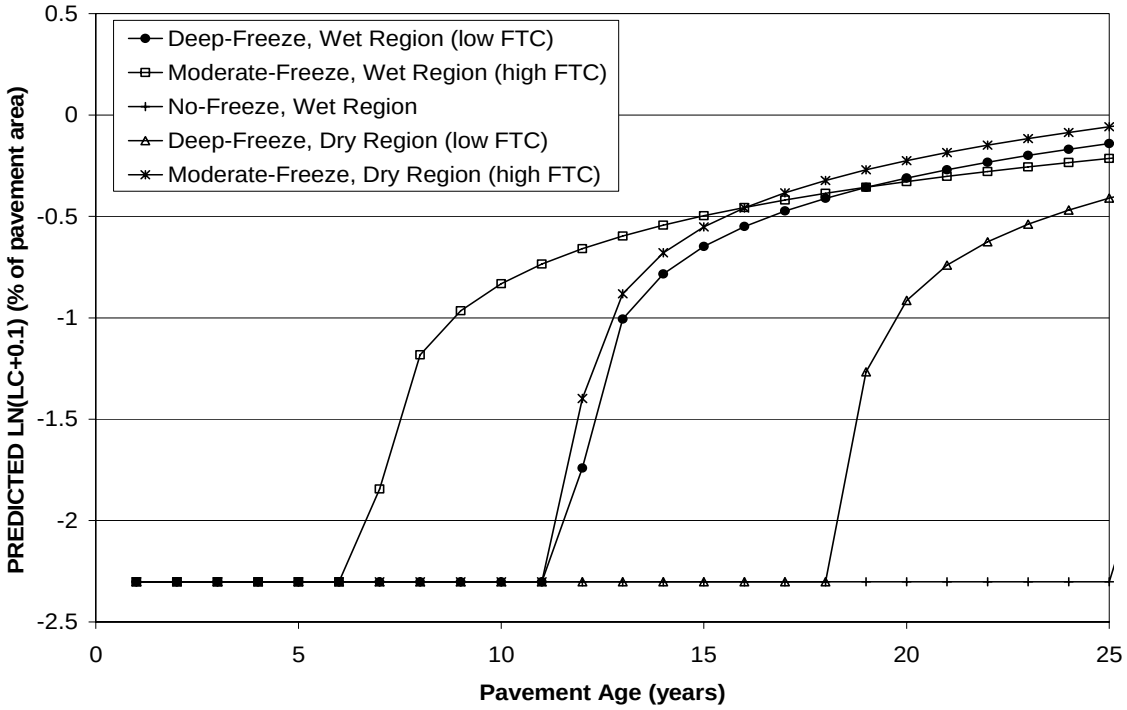

Figure 54. Scatter graph. Mean predicted rigid pavement LC values for each climatic region (BASE=DGAB/SG=FINE).

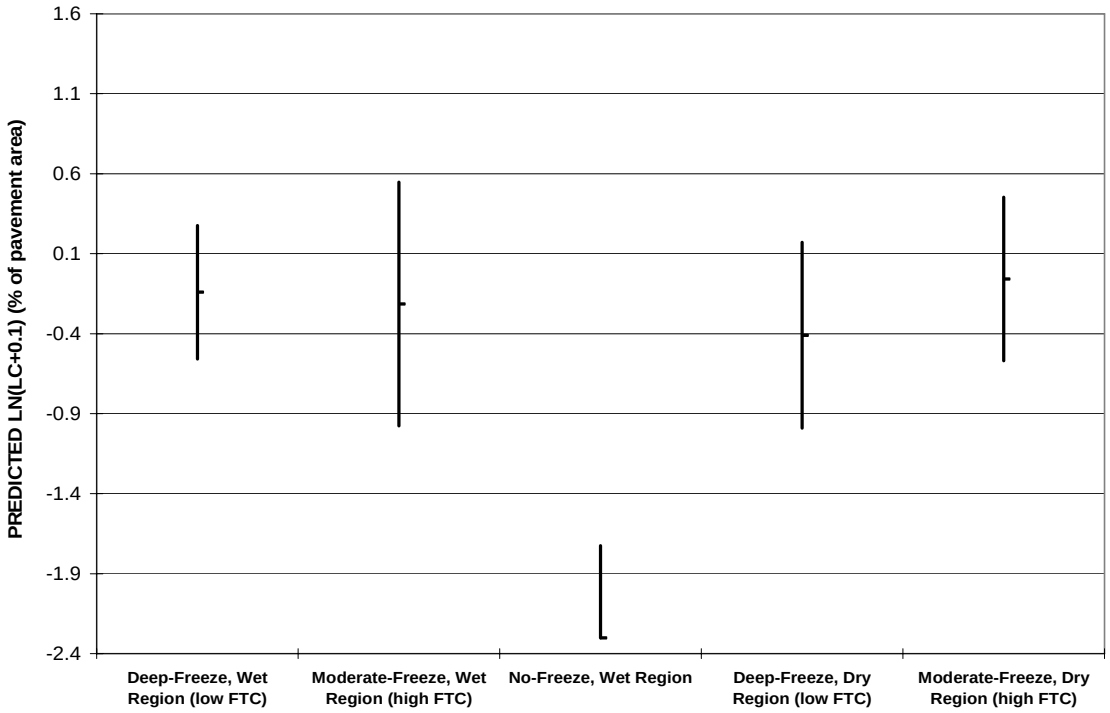

Figure 55. Bar chart. Predicted rigid pavement LC values at 25 years for each climatic region (BASE=DGAB/SG=FINE).

Comparing the deep-freeze region to the moderate-freeze region for both wet and dry climates shows no significant difference in LC performance. On the other hand, the no-freeze wet region at 25 years exhibits significantly lower LC accumulation than the other regions.

The same observations can be made when evaluating longitudinal cracking for different subgrade and base combinations.

TRANSVERSE CRACKING SURFACE DISTRESS COMPARISONS FOR RIGID PAVEMENTS

Figure 56 shows transverse cracking predictions in for each of the climatic scenarios. Figure 57 shows confidence intervals. Crack initiation varies significantly with the moderate-freeze dry region initiating first and the deep-freeze wet region initiating 11 years after construction.

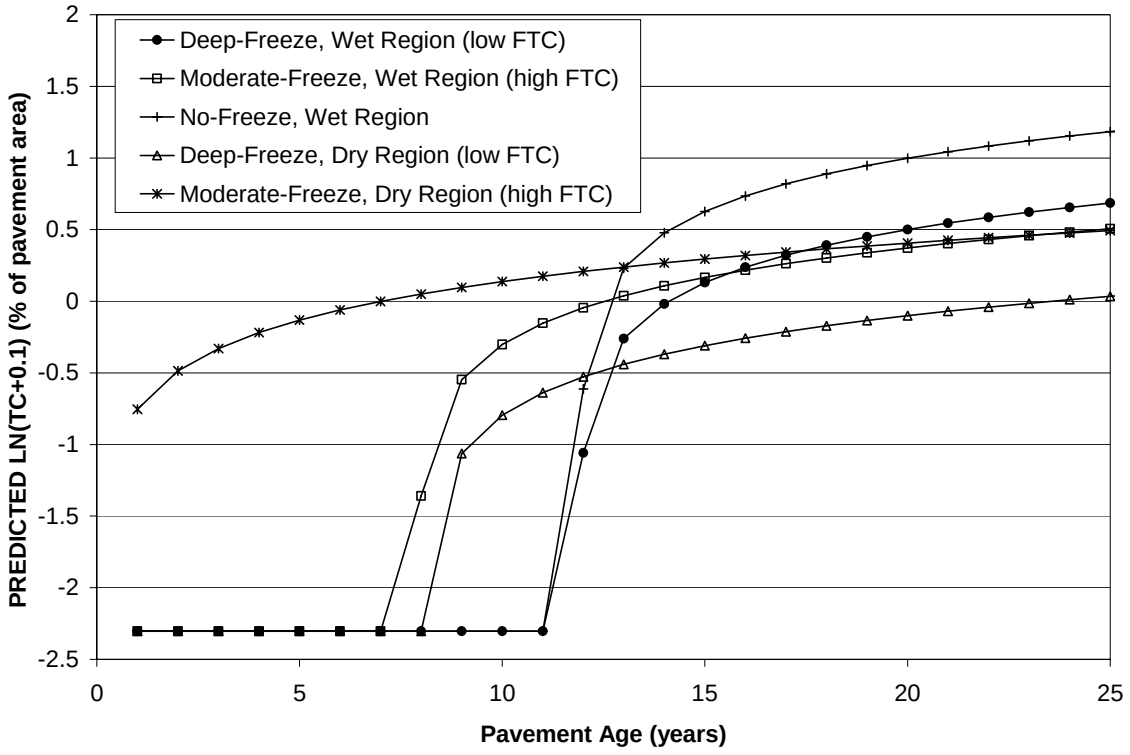

Figure 56. Scatter Graph. Mean predicted rigid pavement TC values for each climatic region (BASE=DGAB/SG=FINE).

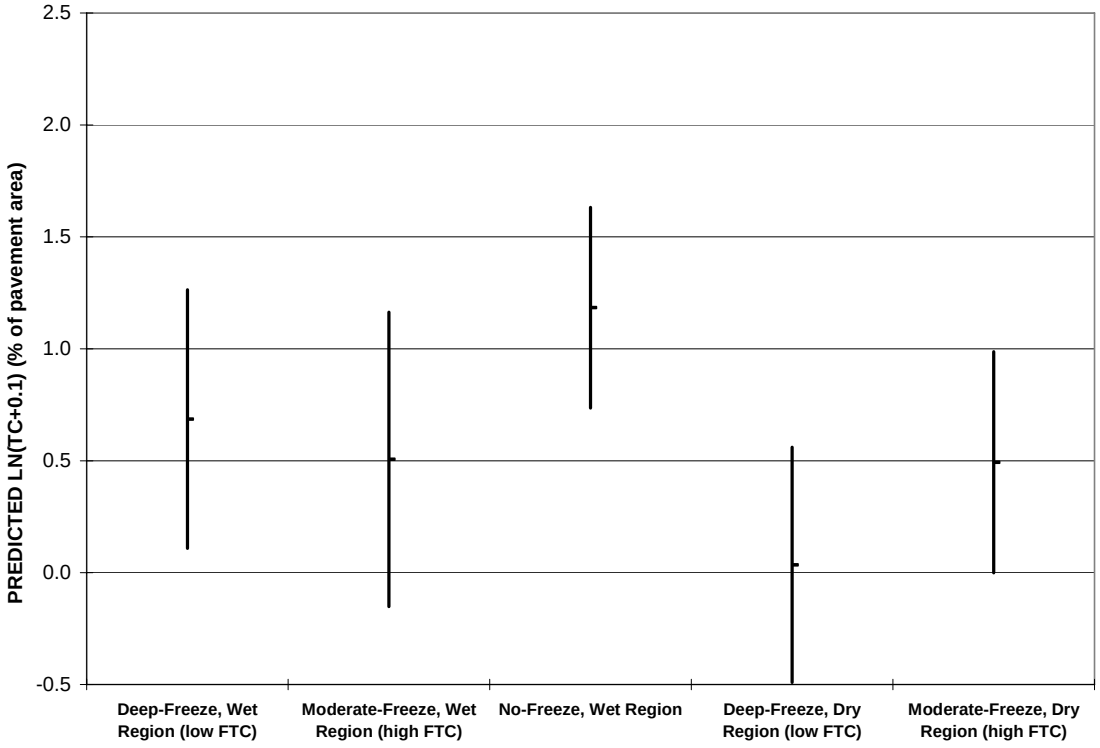

Figure 57. Bar chart. Predicted rigid pavement TC values at 25 years for each climatic region (BASE=DGAB/SG=FINE).

For wet environments, the contribution of deep frost and multiple FTCs did not result in significant transverse crack accumulation differences as compared to the no-freeze region. In addition, transverse cracking differences between the deep-freeze and moderate-freeze climates in dry environments are insignificant; however, the effect of the wet no-freeze region resulted in significantly larger quantities of transverse cracking than the deep-freeze dry region at 25 years.

These observations hold true for the majority of base/subgrade combinations. Rigid pavement structures with PATB and asphalt-treated base (ATB) type categories exhibit considerable variability resulting in all performance differences to be insignificant and confounded by model error.

TRANSVERSE JOINT FAULTING COMPARISONS FOR RIGID PAVEMENTS

Mean transverse joint faulting predictions as a function of age are shown in figure 58 for each climatic scenario. The models used to develop the predictions were based on average faulting over the entire test section; therefore, the model does not predict faulting for one joint but rather for the average for a pavement segment.

Figure 59 provides confidence interval data at a pavement age of 20 years. Faulting in climates with considerable amounts of annual precipitation is not significantly different between any of the frost settings.

In drier climates, deep-frost penetration contributes to an increased accumulation of faulting as compared with the multiple FTC and no-freeze wet regions.

The same observations can be made for the majority of the base/subgrade combinations. The variability inherent in all combinations with ROCK/STONE subgrade is relatively high, which confounds the differences in predicted performance. For structures with ATB and NONBIT, deep frost (in the dry climate) contributes to significantly larger accumulations of faulting than the multiple freeze-thaw (dry) climate at a pavement age of 20 years; however, predictions in these climates are not statistically different than the no-freeze wet region.

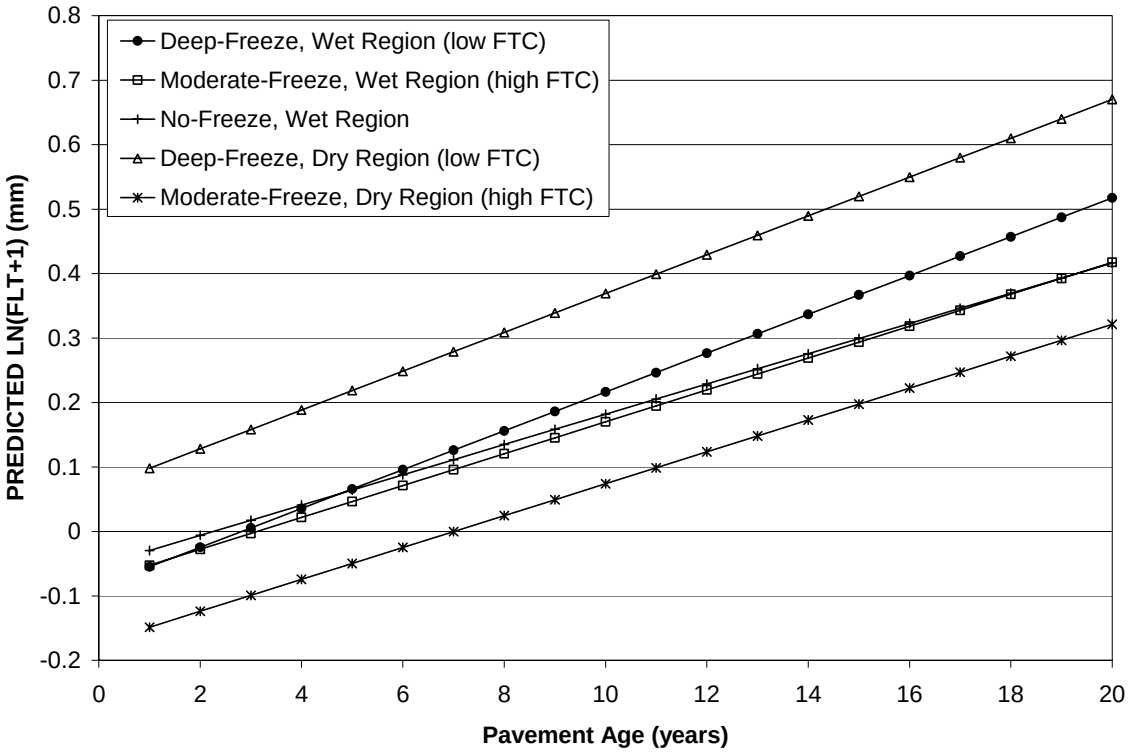

1 mm = 0.04 inch

Figure 58. Scatter chart. Mean predicted rigid pavement FLT values for each climatic region (BASE=DGAB/SG=FINE).

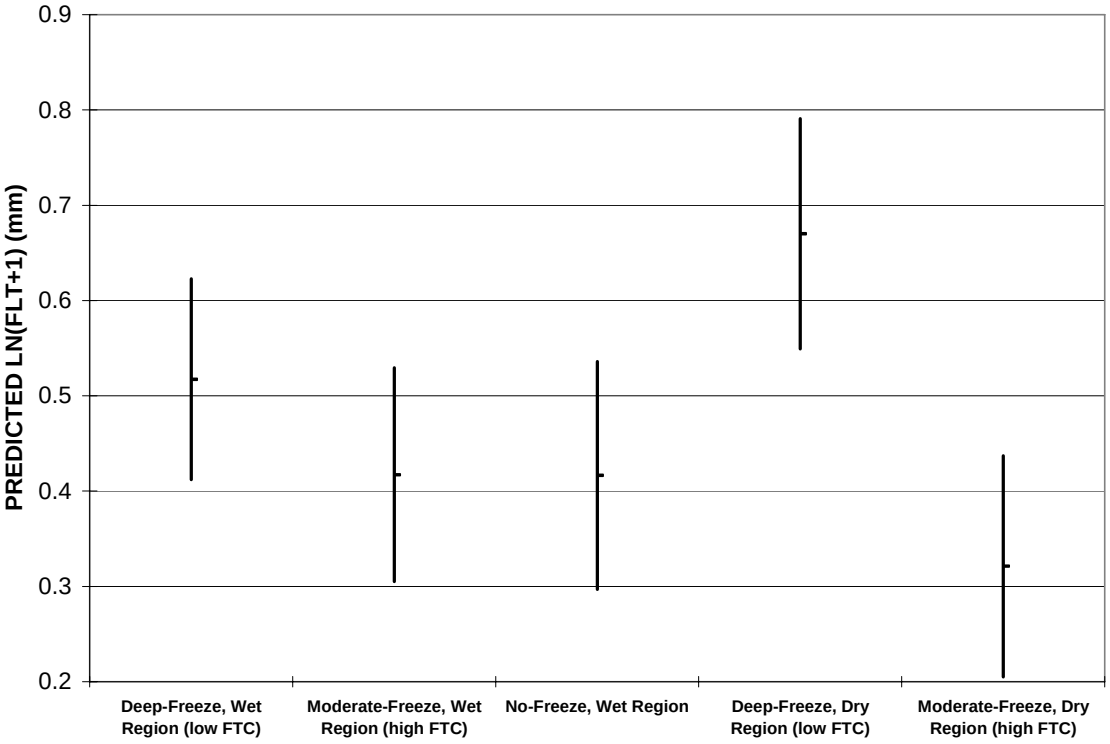

1 mm = 0.04 inch

Figure 59. Bar chart. Predicted rigid pavement FLT values at 20 years for each climatic region (BASE=DGAB/SG=FINE).

7. INDEPTH AGENCY COMPARISONS

To further the investigation of frost penetration and multiple FTCs, an indepth comparison of predicted performance was conducted for all of the States contributing to the pooled fund study. Information on the environment for every test section used in the analysis dataset and located in one of the PFS is provided in table 23. The test sections highlighted in the table were selected as the representative climate conditions for the respective agency. These values were used along with constant nonenvironmental factors, shown in table 20, to predict flexible pavement performance.

Table 23. Measured environmental data for LTPP sites.

State	Site	FTC	FI	CI	PRECIP
Alaska	1002	112	793	0	2020
Alaska	1001	124	890	0	1116
Alaska	1004	87	1110	2	420
Alaska	6010	92	1248	1	413
Alaska	9035	106	1513	3	729
Alaska	1008	74	2584	23	317
Alaska	***average***	***99***	***1356***	***5***	***836***
Idaho	1001	113	217	158	693
Idaho	1005	121	399	339	627
Idaho	1007	121	326	271	254
Idaho	1009	137	351	221	262
Idaho	1010	136	665	144	303
Idaho	1020	128	328	331	280
Idaho	1021	129	622	149	342
Idaho	3017	125	356	344	342
Idaho	3023	107	278	400	295
Idaho	6027	162	817	57	380
Idaho	9032	111	259	121	718
Idaho	9034	117	316	89	807
Idaho	***average***	***127***	***432***	***213***	***398***
Illinois	1003	79	212	742	1052
Illinois	6050	78	239	747	995
Illinois	1002	96	652	383	871
Illinois	***average***	***84***	***368***	***624***	***973***

Table 23. Measured environmental data for LTPP sites (continued).

State	Site	FTC	FI	CI	PRECIP
Indiana	1028	80	217	696	1209
Indiana	1037	73	152	821	1186
Indiana	2008	84	399	471	963
Indiana	3002	84	451	520	950
Indiana	3003	88	454	453	1005
Indiana	3030	88	386	476	1017
Indiana	3031	70	230	772	1165
Indiana	6012	71	215	798	1165
Indiana	***average***	***80***	***313.1***	***625.9***	***1082.5***
Michigan	0200	86	382	443	866
Michigan	0100	105	510	324	870
Michigan	1010	91	532	309	825
Michigan	1013	109	568	251	915
Michigan	1012	115	612	230	931
Michigan	3068	109	670	215	827
Michigan	1001	109	759	174	790
Michigan	6016	100	787	173	751
Michigan	1004	77	960	131	878
Michigan	***average***	***100***	***642***	***250***	***850***
New York	0800	87	437	319	891
New York	1011	90	505	298	1007
New York	1008	87	582	257	1133
New York	1643	99	618	270	1006
New York	1644	109	990	111	1110
New York	***average***	***94***	***627***	***251***	***1029***
North Carolina	0800	47	14	998	1343
North Carolina	1645	57	19	975	1260
North Carolina	1030	50	24	951	1192
North Carolina	2825	52	28	965	1093
North Carolina	1352	69	32	876	1232
North Carolina	1028	54	32	870	1186
North Carolina	3008	67	33	815	1212
North Carolina	1006	60	35	887	1153
North Carolina	2819	69	43	799	1139
North Carolina	3816	71	44	830	1141
North Carolina	3011	71	45	867	1151
North Carolina	3807	77	46	772	1142
North Carolina	1817	74	46	779	1126
North Carolina	0200	83	47	773	1151
North Carolina	3044	77	49	784	1161
North Carolina	1992	73	53	779	1221
North Carolina	2824	73	54	780	1224

Table 23. Measured environmental data for LTPP sites (continued).

State	Site	FTC	FI	CI	PRECIP
North Carolina	1802	82	58	775	1110
North Carolina	1024	93	59	475	1308
North Carolina	1814	100	70	446	1477
North Carolina	1803	107	86	407	1371
North Carolina	1801	88	116	323	1205
North Carolina	1040	109	141	218	1441
North Carolina	***average***	***74***	***51***	***745***	***1219***
Ohio	3801	89	249	480	1037
Ohio	3013	89	250	533	1140
Ohio	0100	96	375	414	972
Ohio	0200	96	375	414	972
Ohio	0800	96	375	414	972
Ohio	***average***	***93***	***325***	***451***	***1018***
Pennsylvania	3044	99	269	433	1164
Pennsylvania	1623	95	309	415	1004
Pennsylvania	1608	107	311	334	944
Pennsylvania	1605	107	331	339	1092
Pennsylvania	1618	100	343	270	1028
Pennsylvania	1597	111	514	196	865
Pennsylvania	1599	124	546	141	1121
Pennsylvania	***average***	***106***	***375***	***304***	***1031***

Note: Shaded cells denote climate selected as representative for agency.

Figure 60 shows pavement roughness predictions. In comparing these results with the confidence interval results in figures 44 and 45, it appears that Alaska's climate contributes to larger accumulations of pavement roughness compared to the other agencies; however, because the differences in performance are relatively small, it is doubtful that they are significant.

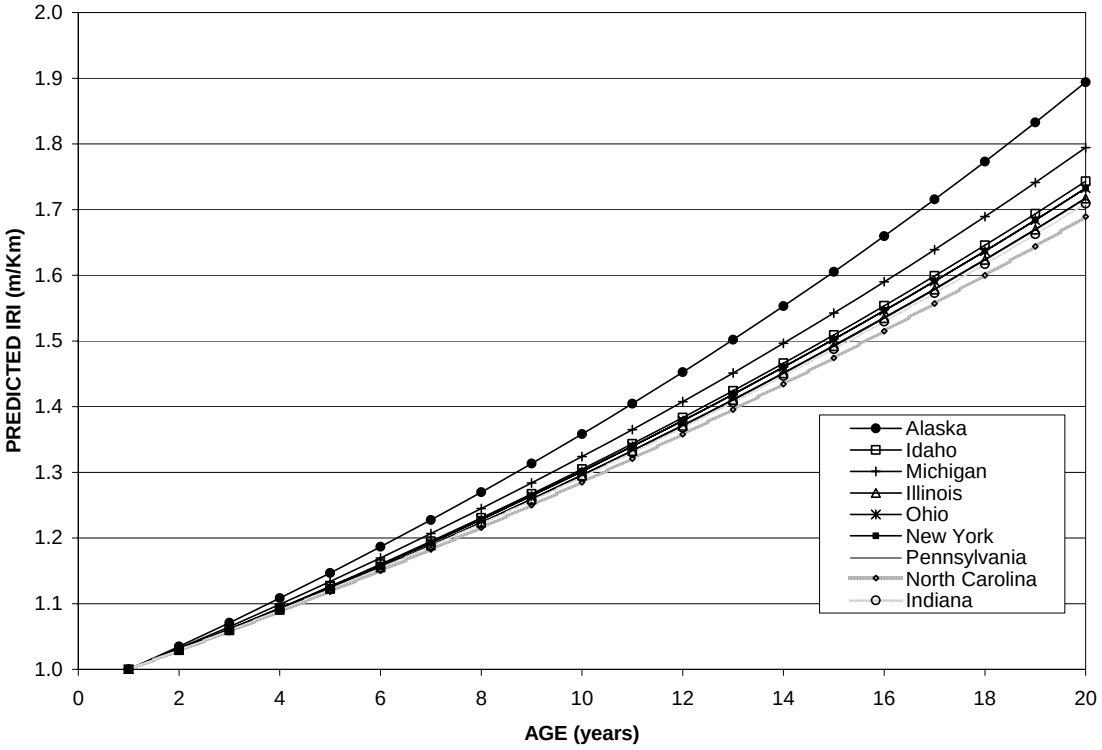

1 m/km = 5.28 ft/mi

Figure 60. Scatter chart. Flexible pavement IRI for selected sites in each agency.

Figure 61 lists rutting performance predictions for each of the agency's representative climates. The confidence interval information in figures 48 and 49 can be used to determine the significance of the predicted differences between the participating agencies. The most obvious observation is the small accumulation of rutting predicted in Alaska and North Carolina in comparison with all other PFS, which appears to be significantly less than the climates in Idaho, Pennsylvania, and New York. All other variations in rutting performance do not appear to be significant.

While the climate in Alaska contributes to minimal amounts of rutting, the tradeoff is evident in the development of transverse cracking. From figure 62, transverse cracking in Alaska initiates very early in the pavement life and reaches a maximum deduct value at age 16 years. This is the likely source of increased pavement roughness values predicted for Alaska in figure 60. Transverse cracking predictions for North Carolina are significantly smaller than all of the other agencies. Climates in Illinois and Indiana exhibit transverse cracking that is very similar, and the contribution of these climates results in significantly smaller amounts of transverse cracking compared to Michigan and New York. Predictions for Idaho, Ohio, and Pennsylvania fall in between the Illinois/Indiana and Michigan/New York climates; however, the differences are insignificant, and they may be the result of error within the regression models.

Last, figure 63 provides fatigue and wheelpath cracking predictions for each of the respective agency climates. Predicted cracking in the New York and Indiana regions are slightly less than the other agencies. These differences, however, are not significant.

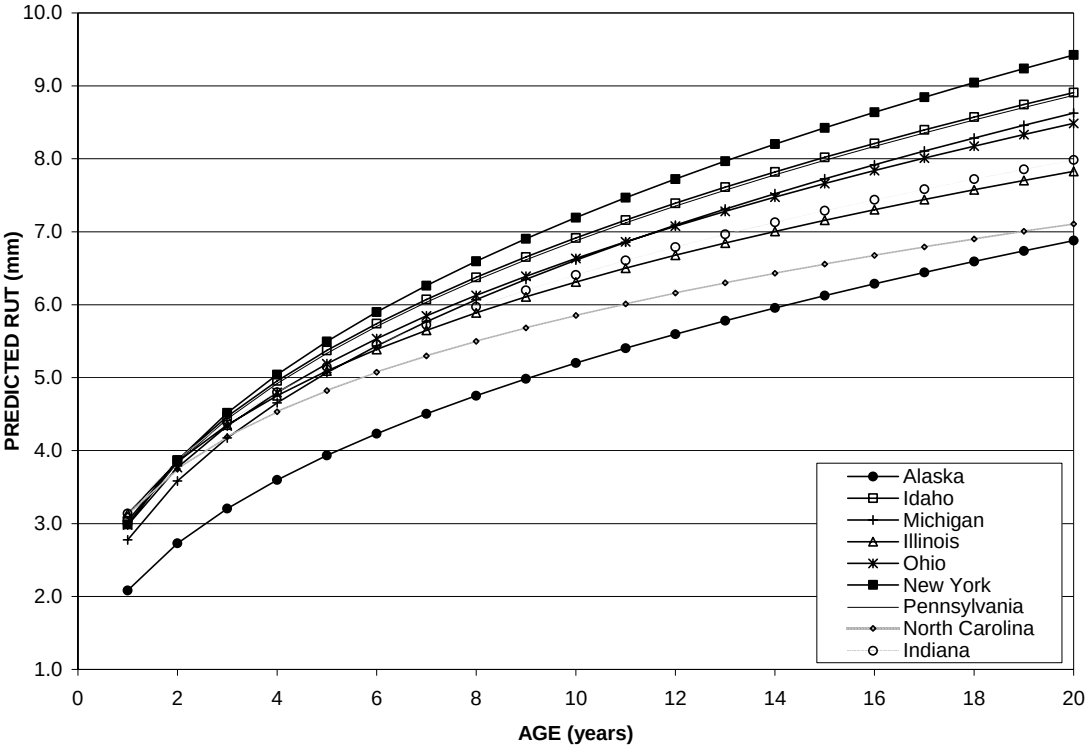

1 mm = -0.04 inch

Figure 61. Scatter chart. Flexible pavement RUT for selected sites in each agency.

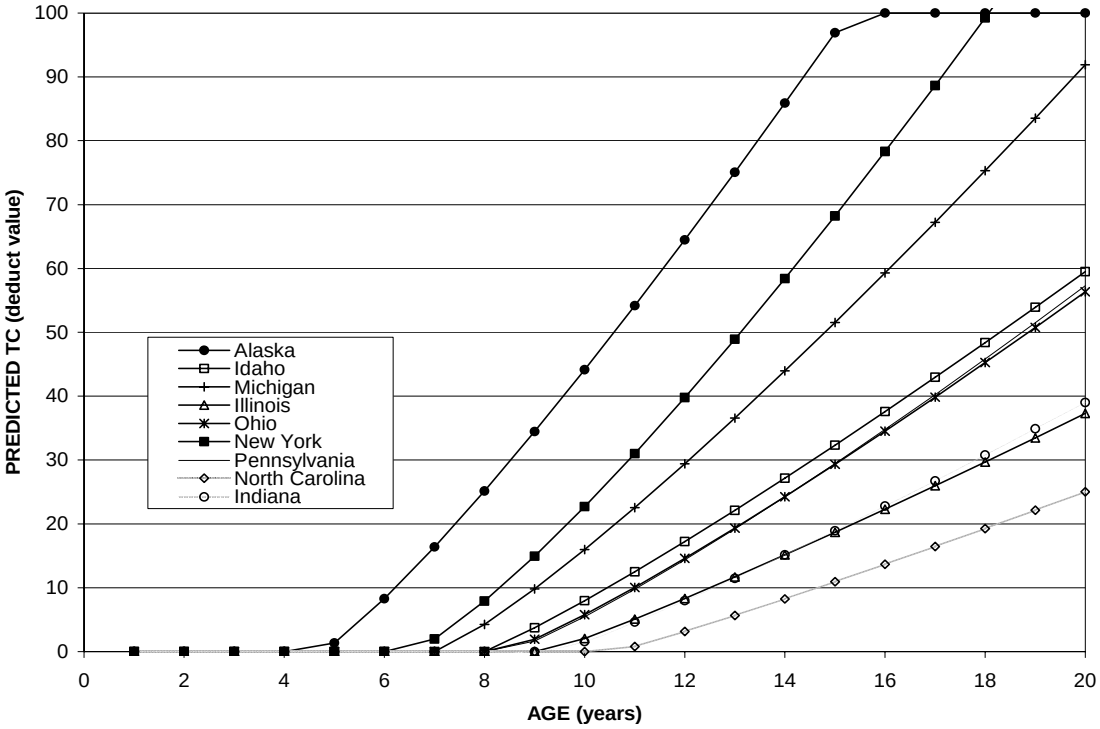

Figure 62. Scatter chart. Flexible pavement TC for selected sites in each agency.

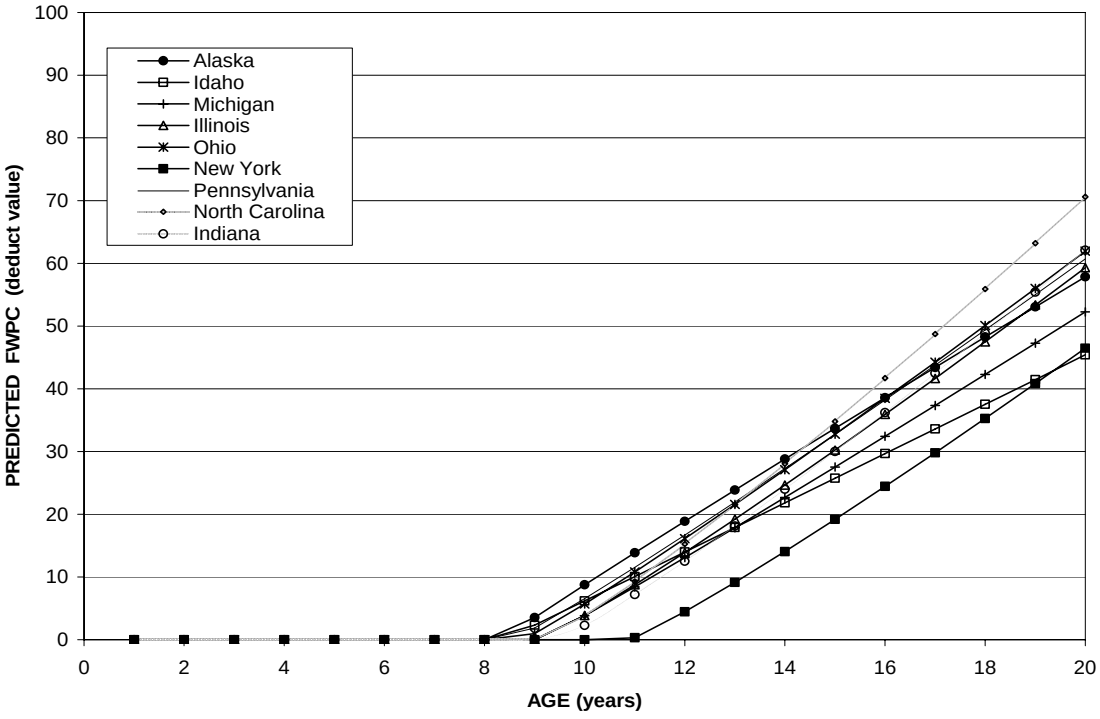

Figure 63. Scatter graph. Flexible pavement FWPC for selected sites in each agency.

It should be noted that these comparisons were based on the environmental conditions observed at one representative location within the agency. It is well known that climates can vary drastically from one location to the next within an agency and a so-called representative climate does not accurately describe climatic conditions for all areas of the agency. As such, an evaluation of regional environments was conducted for each participating state.

Figures 83 through 91 in appendix C show State maps containing the geographic location of each test section used in the study. Tables below each of the figures contain environmental and pavement structure information (GPS test sections only) corresponding to the test sections. Test sections in each agency were grouped based on FI. Some States exhibit climates that fall within the different climatic zones established for the analysis (i.e., deep-freeze, moderate-freeze, and no-freeze). Test sections were grouped based on climatic zone for these cases. In other States, all climates were characteristic of one of the defined zones; however, the test sections were divided where large differences in FI were noted. For example, all test sections in New York fall into the deep-freeze region, but the FI at site 1644 is considerably higher; therefore, this site was separated from the average of the remaining sites in New York.

Some of the largest climatic variations occur in Idaho and Michigan. To highlight the differences in performance across one state, environmental factors from two sites in each of these States were used, along with the standard nonenvironmental factors in table 19, to predict performance. In Idaho sites 1001 and 6027 were selected because they are at the two climatic extremes in the State. Similarly, sites 0200 and 1004 were selected from Michigan.

Figure 64 provides FWPC predictions for the Idaho sites. Site 1001 exhibits a predicted deduct value of more than 2.5 times larger than the prediction for site 6027 at 20 years. This is a significant difference. It is interesting to note that site 1001 has lower FI and FTC values in comparison with site 6027. However, site 1001 is in the wet region while site 6027 is in the dry region. In addition, site 6027 has a larger CI than site 1001.

TC predictions for the two sites in Michigan can be found in figure 65. Predictions for site 1004 reach a maximum level of 100, while the predictions for the environment at site 0200 are at approximately 50. The environment at site 1004 has a very large FI value in comparison to site 0200. Conversely, CI is smaller at site 1004 than at site 0200. Both are in the wet region and experience similar amount of FTCs (77 and 86 for site 1004 and 0200, respectively).

These examples highlight the regional differences in performance that can be expected in one State given a constant pavement structure and traffic loading conditions.

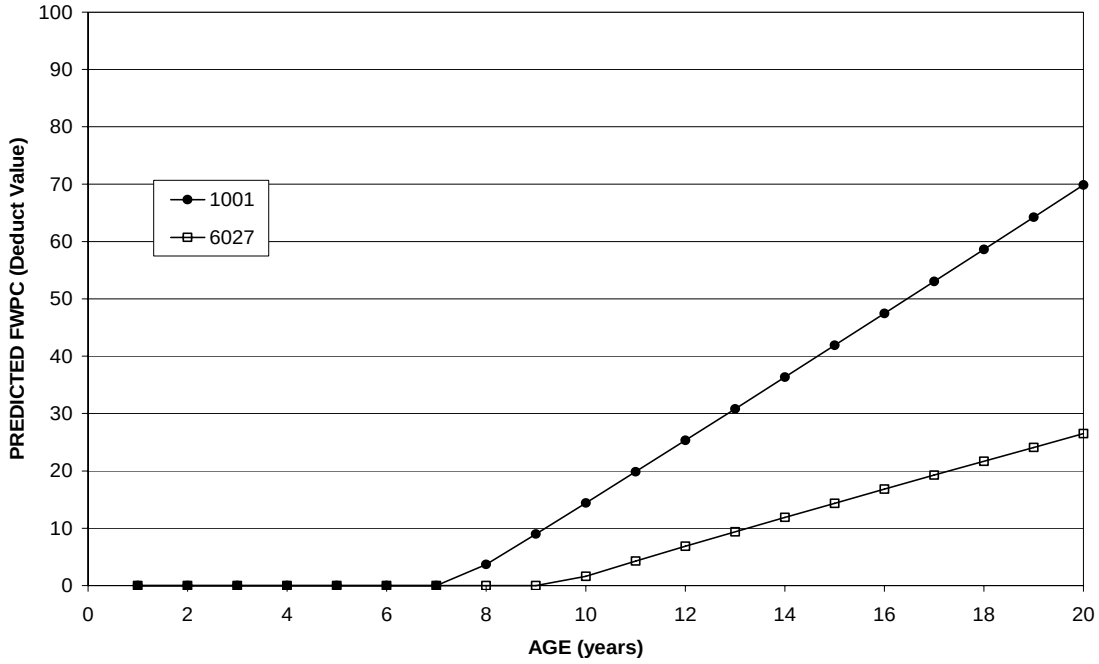

Figure 64. Scatter graph. FWPC predictions for sites 1001 and 6027 in Idaho.

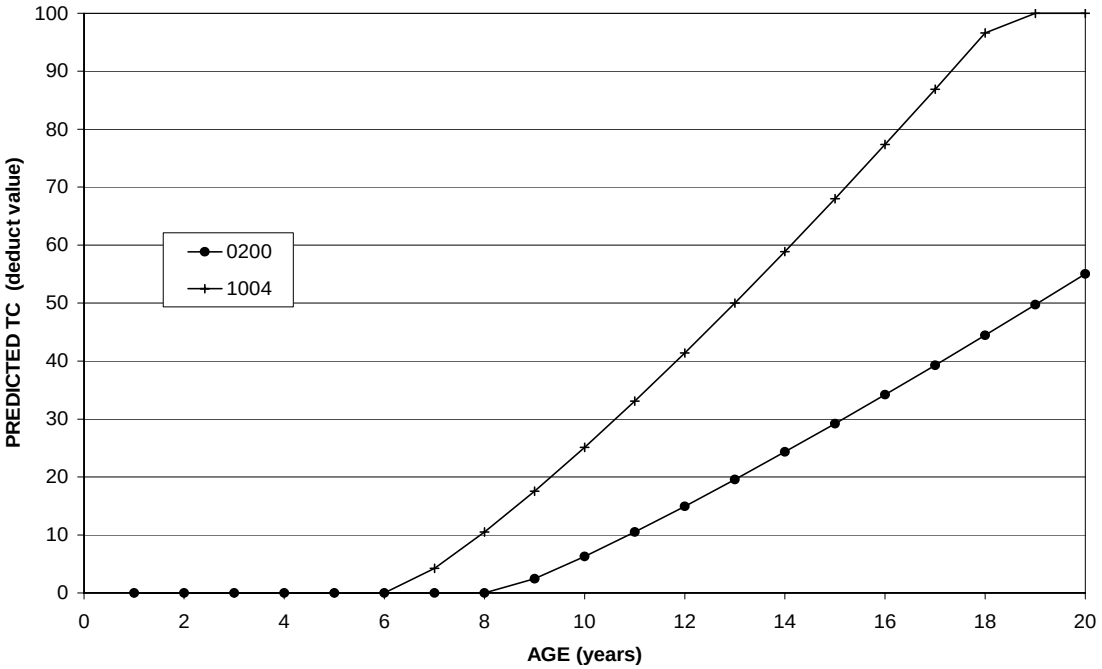

Figure 65. Scatter graph. Flexible TC predictions for the environments at sites 0200 and 1004 in Michigan.

8. LOCAL ADAPTATIONS OF EMPIRICAL PAVEMENT DESIGN PRACTICES AND MATERIALS STANDARDS

One of the primary study areas requested in the proposal was for the *"Analysis of the extent to which local adaptations of materials standards and empirical pavement design practices have been effective at reducing the rate of pavement deterioration."*

To gain an understanding of State design practices, a questionnaire was developed and sent to the PFS participants. The complete questionnaire is provided in appendix D. Basic information on standard roadway sections including structural design for given scenarios, standard specifications, and test procedures was requested. Questions regarding average unit bid prices and typical service life estimates were included for purposes of LCCA. A query on the knowledge of current treatment practices implemented by adjacent SHAs was also incorporated.

The pavement sections or specific pavement designs provided by the States are shown in tables 24 through 27.

Table 24. Primary highway flexible pavement design summary.

States	AC (mm (inch))	Treated Base (mm (inch))	Untreated Base (mm (inch))	Total Depth (mm (inch))	Treated SG (mm (inch))	Total FF[a] Depth (mm (inch))
Alaska	130 (5)	NA	480 (19)	710 (24)	915 (36) select	1270 (50)
Idaho	165 (6.6)	NA	305 (12)	470 (18.6)	NA	470 (18.6)
Illinois	355 (14)	NA	0 (0)	355 (14)	305 (12) lime	660 (26)
Michigan	170 (6.5)	NA	710 (24)	775 (30.5)	var. gr. surf	1065-1525 (42–60)
New York	150 (6)	100 (4) ATPB	305 (12)	560 (22)	NA	560 (22)
North Carolina	265 (10.5)	NA	255 (10)	NA	NA	520 (20.5)
Ohio	203 (8)	NA	150 (6)	355 (14)	no A-4b for 915 (36)	1270 (50)
Pennsylvania	445 (17.5)	NA	0 (0)	445 (17.5)	NA	445 (17.5)

[a]FF=frost-free.
Design conditions: 30-year design; 5 million ESALs; frost-susceptible fine-grained soil with resilient modulus of 68,950 kilopascals (kPa) (10,000 pounds of force per square inch (lbf/in^{2})).

Table 25. Primary highway rigid pavement design summary.

States	PCC (mm (inch))	Treated Base (mm (inch))	Untreated Base (mm (inch))	Treated SG (mm (inch))	Total FF[a] Depth (mm (inch))
Alaska	NA	NA	NA	NA	NA
Idaho	230 (9)	50 (2) ATPLC	305 (12)	NA	585 (23)
Illinois	250 (9.75)	100 (4)	NA	305 (12) lime	655 (25.75)
Michigan	215 (8.5)	150 (6) UTB	255 (10)	var. gran. mat	1065-1525 (42–60)
New York	255 (10)	100 (4) ATPB	305 (12)	NA	660 (26)
North Carolina	205 (8)	115 (4.5)	NA	205 (8) lime	520 (20.5)
Ohio	205 (8)	NA	152 (6)	no A-4b for 915 (36)	1270 (50)
Pennsylvania	205 (8)	NA	205 (8)	NA	405 (16)

[a]FF=frost free

Design conditions: 30-year design; 5 million ESALs; frost-susceptible, fine-grained soil with resilient modulus of 68,950 kPa (10,000 lbf/in^2).

Table 26. Interstate highway flexible pavement design summary.

States	AC (mm (inch))	Treated Base (mm (inch))	Untreated Base (mm (inch))	Treated Subgrade (mm (inch))	Total Depth (mm (inch))
Alaska	NA	NA	NA	NA	NA
Idaho	200 (7.8)	NA	710 (24)	NA	810 (31.8)
Illinois	515 (20.25)	NA	0 (0)	305 (12) lime	820 (32.25)
Michigan	185 (7.25)	NA	710 (24)	1065 (42) granular	1860 (73.25)
New York	180 (7)	100 (4) ATPB	305 (12)	NA	585 (23)
North Carolina	405 (16)	NA	255 (10)	NA	660 (26)
Ohio	290 (11.5)	NA	150 (6)	no silt for 915 (36)	1360 (53.5)
Pennsylvania	420 (16.5)	NA	255 (10)	NA	675 (26.5)

Design conditions: 30-year design; 10 million ESALs; frost-susceptible fine-grained soil with resilient modulus of 68,950 kPa (10,000 lbf/in^2)..

Table 27. Interstate highway rigid pavement design summary.

States	PCC (mm (inch))	Treated Base (mm (inch))	Untreated Base (mm (inch))	Treated Subgrade (mm (inch))	Total Depth (mm (inch))
Alaska	NA	NA	NA	NA	NA
Idaho	305 (12)	50 (2) ATPLC	305 (12)	NA	660 (26)
Illinois	265 (10.5)	100 (4)	0 (0)	305 (12) lime	675 (26.5)
Michigan	290 (11.5)	NA	405 (16)	1065 (42) granular	1765 (69.5)
New York	255 (10)	100 (4) ATPB	305 (12)	NA	660 (26)
North Carolina	280 (11)	115 (4.5)	0 (0)	205 (8) lime	600 (23.5)
Ohio	290 (11.5)	NA	150 (6)	no silt for 915 (36)	1360 (53.5)
Pennsylvania	330 (13)	100 (4) ATPB	100 (4)	NA	535 (21)

Design conditions: 30-year design; 10 million ESALs; frost-susceptible fine-grained soil with resilient modulus of 68,950 kPa (10,000 lbf/in^2).

LOCAL ADAPTATIONS OF PAVEMENT DESIGN PRACTICES

As can be seen from these tables, there was a large variation in the roadway design sections reported for each SHA. There was no specific trend in the pavement designs between those SHAs that experience deep frost and those that experience moderate to no frost penetration. No SHA reported any specific design thickness requirement based on frost depth. One SHA, Pennsylvania, noted design consideration for frost heave in accordance with the 1993 AASHTO *Design Guide*. In particular, the design is based on the loss in serviceability because of frost heave as described in appendix G of the 1993 *AASHTO Guide for Design of Pavement Structures*.(1)

All of the SHAs provided a pavement design based on the subgrade soils resilient modulus (M_R) value noted in the questionnaire without accounting for frost effects; however, one SHA does not design pavement structures for M_R values greater than 41,370 kPa (6,000 lbf/in^2). This may reflect either the weaker soils that are encountered in the State or a method to partially account for thaw weakening in the environment of the State. Two SHAs indicated that their standard construction procedures require that frost-susceptible subgrade soils be removed for a depth of 1m (3 ft) or more. This additional provision is shown as treated subgrade in tables 24 through 26 (Michigan and Ohio).

Alaska traditionally places roadways on embankment sections that consist of a minimum height of 1m (3 ft) of select frost-free material. This practice provides for a minimum of

1 m (3 ft) of frost-free material, in addition to the normal pavement design thickness, to protect the pavement against weakening from frost heave and thaw.

To be consistent with the pavement performance indicated from the LTPP database, Idaho reported design sections that generally represent design procedures that were in place during the development of the LTPP test sections. The SHA is now incorporating a rock cap in much of its new construction that consists of 0.3 to 0.6 m (1 to 2 ft) of rock ballast placed between the subgrade and the surfacing layers, which has been shown to provide long-term benefits in the reduction of frost and moisture-related pavement damage. Nordic countries such as Sweden typically use a similar ballast layer that is usually placed at depths of a little more than 1 m (3 ft).[17] Figure 66 provides a photograph of a deep-base section in Sweden.

In earlier studies, many northern SHAs were found to require a minimum depth of frost-free material ranging from 50 to 100 percent of the maximum measured frost depth[4] for the specific design area. SHAs such as Utah require 100 percent of the measured frost depth, which ranges from 0.6 m (2 ft) to more than 1.2 m (4 ft) in that region. The recent reconstruction of I-15 through Salt Lake City used a 330-mm (13-inch) thick PCC over a 205-mm (8-inch) open graded drainage layer with an additional 380 mm (15 inches) of granular subbase to provide for the required 915 mm (36 inches) of frost measured in the area.[18]

The effect of these treatments is difficult to quantify because the treatments may or may not be incorporated into the existing LTPP sites depending on individual SHA practice. This may be accounted for in the models developed from the LTPP database because these practices are part of the roadway sections in the GPS experiment. The consultant did not directly separate sites with extra surfacing depths based on individual agency policy to either subexcavate frost-susceptible soils or add additional granular base based on local frost depths from the remaining sites. To a limited extent, additional surfacing beyond normal AASHTO design depths is represented and accounted for in the LESN term that was found to have a significant contribution as an explanatory variable in the models developed in this research study.

In general, it appears that many SHAs deal with greater frost depths by adding additional granular surfacing to reduce or prevent frost heaving. Some SHAs accomplish this by replacing the frost-susceptible subgrade with an acceptable frost-free material at fairly specific depths or at variable depths depending on the environmental range in that State. Other SHAs increase the pavement depth using additional gravel surfacing consistent with measured frost depths. Not all SHAs follow these practices, and the LTPP database incorporates pavement deterioration trends from all SHAs including northern SHAs that increase the surfacing and those who do not.

Many SHAs increase the depth of frost-free material over that required by the *AASHTO Guide for Design of Pavement Structures*[1] to minimize frost heaving effects where significant frost depths occur. The literature review and SHA research review did not find any specific examples where a difference in pavement performance was quantified relative to increased surfacing depths or removal of frost-susceptible soils. Considering

the prevalence of the practice across the northern tier SHAs, it appears to be a general, but not universal, practice.

For years, Washington has minimized frost heaving effects and thaw weakening on low-volume roadways by adding gravel surfacing beyond that designated by the AASHTO pavement design procedure for frost depth. The use of additional surfacing significantly increased the service life of the roadway and minimized or eliminated the need for spring load restrictions to protect the roadway. Washington State, as part of its Highway System Plan, includes an Economic Initiative Strategy and subprogram for "All Weather Roadways (Freeze/Thaw)," which is directed to improving low-volume roadways that should be open throughout the winter for the transportation of goods and services.[19] That program consists largely of rebuilding low-volume roadways by increasing the surfacing depth to minimize the effect of frost heaving and thaw weakening. The ultimate goal is to minimize or eliminate the need for spring load closures to protect the roadway, which often causes an economic hardship to the local community. That program has been quite successful.

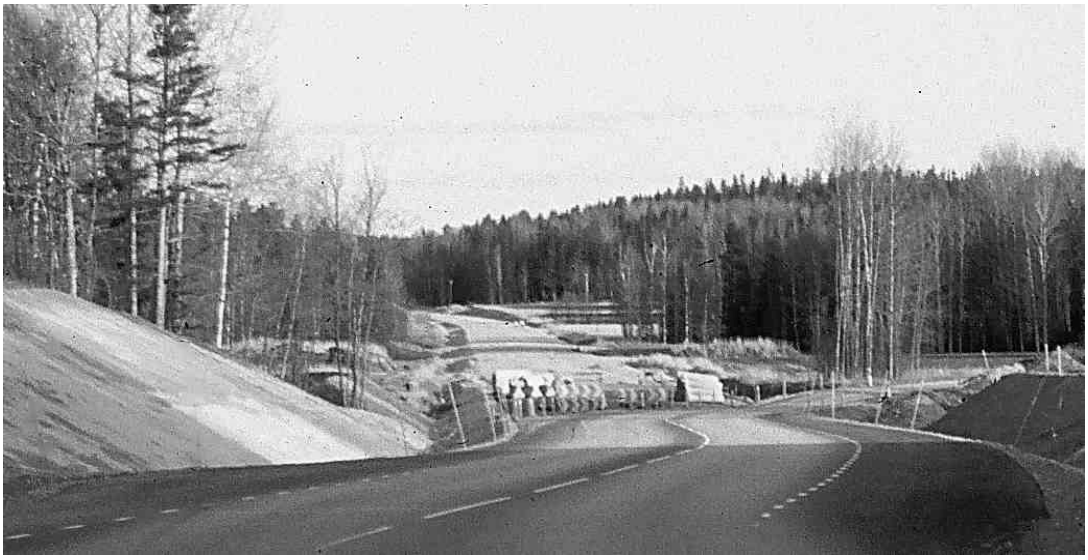

Figure 66. Photo. Road construction in Sweden with deep base section.

There was a very limited amount of literature available from the participating and adjacent SHAs regarding frost penetration and FTC mitigation. A study conducted for Ohio found that overlays in areas with high snowfall deteriorate faster than those in other areas.[20] Two studies performed in Alaska considered differential thaw settlement when considering pavement structural performance and the statewide pavement management system.[21,22] Soil characteristics were investigated and empirically linked to pavement performance.

One source of information on frost heaving and thaw weakening was the WSDOT Pavement Guide, which includes a description of frost action as well as several reviews of other SHA practices.[4] It provides a general description of frost heaving and thaw

weakening as well as a discussion on other SHA practices including added surfacing based on depth of frost. Drainage and the use of capillary blankets are also addressed.

In special cases, such as in the Western States and Northeastern States, where rolling to mountainous terrain are present, moisture enters the roadway prism flowing along lateral soils deposits. This happens in varied silt and sand layers or on top of rock contact zones. Washington State has this terrain, where much of the moisture enters the roadway prism laterally instead of vertically from capillary tension, which also produces ice lenses and causes frost heaving. WSDOT has significantly reduced frost heaving in these areas through the use of longitudinal drainage where the water can be intercepted before it enters the roadway prism, as shown in the photograph in figure 67. Most of the worst frost heaving areas in the State highway system exists in the northeastern slopes of the Cascade Mountain Range. This has been corrected either by digging out and increasing the surfacing depths, adding more surfacing depth, or installing longitudinal drainage along the inslope of the ditch line.(23)

Similar treatments have been used by the New York State Department of Transportation (NYSDOT).(24) In addition, NYSDOT has required the use of rock subgrade fragmentation where the rock is fragmented for a depth of .9 to 1.2 meters (3 to 4 ft) below subgrade during rock excavation to provide adequate drainage in areas of rock cuts.

Figure 67. Photo. Installation of longitudinal drainage to reduce frost heaving.

The photograph in figure 67 shows the installation of a longitudinal drain in the in-slope of the ditch line. A geotechnical study revealed that considerable moisture was entering the roadway prism from lateral flow in and below the cut slope, which caused the frost

heaving in the limits of the cut section. Longitudinal drains were installed to intercept this water and reduce or eliminate the frost heaving. It should be noted that this application was successful but its potential application is limited by the nature of the area and local environment. In this particular case, the frost penetration is approximately 1 m (3 ft) deep, and the ditch line is covered with snow through most of the winter. This significantly reduces the frost depth along the ditch line and does not allow the drain line to freeze.

There was, for a period, some application of foam board to reduce or eliminate frost heaving. There were several installations across the country from Colorado to Maine as well as in Canada and the Nordic countries.[25] The use of foam provided favorable results as far as reducing frost heaving; however, several States experienced a problem with the roadway frosting in the area where the foam was used. There is currently very little or no use of foam insulation for this application.

Maintaining the same frost-free surfacing depth throughout the roadway prism is an additional design consideration to reduce differential frost heave. This was not mentioned in the SHA responses to the questionnaire, but it was recognized in the literature of one adjacent SHA as having contributed to shoulder heave,[26] which resulted in early distress initiation. This appears to be a treatment required more by Western States than those in the Midwest or East.

Most western SHAs maintain the same depth of frost-free surfacing, be it bound pavement or untreated surfacing, throughout the entire roadway prism. This is usually done to prevent differential frost heaving over the full width of the roadway section.

Some of the roadway sections that were provided in response to the questionnaire indicated that the pavement section would not have been designed with a uniform depth of frost-free material across the full roadway prism. In States where a significant depth of frost-susceptible subgrade is removed and replaced (such as in Michigan and Ohio), there would be no frost-susceptible material within 1 m (3 ft) or more of the subgrade surface. In other States where frost-susceptible soils can be placed in the roadway prism, such as that shown in figure 68, there is a potential for differential frost heaving across the roadway prism.

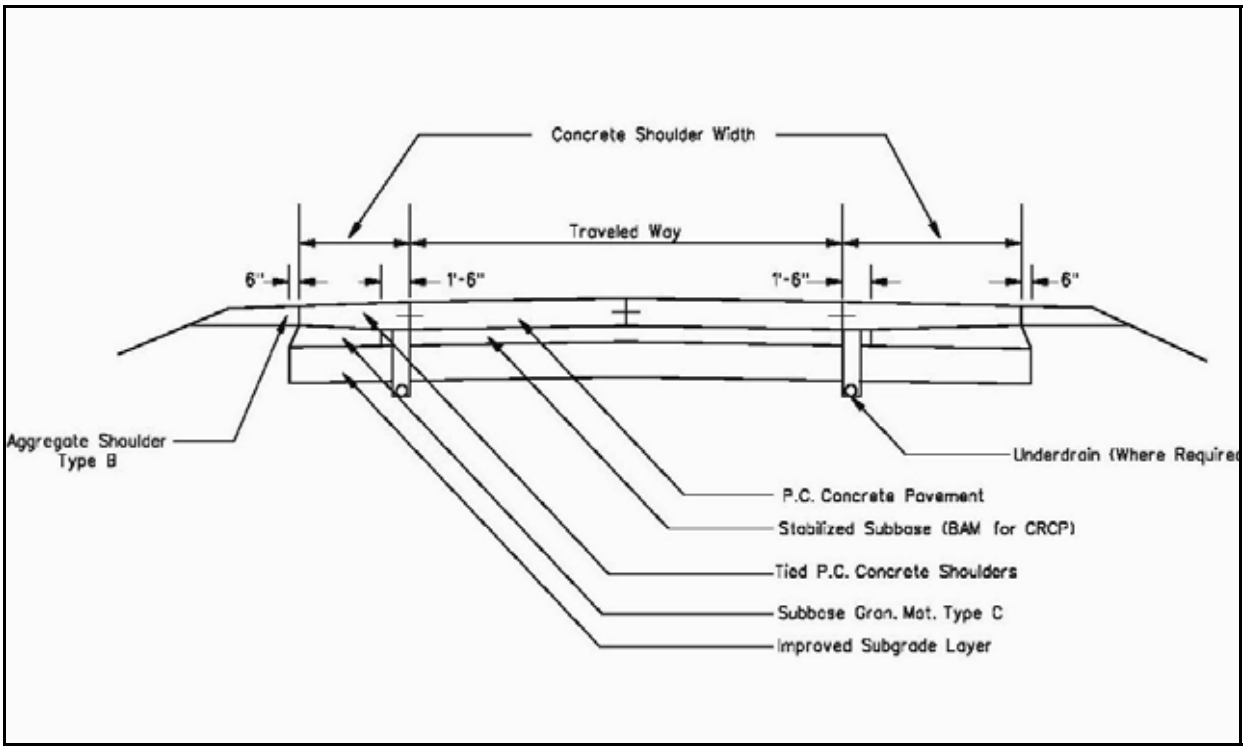

1 inch = 2.54 cm; 1 ft = 0.3 m

Figure 68. Diagram. Standard pavement section from a Midwestern State.

Using a uniform depth of frost-free material across the entire roadway prism appears to represent standard practice by some SHAs, but it may not represent universal or even general practice. The amount of differential frost heaving that would be experienced in a roadway section such as that shown in figure 68 is likely dependent on the environment where it is used. In milder environments, where the freezing front advances slowly through the upper portion of the roadway prism, the amount of moisture that is brought into the frost-susceptible material in the outer edges of the prism might be enough to cause greater heaving in that area, causing differential heaving of the roadway prism. On the other hand, a rapidly advancing freezing front in a more extreme climate may plunge below the surfacing layers quickly enough to minimize any increase in moisture and heaving in the outer sections of the roadway prism. SHAs experiencing differential heaving of the outer edges of the roadway prism could benefit by investigating the use of uniform depths of frost-free material across the entire roadway section.

Applying chip seals on hot-mix asphalt pavements is standard practice in many northern tier SHAs. Idaho, Montana, Wyoming, North Dakota, and South Dakota chip seal hot-mix pavements just after construction, and continue chip seal applications at 6 to 8 year intervals until the next resurfacing project, which might be 25 years or more after initial construction.[10]

A limited amount of research is available that addresses the use of chip seals to improve pavement performance in deep frost areas. North Dakota has documented the used of sand and chip seals to protect pavements from FTCs and expansive soil problems.[10] It is

quite likely that the use of chip seals on hot-mix asphalt pavement reduces the amount of surface raveling in areas with deep frost penetration and numerous FTCs. While the treatment appears to provide some protection against raveling, the relative advantage in improving pavement performance was not quantified. It should be noted that the use of chip seals on hot-mix asphalt pavement was confined to SHAs that generally have lower traffic volumes, where the application of chip seals are usually more acceptable.

LOCAL ADAPTATIONS OF MATERIAL STANDARDS

The responses from SHAs on material standards appear in appendix E, as well as in data gathered from standard specifications available on individual State Web sites.

Most SHAs indicated that they have adopted the use of the Superpave PG binder specification and the Superpave mix design procedures. An abbreviated summary of the responses to the questionnaire and the review of standard specifications on the web sites are shown in table 28.

Table 28. Hot-mix asphalt concrete binder grading and mix designs used by the PFS for surfacing courses.

State	HMAC Reference	AC Grade	Mix Design
Alaska	Hot-Mix Asphalt (HMA), Type II, Class B	PG 58/64–28	Marshall
Idaho	Plant Mix Pavement	PG 64–28	Marshall
Illinois	SP HMA Surface Course	PG 58/64–22	Superpave/Marshall
Michigan	Gap Graded SP	PG 70–22P	Superpave
New York	12.5 mm Superpave HMA	PG 64–28/PG 70–22	Superpave
North Carolina	S-12.5C	PG 70–22	Superpave
Ohio	Item 880 (7 yr warranty)	PG 64–22/PG 70–22M	Superpave/Marshall
Pennsylvania	Superpave HMA Wearing Cr	PG 64–22/PG 58–22	Superpave/Marshall

Appendix F contains the full set of specification comparisons for wearing course and base course, as well as treated and untreated surfacing. An overview of standard design practices for each SHA is also provided in the appendix.

Because cold weather performance was a major consideration in the development of the Superpave binder specifications, it is logical that their use will lead to improved performance; however, the use of Superpave mix design procedures has, to a large extent, eliminated local adaptations in mix design procedures and specifications that might have provided improved performance in areas of deep frost penetration and numerous FTCs. The Superpave mix design procedure does not differentiate between mix designs where mixes will be exposed to numerous FTCs and those that will experience little or no FTCs.

A review of mix specifications shows there are still some local adaptations in acceptable Los Angeles (L.A.) wear values (35 to 55 maximum) and sulfide soundness values (9 to 18 percent maximum). These differences probably represent material availability issues more than environmental issues in the respective SHAs. In addition, minor differences exist in the requirements for antistrip agents. Most agencies required a minimum retained strength of 70 to 80 percent after Lottman conditioning of the test samples to eliminate the need to add antistrip to the mix design. North Carolina requires a minimum of 85 percent of the retained strength after a modified Lottman conditioning. The modified test procedure excludes freezing the sample before the tensile strength ratio (TSR) tests were run. That requirement may not be as demanding as a 70-percent requirement based on the normal Lottman conditioning (with the FTC). It is interesting to note that North Carolina also has the mildest environment as far as frost depth and freeze-thaw cycling is concerned when compared with the other SHAs evaluated in the study. As such, SHAs with more aggressive winter climates should not consider the same modification to antistrip requirements.

Because many SHAs are in the process of adopting the Superpave binder specifications as well as the mix design procedures, local adaptations in mix designs and specifications do not indicate improved pavement performance in areas with either deep frost penetration or numerous FTCs. Many other SHA specifications were reviewed to determine if differences in grading and density requirements existed between the more northern SHAs as compared to the more southern SHAs. Most agencies showed control points and density requirements similar to those contained in the Superpave mix guidelines. Some SHAs have maintained their grading requirements, but there was no consistent pattern to lead to strong conclusions.

9. COST CONSIDERATION

An additional objective of the study involved evaluating the costs associated with performance in the various environments. Cost differences associated with maintaining pavements in deep frost or multiple freeze-thaw climates relative to costs in other areas (i.e., no-freeze) were of particular interest. The following excerpt was taken from the problem statement for this study:

> *"Determination of the cost associated with building and maintaining similar pavements to equal performance standards in various freeze to no-freeze climatic region…These costs should highlight any changes in material quality cost for new construction and life cycle cost associated with rehabilitation needed to maintain the pavement at similar levels of service."*

LCCA was used to evaluate pavement costs in the various climatic settings because it produces comparable results (i.e., equivalent uniform annual costs). Comparisons were made using both deterministic and probabilistic LCCA methods. The deterministic method does not account for variation inherent in the inputs, and therefore, it does not provide information on the distribution of the resulting annualized costs. Because only mean input values are used in the deterministic approach, the results are in terms of mean values with no indication of variability. Probabilistic analysis does incorporate the variation of the inputs and provides distribution statistics of the resulting annualized costs. Realcost version 2.2 was used to conduct the probabilistic analysis. Distributions of construction cost and treatment timings were modeled as a triangle distribution, which required maximum, minimum, and most likely values as inputs. The maximum and minimum unit costs received from the PFS were used to develop the maximum and minimum distribution inputs for construction cost. The average unit costs were used as the most likely value. For the treatment timing distributions, the upper and lower 95-percent confidence intervals were used to determine the maximum and minimum inputs, respectively, while the mean prediction was used as the most likely value.

Annualized and present worth costs for maintaining pavements over a 30-year period were used in the following comparisons. Preventive maintenance activities were assumed to be consistent for all regions, and they were not included in the analysis. It should be noted that some northern SHAs have implemented the routine application of chip seals to pavement sections to mitigate freeze-thaw deterioration. Chip seals are not represented in the performance models; therefore, the contribution to the reduction in deterioration cannot be incorporated in the LCCA, and they were not included in the cost analysis. User costs were assumed to be constant, and they were not included in the analysis. The models developed in this study were used to predict pavement performance for typical roadway sections in the following five region climates:

- Deep-freeze wet (low FTC).
- Deep-freeze dry (low FTC).
- Moderate-freeze wet (high FTC).

- Moderate-freeze dry (high FTC).
- No-freeze wet region.

The performance trends for both new and overlay flexible pavements were determined for fatigue cracking, transverse cracking, rut depth, and ride. Similarly, the performance trends for rigid pavement designs were determined for longitudinal cracking, transverse cracking, faulting, and ride.

Performance trends were evaluated only for pavement aged less than 30 years, so that the inference space of the data used to develop the models was not exceeded. For the rigid pavement designs, the performance trends indicated that no specific damage category reached an action level before 30 years. Because any performance prediction beyond 30 years would greatly exceed the inference range, it was decided not to continue with the economic analysis of the rigid pavements.

Standard flexible pavement sections were developed based on the standard 1993 *AASHTO Guide for Design of Pavement Structures* design procedures[1] using the input variables contained in the questionnaire. One cost comparison was performed using this standard section for all environmental zones; therefore, the initial and rehabilitation costs were constant for all regions. Cost differences were the result of treatment timing differences because of performance differences between the regions. The resulting roadway sections were similar to the average pavement sections provided by the PFS.

To account for local adaptations used to mitigate damage associated with freezing and thawing climates, an additional cost evaluation was performed in which the initial costs of the deep- and moderate-freeze regions included additional frost-freeze material (i.e., unbound base) to obtain a pavement structure with a total depth of 915 mm (36 inches). The 915 mm (36 inches) depth was used because it represents a typical frost-free depth for many SHAs where 1 to 1.2 m (3 to 4 ft) of frost is experienced. The standard section derived from the 1993 AASHTO design guide was used for the no-freeze region. In this evaluation, variations in cost resulted from differences in treatment timing as well as in initial cost (rehabilitation treatment costs were constant).

For the flexible pavement design, the action timing for resurfacing was based on the following distress levels:

- Fatigue cracking—35 deduct points or a fatigue cracking index of 65.
- Transverse cracking—50 deduct points or a transverse cracking index of 50.
- Rut depth—12 mm (0.5 inch).
- Ride—IRI of 2.7 m/km (171.2 inch/mi).

The fatigue cracking deduct value of 35 represents about 10 to 15 percent medium severity fatigue cracking in the wheelpaths. This lower level of fatigue cracking was picked so that a 50-mm (2-inch) overlay would provide reasonable service, and a more intensive overlay design process would not need to be incorporated.

The transverse crack deduct level of 50 represents fairly extensive transverse cracking with medium severity transverse cracking occurring at about 9-m (30-ft) spacing. This is about the level where many SHAs decide to take action to resurface the pavement.[10,27] The common treatment at this level is to place a 50-mm (2-inch) overlay. The rut depth of 12 mm (0.5 inch) is a common level to initiate some type of treatment.

The ride value of 2.7 m/km (171.2 inch/mi) represents a roughness level at which many SHAs will generally place a 50-mm (2-inch) overlay. FHWA has also established this as the maximum acceptable roughness level for primary highway facilities in the Federal aid system.[28]

The timing at which the various distress categories reached the level to trigger improvement was then determined for each of the five environmental zones. Table 29 summarizes the service life at which treatment was initiated along with the distress type driving the event. The timeline includes multiple treatment events for each of the climates. Only fatigue and transverse cracking were included in the table because they were achieved before the rutting and ride levels by significant margins.

Table 29. Action timing for individual distress categories.

Region	Service Life (years)															
	13	**14**	**15**	**20**	**21**	**23**	**24**	**25**	**26**	**35**	**36**	**37**	**38**	**41**	**42**	**43**
Deep-Freeze Wet Region (low FTC)		FC	TC						FC				FC			
Deep-Freeze Dry Region (low FTC)	FC		TC				FC			FC						
Moderate-Freeze Wet Region (high FTC)				FC		TC								FC		
Moderate-Freeze Dry Region (high FTC)					FC		TC									FC
No-Freeze Wet Region		FC						FC			FC	TC				

FC=50.8-mm (2-inch) overlay initiation based on fatigue cracking level.
TC=50.8-mm (2-inch) overlay initiation base on transverse cracking level.

In table 29, the fatigue cracking criteria was reached before the other criteria for all environmental settings; therefore, treatment timing was based on fatigue cracking accumulation for all regions. The timing of the first treatment (using fatigue as the driving factor) was then used as a basis for determining the frequency of subsequent treatments, which were obtained from performance curves for overlay pavements.

Based on this information, a standard deterministic LCCA was performed for both the primary highway design and the interstate highway design. Figures 69 through 71 provide the cross sections for primary and interstate standard sections. These initial pavement sections were developed using the design criteria in the PFS questionnaire and the 1993 *AASHTO Guide for Design of Pavement Structures*.[1] The sections did not

include the added surfacing observed in the PFS response nor the literature review. To account for the added surfacing that is used in the frost areas, a second set of roadway sections were set up that included the extra surfacing or layer of frost-free material used by many States to mitigate frost effects. A second cost analysis was performed that considered the local adaptation of additional frost-free material and used the same geometric cross section with the exception of the increased depth of base material for the deep- and moderate-freeze regions. The additional surfacing depth was based on an assumed frost depth of 1 to 1.2 m (3 to 4 ft), which would usually be met with a requirement of around 915 mm (36 inch) of total surfacing depth. The base course under the mainline of the primary section was increased to 762 mm (30 inch), while the interstate section was increased to 660 mm (26 inch) of base course for the deep- and moderate-freeze regions to provide a minimum frost-free surfacing depth of 762 mm (36 inches). These mitigated pavement sections come much closer to matching the pavement sections from the PFSs in response to the questionnaire.

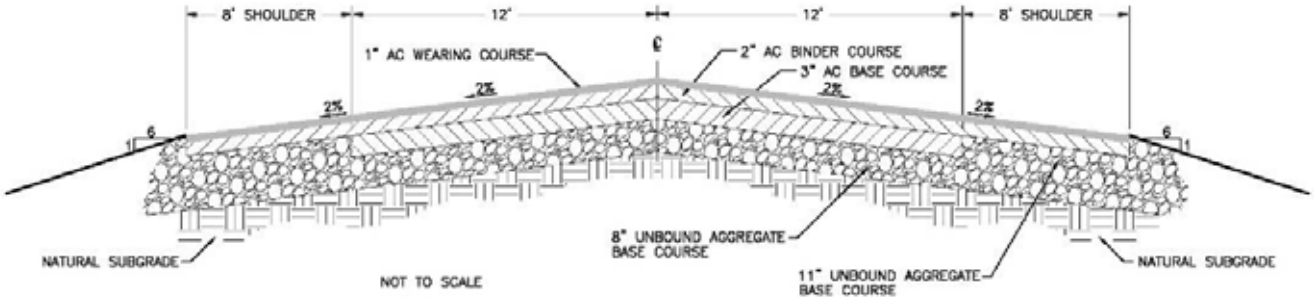

1 inch = 25.4 mm; 1 ft = 304.8 mm

Figure 69. Diagram. Primary highway cross section.

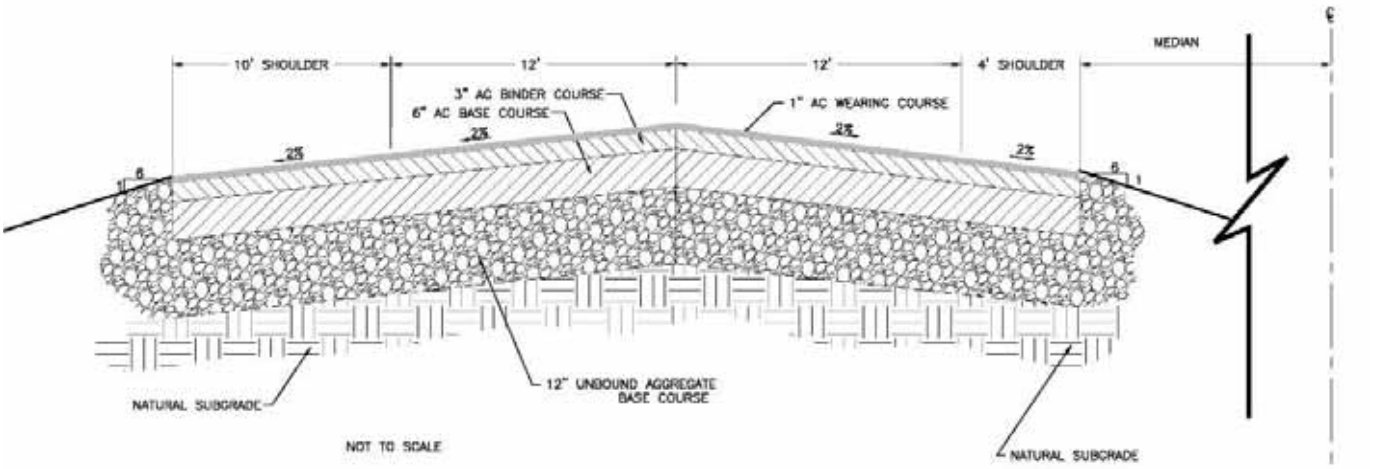

1 inch = 25.4 mm; 1 ft = 304.8 mm

Figure 70. Diagram. Interstate highway, left section.

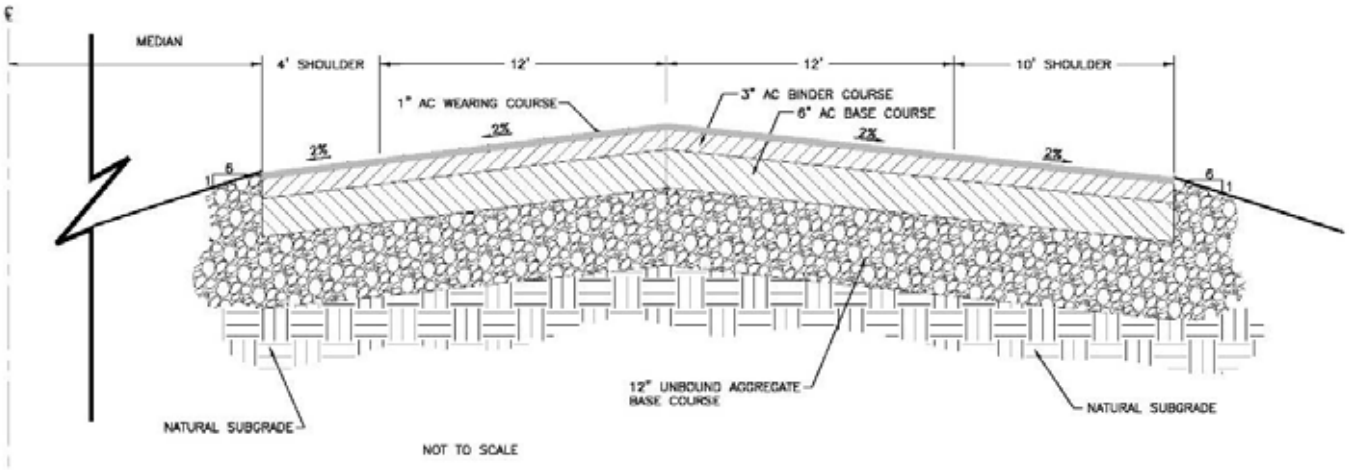

1 inch = 25.4 mm; 1 ft = 304.8 mm

Figure 71. Diagram. Interstate highway, right section.

As can be seen, a typical two lane section 1.6 km (1 mi) long with shoulders was used for the primary highway section. The interstate highway system consisted of a typical four-lane divided highway 1.6 km (1 mi) in length.

Table 30 provides the treatment events used in the deterministic LCCA over the 30-year analysis period. The timing of the first overlay was based on the new construction performance curves. Subsequent events were obtained from overlay performance curves. All events were estimated from the mean predicted performance values. The values in this table are all with respect to the total pavement age. For example, the second overlay on the deep-freeze wet region takes place 26 years after initial construction and 12 years after the first overlay.

Table 30. Overlay timing for the five environmental zones.

Region	Overlay 1	Overlay 2	Overlay 3
Deep-Freeze Wet Region (low FTC)	14 yr	26 yr	38 yr
Deep-Freeze Dry Region (low FTC)	13 yr	24 yr	35 yr
Moderate-Freeze Wet Region (high FTC)	20 yr	41 yr	NA
Moderate-Freeze Dry Region (high FTC)	21 yr	43 yr	NA
No-Freeze Wet Region	14 yr	25 yr	36 yr

Treatment timing inputs for the probabilistic analysis can be found in table 31. The values in this table are not relative to the total pavement age. Rather, the format of Realcost was such that the performance life of each treatment (relative to the application of that treatment) was required.

Table 31. Distribution of performance life for probabilistic analysis.

Region	Initial Construction Life (year)			Overlay Life (year)		
	Min	Likely	Max	Min	Likely	Max
Deep-Freeze Wet (low FTC)	11	14	15	11	12	14
Moderate-Freeze Wet (high FTC)	18	20	23	17	21	25
No-Freeze Wet	12	13	14	10	11	13
Deep-Freeze Dry (low FTC)	11	13	15	9	11	15
Moderate-Freeze Dry (high FTC)	18	21	26	18	22	30

Table 32 summarizes the unit cost information provided by the participating SHAs that was used to determine initial and treatment costs. For the deterministic LCCA evaluation, the average unit price for each material was used. The maximum, minimum, and mean values were used to determine the distribution of costs in the probabilistic analysis. A discount rate of 4 percent was used for all analysis. Salvage value was also included in the analysis for remaining life at the end of the analysis period.

The results from the deterministic analysis for both the standard and mitigated sections can be found in tables 33 and 34, respectively. As can be seen, differences do exist between the regions. Using the standard section for all regions resulted in the deep-freeze regions having approximately the same costs as the no-freeze regions. The moderate-freeze regions were slightly lower in costs than the other regions.

The cost differences in this analysis were due solely to changes in treatment timing because of variations in performance. The no-freeze region accumulated fatigue cracking relatively rapidly in comparison with the other regions. The addition of frost-free material to pavements in the Northern States could be contributing to this improved performance period compared to the Southern States. The frost-free material adds structural capacity to the pavement section. Increases in strength relate to smaller stresses and strains leading to slower accumulation of damage, and hence improved performance in the deep- and moderate-freeze regions.

Considering this, the mitigated sections provide more accurate cost comparisons because they include the additional costs associated with placement of a deeper unbound base course, which has contributed to extended performance. Mitigated pavements in the deep-freeze climates have the highest costs followed by the moderate-freeze regions. The no-freeze region exhibits the lowest annual cost.

While there are differences in the deterministic analysis, there is no means to compare these differences to the distribution of data. The probabilistic analysis is a vital component of LCCA because it provides distribution statistics that can be used to determine if cost differences are significant. Figures 72 and 73 provide the distribution of total present worth costs for the primary and interstate standard sections. One standard deviation was used to compute the distributions provided in the figures.

Table 32. Unit cost information.

State	Reference	Standard Unit Cost - $/m^2 per 1 cm depth ($/yd^2 per 1 inch depth)
AC Wearing Course		
Alaska	HMA, Type II, Class B	0.67 (1.43)
Idaho	Plant Mix Pavement	N/A
Illinois	SP HMA Surface Course	0.93 (1.98)
Michigan	Gap Graded SP	N/A
New York	12.5 mm Superpave HMA	1.59 (3.39)
North Carolina	S-12.5C	1.11 (2.37)
Ohio	Item 880 (7 yr warranty)	0.72 (1.53)
Pennsylvania	Superpave HMA Wearing Cr.	1.32 (2.81)
MINIMUM		0.67 (1.43)
MAXIMUM		1.59 (3.39)
AVERAGE		1.05 (2.25)
AC Binder/Leveling Course		
Alaska	HMA, Type II, Class B	0.67 (1.43)
Idaho	Plant Mix Leveling Course	N/A
Illinois	SP HMA Binder Course	0.93 (1.98)
Michigan	4E50	1.09 (2.33)
New York	Binder Course/19.0 SP HMA	1.35 (2.87)
North Carolina	I-19.0 C	0.98 (2.10)
Ohio	Item 880 (7 yr warranty)	0.72 (1.53)
Pennsylvania	Superpave HMA Binder Cr	1.09 (2.33)
MINIMUM		0.67 (1.43)
MAXIMUM		1.35 (2.87)
AVERAGE		0.97 (2.08)
AC Base Course		
Alaska	HMA, Type II, Class B	0.67 (1.43)
Idaho	Plant Mix Base Course	NA
Illinois	SP HMA Base Course	0.93 (1.98)
Michigan	4E50	1.09 (2.33)
New York	Base Course/25.0 mm SP HMA	1.22 (2.60)
North Carolina	B-25.0C	1.03 (2.19)
Ohio	Item 880 (7 yr warranty)	0.72 (1.53)
Pennsylvania	Superpave HMA Base Cr	1.12 (2.39)
MINIMUM		0.67 (1.43)
MAXIMUM		1.22 (2.60)
AVERAGE		0.97 (2.06)

Table 32. Unit cost information, continued.

State	Reference	Standard Unit Cost - $/m^2 per 1 cm depth ($/yd^2 per 1 inch depth)
Untreated Base Course		
Alaska	Grading D - 1	0.32 (0.68)
Idaho	Rock Cap	NA
Illinois	NA	0.44 (0.93)
Michigan	21AA	0.34 (0.72)
New York	Sub-base	0.34 (0.73)
North Carolina	Aggregate Base Course	0.49 (1.04)
Ohio	Aggregate Base	0.37 (0.80)
Pennsylvania	2A	NA
MINIMUM		0.32 (0.68)
MAXIMUM		0.49 (1.04)
AVERAGE		0.38 (0.82)

Table 33. Deterministic LCCA results for standard sections.

Region	Equivalent Uniform Annual Costs	
	Primary ($)	Interstate ($)
Deep-Freeze Wet Region (low FTC)	28,445	87,634
Deep-Freeze Dry Region (low FTC)	29,165	89,002
Moderate-Freeze Wet Region (high FTC)	25,771	82,556
Moderate-Freeze Dry Region (high FTC)	25,538	82,112
No-Freeze Wet Region	29,165	89,002

Table 34. Deterministic LCCA results for mitigated sections.

Region	Equivalent Uniform Annual Costs	
	Primary ($)	Interstate ($)
Deep-Freeze Wet Region (low FTC)	52,924	117,231
Deep-Freeze Dry Region (low FTC)	53,644	118,599
Moderate-Freeze Wet Region (high FTC)	50,251	112,153
Moderate-Freeze Dry Region (high FTC)	50,017	111,709
No-Freeze Wet Region	29,165	89,002

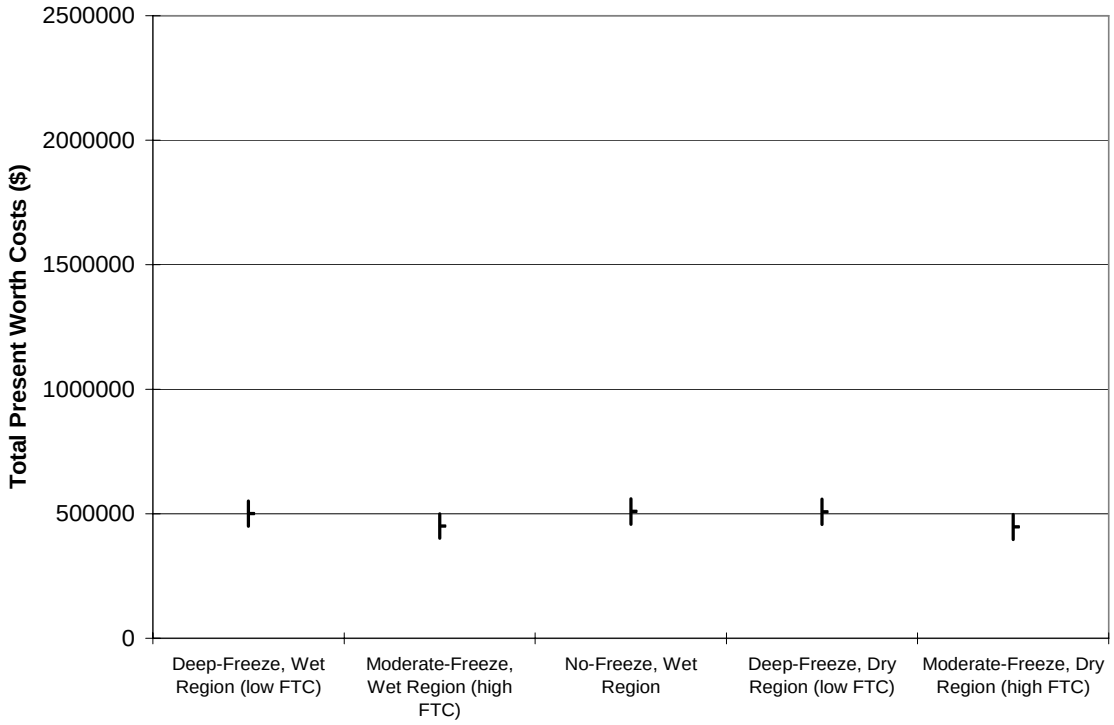

Figure 72. Distribution chart. Annualized costs for standard primary pavement sections.

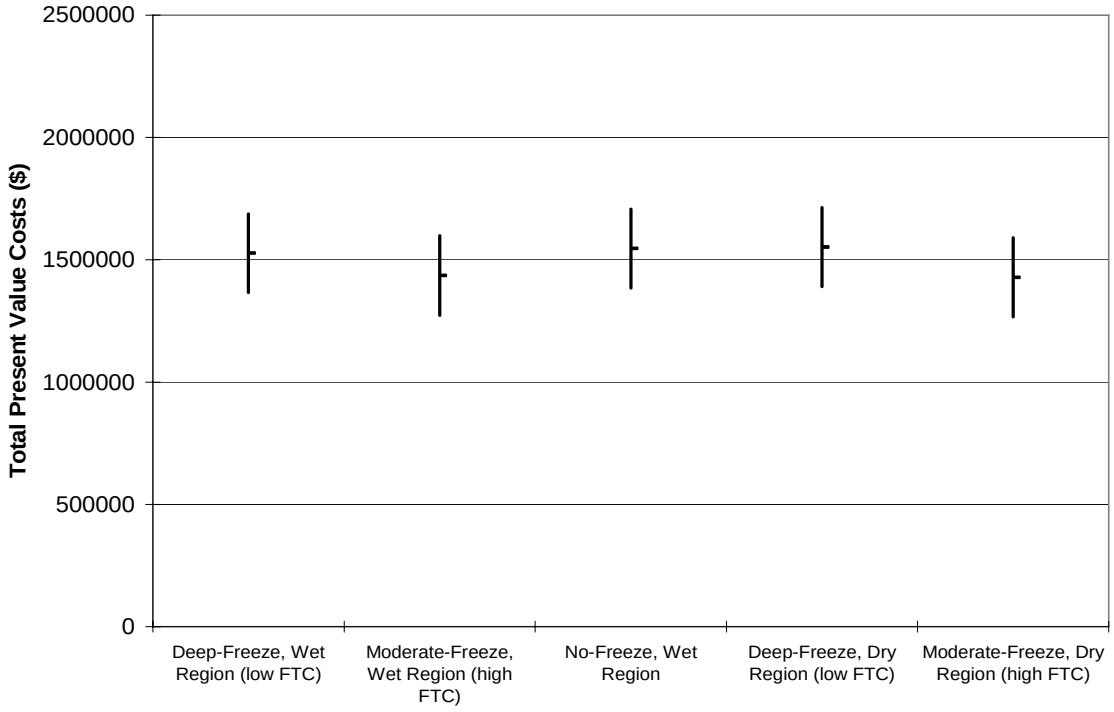

Figure 73. Distribution chart. Annualized costs for standard interstate pavement sections.

All of the mean cost differences between the regions fall within one standard deviation; therefore, it cannot be concluded that significant differences exist among the different climates based on the standard roadway sections.

However, as noted above, comparisons based on the mitigated sections are more representative of the standard practice of northern SHAs. The results using these mitigated primary and interstate sections can be found in figures 74 and 75, respectively.

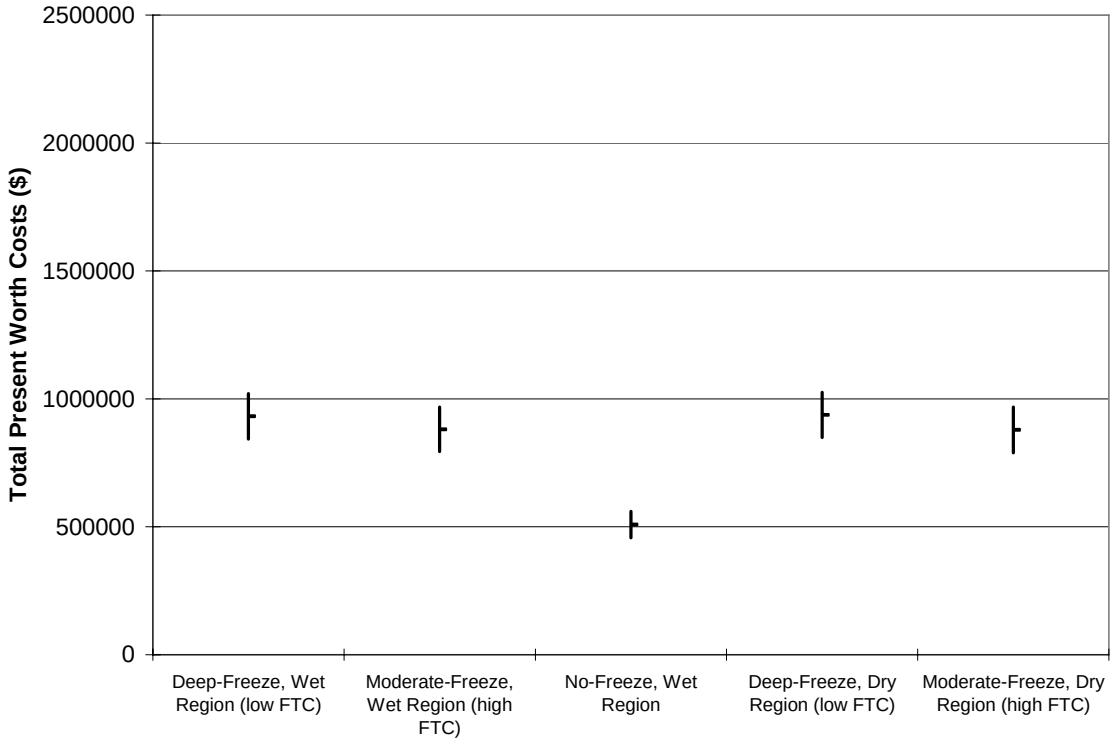

Figure 74. Distribution chart. Annualized costs for mitigated primary pavement sections.

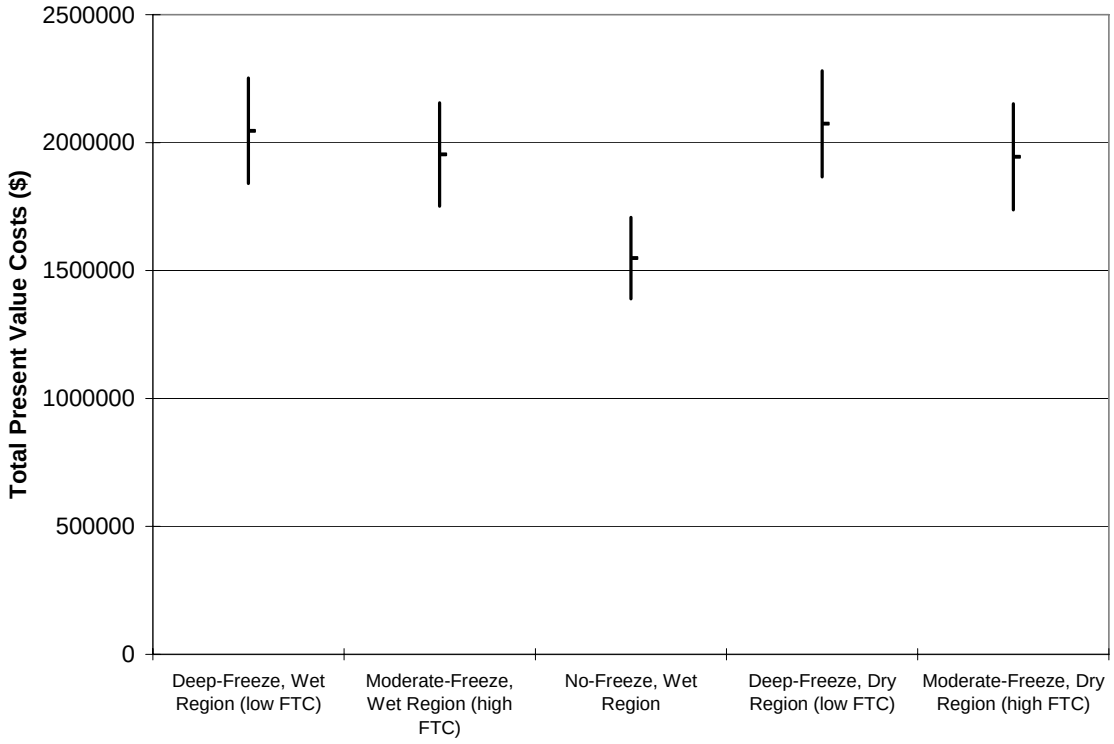

Figure 75. Distribution chart. Annualized costs for mitigated interstate pavement sections.

For the mitigated pavement sections on both primary and interstate highways, the annualized cost for the no-freeze region was lower than any other region. These differences fell outside the one standard deviation range.

The mitigated pavement sections provide a more representative comparison of costs between the regions. The costs to maintain pavements in the no-freeze region are lower than the other regions. These differences do fall outside one standard deviation of the data. Using one standard deviation does not provide direct confidence intervals, but it does allow the distribution of the data to be evaluated because it relates to observed cost differences.

10. APPLICATION TO MECHANISTIC DESIGN

One of the additional objectives indicated in the proposal for this research was for the contractor to make:

> *"...recommendation as to ways in which mechanistic design methods can appropriately consider the most effective adaptations or materials standards to minimize the acceleration of pavement damage due to freezing and thawing."*

NCHRP 1-37A *Guide* procedures basically model a set pavement section and determine the stresses and strains that are produced in that pavement section based on given material properties and dimensions, as well as the loads imposed on those materials. These strains are compared to empirically based damage models to determine the incremental damage for each loading. The incremental damage values are totaled over time to predict the performance of the selected pavement section relative to the specific damage categories (i.e., rutting or fatigue cracking). While only a limited amount of local adaptations were discovered in this study, most can be accounted for in the M-E design procedures.

The effect of local adaptations in M-E design procedures can be applied to the basic material properties or to the empirical damage models. Increasing the depth of frost-free material can be reflected in the M-E design procedures through an adjustment to the material strength properties (i.e., thaw weakening will not be as pronounced, yielding less reduction in subgrade stiffness during the springtime). This same local adaptation can also be accounted for by adjusting the empirical damage models so that the accumulation of deterioration is less rapid over time, given the same stress and strain.

The use of additional frost-free material incorporated either in the pavement design or as a specific subgrade treatment can be accommodated in most mechanistic design procedures. Seasonal subgrade stiffness variation can be accounted for by inputting into the design strength parameters and the duration at which they occur. In these cases, the added frost-free layers are considered as either an improved subgrade or added subbase in the program. For instance, the basic AASHTO pavement design used for the cost analysis described in the previous chapter produced a pavement section consisting of 150 mm (6 inches) of ACP over 205 mm (8 inches) of untreated base. Constructing this section over frost-susceptible soil and in an area experiencing 1 m (3 ft) or more of frost penetration would result in a structure that is significantly weakened during spring thaw—possibly a reduction of up to 50 percent in the subgrade stiffness. This is addressed in the 1993 *AASHTO Guide for Design of Pavement Structures*[(1)] by using the effective modulus to account for the reduced springtime stiffness. In a design procedure based on the NCHRP 1-37A *Guide*, the increased damage accrued during the spring weakening of the subgrade can be accounted for in the program by a reduction in the subgrade stiffness and subsequent increase in stresses incurred during that period as a result of the lower stiffness. If the subgrade soil was replaced with 0.6 m (2 ft) or more of frost-free material, as is done in several of the PFSs, the stiffness of the subgrade can be increased because of the increased layer thickness and the reduced spring weakening effects. Combined, these inputs reduce the tensile stresses on the bottom of the pavement

as well as reducing the compressive stresses on the top of the subbase and subgrade layers, thus resulting in longer service life for the pavement section being analyzed.

The NCHRP 1-37A *Guide* pavement design procedure [2] was developed using damage models that represent average pavement damage trends for the entire United States. The program computes different stress levels in a pavement section depending on the input, which can reflect different material properties based on environmental input. The empirically based damage models, however, were developed to produce the same increment of damage in New York, Los Angeles, and Chicago for a given stress. This was done so that the program could produce reasonable results throughout the country. This is acknowledged in the NCHRP 1-37A *Guide* [2], which provides a process for agencies to calibrate the damage models to local conditions.

Section 3.3.6 of the NCHRP 1-37A *Guide* describes the need and recommended approach for local calibration of the M-E models. Following are specific directions recommended in the report:[2]

> *Because this design procedure is based on mechanistic principals the procedures should work reasonably well within the inference space of the analytical procedure and the performance data from which the procedure was calibrated. However, this is a very complex design procedure and it must be carefully evaluated by highway agencies wishing to implement. The following is the recommended calibration/validation effort required to implement this mechanistic-empirical design procedure….*
>
> - *Review all input data.*
> - *Conduct sensitivity analysis.*
> - *Conduct comparative studies.*
> - *Conduct validation and calibration studies.*
> - *Modify input defaults and calibration coefficients as needed.*

While all five items listed above are necessary in the M-E implementation process, the last two address the adjustment of the M-E damage curves to match local experience. These processes were thoroughly explored with consideration given to the use of the models discussed in chapter 5 in accomplishing local calibration and validation. The following excerpts were taken directly from the NCHRP 1-37A *Guide*:[2]

- Calibrate to local conditions.

  The national calibration-validation process was successfully completed [as part of the NCHRP 1-37A project]. Although this effort was very comprehensive, further validation studies are highly recommended as a prudent step in implementing a new design procedure…A validation database should be developed to confirm that the national calibration factors or functions are adequate and appropriate for the construction, materials, climate, traffic, and other conditions that are encountered within the agencies' highway system.

  Prepare a database of agency performance data and compare the new design procedure results with the performance of these "local" sections. This will require the selection of at least 20 flexible pavement sections around the state. If the state has very distinct climates this should be done in each climate.

  The goal of the calibration-validation process is to confirm that the performance models accurately predict pavement distress and ride quality on a national basis. For any specific geographic area, adjustments to the national models may be needed to obtain reliable pavement designs.

- Modify the calibrations/inputs.

  If significant differences are found between the predicted and measured distresses and IRI for the agencies highways, appropriate adjustments must be made to the performance models. This study will also establish the level of accuracy desirable for key input parameters and default input values. Make modification to the new procedures as needed based on all of the above results and findings.

In light of these guidelines, a few SHAs are now in the process of refining the calibration factors for the performance models. The University of Washington is developing calibration factors for the WSDOT, which is described in the *PCCP Models for Rehabilitation and Reconstruction Decision-Making* report.[29] The steps outlined in the NCHRP 1-37A *Guide* were followed in the referenced work. The comparative analysis considered three major categories for rigid pavement performance: undoweled short jointed PCCP, undoweled short jointed PCCP mountain passes, and doweled bar retrofitted PCCP. Information from the SHA pavement management system, which contains more than 30 years of performance data for all pavements in the network, was used in steps four and five. Typical pavement sections consistent with those in place were used to estimate pavement performance for the three categories of pavement using the 1-37A M-E design program. The resulting predictions were then compared to the average performance history for each category. Through several cycles of iterations, and a subsequent verification activity, a new set of C values were developed for the cracking and faulting models for the three categories of PCCP in Washington State.

Not all SHAs have the advantage of having 30-plus years of network wide continuous pavement condition data. Those that do not may be able to fine-tune the NCHRP 1-37A

Guide output through the use of the models described in chapter 5. That would be particularly true for those agencies that have an environment significantly different than what would be represented by the national models developed for the M-E design procedure. The models developed in this project could be used to predict average rutting or fatigue cracking trends for a specific (regional or statewide) environment. These estimates could be used to then go through the same iteration and verification process described in the NCHRP 1-37A *Guide*, or the WSDOT research project, to determine if modified calibration factors are needed in the design program to accurately reflect performance in the SHA. An example of the NCHRP 1-37A *Guide* calibration methodology flowchart is shown in appendix G.

To provide an example of the use of the models described in chapter 5, the calibration process outlined in the NCHRP 1-37A *Guide* was performed for a typical site in North Carolina. This sample calibration was performed for the basic roadway design parameters and pavement design section used in the economic analysis (chapter 9 of this report) for a rural primary highway. The representative climate for North Carolina presented in table 22 was used for environmental inputs.

In the NCHRP 1-37A pavement design program there are input procedures that allow the user to adjust the damage models used for fatigue cracking, rutting, and thermal cracking. For the AC fatigue cracking model there are three calibration factors (referred to as Bf1, Bf2, and Bf3) that adjust the K1, K2, and K3 correlation coefficients. In the current version of the NCHRP 1-37A pavement design software, these calibration settings can be found through the tools menu and the calibration settings for new flexible pavement under "Distress Model Calibration Settings–Flexible." Four categories of calibration conditions are available for AC fatigue analysis:

- Special analysis—Bf1 input only.
- National calibration—No adjustments available.
- State/regional calibration—Bf1, Bf2, and Bf3 inputs available.
- Typical agency values—K1, K2, and K3 adjustments available.

The same set of inputs is available for AC rutting, except that the adjustments for K1, K2, and K3 are termed Br1, Br2, and Br3, respectively. Conversely, only the State/Region Calibration category is available for AC thermal fracture with the adjustment inputs termed Bt1, Bt2, and Bt3 respectively.

Similar adjustments are available for chemically stabilized material (CSM) fatigue and subgrade rutting. The correlation coefficients (C1 through C4 and C1 through C6) can be individually modified for the AC cracking, CSM cracking, and IRI categories.

The roadway section used for this sample consisted of 150 mm (6 inches) of hot mix asphalt (HMA) concrete pavement over 205 mm (8 inches) of granular base with a fine-grained, frost-susceptible subgrade soil, which was assumed to be A-6 soil as defined in the AASHTO classification system.[30] The values input into the NCHRP 1-37A pavement design software matched the mix properties and typical specifications provided by North Carolina. The traffic loading was input as load spectra, but it was very similar to

the 3 million ESAL loading over 20 years used in previous analysis described in this report.

The calibration process consisted of running the NCHRP 1-37A pavement design software with the national calibration factors to estimate performance and compare output to the predictions of the models from this study. The NCHRP 1-37A pavement design software (using the nationally calibrated models) indicated that the pavement would experience rapid top-down cracking with an accumulation of more than 750 m/km (4,000 ft/mi), more than 13 mm (0.5 inch) of rutting, and ride values progressing from 1 m/km (64 inch/mi) to more than 8.3 m/km (525 inch/mi) in 20 years. The design section used for this analysis was developed using the 1993 AASHTO *Guide for the Design of Pavement Structures*[1] with 85 percent reliability, so it did not seem reasonable for it to experience that much longitudinal cracking and ride deterioration. Looking at the pavement distresses recorded at the various LTPP sites around North Carolina, similar pavement sections have not experienced that level of distress accumulation over a 20-year period. Dominate pavement distress recorded at the LTPP sites in North Carolina consisted of some fatigue cracking, isolated transverse cracking, and rutting, so regional calibration seemed appropriate. For this example, that calibration focused on the accumulation of fatigue cracking, rutting, and ride values because those were the predominant distresses indicated by the local LTPP sites. The calibration was achieved through an extensive iterative process of varying either the B values for the fatigue and rutting models or the C values for the ride model.

Figure 76 provides the fatigue cracking predictions for the sample design. The NCHRP 1-37A damage trends for fatigue cracking are generally continuous trends without the observation of a crack initiation point, which is included in the models developed under this study. The calibration was thus set to match the frost model at 20 years, but it could have been adjusted to fit the model at 10 or 15 years as well. The Bf1 term was set at 0.47 to provide the NCHRP 1-37A *Guide* fatigue cracking prediction shown in figure 76 as local calibration.

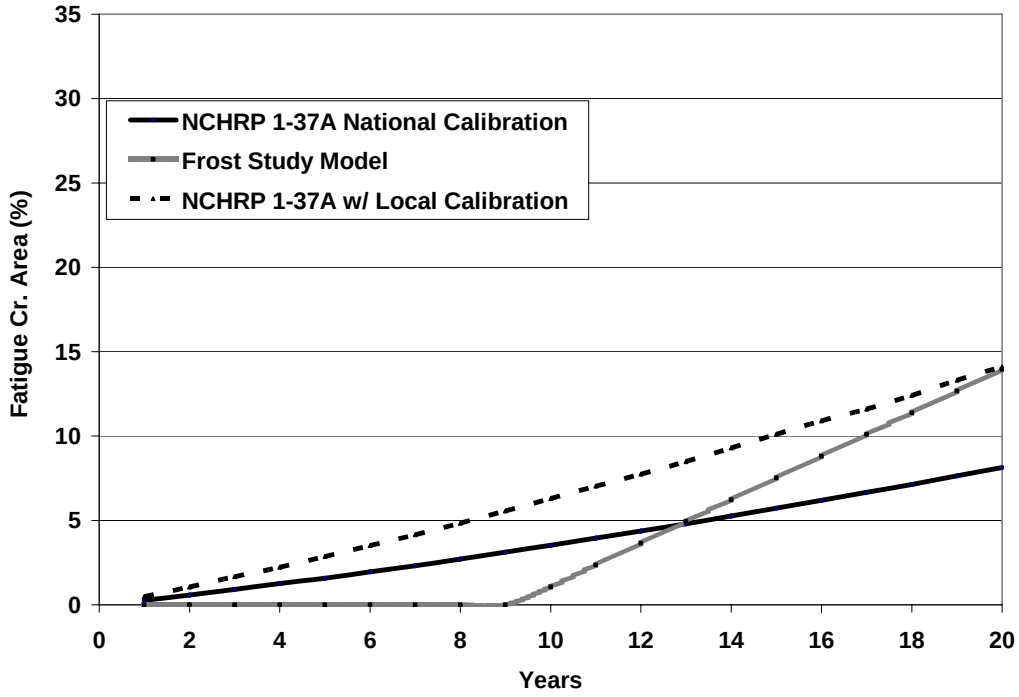

Figure 76. Graph. Comparison of fatigue cracking trends before and after local calibration.

The rutting prediction model developed in this study and the NCHRP 1-37A *Guide* model are similar in form. Therefore, the NCHRP 1-37A rutting models could be calibrated to local conditions for the full range of the pavement ages as opposed to the fatigue models which had to be calibrated at a certain age. The Br1 factor was set to 0.1 to obtain the rutting prediction for the local calibration shown in figure 77. This resulted in rut development predicted primarily in the base and subgrade soils by the NCHRP 1-37A design software. Similar trends were also developed by increasing the Br1 factor to above 1 and setting the Bs1 terms to 0.05 or less, which moved the rutting prediction from occurring in the subgrade and aggregate base to occurring in the HMA based on the NCHRP 1-37A design software. Either approach provided the same basic rutting trend over time.

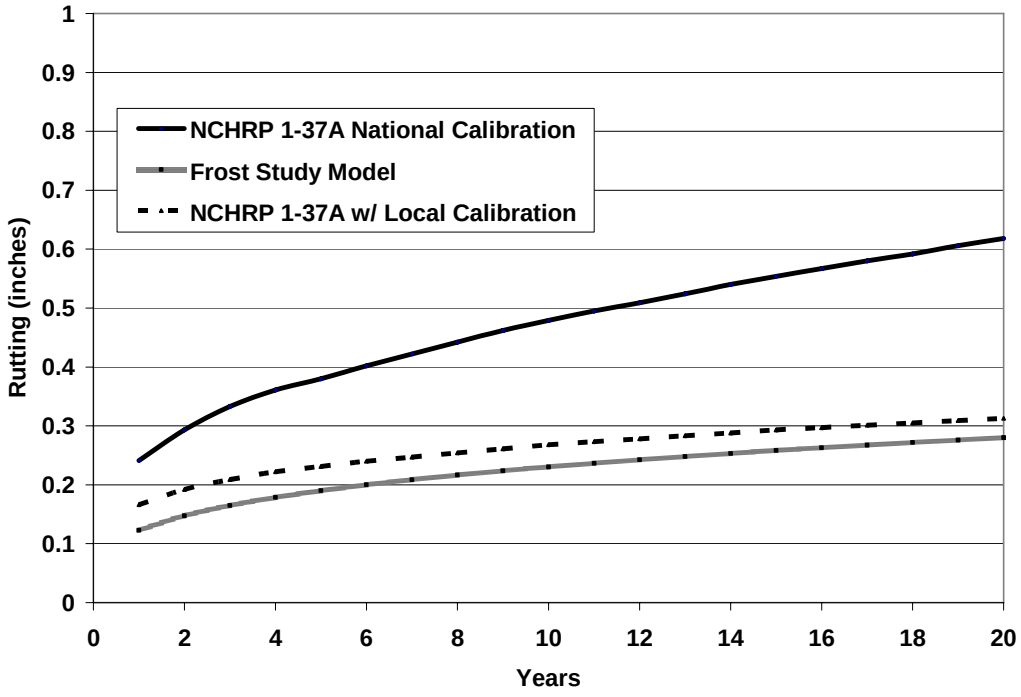

1 inch = 25 mm

Figure 77. Graph. Comparison of rutting trends before and after local calibration.

Similar to the rutting models, the form of models for ride deterioration in terms of IRI was also consistent over time; therefore, the NCHRP 1-37A model could be calibrated over the full range of pavement ages and not at a specific age. The C values were adjusted to bring the NCHRP 1-37A model more in line with the ride model developed for this study using the North Carolina conditions. As can be seen in figure 78, a very good fit was achieved after the local ride calibration. To get this fit, the C1 value was lowered to 0.10 of the value for the national calibration. The rest of the C values were not as sensitive as the C1 value in providing a better fit to the performance model from this study.

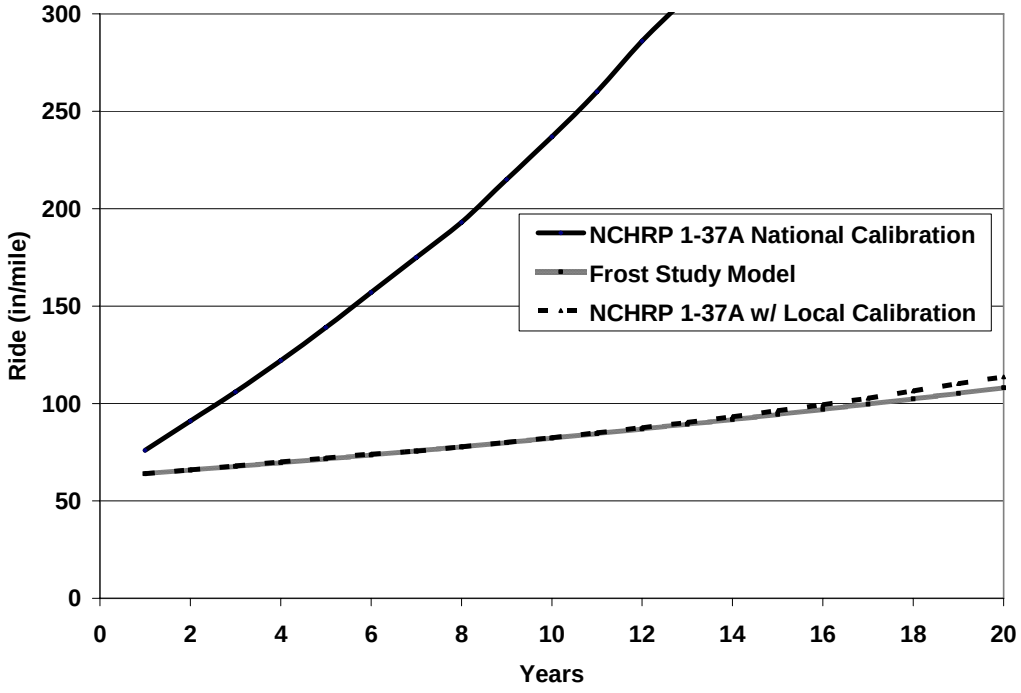

100 inches/mi = 1.5 m/km

Figure 78. Graph. Comparison of ride trends before and after local calibration.

This was one set of iterations for a pavement with 150 mm (6 inches) HMA over 205 mm (8 inches) of granular base. Similar iterations would need to be performed on a range of pavement sections with both higher and lower traffic loadings and the resulting average calibration factors would then be used to produce pavement design performance predictions that would be calibrated to the local environmental conditions.

This type of calibration procedure should be used only if the local agency does not have its own performance data for developing local calibrations for use in the NCHRP 1-37A pavement design software. If an agency has limited pavement performance data, the models developed in this study could be used to estimate general pavement performance trends adjusted to fit the relative values of the local data in a process similar to that described in the next chapter on pavement management systems.

The performance trends from this study were developed with the intent to represent a broad array of inservice pavements throughout North America. As such, the contributions of surface treatments such as chip seals were not incorporated in the models and cannot be used to calibrate the NCHRP 1-37A *Guide* performance curves for sealed HMA pavement. SHAs using these treatments must develop damage models that are specific to the performance of pavements with surface treatments.

11. APPLICATION TO PAVEMENT MANAGEMENT

The models developed for this project can be used as a pavement management tool. Most PMSs in North America collect pavement condition data in a manner similar to that used in the LTPP program. The LTPP program collects pavement distress in more detail than most agencies do for pavement management purposes, but most agencies follow the same basic surface distress categories. Fatigue cracking, longitudinal cracking, and transverse cracking data are collected for flexible pavements and faulting, transverse, and longitudinal cracking are recorded for rigid pavements. The LTPP method also uses three severity levels that are similar to those used in PMSs. In some cases the extent conventions need to be modified, but that is fairly easily accomplished. For example, fatigue cracking is collected in square meters for LTPP purposes, but most SHAs measure the percentage of area or length of the fatigue cracking in the wheelpaths for use in their PMS. This is easily rectified because the dimensions of the LTPP test section are known, and fatigue cracking is assumed as occurring in the wheelpaths, so quantities can be converted to percentages in terms of wheelpath area.

In consideration of PMS application, several of the models developed in this study were based on LTPP measurements that were converted to be consistent with PMS extant conventions. In turn, these values were extended to standard PMS deduct values so that the measured distress could be represented in terms of deduct values or a pavement condition index (i.e., 100 less the sum of deduct values for a given test section). This approach provided for the characterization of the various levels of distress severity that is consistent with common PMS practices. A complete discussion on the development of deduct value development can be found in chapter 3 of this report.

One of the more difficult exercises in implementing PMS applications is the development of a family of curves that represent the standard deterioration trends unique to an agency's roadways and environment. Few SHAs have been able to measure pavement conditions in a consistent manner. Relating one set of measurements over a specific area to another set of measurements over that same area from year to year (as was done at the LTPP sites) has proven to be a difficult task. To overcome this, some SHAs have relied on models developed based on test sites that could be monitored with time or expert opinion, while others have used models developed based on other SHA data.

Pavement performance models are used to predict future deterioration of a highway network's pavements based on the last set of pavement condition survey data. The models (or condition data) have a large effect on the information the PMS provides for future construction program decisions, and also influence the future pavement condition trends as well as the funding needs for that agency.

SHAs with little historical pavement condition information or limited amounts of composite indices can use the models from this study to develop a family of curves to help implement a PMS or convert a PMS from one with only composite indices available. Not all agencies have maintained their raw pavement condition survey data and only have files with the computed index for prior years. Because the location referencing system can change from year to year or the posting of those locations can change, there is often

no attempt to correlate the pavement condition data taken at a specific location with future or past data taken at that same location.

Unfortunately, most SHAs use different pavement distress indices based primarily on the specific pavement management system they have adopted, and there is a wide range of systems in use throughout the United States. Deduct curves developed for South Dakota,[10] which are now in use by several other SHAs, were used to develop pavement performance trends for this study. The extent of pavement distress (i.e., area or length) for each severity level was accumulated in terms of the sum of the pavement distress deduct values. As noted in the chapter on database development, the deduct values were determined using the expressions shown in equations 7 through 10 for each severity level.

$$D_L = 3.4082 * P_L^{0.514} \quad (7)$$

$$D_M = 4.4575 * P_M^{0.6107} \quad (8)$$

$$D_H = 5.2064 * P_H^{0.6956} \quad (9)$$

$$D_T = D_L + D_M + D_H \quad (10)$$

These equations are represented in figure 79.

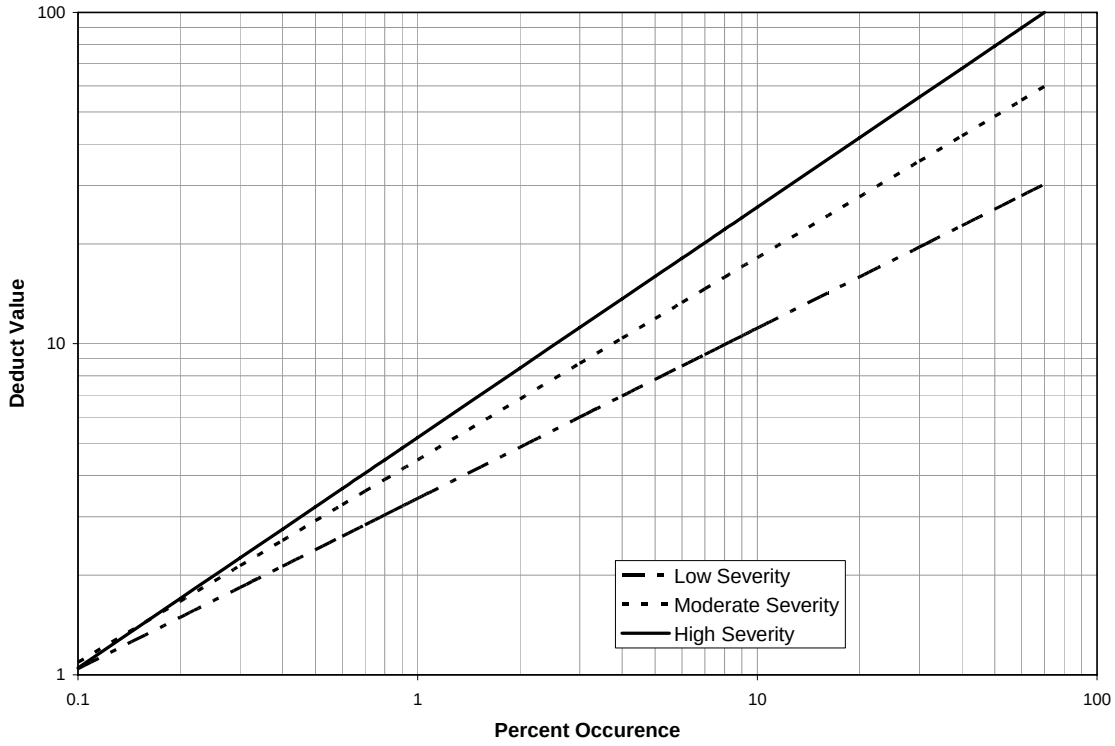

Figure 79. Graph. Individual distress deduct curves.

The individual distress indices were developed so those deduct values represented desired action times for most SHAs. For example, a fatigue distress deduct accumulation level of about 35 represents about 10 to 15 percent medium severity cracking over the length or area of the wheelpath assuming each wheelpath is 1 m (3 ft) wide. For transverse cracking, an accumulation level of about 50 represents a sufficient length of medium severity transverse cracking to indicate a crack spacing of approximately 9 m (30 ft) between transverse cracks. These values represent damage levels that affect or initiate repair or rehabilitation project timing for most SHAs.[10]

Figure 79 can be used by SHAs to gain an understanding for the distress magnitudes represented by deduct values. The medium severity deduct curve can be used to get the average magnitude required to produce that value. This process can also be used to make comparisons between SHA-specific damage indices and those used in this study.

The pavement performance curves for any specific distress can be used to develop general deterioration trends to forecast future pavement conditions from current condition measurements.

As an example, the fatigue deduct values shown in figure 80 (from the environmental sensitivity study) for the no-freeze wet region were converted to a pavement condition index by subtracting the accumulated deduct values from 100. The resulting pavement deterioration trend for fatigue cracking for a pavement with the characteristics outlined in table 19 can be found in figure 81.

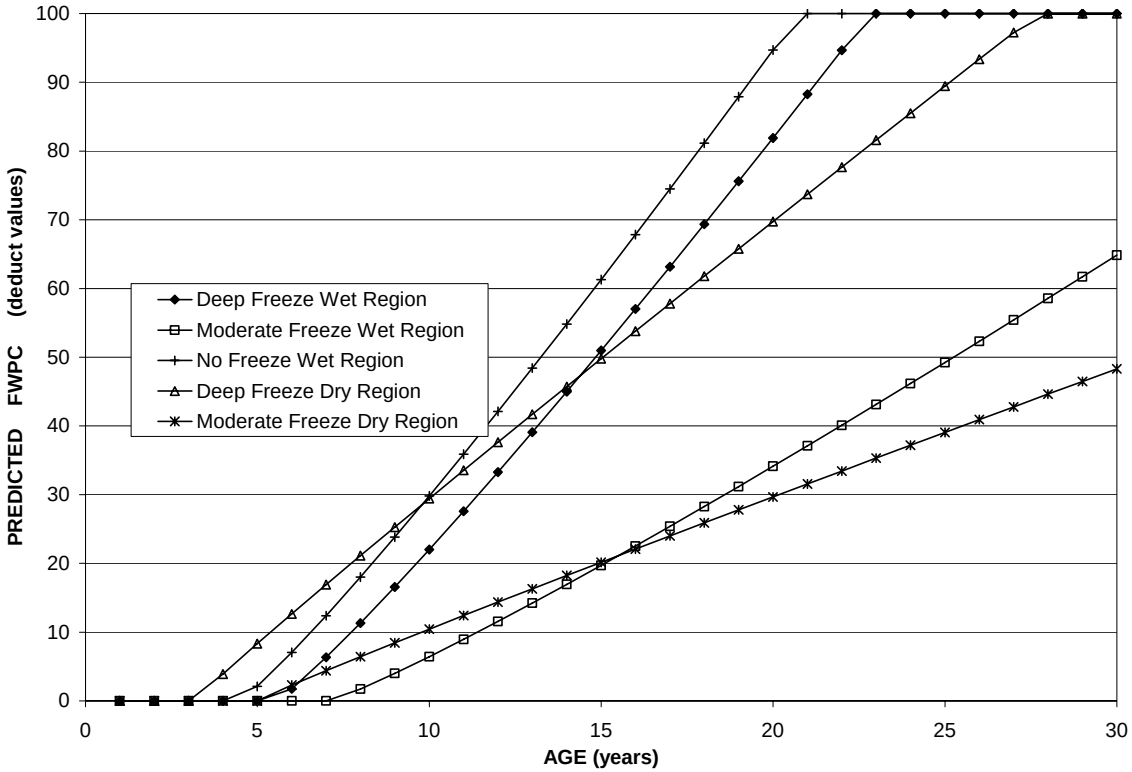

Figure 80. Graph. Example of fatigue cracking trends for different environments.

Figure 81. Chart. Fatigue cracking index trend for environmental case wet no-freeze.

This trend line represents the average trend found for a specific set of conditions used in the sensitivity study for this project. SHAs can determine a set of input parameters that represents the regional-specific conditions (environment, traffic, and pavement structure) and develop a similar deterioration trend line using the performance models from this project. A series of these trend lines can be developed for the range of conditions expected across a region and used as a tool to predict future pavement conditions. As condition data are collected on pavement structures, the average deterioration line can be updated or shifted to match the most recently collected data. For example, a highway section that matches the criteria used to develop figure 81 surveyed at year 10 exhibits a fatigue cracking index of 75. The trend in figure 81 would be shifted to the right so that it predicts a value of 75 at year 10 without altering the slope. This would result in the life of the particular highway section being extended by approximately 2 years based on the condition data collected at year 10. This is shown in figure 82.

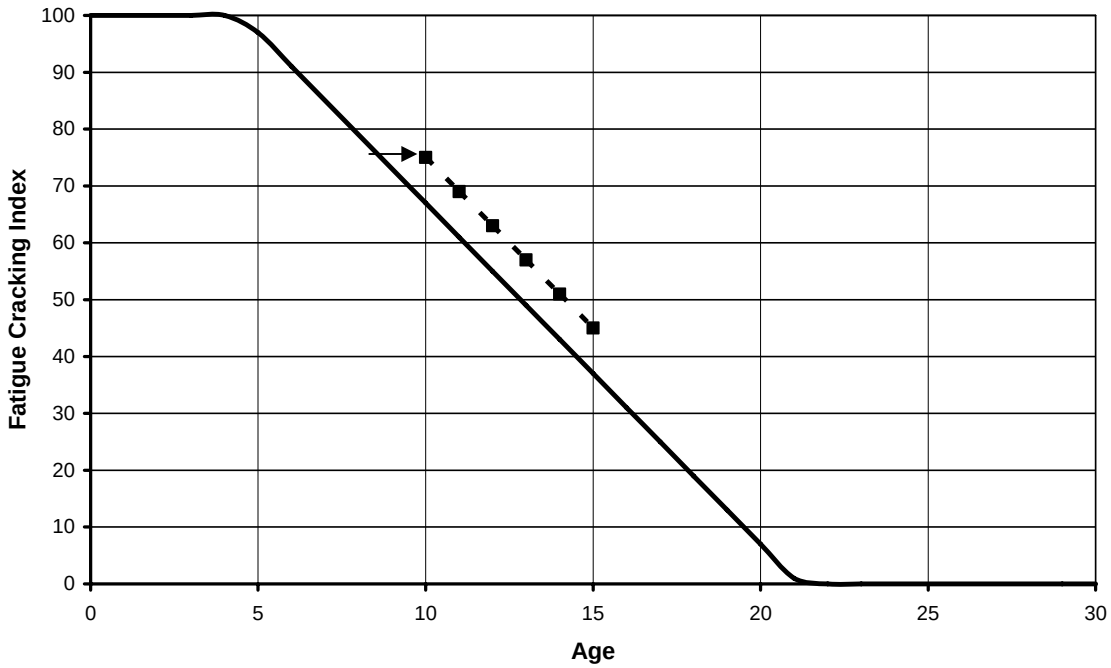

Figure 82. Chart. Example of shifting trend line to fit index for a given location.

Where an agency used different pavement condition indices, it would need to develop the area of medium severity fatigue cracking using equations 7 through 10 for medium pavement deterioration trend lines. The amount of medium-severity fatigue-cracking values would then be used to convert to the pavement condition deduct values the agency uses.

Where an agency uses a composite index that combines several of the distresses modeled individually in this study, the process would be more complicated. The agency would probably need to use each pavement deterioration curve to predict the future distress level for each distress and then combine the distress levels according to their combined equation into a composite index for set program dates rather than developing a trend line for the composite index.

12. KEY FINDINGS

An overview of the findings from the performance comparisons between the five climatic scenarios established for the study can be found in table 36. The "X" symbol indicates differences exist, and they are statistically significant at a 95-percent confidence.

Table 35. Summary of statistical comparisons.

Performance Measure	Deep-Freeze Wet Region	Moderate-Freeze Wet Region	No-Freeze Wet Region	Deep-Freeze Dry Region	Moderate-Freeze Dry Region
Roughness (flexible)					
Fatigue/wheelpath cracking (flexible)	X	X	X	X	X
Transverse cracking (flexible)	X	X	X	X	X
Rut dept (flexible)		X	X		X
Roughness (rigid)	X		X	X	
Longitudinal cracking (rigid)	X	X	X	X	X
Transverse cracking (rigid)	X		X		
Faulting (rigid)				X	X

Following is a list of descriptions of the significant differences noted in table 36:

- Differences in flexible pavement roughness between the various climates at 20 years were not found to be significant.
- The no-freeze wet region exhibits significantly lower rigid pavement roughness than the deep-freeze regions (both wet and dry) at 20 years.
- Rutting accumulations in the moderate-freeze regions (both wet and dry) are significantly larger than the no-freeze wet region at 20 years.
- The deep-freeze regions (both wet and dry) and no-freeze wet region accumulate significantly larger quantities of fatigue/wheelpath cracking at 20 years compared to the moderate-freeze regions (both wet and dry).
- Predictions for flexible pavement transverse cracking at 20 years result in the deep-freeze regions (both wet and dry) having significantly larger quantities than the moderate-freeze regions (both wet and dry). In addition, the moderate-freeze

regions (both wet and dry) have significantly larger accumulations than the no-freeze wet region.

- Accumulations of rigid pavement longitudinal cracking at 25 years were significantly lower in the no-freeze wet region as compared with all other regions.
- At 25 years, rigid pavement transverse cracking was significantly larger for the no-freeze wet region as compared to the deep-freeze wet region. All other comparisons were found to be insignificant.
- The magnitude of joint faulting at 20 years was found to be significantly larger in the deep-freeze dry region as compared with the moderate-freeze dry region.

It should be noted that the data in this study do not support the notion that deep frost penetration and multiple FTCs are mutually exclusive. Areas do exist with high freezing indices and large quantities of annual FTCs.

A review of information provided by participating SHAs and relevant literature regarding local adaptations to mitigate frost was performed. There was a large variation in typical cross sections for similar design situations, and no specific treatment was universally used to counter frost effects. Many States with frost penetration did required additional surfacing or the replacement of frost-susceptible soils with frost-free material. In addition, most of the States have adopted Superpave PG binder specifications and mix design procedures. This relatively recent development has to a large extent eliminated local adaptations to materials specifications and mix designs for HMA pavements.

Life cycle cost analysis was conducted using two different approaches. The first approach used initial construction costs that were consistent for each of the five climatic scenarios and were based on a standard roadway design. This resulted in equivalent uniform annual costs that were not significantly different between the regions. The second approach used initial construction costs that varied with the climatic scenario. The typical section for the deep- and moderate-freeze regions included additional frost-free material to represent the mitigation found in the review of SHA information. This cost analysis resulted in the no-freeze region having equivalent uniform annual costs that were lower than the other regions.

The models developed from this study can be used in pavement management system applications as well as to perform local calibration for the NCHRP 1-37A *Guide*.

13. SUMMARY AND CONCLUSIONS

To meet the objectives of this study, the research was separated into three basic steps. The first step was to develop models to quantify the effect of the environment, particularly related to deep frost or multiple FTCs, on pavement performance in terms of pavement distress. The second measure was to look at pavement design and materials standards that compensate for or mitigate the effect of seasonal frost. The third step was to evaluate costs associated with pavement design elements considering frost-related effects. Supplementary to these efforts, the application to mechanistic-based pavement design was also addressed.

Findings from phase one of this study were incorporated into the work performed in phase 2. As part of phase 1, a literature review was conducted to guide and supplement the analysis. It was also discovered in phase 1 that the dataset necessary to represent the number of variables required in the analysis needed to be expanded from only SMP sites to include other LTPP sections. GPS-1, GPS-2, GPS-6, SPS-1, and SPS-8 experiments were used in the dataset for flexible pavements, while the rigid pavement dataset consisted of GPS-3, SPS-2, and SPS-8 projects. Because frost penetration data are not directly measured at all of these sites (as is the case for SMP projects), surrogate factors were investigated. FI was found to represent relative frost conditions in the dataset, and that information was used in place of frost penetration. The analysis database developed for phase 2 included data to represent the following factors:

- Pavement types (rigid, flexible).
- Climatic data (rainfall, FI, and thawing index from temperature data).
- Frost depth (temperature sensors and resistivity data).
- Deflection data (stresses and strains calculated from layer material properties).
- Performance data (distress and permanent deformation).
- Soils and material properties.
- Traffic data.

The dataset included test sections located in the deep-freeze wet region, deep-freeze dry region, and the no-freeze wet region. The data were not separated by climatic setting, and they were analyzed independently to reduce the number of observations per grouping and because the information is largely dependent on the method used to group the data. Rather, all data for one pavement type were combined. Climatic differences were accounted for through the use of explanatory variables in the regression analysis. Test sections with surface treatments were excluded from the analysis. This resulted in more than 520 and 280 test sections for flexible and rigid pavement structures, respectively.

This study considered the following performance data:

- Roughness—flexible and rigid.
- Rut depth—flexible.

- Distress (fatigue, transverse, longitudinal, block, raveling)—flexible.
- Distress (corner breaks, transverse, longitudinal, durability, pumping)—rigid.
- Faulting—rigid.
- Strain—flexible.

Some of the distress types were excluded from further analysis because of the limited number of nonzero observations or because the variation at one site over time was relatively large. This included raveling and durability cracking.

Models were developed using multivariate regression analysis through an iterative process. All explanatory variables were investigated through the use of P-values to determine if their contribution to the prediction was significant. Variables that were marginally significant were included in the model only if they improved the prediction capability of the regression. In addition, various transformations and relationships between the performance measure and pavement age were investigated. The models with the smallest deviation were selected for use.

Some of the models resulted in predictions that were not logical based on general engineering experience. For example, the strain model estimated a reduction in strain as the pavement age increased. Models exhibiting these types of errors were excluded from the performance comparison evaluation. Table 35 provides an overview of the selected models including R-squared data.

Table 36. Overview of developed performance models.

Model	Pavement	Model Type	R-squared	Observations
Roughness	Flexible	regression (shifted)	0.78	4,544
Roughness	Rigid	regression	0.78	2,652
Rut Depth	Flexible	regression	0.45	1,966
Faulting	Rigid	regression	0.47	1,384
Fatigue and Wheelpath Cracking	Flexible-deduct	logistic	NA	1,977
		regression	0.63	1,486
Fatigue and Wheelpath Cracking	Flexible-percent	logistic	NA	1,977
		regression	0.49	1,481
Transverse Cracking	Flexible	logistic	NA	1,920
		regression	0.71	1,077
Longitudinal Cracking	Rigid	logistic	NA	475
		regression	0.38	240
Transverse Cracking	Rigid	logistic	NA	489
		regression	0.54	228

Using these models, performance comparisons were made for the following five climatic scenarios. Performance curves, as a function of pavement age, were evaluated and mean comparisons were made using 95 percent confidence intervals at select pavement ages, generally between 20 and 25 years. These comparisons were used to identify statistically significant performance differences.

- Deep-freeze, wet region.
- Deep-freeze, dry region.
- Moderate-freeze, wet region.
- Moderate-freeze, dry region.
- No-freeze, wet region.

In addition, performance predictions in each of the PFS were evaluated using typical climates found in each SHA. It was also observed that regional environmental conditions can vary widely in one state. Climatic differences in each PFS were presented as well.

The PFSs were asked to provide information on the pavement design they would use for a standard primary and interstate highway with set design parameters as well as the material specifications, test procedures, and costs associated with those designs.

The questionnaire responses produced a wide variation in pavement design sections for essentially the same design parameters. The PFSs did not identify any particular treatment in their designs that addressed frost effects other than one reference to the frost heave design procedure contained in the *AASHTO Guide for Design of Pavement Structures*.[1] In a secondary query, it was found that several of the northern SHAs did require that frost-susceptible subgrade soils must be removed as part of their construction specifications.

The project also called for the review of practices in adjacent States to see if any treatments could be of use; however, only limited contacts were provided. To augment this process, existing research reports or ongoing research for all SHA were reviewed from Web sites for anything available for this process. This query produces nothing to add to that already found for the PFS and the earlier literature review.

Many of the northern SHAs add additional untreated frost-free surfacing as part of their pavement designs based on the maximum measured frost depth.[12] For some SHAs, frost-susceptible subgrade soils are removed and replaced with frost-free material for depths ranging from 0.61 to 1.22 m (2 to 4 ft) as part of their normal construction requirements to eliminate the need to consider frost depth in the design procedures. There is no real way to show the relative value of the extra depth of frost-free material other than to note its widely accepted use. The extra surfacing depth is probably already accounted for in the pavement performance models developed considering that many SHAs follow that practice, and GPS test sections represent standard SHA design procedures. It may be one of the reasons for the longer service lives observed in fatigue cracking on flexible pavements in the moderate-freeze environments, which would have the extra surfacing compared to the wet no-freeze environments that would not have the extra surfacing.

A possible consideration was noted relative to the use of a uniform surfacing section across the full roadway prism. For those SHAs that use frost-susceptible subgrade soils in part of their shoulder section or outside their shoulder surfacing materials, there is the potential for differential frost heaving. The extent to which this is a problem or the effect it has on pavement performance could not be quantified. Any SHA that has experienced differential frost heave may wish to look more closely at the capillary flow of moisture into the roadway section during the advancement of the freezing front and onset of frost.

The possible use of surface seals was also noted in the northern tier States where highway volumes were low enough to allow their use. This treatment did not seem to be practical in SHAs where chip sealing is not usually done, particularly on higher volume roadways.

Little was noted in the area of material specifications. Prior to Superpave, the researchers would have expected to find different (softer) binders used in the more Northern States as well as the use of a finer, lower-void mix compared to the Southern States. In the response provided by the PFSs, most SHAs have or are in the process of switching to Superpave. The use of the Superpave binder specifications should improve cold weather performance, a major consideration in the development of those specifications. The use of Superpave mix design procedures has to a large extent eliminated local adaptations in mix design procedures and specifications that might have provided improved performance in areas of deep frost penetration or numerous FTCs.

Very little was found in the SHA specifications that indicated a trend in specifications that would have had an impact on mitigating frost effects. What variation there was seemed most likely due to the availability or type of aggregate found in the State.

An economic evaluation was conducted, which consisted of computing equivalent uniform annual costs and present worth costs using deterministic and probabilistic LCCA. Standard cross sections were developed for interstate and primary highways using the 1993 AASHTO *Pavement Design Guide*.[1] LCCA was performed using these standard sections for all of the five regions. However, because many northern SHAs use additional depths of frost-free material to mitigate frost effects, an additional LCCA was performed. In this analysis, the roadway sections for the deep- and moderate-freeze regions included additional unbound base course thickness while the no-freeze region remained unchanged from the standard AASHTO design.

The differences between the costs using the standard sections were relatively small and well within one standard deviation when considering the distribution of the data. Using the mitigated section, which is more representative, resulted in the no-freeze region having life cycle costs that were less than the costs of the other regions and fell outside the range of one standard deviation.

The application of the results of this study to M-E design procedures was also explored. Potential uses of the models in implementing the NCHRP 1-37A *Guide* design procedure were also discussed. The use of additional frost-free material incorporated either in the pavement design or as a specific subgrade treatment can be accommodated in mechanistic design procedures. In most mechanistic design procedures there is a process

that accounts for changing subgrade stiffness experienced throughout the year. In those areas with significant thaw weakening, the amount of time that the subgrade is weaker as well as the amount of weakening that occurs during the spring thaw is input into the program. In these cases, the added frost-free layers would be considered as either an improved subgrade or added subbase in the program. For instance, in the basic pavement design used in the economic analysis in the previous chapter, the AASHTO design procedures produced a pavement section consisting of 150 mm (6 inches) of ACP over 205 mm (8 inches) of untreated base for the design considerations included in the PFS design questionnaire.

In an area where there is 1 m (3 ft) or more of frost penetration during the winter, that subgrade would weaken significantly during spring thaw, possibly as much as 50 percent. That weakening is addressed in the 1993 AASHTO guide by using the effective modulus to account for the reduced springtime stiffness. In a mechanistic-based design procedure, the increased damage accrued during the spring weakening of the subgrade would be accounted for in the program by an increase in stresses incurred during that period as a result of the lower stiffness. If the subgrade soil was replaced with 0.61 m (2 ft) or more of frost-free material, as is done in several of the PFSs, then the stiffness of the subgrade can be increased because of the replaced layer, and the reduced spring weakening effects can be eliminated or significantly reduced. Combined, these inputs would reduce the tensile stresses on the bottom of the pavement and reduce the compressive stresses on the top of the subbase as well as the subgrade. The results should be demonstrated in longer service life for the pavement section being analyzed.

Probably of greater significance is the potential use of the models from this study to help provide a regional calibration for the 1-37A mechanistic-based design procedure. The 1-37A M-E design program uses nationally calibrated damage trends, but the NCHRP 1-37A *Guide* recommends that the users consider a regional calibration- verification procedure. For those SHAs that do not have the regional data to support the activity, the potential use of the models developed in this project as well as the general procedures to develop regional calibration factors were described.

There is also a potential for using the models developed in this study to augment SHA-collected data for the development of a family of curves for regional use in PMSs. Where an agency does not have sufficient regional data to develop project-specific pavement deterioration curves, the models from this study could be used to develop a family of curves that would fit the local environment. It is not envisioned that these models could be used in place of SHA-specific data but, in the beginning—during the implementation of a PMS—the models could be used to make an initial trial of developing the pavement deterioration trends used in the PMS. As with the implementation of any PMS, as data become available, the SHA should refine the performance trends based on its own actual experience, but these models would provide a very good starting point.

APPENDIX A. LITERATURE REVIEW

This appendix details relevant literature reviewed for this study to gain an understanding of pavement response in various freezing conditions. Although the available literature directly related to the study was relatively limited, it provided insight that was used to formulate the activities conducted. The majority of the literature regarding frost effects dealt with quantifying the change in material properties and performance characterization on particular projects. In addition, some limited information was found on using LTPP data to model pavement performance in frost areas.

THE EFFECTS OF FREEZE-THAW PERIODS ON A TEST PAVEMENT IN THE DANISH ROAD TESTING MACHINE

In this literature example, Zhang and MacDonald[31] reported frost studies using the Danish road testing machine in their paper "The Effects of Freeze-Thaw Periods on a Test Pavement in the Danish Road Testing Machine" presented at the Ninth International Conference on Asphalt Pavements, International Society for Asphalt.

Tests performed in the testing machine were subjected to freeze-thaw cycles to study the effects of frost on pavement performance. Initially, Road Test Machine 2 (RTM2) was loaded with more than 150,000 repetitions of a 60,000 newton (N) (13,488 lbf) wheel load. A freeze-thaw cycle was then simulated and the pavement structure was loaded with 1,800 additional repetitions during the thawing period. This process was then repeated; however, the number of load repetitions during thawing was modified to 3,000. Rut level-up and overlay layers were then placed on the RTM2 pavement structure. The resulting structure was labeled as RTM3. It was subjected to one freeze-thaw cycle and loaded with 2,800 repetitions during the thawing period, followed by 50,000 repetitions after the completion of the thawing process. Soil suction, material response, profile, and temperature data were collected throughout the testing periods. The profile data were obtained using a profiler specially built for profile measurements in the RTM. To simulate freezing conditions, the chamber was maintained at –15 °Celsius (C) (5 °Fahrenheit (F)). During thawing, the temperature of the chamber was gradually raised to 10 °C (50 °F) and then to 25 °C (77 °F). The water table level in the RTM was maintained at 0.8 m (2.62 feet (ft)) below the level of the pavement surface.

As a result of the testing, a new subgrade permanent strain model was developed as well as roughness models in terms of slope variance, international roughness index (IRI), and rut depth. Equation 11was developed for permanent strain in the subgrade.

$$\varepsilon_{PZ} = 0.087 * N^{0.333} * (\sigma_Z / p)^{0.333} * \varepsilon_Z \quad (11)$$

Where:

ε_{PZ} = plastic strain at depth Z in microstrain

N = number of load repetitions

σ_Z = vertical stress at depth Z

P = reference stress (atmospheric pressure 0.1 MegaPaschal)

ε_Z = vertical resilient (elastic) strain at depth Z in microstrain

A, α, β = constants

Plastic strain in the subgrade material was determined to increase 60 to 75 percent during the thaw-loading period, while the transient resilient response increased 40 percent. The increase in strain was attributed to movement, reorientation, and resettlement of the soil particle displaced by previous frost heave. This study provided good numerical information on the change in material properties from frost effects.

A DETERIORATION MODEL FOR PAVEMENTS IN FROST CONDITIONS

Doré, Konrad, and Roy[32] presented a paper, "A Deterioration Model for Pavements in Frost Conditions," analyzing thermal cracking. Using data from test sections in Quebec, Finland, and Minnesota (the Minnesota Road Research Project (Mn/ROAD) as well as two LTPP SMP sites, Doré, Konrad, and Roy developed two empirical models. The first model provides curves for delimiting different levels of cracking extents based on the solicitation index. The second model estimates the equivalent annual evolution of cracking, which is defined as the total cracking developed over 1 year divided by the age (in years) of the pavement.

A sensitivity analysis was performed by altering all contributing factors used in the model to predict the life span of the pavement. The results showed that the frost depth and width of snow removal contribute the most to pavement performance. The model is based on a number of assumptions, and it is valid only for pavements with substantial frost penetration. In addition, the data used in generating the model came from a small set of locations. Construction variability was not taken into account and would contribute significantly to crack development in areas of local weak spots.

ANALYSIS OF SEASONAL PAVEMENT DETERIORATION

Doré and Savard[33] reported additional studies of thermal cracking which in their paper "Analysis of Seasonal Pavement Deterioration." Two test sites in Quebec, Canada, were monitored for 3 years to evaluate seasonal accumulation rates of distress. One site was constructed in 1994 specifically for this project. It consisted of five test sections (three of which were insulated). The other site was part of C-SHRP and consisted of four

noninsulated test sections. Each of these sections had the same structural design and differed only in the grade of asphalt used. Noninsulated sections were used to compare the accumulation of different distress types in each season. Similar analysis was performed on the insulated sections, thus evaluating the effectiveness of insulation in preventing frost-related distress.

The noninsulated sections were found to experience 65 percent of transverse cracking damage in the winter followed by 25.5 percent in the spring. Transverse cracking is caused by the accumulation of tensile stress in the pavement due to thermal shrinkage. The relatively large amount of damage incurred during the spring is likely to be the propagation of existing transverse cracks originally developed in the winter. Similarly, 55 percent of longitudinal cracking damage occurred in the winter compared with 23 percent in the spring and 22 percent in the summer. The research team believed that differential heaving during winter was the main mechanism in longitudinal cracking; however, the data does not support this belief. Other factors may also contribute to the longitudinal cracking. Approximately one-half (49 percent) of the fatigue damage was accumulated during the winter, while 42 percent occurred in the spring. The large fatigue damage in the winter is believed to be due to partial thawing of the pavement base that occurred during the winter season. The ratio of winter-to-fall roughness was approximately 1.7 to 1. A residual roughness was found to remain after the spring thaw. The increase in roughness is believed to be caused by frost heave. Based on the data collected, seasonal effects are not significant in terms of rutting damage. Last, the comparison of distress accumulated on insulated and noninsulated sections revealed that insulation is effective in reducing overall distress by 40 percent.

DEVELOPMENT OF PERFORMANCE PREDICTION MODELS FOR DRY NO FREEZE AND DRY FREEZE ZONES USING LTPP DATA

More specific to this project was a report by Senn, et al.[34] on "Development of Performance Prediction Models for Dry No Freeze and Dry Freeze Zones Using LTPP Data." Using data from approximately 50 GPS sites in the LTPP Western Region, performance trends were developed based on roughness, fatigue cracking, transverse cracking, and rut depth. For purposes of analysis, the sites were categorized by climatic region and structural number. Only two climates were considered in this study (dry freeze and dry no-freeze). Similarly, two structural number levels were used to group the sites using a structural number of four as the breakpoint between the two levels. This was done to distinguish between the relatively thick and thin pavement sections. Regression analysis was performed using ESALs as the independent variable for all parameters with the exception of transverse cracking, which incorporated pavement age as the independent variable.

From the analysis, fatigue cracking and transverse cracking both increased with traffic or time:

- In the dry no-freeze zone, larger amounts of fatigue cracking were present in thinner pavements compared to thicker pavements.
- The opposite was true for sites located in the dry freeze zone.

- Thinner pavements in the dry no-freeze zone were more susceptible to transverse cracking than thicker pavements.
- The increase in roughness of sites located in the dry freeze region was more rapid than the increase in the dry no-freeze zone.
- Similar to the other distress types, opposing roughness trends were found for thick and thin pavements in each climate.
- Thin pavements experience a greater increase in roughness in the dry freeze climate, while the opposite is true for the dry no-freeze environment.
- Rutting in the dry no-freeze climate was much greater than in the dry freeze climate.

Although the preceding conclusions could be drawn from the data, the correlations were very poor, and many factors made the analysis difficult. In some cases, monitoring terminated before the failures in the pavement were exhibited. Without data on pavement structures near the end of their service life, developing a prediction model is very difficult. Adding to the difficulties was the variability in the field measurements. In particular, the difference between longitudinal cracking in the wheelpath and fatigue cracking is very subjective, resulting in drastically different amounts of fatigue cracking on the same section. Last, there is a large difference in the traffic levels experienced in the Western Region's dry freeze and dry no-freeze zones.

DETERMINATION OF THE CRITICAL THAW-WEAKENED PERIOD IN ASPHALT PAVEMENT STRUCTURES

A study[35] was undertaken to evaluate the spring thaw period on a forest highway in northwestern Montana. By developing a methodology to accurately and easily determine the thaw conditions of the highway at various locations, responsible entities could place load restrictions at optimum times throughout the year. Air and subsurface soil temperature thermistors were installed at 17 sites equating to a density of one site every 5.63 km (3.5 mi). The locations of the instrumentation were selected based on divisions of the highway that could be easily closed without affecting the remaining segments. Data were collected throughout the year with increased frequency during the spring season.

The research attempted to predict the thaw condition based solely on soil temperature. Because of the presence of dissolved minerals in soil moisture, the soil will freeze at temperatures below 0 °C (32 °F). Therefore, laboratory testing was performed on eight soil samples typical of the region to determine the actually freezing temperature. An average value of −0.17 °C (31.7 °F) was determined from this testing and used in the analysis. In addition, pavement strength was measured using Benkelman beam deflection testing.

Through the combination of temperature and strength testing the following results were obtained. The thawing period did not begin until a temperature of −0.17 °C (31.7 °F) was achieved at the base of the asphalt. It is interesting to note that this condition was not met

until the average soil temperature rose to approximately 1.11 °C (30 °F). Pavement strength data were used to determine the pavement strain, and thus, damage factors throughout the year. The end of the critical thaw weakening period was determined by identifying the time when the damage factor returned to unity, indicating the pavement strength returned to prefreeze levels. From this analysis, a thaw depth of approximately 1.22 m (4 ft) was indicated as the end of the critical thaw period. These results are based on limited data from a very specific region of Montana.

CALCULATED MAXIMUM FROST DEPTHS AT MN/ROAD WINTERS 1993–1994, 1994–1995, AND 1995–1996

The Modified Berggren equation (MBE) was used to estimate the maximum frost penetration experienced at 40 Mn/ROAD test sections over three winters.[36] These predictions were compared with the measured maximum frost penetration values obtained from electrical resistivity probes installed at the site. Further, sensitivity analysis was conducted to study the contribution of many factors on estimated frost depth. The factors considered in the analysis were pavement material properties, moisture content, density, layer thickness, and mean soil temperature, as well as factors dealing with thermal properties of materials.

The results from the comparison were inconsistent between the three winters. For the 1993–1994 winter, the difference between calculated and measured frost depth was within ±10 percent for most of the sections. Generally, the calculated values underestimated the actual frost depths measured. Similar results were obtained for the 1995–1996 winter. Conversely, only approximately 50 percent of the data from the 1994–1995 winter were within ±20 percent. The rest of the data exhibited greater differences. Using the MBE resulted in an overestimation of frost depth in the majority of the test sections for that winter. For all three winters, test sections with granular subgrade experienced measured frost depths far less than the estimated values. In this case, it is believed that errors in the frost penetration measurement caused the discrepancy.

Several conclusions were drawn from the sensitivity analysis. The effect of small variations in layer thickness on estimated frost depth can be considered negligible. Sizeable deviation in moisture content will result in a change in calculated frost depth of less than 10 percent. One of the variables in the MBE is the n-factor, which is used to convert air freezing index to surface freezing index. The most appropriate n-factors were found to be 0.90 for flexible pavements and 0.95 for rigid pavements based on the conditions at Mn/ROAD. Thermal conductivity values were estimated using equations developed by Kersten. Better results of frost penetration were observed when the thermal conductivity estimates were increased by 25 percent. Last, a reduction of the estimated mean annual soil temperature from 11.1 °C to 9.4 °C (51.98 to 48.92 °F) resulted in better agreement of frost penetration data. If the changes in n-factors, thermal conductivity, and mean annual soil temperature are implemented, the majority of the calculated depths fall within ±13.3 (excluding granular subgrade data).

PARKS HIGHWAY LOAD RESTRICTION FIELD DATA ANALYSIS: A CASE STUDY

In an effort to evaluate the effect of thaw weakening on pavement structures, eight test sections were monitored in 1993, 1995, and multiple times in 1996.[37] FWD, distress, rut, roughness, and traffic data were collected and used in the analysis. To monitor thaw propagation, hourly subsurface temperatures were collected to a depth of 1.93 m (6.33 ft) below the surface. Regression analysis was performed on the temperature data to develop thaw propagation models, which were used to determine the limits of the thaw period in the spring of 1996. For this study, the end of the thaw period was set as the time at which the thaw depth reached 1 m (3.28 ft).

Results from distress data revealed that rutting and water bleeding were the most common forms of distress accumulated during the thaw period. Rutting occurred very rapidly, and it first occurred when the thaw depth was at approximately 0.3 m (0.98 ft). The southern lane, which carries 70 percent less EALs, was found to exhibit more damage than the northern lane. Dynamic effects of lighter weight traffic are believed to be the cause of this phenomenon. Rut depth and roughness were both found to be larger in the early spring than in the late spring. The improvement in remaining life based on fatigue damage obtained when load restrictions were enforced was determined using FWD.

COMMON CHARACTERISTICS OF GOOD AND POORLY PERFORMING PCC PAVEMENTS

A study[38] was undertaken to evaluate the factors contributing to both good and poor performance of PCC pavements. To conduct this analysis, definitions of good and poor performance needed to be determined in terms of specific distress types. This was achieved through the collaboration of a panel of experts who set limits on performance considering roughness, faulting, cracking, and localized failures such as a function of pavement age. Data from the LTPP database were the sole source of information used for this study.

Based on the analysis, jointed plain concrete pavements (JPCP) were found to exhibit increased roughness values when subjected to multiple freeze-thaw cycles. In addition, sections in colder climates were rougher, as were sections in wetter climates. Seventy-one percent of the poor performing JPCP (in terms of roughness) sections had fine-grained subgrade. Similarly, all of the poor performing JRCP sections (roughness) were on fine-grained subgrade. Increased subdrainage was also found to decrease roughness in three surface types: JPCP, JRCP, and continuously reinforced concrete pavements.

Faulting of nondoweled JPCP was found to be higher in wet climates. This trend did not hold true for doweled JPCP or JRCP. Fine-grained soils contributed to increased faulting of both JPCP and JRCP. Adequate subdrainage resulted in lower amounts of faulting for both types of jointed concrete but particularly for nondoweled JPCP.

Transverse cracking of JPCP was found to occur more often in the western part of North America. It is believed that the increase in solar radiation in the west contributes to a larger thermal gradient through the slab leading to increased warping and curling.

Cold and wet climates increased the amount of localized failures experienced in continually reinforced concrete pavement (CRCP); However, more information is required to fully understand all factors contributing to these failures.

DETERMINATION OF FROST PENETRATION IN LTPP SECTIONS, FINAL REPORT

In this study[39] data obtained from LTPP SMP sites were used to determine the presence and extent of frost penetration. Three types of electrical resistance measurements (2-point resistance, 4-point resistivity, and voltage drop) were used in conjunction with subsurface temperature profile data to estimate frost penetration. A computer program (FROST) was developed to assist in evaluating the temperature and electrical resistance data.

Overall, temperature profile data produced reasonable and expected trends. Based on the concept of latent heat of fusion, two conditions were defined to indicate a phase change in subsurface material. The temperature must be less than or equal to 0 °C (32 °F), and it must remain constant for 2 days. Reasonable frost predictions were obtained using these criteria and the temperature data; however, some limitations exist using the established method. The 2-day minimum time period for constant temperature prevents short freeze-thaw cycles from being captured. On the other hand, temperature data from lower in the pavement structure usually exhibit less than 1 °C (33.8 °F) daily variation throughout the year. Therefore, the 2-day time period erroneously identifies phase changes in some cases. Because of these limitations, temperature data alone cannot be used in predicting phase changes.

There is a large increase in resistivity when frozen conditions exist, thereby allowing for the identification of phase changes; however, many factors influence the bulk resistivity of soils: the type of soil, moisture content, dissolved salt concentration, and temperature. Identifying an increase in resistance due to frozen soil is very difficult. When comparing the three resistance measurement techniques it was discovered that agreement between all three methods occurred 60 percent of the time. Coupling this with the fact that each method had unique advantages and disadvantages, the use of all three techniques simultaneously would produce the most reliable results. Concurrently using all resistance data still produced large nonwinter, seasonal, and diurnal variability that could not predict phase changes with accuracy.

As a result of the analyses of temperature and electrical resistance data, algorithms were developed to incorporate data from all three resistance measurement techniques, temperature data and time of year to identify the extent of frost penetration. These algorithms were packaged into the FROST program. The FROST program will normalize all three resistance measurements. The user must then select an appropriate threshold based on these normalized values. All data points below the threshold are considered to

be in the nonfreeze state. Data points above the threshold are analyzed further based on the average temperature. If the temperature is greater than zero, the data point is considered to be in the nonfreeze state. Conversely, temperatures below zero yield a data point classified in the freeze state. Graphs are then produced that visually depict the extent of frost throughout the monitoring period.

The output from FROST was compare with historical data and found to be in reasonable agreement. Time domain reflectometry (TDR) data, also collected at LTPP SMP sites, was compared with the FROST output. TDR data provide information about the moisture content of soil; however, this information does not reflect frozen water. Therefore, a sudden drop in moisture content recorded by the TDR is expected during freeze periods. In almost all cases, prediction of frost by the program corresponded to a drop in moisture content recorded by TDR. The overall reliability of the freeze-state determination is 93 percent. These results have been added to the LTPP IMS and can be found in two tables: SMP_FREEZE_STATE and SMP_FROST_PENETRATION.

DEVELOPMENT OF A PAVEMENT RUTTING MODEL FROM EXPERIMENTAL DATA

An empirical rutting progression model was developed using data from the AASHO Road Test.[40] One of the major differences between this and other models is the inclusion of a thawing index to capture the effects of the environment on rutting. Considerable accumulation of permanent deformation was experienced during spring thaw periods; therefore, including a thawing index seems logical. Furthermore, it is well accepted that the strength of unbound layers reduces considerably with excess moisture. The largest increase in moisture content of subsurface material is experienced during thaw periods.

To determine a thawing index, some measure of freezing is necessary. An accumulated freeze index was utilized to quantify freezing and was based on the mean minimum temperature of each two week period. This index was combined with the mean maximum temperature over each two week period to determine the thawing index. The thawing index was then incorporated in the permanent deformation model by increasing the rate of rutting as a function of thawing index.

Overall, the model was found to estimate rut depth with a standard error of regression of 3.3 mm (0.13 inch). The predicted rut depth values compare very well to the observed rut depth measurements for sections used in the model development. In addition, actual rutting measurements from other sections, not used in the model development, were compared with predicted values and found to be in agreement, further confirming the model. Note that this model is specific to the conditions of the AASHO road test.

ANALYSIS OF EXPERIMENTAL PAVEMENT FAILURE DATA USING DURATION MODELS

A study[41] was undertaken to develop a new pavement performance equation using duration models based on data from the AASHO road test. Duration models incorporate the variable nature of pavement failure as well as accounting for censoring and truncation biases, which are introduced into models when failure events are not observed due to limited duration data collection. In some instances, pavement failure is reached before the monitoring period begins, while other failures occur after the completion of the monitoring period. Although these data points were not observed, they need to be accounted for in model development. An extension of the Weibull model can be used to eliminate this bias.

From the Weibull model, the rate at which pavement failure will occur after a given time can be estimated using the hazard rate function. In addition, the survival function can be used to estimate the probability that a pavement will last longer than a given time period. In turn, the probability distribution can be determined using the previous two functions. Of the three models discussed above, only the hazard rate function was used in this study.

For comparison, a model using the hazard function with the same variables as the original AASHO equation was developed to predict pavement life. Results from this duration model were compared with the predicted values of the original model using data from the AASHO road test. Overall, the life prediction from the new duration model estimated the life of the test section with more accuracy than the original model. The standard error of the new model was 0.42 compared with 0.65 from the original model. However, the duration model overestimated the life of pavement structures that failed relatively early in the testing period. Conversely, the model underestimated the pavement life of pavement structures failing relatively late. By the end of the testing phase, 237 test sections reached failure. The new equation predicted 253 failures with an error of 6.8 percent, while the original equation predicted 215, which equates to an error of –9.3 percent.

PAVEMENT PERFORMANCE DURING THAW WEAKENING

Test sections in the Frost Effects Research Facility at the Cold Regions Research and Engineering Laboratory were loaded with a 133-kN wheel load during a simulated thawing period.[42] Using in situ measurement equipment, base and subgrade responses such as stress, strain, resilient modulus, and permanent deformation were monitored before and throughout one freeze-thaw cycle to quantify the changes induced by this environmental process. In addition, the timing of these changes was of interest to researchers to define critical periods in the cycle. Results from this research were used to evaluate the validity of the U.S. Army Corps of Engineers Modulus Reduction Factors for Frost-Susceptible Soils. This table is used for design to adjust modulus values obtained during frost-free conditions to reflect values experienced during thawing periods.

From this testing, the base was found to experience a 67 percent maximum reduction in resilient modulus during the thaw-weakening period, which was approximately 2 weeks. Similarly, the subgrade experienced a reduction of 56 percent over a 3-week period. The vertical strain in the base reached a maximum level 15 days into the thawing phase, which was approximately 530 percent of the prefreeze value. The strain never fully recovered, remaining at 160 percent on completion of the cycle. The subgrade behaved in the same manner, reaching a maximum strain 1,100 percent higher than the prefreeze strains 15 days into the thaw process and recovering to only 241 percent. The stress values followed similar patterns. The minimum stress did occur at the same time as the maximum strain in the subgrade but not in the base layer. Permanent deformation was found to increase rapidly within the first 10 days. Based on these findings, the reduction factors used in the design process significantly overestimate the stiffness of both the base and subgrade material during the thawing period.

EFFECTS OF FROST HEAVE ON THE LONGITUDINAL PROFILE OF ASPHALT CONCRETE PAVEMENTS IN COLD REGIONS

The cyclic increase of pavement roughness in roadways subjected to frost penetration prompted a study of the change in IRI on a section of the Doto Expressway in east Hokkaido, Japan.[16] The section of road was divided into 31 consecutive sections each with a length of 1 km (0.62 mi). The IRI values were obtained from longitudinal profile data collected using an inertial profiler. Profiles were collected once in August 1999 and once in November 1999 to establish prefrost values. Between February and April 2000, longitudinal profile data were collected once a week to monitor the change in IRI during the propagation of frost penetration and subsequent thaw period. Weather data were also gathered from a weather station adjacent to the test sections. Using a modified Berggren's formula with this data and knowledge of the subsurface material, the depth of frost penetration was estimated to reach a maximum in late March 2000. In addition, frost penetration was estimated to reach the subgrade layer on February 11, 2000.

The IRI in the summer and fall were found to be similar and considerably less than the winter IRI values. The winter IRI values increased as the temperature decreased, and they reached a maximum value in early to mid-March just before the maximum depth of frost penetration was achieved. The spring IRI values appeared to have returned the level of the prefreeze values of the summer and fall. For further analysis, the test sections were divided into 100-m (328.1-ft) segments and categorized into following three groups based on the nature of material under the pavement structure: cut, embankment, and bridge. The average IRI values in each category were compared and the cut sections were found to exhibit the greatest increase in roughness during the frost penetration. Additional evaluation of the six sections demonstrating the largest increase in IRI established a linear relationship between IRI and freezing index.

THERMAL ASPECT OF FROST-THAW PAVEMENT DIMENSIONING: IN SITU MEASUREMENT AND NUMERICAL MODELING

Multiple models have been developed to forecast the propagation of frost and resultant heave of roadways both in Quebec and France. In order to validate these models, in this

study[43] four test sections were constructed and monitored for 3 years. The test sections were equipped with temperature sensors, TDRs, frost tubes, piezometers, and heaving sensors to monitor frost depth as well as the amount of heaving in the subsurface layers of the pavement structure. Weather data were obtained from a weather station in the nearby vicinity. Two pavement structures commonly constructed in France were selected for the monitoring sections. Two test sections conforming to each typical pavement structure were constructed; however, only one test section of each structure was insulated with extruded polystyrene. This allowed for the evaluation of the effect of frost on pavement performance while keeping all other variables (i.e., traffic, natural subgrade, climate, and pavement structure) constant. Furthermore, the efficiency of the insulation could also be assessed.

Frost depth and soil heave estimates from the SSR, GEL1D, and CESAR-GELS models were compared with actual values obtained for the onsite monitoring equipment. The SSR model is based on thermal equilibrium at the frost front, and it estimates soil heave using water migration as a function of thermal gradient. The GEL1D and CESAR-GELS models are similar; they use finite element analysis as the foundation for frost-depth estimation. These two models do not incorporate heave estimates into their frost-depth calculations.

All three models were found to estimate frost penetration within 10 percent of the values recorded onsite. Because the GEL1D and CESAR-GELS models are dependent on initial conditions and do not incorporate frost heave, substantial differences between the models were observed. The SSR model was found to predict frost heave within the same order of magnitude with the maximum difference between predicted and measured values found to be 7 mm (0.276 inch). The ability of the insulation layer to protect subsurface materials from frost penetration was confirmed.

PROBABILISTIC ANALYSIS OF HIGHWAY PAVEMENT LIFE FOR ILLINOIS

Survival analysis has been performed four times over the past 15 years on the majority of the freeway system in Illinois. This analysis[44] provides the probability of failure as a function of age or cumulative ESALs. Original pavement structures were categorized by pavement type and thickness. JRCP and CRCP were further separated with the presence of durability cracking. All pavement types were also classified by geographical location. Receiving rehabilitation treatment was defined as the failure criteria. Due to the length of the study, some pavement structures experienced failure multiple times, with some sections receiving three overlays; therefore, overlays were also included in the analysis.

Durability cracking greatly reduced the life expectancy of both JRCP and CRCP sections in the southern region of Illinois. JRCP sections without durability cracking are expected to carry 30 percent more ESALs than sections with durability cracking before reaching the 50th percentile life expectancy. Similar results were found in CRCP sections with a reduction in cumulative ESALs ranging between 32 and 63 percent. Thick asphalt cement overlays placed over both JRCP and CRCP experienced a larger reduction in life expectancy due to durability cracking compared with thin overlays.

One major downfall of this study was the failure criteria selected. Due to budgetary and other issues, rehabilitation activities are not performed on roads with consistent conditions. One road may receive treatment 1 year after the pavement has reached a poor condition, while other roads may be overlaid within 1 month of deteriorating to a similar condition. Further, some sections receive rehabilitation before failure occurs, introducing censoring bias.

EFFECTS OF ENVIRONMENTAL FACTORS ON PAVEMENT PERFORMANCE-THE INITIAL EVALUATION OF THE LTPP SPS-8 EXPERIMENT

Using data available from the LTPP database, a study was conducted to examine the effects of climate and subgrade on pavements subjected to limited loading.[45] All SPS-8 projects, monitored under LTPP, were considered in this analysis. Each site was categorized based on climate (precipitation and temperature), subgrade type, pavement structure, and age. Distress and roughness data were the only parameters evaluated in the study.

The research effort revealed that sections constructed on active subgrade soil in wet-freeze climates exhibited significantly more nonwheelpath longitudinal cracking. Statistical analysis of pavement roughness showed that subgrade type was the most influential factor for flexible pavements, while precipitation was most important in rigid pavements. It should be noted that these statements were not statistically significant at the 95 percent confidence interval. Sections constructed on active subgrade (in any climate) had the highest average IRI.

LTPP DATA ANALYSIS: INFLUENCE OF DESIGN AND CONSTRUCTION FEATURES ON THE RESPONSE AND PERFORMANCE OF NEW FLEXIBLE AND RIGID PAVEMENTS

LTPP data from the SPS-1, SPS-2, and SPS-8 experiments were used to study the relative influence of structural design factors as well as site conditions on pavement performance.[46] The SPS-1 projects were used to investigate HMA layer thickness, base type, base thickness, and drainage. The SPS-2 experiments were evaluated to determine the effects of PCC slab thickness, flexural strength, base type, drainage, and slab width. The SPS-8 experiments were used to look into environmental effects without the contribution of heavy traffic. Performance comparisons were made for various surface distress types as well as roughness, rutting (HMA), and transverse joint faulting (PCC). The results from this study can be used to improve and implement design procedures that make better use of design options. Also, the contribution of environment and site conditions can be evaluated. Following are a few of the findings from the final report:

- Based on the data evaluated, drainage improves rutting performance of pavements with dense graded aggregate base (DGAB) in wet no freeze climates.
- Pavements with underlying asphalt treated base (ATB) exhibit the lowest accumulation of fatigue cracking.

- PCC pavements with fine-grained subgrade soils have higher accumulations of transverse cracking as compared to coarse-grained subgrades, although the difference is only marginally significant based on statistics.
- Because SPS-8 projects have accumulated low amounts of distress to date, pavement with frost-susceptible subgrade have more longitudinal cracking, transverse cracking, and fatigue cracking compared with other soil types.

APPENDIX B. PERFORMANCE PREDICTION MODELS

This appendix provides details on the prediction models for each of the performance measures evaluated in the study. In addition, the use of each model is illustrated through examples. Following is a list of the performance measures:

IRI = Pavement roughness (m/km (ft/mi))—flexible and rigid.

RUT = Rut depth (mm (inch))—flexible.

FWPC = Fatigue and wheelpath cracking (deduct value)—flexible.

fwpc = Fatigue and wheelpath cracking (percentage of wheelpath area)—flexible.

TC = Transverse cracking (deduct value)—flexible.

TC = Transverse cracking (percentage of total section area)—rigid.

LC = Longitudinal cracking (percentage of total section area)—rigid.

FLT = Transverse joint faulting (mm (inch))—rigid.

Following is a list of the explanatory variables input into the equations:

ACTHICK = Thickness of AC layer (mm (inch)).

ADJ_AGE = Pavement age after distress initiation (years).

AGE = Pavement age (years).

BASE = Base type (DGAB, ATB, PATB, LCB, NONBIT, NONE).

CI = Cooling index (degree-Celsius days).

DEPTH = Thickness of PCC layer (mm (inch)).

FC = Functional classification of roadway.

FI = Freezing index (degree-Celsius days).

FTC = Annual number of freeze-thaw cycles (each).

LESN = Logarithm of annual ESAL divided by structural number.

LEDT = Logarithm of annual ESAL divided by PCC layer thickness.

MIRI = Initial IRI (m/km (ft/mi)).

MIRI_AGE = Pavement age when MIRI was recorded (years).

Pavement Structure = AC nonoverlay with unbound base, AC nonoverlay with bound base, AC overlay (either bound or unbound base), JPCC.

PRECIP = Annual precipitation (mm (inch)).

SG = Subgrade classification (FINE, COARSE, ROCK/STONE, OTHER).

ABSOLUTE IRI PREDICTION MODEL FOR FLEXIBLE PAVEMENTS

Equation 12 shows the IRI regression equation (R-squared = 0.78, total observations = 4,544) and equation 13 defines the delta equation.

$$\ln(IRI+0.1)=\alpha-\Delta+0.115*\left(\frac{\log(ESAL)}{SN}\right)+3.29\times10^{-2}*AGE-4.33\times10^{-5}*CI+2.28\times10^{-6}*FI$$
$$+5.90\times10^{-5}*PRECIP+2.21\times10^{-4}*FTC+8.59\times10^{-5}*ACTHICK$$
$$-5.39\times10^{-3}*\left(\frac{\log(ESAL)}{SN}\right)*AGE+1.77\times10^{-6}*AGE*CI+4.55\times10^{-6}*AGE*FI+0.643*MIRI$$
$$-2.50\times10^{-2}*MIRI\_AGE-2.40\times10^{-6}*AGE*PRECIP-1.09\times10^{-5}*AGE*FTC \quad (12)$$

Where:

$$\Delta=\alpha+0.115*\left(\frac{\log(ESAL)}{SN}\right)+7.90\times10^{-3}MIRI\_AGE-4.33\times10^{-5}*CI+2.28\times10^{-6}*FI$$
$$+5.90\times10^{-5}*PRECIP+2.21\times10^{-4}*FTC+8.59\times10^{-5}*ACTHICK$$
$$-5.39\times10^{-3}*\left(\frac{\log(ESAL)}{SN}\right)*MIRI\_AGE+1.77\times10^{-6}*MIRI\_AGE*CI$$
$$+4.55\times10^{-6}*MIRI\_AGE*FI+.643*MIRI-2.40\times10^{-6}*MIRI\_AGE*PRECIP$$
$$-1.09\times10^{-5}*MIRI\_AGE*FTC-\ln(MIRI+0.1) \quad (13)$$

Table 37 shows the coefficients for a flexible IRI model.

Table 37. Coefficients for flexible IRI model.

α Values for FINE SUBGRADE			
BASE	**Nonoverlay, Unbound Base**	**Nonoverlay, Bound Base**	**Overlay, Bound or Unbound Base**
ATB	NA	−0.714	−0.759
DGAB	−0.713	NA	−0.753
LCB	NA	−0.658	−0.702
NONBIT	NA	−0.674	−0.718
NONE	−0.658	NA	−0.698
PATB	NA	−0.734	−0.779
α Values for COARSE SUBGRADE			
ATB	NA	−0.77	−0.815
DGAB	−0.769	NA	−0.810
LCB	NA	−0.714	−0.759
NONBIT	NA	−0.730	−0.774
NONE	−0.714	NA	−0.755
PATB	NA	−0.790	−0.835
α Values for ROCK/STONE SUBGRADE			
ATB	NA	−0.671	−0.716
DGAB	−0.670	NA	−0.711
LCB	NA	−0.615	−0.660
NONBIT	NA	−0.631	−0.676
NONE	−0.615	NA	−0.656
PATB	NA	−0.691	−0.736

Example of Absolute IRI Prediction Model for Flexible Pavements

As discussed in the main body of the report, the flexible IRI prediction model incorporates a delta factor that shifts the model to correspond with the measured initial IRI value (MIRI). The first step in predicting IRI for flexible pavements is to calculate that delta factor. With this factor determined, the IRI can be estimated from the regression equation. A pseudopavement section was fabricated with the explanatory conditions in table 38 for use as an example.

Table 38. Example pavement section information.

Input	Value
Pavement Structure	Nonoverlay, Unbound Base
BASE	DGAB
SG	FINE
ESAL	126,000
SN	5.0
ACTHICK	6.5
FTC	80
FI	688
CI	205
PRECIP	1,140
MIRI_AGE	1
MIRI	1
Age	2

Substituting the inputs from table 38 into the delta equation and extracting the alpha value from table 37 based on pavement structure, base type, and subgrade type appears in equation 14.

$$\Delta = -0.713 + 0.115 * \left(\frac{\log(126000)}{5} \right) + 7.90 \times 10^{-3} * 1 - 4.33 \times 10^{-5} * 205 + 2.28 \times 10^{-6} * 688$$
$$+ 5.90 \times 10^{-5} * 1140 + 2.21 \times 10^{-4} * 80 + 8.59 \times 10^{-5} * 6.5$$
$$- 5.39 \times 10^{-3} * \left(\frac{\log(126000)}{5} \right) * 1 + 1.77 \times 10^{-6} * 1 * 205$$
$$+ 4.55 \times 10^{-6} * 1 * 688 + .643 * 1 - 2.40 \times 10^{-6} * 1 * 1140$$
$$- 1.09 \times 10^{-5} * 1 * 80 - \ln(1 + 0.1) \quad (14)$$

Therefore, the result is equation 15.

$$\Delta = 0.032 \tag{15}$$

Using this delta and the regression equation, the result is equation 16.

$$\ln(IRI+0.1) = -0.713-0.032+0.115*\left(\frac{\log(126000)}{5}\right)+3.29\times10^{-2}*2-4.33\times10^{-5}*205+2.28\times10^{-6}*688$$
$$+5.90\times10^{-5}*1140+2.21\times10^{-4}*80+8.59\times10^{-5}*6.5-5.39\times10^{-3}*\left(\frac{\log(126000)}{5}\right)*2+1.77\times10^{-6}*2*205$$
$$+4.55\times10^{-6}*2*688+0.643*1-2.50\times10^{-2}*1-2.40\times10^{-6}*2*1140-1.09\times10^{-5}*2*80 \tag{16}$$

Therefore, the results appear in equations 17 and 18.

$$\ln(IRI+0.1) = 0.123 \tag{17}$$

$$IRI = e^{0.123} - 0.1 = 1.03 \tag{18}$$

ABSOLUTE IRI PREDICTION MODEL FOR RIGID PAVEMENTS

Equation 19 shows the IRI regression equation (R-squared=0.78, total observations=2,652) for rigid pavements.

$$\ln(IRI+0.1) = \alpha+0.501*MIRI+9.85\times10^{-2}*\left(\frac{\log(ESAL)}{DEPTH}\right)+3.21\times10^{-4}*FI-1.84\times10^{-5}*CI$$
$$+4.17\times10^{-5}*PRECIP+7.76\times10^{-4}*FTC-1.64\times10^{-2}*MIRI\_AGE+1.68\times10^{-2}*AGE$$
$$-2.30\times10^{-6}*FI*FTC+8.11\times10^{-8}*CI*FTC-3.57\times10^{-7}*FI*CI+4.30\times10^{-6}*FI*AGE \tag{19}$$

Table 39 lists the coefficients for a rigid IRI model.

Table 39. Coefficients for rigid IRI model.

α Values for FINE SUBGRADE					
	ATB Base	**DGAB Base**	**LCB Base**	**NONBIT Base**	**PATB Base**
FC 1	−0.478	−0.499	−0.497	−0.413	−0.539
FC 2	−0.488	−0.510	−0.507	−0.423	−0.550
FC 6	−0.529	−0.551	−0.548	−0.464	−0.591
FC 7	−0.492	−0.514	−0.511	−0.427	−0.554
FC 9	−0.402	−0.424	−0.421	−0.337	−0.464
FC 11	−0.455	−0.476	−0.473	−0.389	−0.516
FC 12	−0.469	−0.491	−0.488	−0.404	−0.531
FC 14	−0.526	−0.547	−0.544	−0.460	−0.587
FC 17	−0.408	−0.430	−0.427	−0.343	−0.470
α Values for COARSE SUBGRADE					
FC 1	−0.475	−0.497	−0.494	−0.410	−0.537
FC 2	−0.486	−0.507	−0.505	−0.420	−0.547
FC 6	−0.527	−0.548	−0.545	−0.461	−0.588
FC 7	−0.489	−0.511	−0.508	−0.424	−0.551
FC 9	−0.400	−0.421	−0.419	−0.334	−0.461
FC 11	−0.452	−0.473	−0.471	−0.387	−0.513
FC 12	−0.467	−0.488	−0.485	−0.401	−0.528
FC 14	−0.523	−0.544	−0.542	−0.458	−0.584
FC 17	−0.406	−0.427	−0.424	−0.340	−0.467
α Values for ROCK/STONE SUBGRADE					
FC 1	−0.540	−0.562	−0.559	−0.475	−0.602
FC 2	−0.551	−0.573	−0.570	−0.486	−0.612
FC 6	−0.592	−0.614	−0.611	−0.527	−0.653
FC 7	−0.555	−0.576	−0.574	−0.490	−0.616
FC 9	−0.465	−0.487	−0.484	−0.400	−0.526
FC 11	−0.517	−0.539	−0.536	−0.452	−0.579
FC 12	−0.532	−0.553	−0.551	−0.467	−0.593
FC 14	−0.588	−0.610	−0.607	−0.523	−0.650
FC 17	−0.471	−0.493	−0.490	−0.406	−0.532

Table 39. Coefficients for rigid IRI model (continued).

α Values for OTHER SUBGRADE					
FC 1	−0.482	−0.504	−0.501	−0.417	−0.544
FC 2	−0.493	−0.514	−0.512	−0.428	−0.554
FC 6	−0.534	−0.555	−0.553	−0.468	−0.595
FC 7	−0.497	−0.518	−0.515	−0.431	−0.558
FC 9	−0.407	−0.428	−0.426	−0.341	−0.468
FC 11	−0.459	−0.481	−0.478	−0.394	−0.520
FC 12	−0.474	−0.495	−0.492	−0.408	−0.535
FC 14	−0.530	−0.551	−0.549	−0.465	−0.591
FC 17	−0.413	−0.434	−0.431	−0.347	−0.474

Example of Absolute IRI Predictions Model for Rigid Pavements

The rigid IRI model does not incorporate a delta factor; therefore, the regression equation can be used directly. The pavement structure shown in table 40 illustrates the use of the regression model.

Table 40. Example pavement section information.

Input	Value
Pavement Structure	JPCC
BASE	DGAB
SG	FINE
ESAL	410,000
FC	2
D	9.5
FTC	80
FI	688
CI	205
PRECIP	1,140
MIRI_AGE	1
MIRI	1
AGE	2

Substituting the inputs from table 40 into the regression equation and extracting the alpha value from the table 39 based on pavement structure, base type, and subgrade type leads to equation 20.

$$\ln(IRI+0.1) = -0.510 + 0.501*1 + 9.85\times10^{-2} * \left(\frac{\log(410000)}{9.5}\right) + 3.21\times10^{-4} * 688 - 1.84\times10^{-5} * 205$$
$$+ 4.17\times10^{-5} * 1140 + 7.76\times10^{-4} * 80 - 1.64\times10^{-2} * 1 + 1.68\times10^{-2} * 2$$
$$- 2.30\times10^{-6} * 688 * 80 + 8.11\times10^{-8} * 205 * 80 - 3.57\times10^{-7} * 688 * 205 + 4.30\times10^{-6} * 688 * 2 \quad (20)$$

Equations 21 and 22 show the results.

$$\ln(IRI+0.1) = 0.223 \quad (21)$$

$$IRI = e^{0.223} - 0.1 = 1.15 \quad (22)$$

FWPC PREDICTION MODEL FOR FLEXIBLE PAVEMENTS (DEDUCT VALUE)

Equation 23 shows the logistic FWPC prediction model for flexible pavements (total observations = 1977).

$$\ln\left(\frac{P}{1-P}\right) = \alpha_1 + 0.917 * \left(\frac{\log(ESAL)}{SN}\right) - 1.12\times10^{-2} * FTC + 1.06\times10^{-4} * FI$$
$$- 2.21\times10^{-4} * CI - 1.01\times10^{-3} * PRECIP + 0.513 * AGE$$
$$- 6.10\times10^{-2} * AGE * \left(\frac{\log(ESAL)}{SN}\right) - 1.15\times10^{-4} * AGE * CI - 1.44\times10^{-4} * AGE * FI \quad (23)$$

Table 41 lists the coefficients for the flexible FWPA logistic model.

Table 41. Coefficients for flexible FWPC (deduct value) logistic model.

	α_1 Values
Nonoverlay, Unbound Base	−1.06
Nonoverlay, Bound Base	−0.635
Overlay, Bound or Unbound Base	0.101

Where crack initiation age is determined as the AGE at which P, cutoff probability, equals 0.7 (percent correct = 72.6). If the crack initiation age is determined to be less than zero from the logistic model, a value of zero is used.

Equation 24 shows the regression equation (R-squared = 0.63, total observations = 1,486).

$$\ln(FWPC + 0.1) = \alpha_2 - 3.65 \times 10^{-3} * \left(\frac{\log(ESAL)}{SN}\right) + 0.875 * \ln(ADJ\_AGE + 0.1)$$
$$- 8.77 \times 10^{-4} * CI - 3.59 \times 10^{-4} * FI - 1.71 \times 10^{-4} * PRECIP - 1.12 \times 10^{-2} * FTC$$
$$+ 2.14 \times 10^{-4} * \ln(ADJ\_AGE + 0.1) * PRECIP \quad (24)$$

Table 42 lists the coefficients for the flexible FWPC regression model.

Table 42. Coefficients for flexible FWPC (deduct value) regression model.

α_2 Values for FINE SUBGRADE			
BASE	**Nonoverlay,**	**Nonoverlay,**	**Overlay, Bound**
ATB	NA	3.13	2.88
DGAB	3.25	NA	2.94
LCB	NA	2.79	2.54
NONBIT	NA	2.76	2.51
NONE	2.91	NA	2.60
PATB	NA	3.06	2.81
α_2 Values for COARSE SUBGRADE			
ATB	NA	2.88	2.63
DGAB	3.00	NA	2.68
LCB	NA	2.54	2.29
NONBIT	NA	2.51	2.25
NONE	2.65	NA	2.34
PATB	NA	2.81	2.56
α_2 Values for ROCK/STONE SUBGRADE			
ATB	NA	3.17	2.91
DGAB	3.28	NA	2.97
LCB	NA	2.82	2.57
NONBIT	NA	2.79	2.54
NONE	2.94	NA	2.63
PATB	NA	3.09	2.84

Where *ADJ_AGE* equals pavement age minus crack initiation age. If the pavement age is less than or equal to the crack initiation age, the predicted FWPC equals zero.

FWPC PREDICTION MODEL FOR FLEXIBLE PAVEMENTS (PERCENTAGE WHEELPATH AREA)

Equation 25 gives the logistic model (total observations = 1977).

$$\ln\left(\frac{P}{1-P}\right) = \alpha_1 + 0.917 * \left(\frac{\log(ESAL)}{SN}\right) - 1.12 \times 10^{-2} * FTC + 1.06 \times 10^{-4} * FI$$
$$- 2.21 \times 10^{-4} * CI - 1.01 \times 10^{-3} * PRECIP + 0.513 * AGE$$
$$- 6.10 \times 10^{-2} * AGE * \left(\frac{\log(ESAL)}{SN}\right) - 1.15 \times 10^{-4} * AGE * CI - 1.44 \times 10^{-4} * AGE * FI \quad (25)$$

Table 43 lists the coefficients for the flexible FWPC logistic model.

Table 43. Coefficients for flexible FWPC (percentage of wheelpath) logistic model.

	α_1 Values
Nonoverlay, Unbound Base	−1.06
Nonoverlay, Bound Base	−0.635
Overlay, Bound or Unbound Base	0.101

Where the crack initiation age is determined as the AGE at which P, cutoff probability, equals 0.7 (percent correct = 72.6). If the crack initiation age is determined to be less than zero from the logistic model, a value of zero is used.

Equation 26 shows the regression equation (R-squared = 0.63, total observations = 1486).

$$\ln(fwpc + 0.1) = \alpha_2 + 7.63 \times 10^{-2} * \left(\frac{\log(ESAL)}{SN}\right) + 0.737 * \ln(ADJ\_AGE + 0.1)$$
$$- 1.04 \times 10^{-3} * CI - 4.12 \times 10^{-4} * FI + 2.03 \times 10^{-5} * PRECIP - 1.12 \times 10^{-2} * FTC$$
$$+ 2.07 \times 10^{-4} * \ln(ADJ\_AGE + 0.1) * PRECIP \quad (26)$$

Table 44 lists the coefficients for the flexible FWPC regression model.

Table 44. Coefficients for flexible FWPC (percentage of wheelpath) regression model.

α_2 Values for FINE SUBGRADE			
BASE	**Nonoverlay, Unbound Base**	**Nonoverlay, Bound Base**	**Overlay, Bound, or Unbound Base**
ATB	NA	2.43	1.97
DGAB	2.51	NA	2.14
LCB	NA	2.80	2.33
NONBIT	NA	1.97	1.51
NONE	2.15	NA	1.78
PATB	NA	2.45	1.98
α_2 Values for COARSE SUBGRADE			
ATB	NA	2.06	1.59
DGAB	2.14	NA	1.77
LCB	NA	2.43	1.96
NONBIT	NA	1.60	1.13
NONE	1.77	NA	1.40
PATB	NA	2.08	1.61
α_2 Values for ROCK/STONE SUBGRADE			
ATB	NA	2.11	1.64
DGAB	2.19	NA	1.81
LCB	NA	2.47	2.01
NONBIT	NA	1.65	1.18
NONE	1.82	NA	1.45
PATB	NA	2.12	1.66

Where *ADJ_AGE* = pavement Age—crack initiation age. If the pavement age is less than or equal to the crack initiation age, the predicted FWPC equals zero.

Example for FWPC Prediction Model for Flexible Pavements

The prediction model for FWPC involves a two-step process. In the first step, the logistic equation in equation 25 is used to estimate the age of crack initiation. This is done solving for the AGE variable so that P is equivalent to the cutoff value (0.7 for this model). This AGE is denoted as the crack initiation age. In some cases, the resulting crack initiation age may be less than zero. A value of zero is used in place of the estimated negative crack initiation age.

If the FWPC estimate is for a pavement age less than or equal to the crack initiation age, the predicted FWPC value is equal to zero. If the FWPC estimate is for a pavement age

greater than the crack initiation age, the ADJ_AGE is calculated as the pavement age of interest less the crack initiation age. Table 45 lists information for an example pavement section.

Table 45. Example pavement section information.

Input	Value
Pavement Structure	Nonoverlay, Unbound Base
BASE	DGAB
SG	FINE
ESAL	126,000
SN	5.0
ACTHICK	6.5
FTC	80
FI	688
CI	205
PRECIP	1,140
MIRI_AGE	1
MIRI	1
AGE	12

Equation 27 substitutes information from table 45 as well as a P value of 0.7 into the logistic equation and extracting the α_1 value from the appropriate table.

$$\ln\left(\frac{0.7}{1-0.7}\right) = -1.06 + 0.917*\left(\frac{\log(126000)}{5}\right) - 1.12\times10^{-2}*80 + 1.06\times10^{-4}*688 - 2.21\times10^{-4}*205$$
$$-1.01\times10^{-3}*1140 + 0.513*AGE - 6.10\times10^{-2}*AGE*\left(\frac{\log(126000)}{5}\right) - 1.15\times10^{-4}*AGE*205$$
$$-1.44\times10^{-4}*AGE*688 \quad (27)$$

Equation 28 is solving for AGE through an iterative process.

$$AGE = 9.13 = \text{crack initiation age} \quad (28)$$

FWPC prediction of interest occurs at a pavement age of 12. Therefore, ADJ_AGE = 12–9.13 = 2.87. Equation 29 substitutes this age and the information from table 45 into the regression equation.

$$\ln(FWPC + 0.1) = 3.25 - 3.65 \times 10^{-3} * \left(\frac{\log(126000)}{5}\right) + 0.875 * \ln(2.87 + 0.1)$$
$$- 8.77 \times 10^{-4} * 205 - 3.59 \times 10^{-4} * 688 - 1.71 \times 10^{-4} * 1140 - 1.12 \times 10^{-2} * 80$$
$$+ 2.14 \times 10^{-4} * \ln(2.87 + 0.1) * 1140 \quad (29)$$

Therefore, the results are shown in equations 30 and 31.

$$\ln(FWPC + 0.1) = 2.95 \quad (30)$$

$$FWPC = e^{2.95} - 0.1 = 18.9 \quad (31)$$

TC PREDICTION MODEL FOR FLEXIBLE PAVEMENTS

Equation 32 shows the logistic model (observations = 1,920).

$$\ln\left(\frac{P}{1-P}\right) = \alpha_1 + 0.723 * \left(\frac{\log(ESAL)}{SN}\right) - 1.34 \times 10^{-2} * FTC + 2.65 \times 10^{-3} * FI + 1.30 \times 10^{-3} * CI$$
$$+ 1.81 \times 10^{-4} * PRECIP + 0.512 * AGE - 2.88 \times 10^{-2} * AGE * \left(\frac{\log(ESAL)}{SN}\right) - 1.86 \times 10^{-4} * AGE * CI$$
$$- 1.92 \times 10^{-4} * AGE * FI - 7.72 \times 10^{-5} * AGE * PRECIP + 1.56 \times 10^{-3} * AGE * FTC \quad (32)$$

Table 46 lists the coefficients for the flexible TC logistic model.

Table 46. Coefficients for flexible TC logistic model.

	α_1 Values
Nonoverlay, Unbound Base	−3.75
Nonoverlay, Bound Base	−3.29
Overlay, Bound or Unbound Base	−1.97

Where the crack initiation age is determined as the AGE at which P, cutoff probability, equals 0.7 (percent correct = 78.4). If the crack initiation age is determined to be less than zero from the logistic model, a value of zero is used.

Equation 33 is the regression equation (R-squared = 0.71, total observations = 1,077).

$$\ln(TC + 0.1) = \alpha_2 + 0.175 * \left(\frac{\log(ESAL)}{SN}\right) + 1.14 * \ln(AGE + 0.1) - 3.16 \times 10^{-4} * CI$$
$$+ 5.28 \times 10^{-4} * FI - 1.10 \times 10^{-4} * PRECIP + 1.12 \times 10^{-4} * \ln(AGE + 0.1) * PRECIP$$
$$- 1.88 \times 10^{-4} * CI * \ln(AGE + 0.1) \quad (33)$$

Table 47 lists the coefficients for the flexible TC regression model.

Table 47. Coefficients for flexible TC regression model.

α_2 Values for FINE SUBGRADE			
BASE	**Nonoverlay, Unbound Base**	**Nonoverlay, Bound Base**	**Overlay, Bound or Unbound Base**
ATB	NA	1.48	1.10
DGAB	1.03	NA	0.996
LCB	NA	1.58	1.20
NONBIT	NA	1.55	1.17
NONE	1.41	NA	1.37
PATB	NA	1.82	1.44
α_2 Values for COARSE SUBGRADE			
ATB	NA	1.17	0.792
DGAB	0.72	NA	0.687
LCB	NA	1.27	0.891
NONBIT	NA	1.24	0.859
NONE	1.10	NA	1.06
PATB	NA	1.51	1.13
α_2 Values for ROCK/STONE SUBGRADE			
ATB	NA	0.976	0.599
DGAB	0.527	NA	0.494
LCB	NA	1.08	0.698
NONBIT	NA	1.04	0.666
NONE	0.905	NA	0.871
PATB	NA	1.32	0.939

Where *ADJ_AGE* equals pavement age less the crack initiation age. If the pavement age is less than or equal to the crack initiation age, the predicted TC equals zero.

Example for TC Prediction Model for Flexible Pavements

The prediction model for TC involves a two-step process. In the first step, the logistic model in equation 32 is used to estimate the age of crack initiation. This is done by solving for the AGE variable so that P is equivalent to the cutoff value (0.7 for this model). This AGE is denoted as the crack initiation age. In some cases, the resulting crack initiation age may be less than zero. A value of zero is used in place of the estimated negative crack initiation age.

If the TC estimate is for a pavement age less than or equal to the crack initiation age, the predicted TC value is equal to zero. If the TC estimate is for a pavement age greater than the crack initiation age, the ADJ_AGE is calculated as the pavement age of interest less the crack initiation age. Table 48 lists information for an example pavement section.

Table 48. Example pavement section information.

Input	Value
Pavement Structure	Nonoverlay, Unbound Base
BASE	DGAB
SG	FINE
ESAL	126,000
SN	5.0
ACTHICK	6.5
FTC	80
FI	688
CI	205
PRECIP	1,140
MIRI_AGE	1
MIRI	1
AGE	12

Equation 34 substitutes information from table 48 as well as a P value of 0.7 into the logistic equation and extracts the alpha 1 value from the appropriate table.

$$\ln\left(\frac{0.7}{1-0.7}\right) = 1.03 + 0.723 * \left(\frac{\log(126000)}{5}\right) - 1.34\times10^{-2} * 80 + 2.65\times10^{-3} * 688$$
$$+ 1.30\times10^{-3} * 205 + 1.81\times10^{-4} * 1140 + 0.512 * AGE - 2.88\times10^{-2} * AGE * \left(\frac{\log(126000)}{5}\right)$$
$$- 1.86\times10^{-4} * AGE * 205 - 1.92\times10^{-4} * AGE * 688 - 7.72\times10^{-5} * AGE * 1140 + 1.56\times10^{-3} * AGE * 80 \quad (34)$$

Solving for AGE through an iterative process results in equation 35.

$$AGE = 7.54 = \text{crack initiation age} \tag{35}$$

TC prediction of interest occurs at a pavement age of 12. Therefore, ADJ_AGE = 12−7.54 = 4.46. Equation 36 substitutes this age and the information in table 48 into the regression equation.

$$\ln(TC + 0.1) = 1.03 + 0.175 * \left(\frac{\log(126000)}{5}\right) + 1.14 * \ln(4.46 + 0.1) - 3.16 \times 10^{-4} * 205$$
$$+ 5.28 \times 10^{-4} * 688 - 1.10 \times 10^{-4} * 1140 + 1.12 \times 10^{-4} * \ln(4.46 + 0.1) * 1140$$
$$- 1.88 \times 10^{-4} 205 * \ln(4.46 + 0.1) \tag{36}$$

Therefore, the results are shown in equations 37 and 38.

$$\ln(TC + 0.1) = 3.25 \tag{37}$$

$$TC = e^{3.25} - 0.1 = 25.6 \tag{38}$$

LC PREDICTION MODEL FOR RIGID PAVEMENTS

Equation 39 shows the logistic model (total observations = 400).

$$\ln\left(\frac{P}{1-P}\right) = -4.01 + 3.15 * \left(\frac{\log(ESAL)}{DEPTH}\right) + 1.09 \times 10^{-2} * FTC + 1.39 \times 10^{-3} * CI$$
$$- 5.69 \times 10^{-4} * PRECIP + 3.01 \times 10^{-2} * AGE - 8.19 \times 10^{-5} * AGE * CI$$
$$+ 3.45 \times 10^{-5} * AGE * FI + 1.03 \times 10^{-4} * PRECIP * AGE \tag{39}$$

Where the crack initiation age is determined as the AGE at which P, cutoff probability, equals 0.55 (percent correct = 63.5). If the crack initiation age is determined to be less than zero from the logistic model, a value of zero is used.

Equation 40 is the regression equation (R-squared = 0.38, total observations = 240).

$$\ln(LC + 0.1) = \alpha_1 + 0.68 * \left(\frac{\log(ESAL)}{DEPTH}\right) + 4.96 \times 10^{-3} * FTC + 6.44 \times 10^{-4} * PRECIP$$
$$+ 0.354 * \ln(ADJ\_AGE + 0.01) - 7.66 \times 10^{-6} * FTC * PRECIP \tag{40}$$

Table 49 lists the coefficients for the rigid LC regression model.

Table 49. Coefficients for rigid LC regression model.

BASE	α_1
ATB	−1.36
DGAB	−1.89
LCB	−1.03
NONBIT	−0.84
PATB	−2.14

Where *ADJ_AGE* equals pavement age less the crack initiation age. If the pavement age is less than or equal to the crack initiation age, the predicted LC equals zero. If the predicted LC is less than zero for pavement age is greater than crack initiation age, the predicted LC was set to zero.

Example for LC Prediction Model for Rigid Pavements

The prediction model for LC involves a two-step process. In the first step, logistic equation 39 is used to estimate the age of crack initiation. This is done solving for the AGE variable so that P is equivalent to the cutoff value (0.55 for this model). This AGE is denoted as the crack initiation age. In some cases, the resulting crack initiation age may be less than zero. A value of zero is used in place of the estimated negative crack initiation age.

If the LC estimate is for a pavement age less than or equal to the crack initiation age, the predicted TC value is equal to zero. If the LC estimate is for a pavement age greater than the crack initiation age, the ADJ_AGE is calculated as the pavement age of interest less the crack initiation age.

Table 50 gives the information for an example pavement section.

Table 50. Example pavement section information.

Input	Value
Pavement Structure	JPCC
BASE	DGAB
SG	FINE
ESAL	410,000
FC	2
D	9.5
FTC	80
FI	688
CI	205
PRECIP	1,140
MIRI_AGE	1
MIRI	1
AGE	14

Equation 41 substitutes information from the table 50 as well as a P value of 0.55 into the logistic equation and extracts the alpha 1 value from the appropriate table.

$$\ln\left(\frac{0.55}{1-0.55}\right) = -4.01 + 3.15 * \left(\frac{\log(410000)}{9.5}\right) + 1.09\times10^{-2} * 80 + 1.39\times10^{-3} * 205$$
$$- 5.69\times10^{-4} * 1140 - 3.01\times10^{-2} * AGE - 8.19\times10^{-5} * AGE * 205$$
$$+ 3.45\times10^{-5} * AGE * 688 + 1.03\times10^{-4} * 1140 * AGE \quad (41)$$

Equation 42 is solving for AGE through an iterative process.

$$AGE = 11.86 = \text{crack initiation age} \quad (42)$$

LC prediction of interest occurs at a pavement age of 14. Therefore, ADJ_AGE = 14−11.86 = 2.14. Substituting this age and the information in table 50 into the regression equation results in equation 43.

$$\ln(LC + 0.1) = -1.89 + 0.68 * \left(\frac{\log(410000)}{9.5}\right) + 4.96\times10^{-3} * 80 + 6.44\times10^{-4} * 1140$$
$$+ 0.354 * \ln(2.14 + 0.01) - 7.66\times10^{-6} * 80 * 1140 \quad (43)$$

Therefore, the results are shown in equations 44 and 45.

$$\ln(LC + 0.1) = -0.78 \quad (44)$$

$$LC = e^{-0.78} - 0.1 = .358 \quad (45)$$

TC PREDICTION MODEL FOR RIGID PAVEMENTS

Equation 46 shows the logistic model (total observations = 414).

$$\ln\left(\frac{P}{1-P}\right) = -2.20 + 3.06 * \left(\frac{\log(ESAL)}{DEPTH}\right) + 6.58 \times 10^{-3} * FTC + 1.25 \times 10^{-3} * CI$$
$$- 2.07 \times 10^{-3} * PRECIP + 0.126 * AGE - 1.16 \times 10^{-4} * CI * AGE - 7.47 \times 10^{-5} * FI * AGE$$
$$+ 1.31 \times 10^{-4} * PRECIP * AGE \quad (46)$$

Where The crack initiation age is determined as the AGE at which P, cutoff probability, equals 0.6 (percent correct = 63.5). If the crack initiation age is determined to be less than zero from the logistic model, a value of zero is used.

Equation 47 shows the regression equation (R-squared = 0.54, total observations = 228).

$$\ln(TC + 0.1) = \alpha_1 + 1.02 \times 10^{-2} * FTC - 1.20 \times 10^{-3} * FI$$
$$+ 2.23 \times 10^{-3} * PRECIP + 0.388 * \ln(ADJ\_AGE + 0.01) + 1.53 \times 10^{-5} * FTC * FI$$
$$- 1.56 \times 10^{-5} * FTC * PRECIP \quad (47)$$

Table 51 lists the coefficients for the rigid TC regression model.

Table 51. Coefficients for rigid TC regression model.

BASE	α_2
ATB	–3.05
DGAB	–2.28
LCB	–1.76
NONBIT	–2.65
PATB	–2.55

Where *ADJ_AGE* equals pavement age less the crack initiation age. If the pavement age is less than or equal to the crack initiation age, the predicted TC equals zero

Example for TC Prediction Model for Rigid Pavements

The prediction model for TC involves a two-step process. In the first step, the logistic model in equation 46 is used to estimate the age of crack initiation. This is done by solving for the AGE variable so that P is equivalent to the cutoff value (0.6 for this model). This AGE is denoted as the crack initiation age. In some cases, the resulting

crack initiation age may be less than zero. A value of zero is used in place of the estimated negative crack initiation age.

If the TC estimate is for a pavement age less than or equal to the crack initiation age, the predicted TC value is equal to zero. If the TC estimate is for a pavement age greater than the crack initiation age, the ADJ_AGE is calculated as the pavement age of interest less the crack initiation age.

Table 52 lists information for an example pavement section.

Table 52. Example pavement section information.

Input	Value
Pavement Structure	JPCC
BASE	DGAB
SG	FINE
ESAL	410,000
FC	2
D	9.5
FTC	80
FI	688
CI	205
PRECIP	1,140
MIRI_AGE	1
MIRI	1
AGE	18

Equation 48 substitutes information from table 52 as well as a P value of 0.6 into the logistic equation and extracts the alpha 1 value from the appropriate table.

$$\ln\left(\frac{0.6}{1-0.6}\right) = -2.20 + 3.06 * \left(\frac{\log(410000)}{9.5}\right) + 6.58\times10^{-3} * 80 + 1.25\times10^{-3} * 205$$
$$- 2.07\times10^{-3} * 1140 + 0.126 * AGE - 1.16\times10^{-4} * 205 * AGE$$
$$- 7.47\times10^{-5} * 688 * AGE + 1.31\times10^{-4} * 1140 * AGE \quad (48)$$

Equation 49 is solving for AGE through an iterative process.

$$AGE = 11.86 = \text{crack initiation age} \quad (49)$$

The TC prediction of interest occurs at a pavement age of 18. Therefore, ADJ_AGE = 18−11.86 = 6.14. Equation 50 substitutes this age and the information in table 52 into the regression equation shown in equation 50.

$$\ln(TC + 0.1) = -2.28 + 1.02 \times 10^{-2} * 80 - 1.02 \times 10^{-3} * 688 + 2.23 \times 10^{-3} * 1140 + 0.388 * \ln(1.43 + 0.01) - 1.53 \times 10^{-5} * 80 * 688 - 1.56 \times 10^{-5} * 80 * 1140 \quad (50)$$

Therefore, the results are as shown in equations 51 and 52.

$$\ln(TC + 0.1) = 0.02 \quad (51)$$

$$TC = e^{0.02} - 0.1 = 0.92 \quad (52)$$

RUT DEPTH PREDICTION MODEL FOR FLEXIBLE PAVEMENTS

Equation 53 shows the regression equation (R-squared = 0.45, total observations = 1,966).

$$\ln(RUT + 0.1) = \alpha + 0.503 * \ln(AGE + 0.1) + 3.37 \times 10^{-4} * CI + 1.22 \times 10^{-5} * PRECIP + 3.48 \times 10^{-3} * FTC + 2.98 \times 10^{-7} * FI * PRECIP - 8.44 \times 10^{-2} * \left(\frac{\log(ESAL)}{SN}\right) * \ln(AGE + 0.1) - 1.42 \times 10^{-4} * \ln(AGE + 0.1) * CI - 1.38 \times 10^{-5} \ln(AGE + 0.1) * FI + \beta * \left(\frac{\log(ESAL)}{SN}\right) + \gamma * FI \quad (53)$$

Table 53 lists the coefficients for the flexible RUT model.

Table 53. Coefficients for flexible RUT model.

α Values for FINE SUBGRADE			
BASE	**Nonoverlay, Unbound Base**	**Nonoverlay, Bound Base**	**Overlay, Bound or Unbound Base**
ATB	NA	0.136	0.124
DGAB	0.367	NA	0.31
LCB	NA	0.624	0.612
NONBIT	NA	0.436	0.425
NONE	−0.539	NA	−0.597
PATB	NA	−0.309	−0.321
α Values for COARSE SUBGRADE			
ATB	NA	0.0958	0.084
DGAB	0.327	NA	0.269
LCB	NA	0.583	0.572
NONBIT	NA	0.396	0.384
NONE	−0.580	NA	−0.637
PATB	NA	−0.350	−0.361
α Values for ROCK/STONE SUBGRADE			
ATB	NA	−0.0199	−0.0317
DGAB	0.211	NA	0.154
LCB	NA	0.468	0.456
NONBIT	NA	0.280	0.269
NONE	−0.695	NA	−0.753
PATB	NA	−0.465	−0.477
β and γ values			
BASE		β	γ
ATB		0.331	-.000228
DGAB		0.225	-.000266
LCB		0.0236	-.00507
NONBIT		0.108	.00120
NONE		1.13	.000283
PATB		0.769	.000150

Example for Rut Depth Prediction Model for Flexible Pavements

The prediction model for rut depth on flexible pavement uses one regression equation. Table 54 lists information for the example pavement structure to illustrate the model.

Table 54. Example pavement section information.

Input	Value
Pavement Structure	Nonoverlay, Unbound Base
BASE	DGAB
SG	FINE
ESAL	126,000
SN	5.0
ACTHICK	6.5
FTC	80
FI	688
CI	205
PRECIP	1,140
MIRI_AGE	1
MIRI	1
AGE	2

Equation 54 substitutes the information from table 54 into the delta equation and extracts the alpha value from table 53 based on pavement structure, base type, and subgrade type.

$$\ln(RUT + 0.1) = .367 + 0.503 * \ln(2 + 0.1) + 3.37 \times 10^{-4} * 205 + 1.22 \times 10^{-5} * 1140 + 3.48 \times 10^{-3} * 80 + 2.98 \times 10^{-7} * 688 * 1140 - 8.44 \times 10^{-2} * \left(\frac{\log(126000)}{5}\right) * \ln(2 + 0.1) - 1.42 \times 10^{-4} * \ln(2 + 0.1) * 205 - 1.38 \times 10^{-5} \ln(2 + 0.1) * 688 + 0.225 * \left(\frac{\log(126000)}{5}\right) - 2.66 \times 10^{-4} * 688 \quad (54)$$

Therefore, the results are shown in equations 55 and 56.

$$\ln(RUT + 0.1) = 1.29 \quad (55)$$

$$RUT = e^{1.29} - 0.1 = 3.53 \quad (56)$$

TRANSVERSE JOINT FAULTING PREDICTION MODEL FOR RIGID PAVEMENTS

Equation 57 shows the regression equation (R-squared = 0.47, total observations = 1,384).

$$\ln(FAULT+1) = \alpha - 0.337*\left(\frac{\log(ESAL)}{DEPTH}\right) - 1.40\times10^{-3}*FTC - 5.51\times10^{-4}*FI$$
$$+3.15\times10^{-6}*FTC*FI - 5.15\times10^{-4}*CI - 7.92\times10^{-4}*\left(\frac{\log(ESAL)}{DEPTH}\right)*CI + 9.28\times10^{-7}*FI*CI$$
$$-8.42\times10^{-4}*PRECIP + 8.28\times10^{-4}*\left(\frac{\log(ESAL)}{DEPTH}\right)*PRECIP + 7.44\times10^{-7}*CI*PRECIP$$
$$-6.68\times10^{-3}*AGE + 5.09\times10^{-2}*\left(\frac{\log(ESAL)}{DEPTH}\right)*AGE + 9.78\times10^{-6}*FI*AGE \quad (57)$$

Table 55 lists the coefficients for the rigid FLT model.

Table 55. Coefficients for rigid FLT model.

α Values				
BASE	**Fine Subgrade**	**Coarse Subgrade**	**Other Subgrade**	**Rock/Stone Subgrade**
ATB	0.755	0.810	1.20	0.515
DGAB	0.732	0.786	1.18	0.492
LCB	0.665	0.720	1.11	0.425
NONBIT	0.834	0.889	1.28	0.595
PATB	0.693	0.748	1.14	0.453

Example for Fault Prediction Model for Rigid Pavements

The prediction model for faulting on rigid pavement uses one regression equation. Table 56 lists information for an example pavement structure to illustrate the use of the model.

Table 56. Example pavement section information.

Input	Value
Pavement Structure	JPCC
BASE	DGAB
SG	FINE
ESAL	410,000
FC	2
D	9.5
FTC	80
FI	688
CI	205
PRECIP	1140
AGE	15

Equation 58 substitutes the information from table 56 into the delta equation and extracts the alpha value from table 55 based on base type and subgrade type.

$$\ln(FAULT+1) = .732 - 0.337*\left(\frac{\log(410000)}{9.5}\right) - 1.40\times10^{-3}*80 - 5.51\times10^{-4}*688$$
$$+ 3.15\times10^{-6}*80*688 - 5.15\times10^{-4}*205 - 7.92\times10^{-4}*\left(\frac{\log(410000)}{9.5}\right)*205 + 9.28\times10^{-7}*688*205$$
$$- 8.42\times10^{-4}*1140 + 8.28\times10^{-4}*\left(\frac{\log(410000)}{9.5}\right)*1140 + 7.44\times10^{-7}*205*1140$$
$$- 6.68\times10^{-3}*15 + 5.09\times10^{-2}*\left(\frac{\log(410000)}{9.5}\right)*15 + 9.78\times10^{-6}*688*15 \quad (58)$$

Therefore, equations 59 and 60 show the results.

$$\ln(FAULT+1) = 0.367 \quad (59)$$
$$FAULT = e^{0.367} - 1.0 = 0.443 \quad (60)$$

APPENDIX C. AGENCY CLIMATIC INFORMATION

This appendix provides State maps containing the analysis test sections for each of the participating agencies. These maps and the tables link the geographic location of test sections to the climatic setting and aid in evaluating environmental variation within a State. This appendix also contains information on the pavement structure of each GPS test section.

Figure 83 shows geographic locations of analysis test sections in Alaska, and table 57 lists the environmental and pavement structure information for the Alaska test sections.

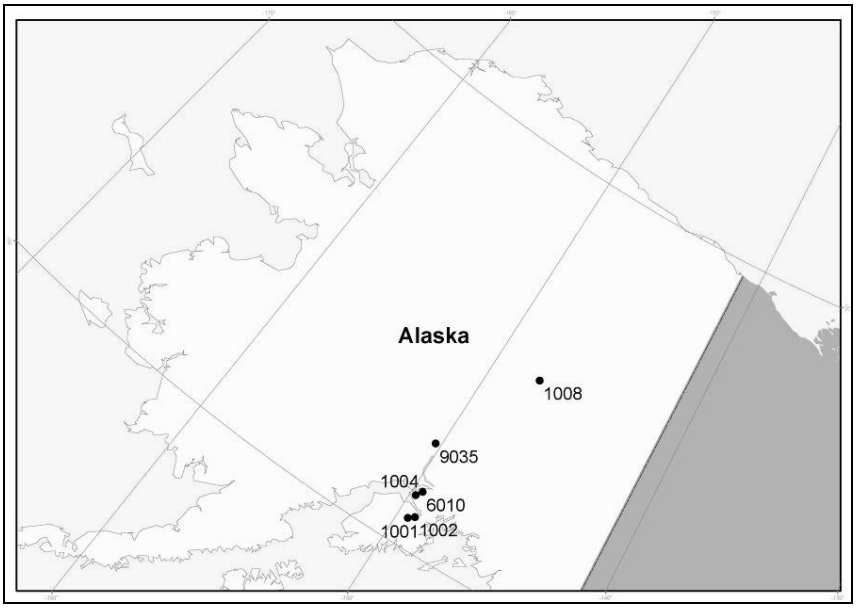

Figure 83. Map. Alaska geographic location of analysis test sections.

Table 57. Alaska environmental and pavement structure information for test sections.

Site	FTC	FI	CI	PRECIP	SN	ACTHICK	D	LESN	LEDT	AC/PC
1002	112	794	0	2020	3.4	4.3	NA	1.4	NA	AC
1001	124	890	0	1116	2.2	3.0	NA	2.0	NA	AC
Average	***118***	***841***	***0***	***1568***	***2.8***	***3.7***	**NA**	***1.7***	**NA**	NA
1004	87	1110	2	420	4.1	4.5	NA	1.2	NA	AC
6010	92	1248	1	413	2.9	3.8	NA	1.7	NA	AC
9035	106	1513	3	729	2.7	3.0	**NA**	1.7	**NA**	AC
1008	74	2584	23	317	2.9	3.1	NA	1.6	NA	AC
Average	***90***	***1614***	***7***	***470***	***3.2***	***3.6***	NA	***1.5***	NA	NA

Figure 84 shows the geographic locations for the analysis test sections in Idaho, and table 58 lists the environmental and pavement structure information for test sections in Idaho.

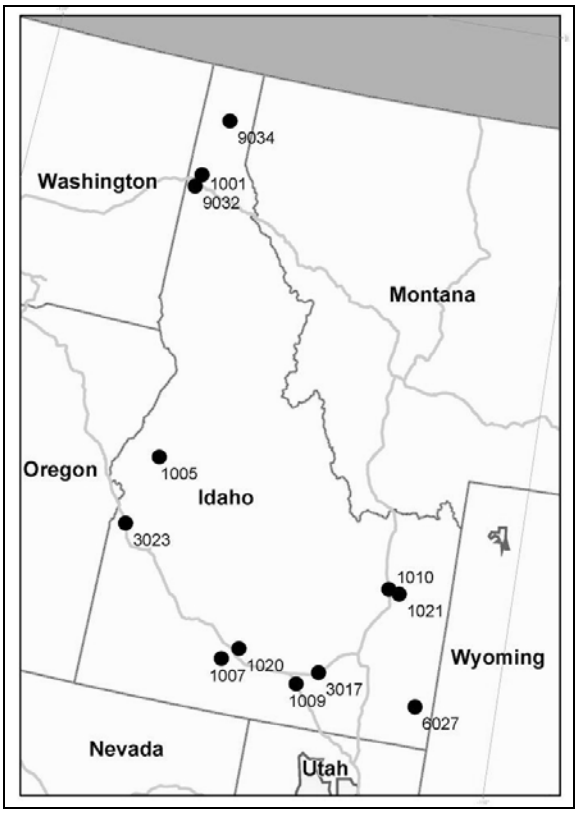

Figure 84. Map. Idaho geographic location of analysis test sections.

Table 58. Idaho Environment and pavement structure information for test sections.

Site	FTC	FI	CI	PRECIP	SN	ACTHICK	D	LESN	LEDT	AC/PC
1001	113	217	158	693	2.2	3.7	NA	2.3	NA	AC
9032	111	259	121	718	5.8	6.1	NA	0.9	NA	AC
3023	107	278	400	295	NA	NA	NA	NA	0.7	PC
9034	117	316	89	807	6.5	9.2	**NA**	NA	NA	AC
1007	121	326	271	254	5.0	5.5	NA	**NA**	NA	AC
1020	128	328	331	280	4.0	3.8	NA	1.2	NA	AC
1009	137	351	221	262	5.9	10.6	NA	0.9	NA	AC
3017	125	356	344	342	NA	NA	10.3	NA	0.6	PC
1005	121	399	339	627	NA	3.8	NA	1.6	NA	AC
Average	***120***	***314***	***253***	***475***	**NA**	***6.1***	NA	***1.2***	***0.6***	**NA**
1021	129	622	149	342	3.2	5.9	**NA**	1.6	NA	AC
1010	136	665	144	303	5.5	10.9	NA	1.0	NA	AC
6027	162	817	57	380	4.6	5.6	NA	1.2	NA	AC
Average	***142***	***702***	***116***	***342***	***4.4***	***7.5***	**NA**	***1.2***	**NA**	**NA**

Figure 85 shows geographic locations for the analysis test sections in Illinois, and table 59 lists environment and pavement structure information for the Illinois test sections.

Figure 85. Map. Illinois geographic location of analysis test sections.

Table 59. Illinois environment and pavement structure information for test sections.

Site	FTC	FI	CI	PRECIP	SN	ACTHICK	D	LESN	LEDT	AC/PC
79	212	742	1052	5.9	12.10	NA	0.8	NA	AC	NA
78	239.4	747	995	4.9	7.00	NA	1.0	NA	AC	NA
79	***225.7***	***745***	***1024***	***5.4***	***9.55***	**NA**	***0.9***	**NA**	**NA**	**NA**
96	651.8	383	871	5.8	13.20	NA	0.9	NA	AC	NA

Figure 86 shows geographic locations of analysis test sections in Indiana, and table 60 lists environment and pavement structure information for the Indiana test sections.

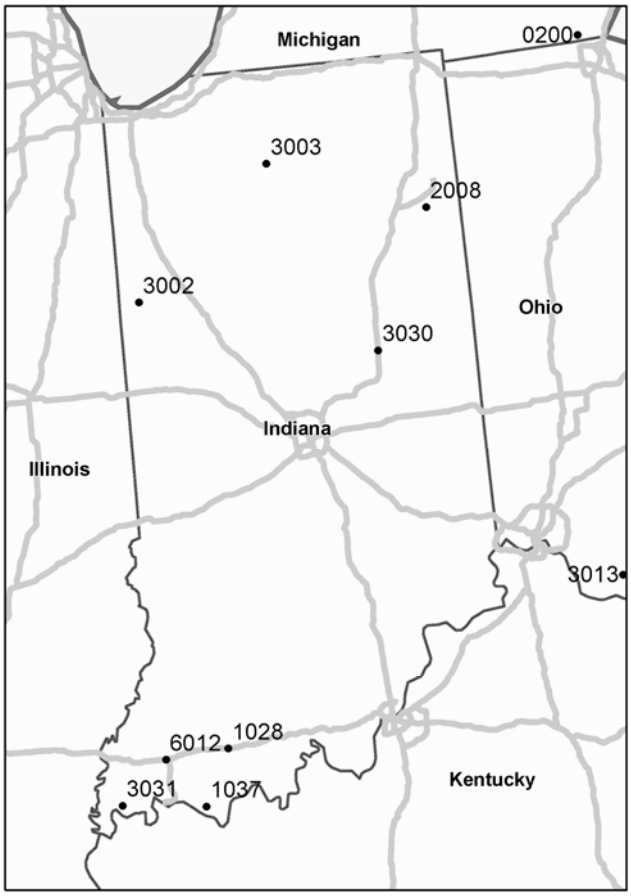

Figure 86. Map. Indiana geographic location of analysis test sections.

Table 60. Indiana environment and pavement structure information for test sections.

Site	FTC	FI	CI	PRECIP	SN	ACTHICK	D	LESN	LEDT	AC/PC
1037	73	152	821	1186	6.3	14.4	NA	0.88	NA	AC
6012	71	215	798	1165	8.6	20.2	NA	0.69	NA	AC
1028	80	217	696	1209	6.7	15.3	NA	0.84	NA	AC
3031	70	230	772	1165	NA	NA	10.0	NA	0.53	PC
3030	88	386	476	1017	NA	NA	8.0	NA	0.72	PC
2008	84	399	471	963	7.0	12.9	NA	0.76	NA	AC
Average	***78***	***267***	***672***	***1118***	***7.2***	***15.7***	***9.1***	***0.79***	***0.63***	**NA**
3002	84	451	520	950	NA	NA	9.5	NA	0.58	PC
3003	88	454	453	1005	NA	NA	10.0	NA	0.58	PC
Average	***86***	***453***	***487***	***978***	**NA**	**NA**	***9.9***	**NA**	***0.58***	**NA**

Figure 87 shows geographic locations of analysis test sections in Michigan, and table 61 lists environment and pavement structure information for Michigan test sections.

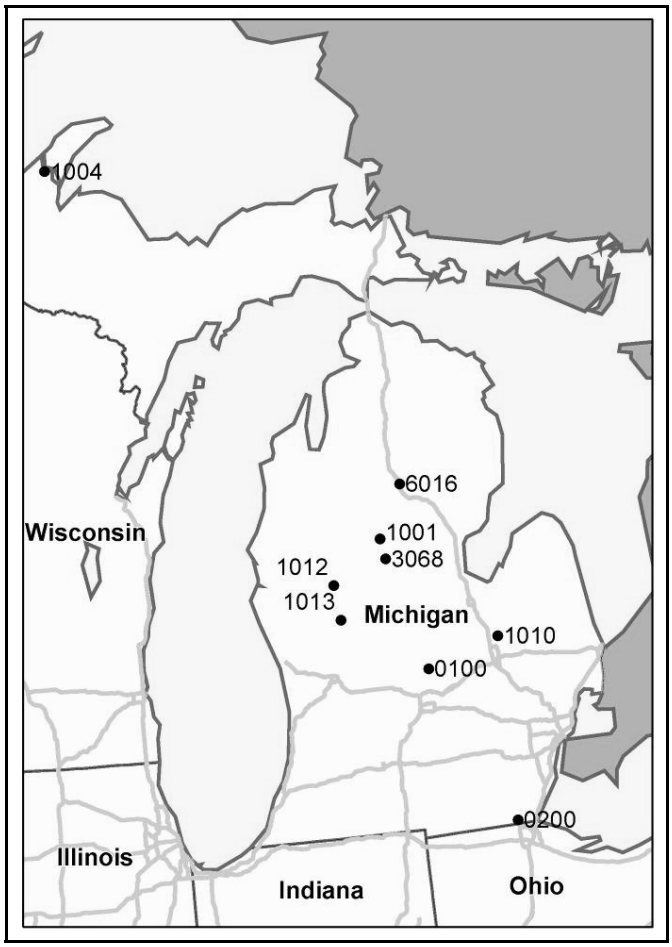

Figure 87. Map. Michigan geographic location of analysis test sections.

Table 61. Michigan environment and pavement structure information for test sections.

Site	FTC	FI	CI	PRECIP	SN	ACTHICK	D	LESN	LEDT	AC/PC
0200	86	382	443	866	NA	NA	NA	NA	NA	PC
0100	105	510	324	870	NA	NA	NA	NA	NA	AC
1010	91	532	309	825	3.7	2.2	NA	1.3	NA	AC
1013	109	568	251	915	5.0	6.7	NA	1.1	NA	AC
1012	115	612	230	931	4.9	6.1	NA	1.1	NA	AC
3068	109	670	215	827	NA	NA	9.0	0.6	0.6	PC
1001	109	759	174	790	2.2	2.2		2.3	NA	AC
6016	100	787	173	751	4.5	4.6	10.3	1.1	0.6	AC
Average	***105***	***634***	***239***	***844***	***4.1***	***4.4***	***9.7***	***1.3***	***0.6***	NA
1004	77	960	131	878	2.5	4.2	NA	2.1	NA	AC

Figure 88 shows geographic locations for analysis test sections in New York.

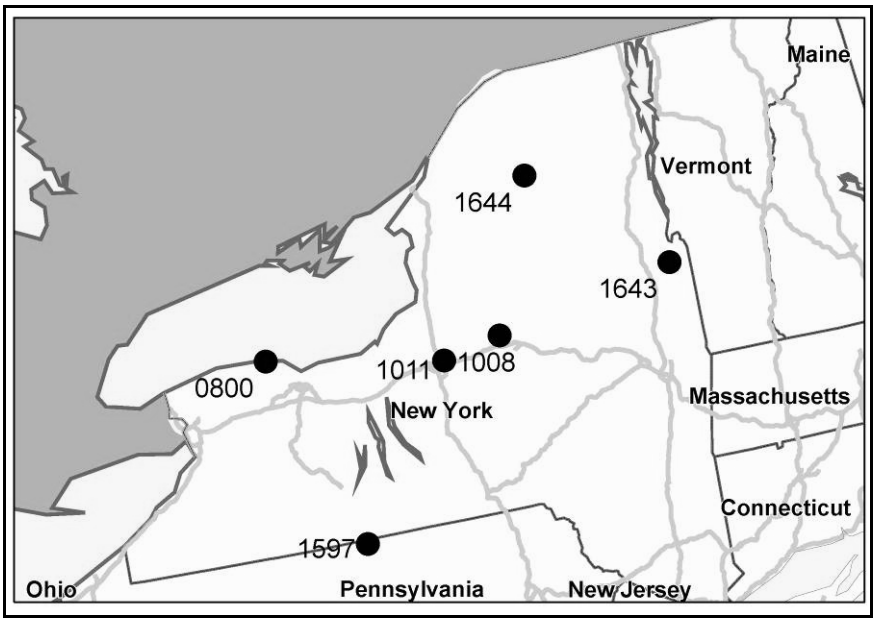

Figure 88. Map. New York geographic location of analysis test sections.

Table 62 lists environment and pavement structure information for analysis test sections in New York.

Table 62. New York environment and pavement structure information for test sections.

Site	FTC	FI	CI	PRECIP	SN	ACTHICK	D	LESN	LEDT	AC/PC
0800	87	437	319	891	NA	NA	NA	NA	NA	AC
1011	90	505	298	1007	7.4	12.0	NA	0.7	NA	AC
1008	87	582	257	1133	5.6	1.8	NA	0.9	NA	AC
1643	99	618	270	1006	5.8	3.7	NA	1.0	NA	AC
Average	***91***	***536***	***286***	***1009***	***6.3***	***5.8***	NA	***0.9***	NA	NA
1644	109	990	111	1110	3.7	3.0	NA	1.3	NA	AC

Figure 89 shows geographic location of analysis test sections in North Carolina. Table 63 lists environment and pavement structure information for analysis test sections in North Carolina.

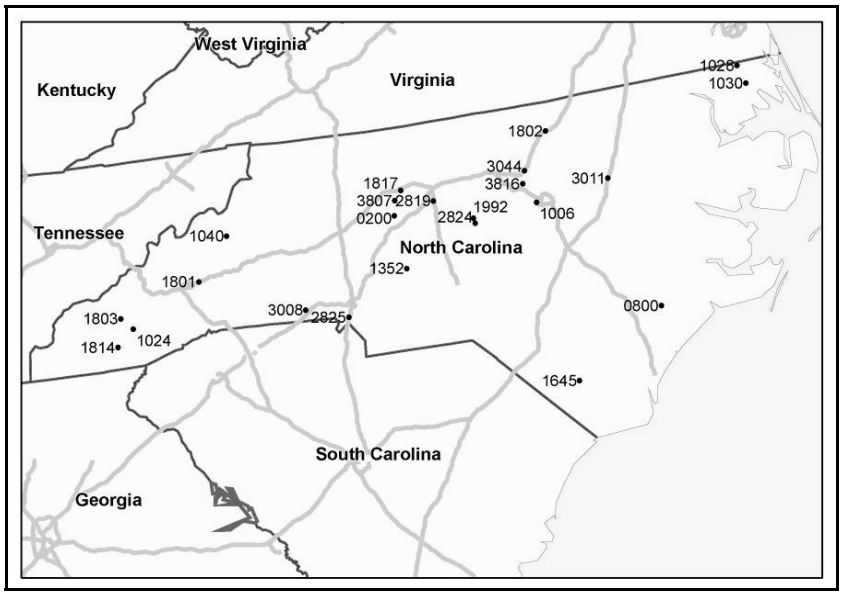

Figure 89. Map. North Carolina geographic location of analysis test sections.

Table 63. North Carolina environment and pavement information for analysis test sections.

Site	FTC	FI	CI	PRECIP	SN	ACTHICK	D	LESN	LEDT	AC/PC
0800	47	14	998	1343	NA	NA	NA	NA	NA	AC
1645	57	19	975	1260	5.2	8.9	NA	1.1	NA	AC
1030	50	24	951	1192	3.6	4.0	NA	1.4	NA	AC
2825	52	28	965	1093	3.9	4.6	NA	1.2	NA	AC
1352	69	32	876	1232	3.7	6.6	NA	1.4	NA	AC
1028	54	32	870	1186	4.6	2.9	NA	1.1	NA	AC
3008	67	33	815	1212	NA	NA	7.9	NA	0.7	PC
1006	60	35	887	1153	NA	10.1	NA	1.0	NA	AC
2819	69	43	799	1139	**NA**	7.0	NA	1.0	NA	AC
3816	71	44	830	1141	NA	NA	9.3	NA	0.6	PC
3011	71	45	867	1151	NA	NA	10.0	NA	0.6	PC
3807	77	46	772	1142	NA	NA	9.4	NA	0.6	PC
1817	74	46	779	1126	3.9	6.7	NA	1.4	NA	AC
0200	83	47	773	1151	NA	NA	NA	NA	NA	PC
3044	77	49	784	1161	NA	NA	9.0	NA	0.7	PC
Average	***65***	***36***	***863***	***1179***	***4.5***	***6.4***	***9.1***	***1.2***	***0.6***	**NA**
1992	73	53	779	1221	4.7	2.4	NA	1.1	NA	AC
2824	73	54	780	1224	4.0	5.8	NA	1.3	NA	AC
1802	82	58	775	1110	3.3	4.9	NA	1.6	NA	AC
1024	93	59	475	1308	5.0	7.6	NA	1.0	NA	AC
1814	100	70	446	1477	4.2	7.1	NA	1.3	NA	AC
1803	107	86	407	1371	3.8	6.3	NA	1.3	NA	AC
1801	88	116	323	1205	4.6	8.5	NA	1.2	NA	AC
1040	109	141	218	1441	3.9	6.2	NA	1.3	NA	AC
Average	***91***	***80***	***526***	***1245***	***4.2***	***6.1***	NA	***1.3***	NA	**NA**

Figure 90 shows the geographic locations of the analysis test sites in Ohio, and table 64 shows the environment and pavement structure information for the analysis test sections in Ohio..

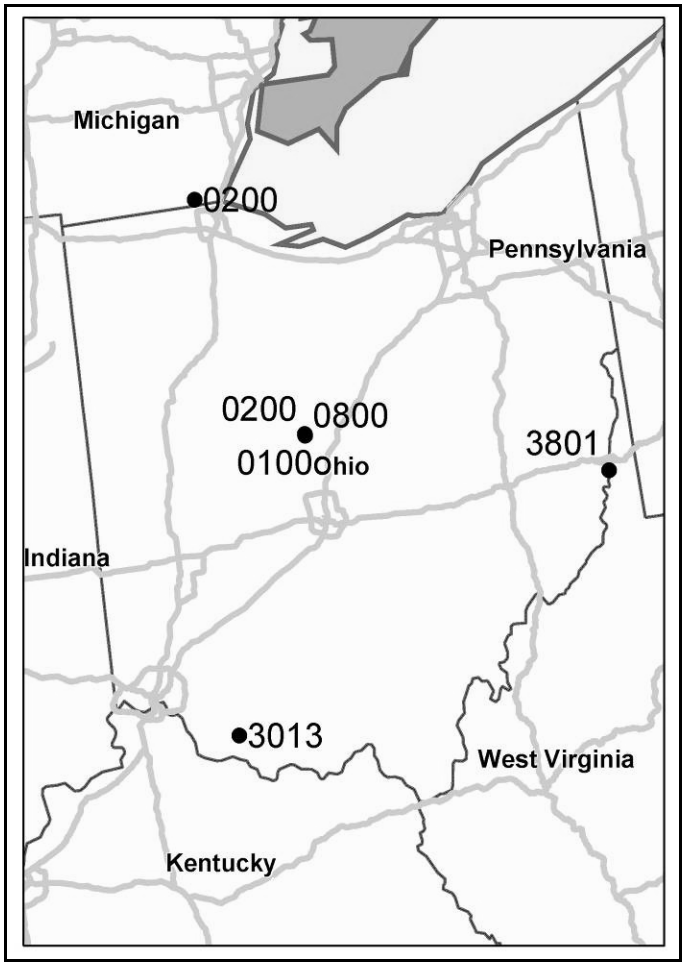

Figure 90. Map. Ohio geographic locations of analysis test sections.

Table 64. Ohio environment and pavement structure information for analysis test sections.

Site	FTC	FI	CI	PRECIP	SN	ACTHICK	D	LESN	LEDT	AC/PC
3801	89	249	480	1037	NA	NA	9.2	NA	0.6	PC
3013	89	250	533	1140	NA	NA	8.3	NA	0.6	PC
Average	***89***	***250***	***507***	***1088***	NA	NA	***8.8***	NA	***0.6***	**NA**
0100	96	375	414	972	NA	NA	NA	NA	NA	AC
0200	96	375	414	972	NA	NA	NA	NA	NA	PC
0800	96	375	414	972	NA	NA	NA	NA	NA	AC
Average	***96***	***375***	***414***	***972***	NA	NA	NA	NA	NA	**NA**

Figure 91 shows the geographic locations for analysis test sections in Pennsylvania.

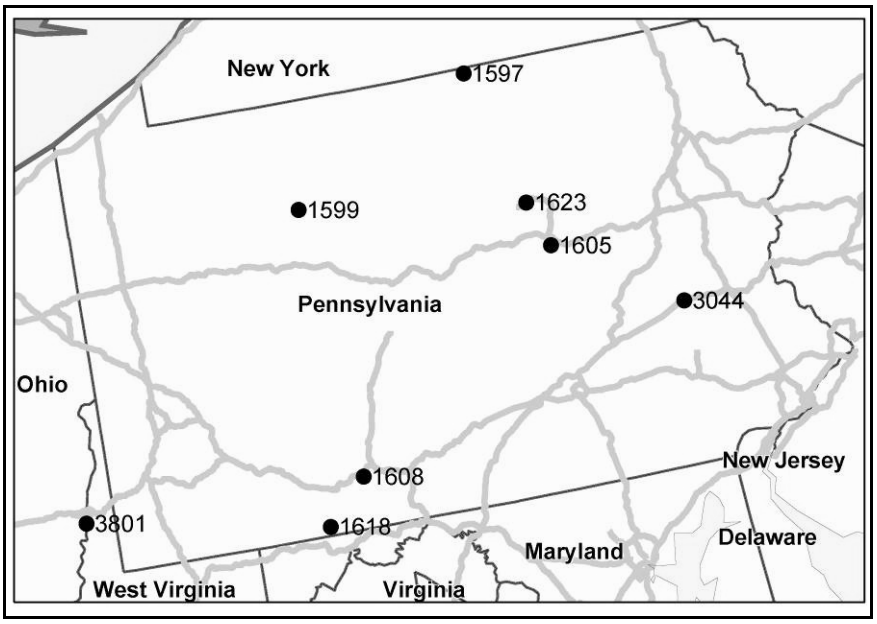

Figure 91. Map. Pennsylvania geographic locations of analysis test sections.

Table 65 lists environment and pavement structure information for analysis test sections in Pennsylvania.

Table 65. Pennsylvania environment and pavement structure information for analysis tests sections.

Site	FTC	FI	CI	PRECIP	SN	ACTHICK	D	LESN	LEDT	AC/PC
3044	99	269	433	1164	NA	NA	12.7	NA	0.5	PC
1623	95	309	415	1004	NA	NA	9.3	NA	0.6	PC
1608	107	311	334	944	3.7	5.0	NA	1.1	NA	AC
1605	107	331	339	1092	6.4	9.5	NA	0.9	NA	AC
1618	100	343	270	1028	3.6	5.1	NA	1.5	NA	AC
Average	***102***	***313***	***358***	***1047***	***4.6***	***6.5***	***11.0***	***1.2***	***0.6***	**NA**
1597	111	514	196	865	5.6	8.7	NA	0.9	NA	AC
1599	124	546	141	1121	6.7	12.3	NA	0.8	NA	AC
Average	***118***	***530***	***169***	***993***	***6.2***	***10.5***	NA	***0.9***	NA	**NA**

APPENDIX D. QUESTIONNAIRE SENT TO POOLED FUND STATES

This appendix provides a sample questionnaire sent to each of the participating PFS. The intent of this survey was to gain an understanding of standard design, specification, and testing procedures as well as unit bid prices and average performance lives.

POOLED FUND STATES QUESTIONNAIRE

Dear State Pooled Fund Panel Members:

As you remember, one of the primary research objectives for this pooled fund study was to determine:

> "The extent to which local adaptations of materials standards and pavement thickness designs have compensated for and/or mitigated the effects of seasonal frost penetration,…"

To accomplish that goal NCE proposed to look at this issue using a couple of standard pavement design sections. NCE anticipates that the roadway design sections as well as the materials and their related specifications may change between States to provide better pavement performance in their respective environment.

To develop these standard section and related material information, we are asking the pooled fund states (PFS) to provide the following information.

Standard Roadway Section

What is your standard pavement section for both flexible and rigid pavements that meets the following design criteria? If you don't have standard sections then what would your designed section be?

Rural Interstate (Four Lanes) Rigid and Flexible

- 30-year design.
- 30,000,000 ESALs.
- Frost-susceptible, fine-grained soil M_R 68,947.6 kilopascals (kPa) (10,000 pounds per square inch (psi)).
-

Rural Primary (Two Lanes) Rigid and Flexible

- 30-year design.
- 5,000,000 ESALs.
- Frost susceptible fine grained soil M_R 68,947.6 kilopascals (kPa) (10,000 psi).

Please provide layer unit names as well as dimensions for both the traveled lanes as well as the shoulder sections. For example, the first section of Rural Interstate Flexible might be shown as follows:

Pavement Course	**Main Line**	**Shoulders**
Wearing Course	7.62 cm (3-inch) Class A HMA	7.62 cm (3-inch) Class A HMA
Leveling Course	7.62 cm (3-inch) Class B HMA	7.62 cm (3-inch) Class B HMA
Base/Binder Course	12.7 cm (5-inch) Class E HMA	
Granular Base Course	15.24 cm (6-inch) Class 1 UTBC	27.94 cm (11-inch) Class 1 UTBC
Granular Subbase Cr.	15.24 cm (6-inch) Class 3 UTBC	15.24 cm (6-inch) Class 3 UTBC
Total Depth	58.42 cm (23 inches)	58.42 cm (23 inches)

The item names noted above are entirely fictional, and are used only to show that the bid item names are important. Each State transportation agency has its own naming conventions.

If special drainage features are included in the roadway section please note those as well.

If possible provide a cross section of the roadway section which shows the configuration of the pavement layers as well as the typical ditch section and depth, subgrade slopes, drainage features, etc.

Standard Specifications

We will also need copies of your standard specifications that apply to the bid items listed for the material properties as well as the placement procedures or in place properties. Where these are available at your agency's Web site, please let us know and we will download the PDF files. If only paper hard copies are available, please provide copies of the applicable specifications or simply send us a specifications book that applies to the materials placed at the LTPP test sites and we will make copies and return the book.

The ongoing adoption of SuperPave mixes will complicate this process. If your agency has adopted SuperPave mixes, please reference the materials that were used in your GPS and SPS test sites that represent the performance data included in the LTPP database.

If your agency has adopted SuperPave, please provide copies of those specifications as well. Please note that many agencies have developed their own SuperPave mix specifications based to varying degrees on the national guidelines. This is the reason we are asking for your specific specifications rather than use the national guidelines.

Test Procedures

Please review your specifications before you send them. If they reference standard AASHTO test procedures, we can access that information. If, however, they reference test procedures that are unique to your agency, please provide copies of those test procedures or provide a reference to the Web site where those test procedures are available.

Average Unit Bid Prices

In addition to the specifications, we will also need the average unit bid prices or the prices you would prefer we use in this study for each of the bid items noted in your standard or design roadway section.

Typical Service Life for Standard Section

We would also like your best estimate of the average service life of the pavement sections until major pavement repair, rehabilitation, or overlay as usually required. Please also provide a description of that treatment as well as the typical pavement condition (amount of fatigue cracking, ride values etc.), when treatment is applied.

Adjacent State Treatments
If there are any unique designs processes or treatments that are used by any adjacent States that seem to help mitigate frost effects, please describe that treatment and, if possible, indicate a contact person to check on that treatment.

Timeline
If possible we would like to receive the typical or design roadway sections as well as the standard specifications and test procedures by June 21. We would like to receive the rest of the material (bid prices, service life estimate, and adjacent state treatments) by July 9.

Sincerely,

Newton Jackson, P.E.
Project Manager
Nichols Consulting Engineers Chtd.

APPENDIX E. RESPONSES RECEIVED FROM POOLED FUND STATES

This appendix provides the information obtained from the PFS in response to the questionnaire in Appendix E. Some of the information provided by the PFS was excluded from this appendix because of publication limitations.

STATE OF ALASKA
Department of Transportation and Public Facilities
2301 Peger Road
Fairbanks, Alaska 99709

June 22, 2004

Newton Jackson, P.E.
Principal Engineer
Nichols Consulting Engineers, Chtd.
1885 S. Arlington, Suite 111
Reno, NV 89509

RE: Alaskan pavement section for "Effects of Multiple Freeze Cycles…" Pooled Fund Study

Dear Newton:

I am enclosing the Alaskan information you requested for the above project:

Standard Roadway Section:

- In Alaska, only flexible pavements are used for roadways
- In Rural Interstate (4 lanes): 30M ESALs is a high traffic level for us, so no pavement section is provided.
- Rural Primary (2 lanes): Enclosed are a drawing and a table detailing the pavement section for this case.

Standard Specifications:
Enclosed are hard copies of the relevant pages from the "Alaska Standard Specifications for Highway Construction – 2004."

Test Procedures:
We mainly use AASHTO specifications; however, two tests are done according to the Alaska Test Methods (ATM); see enclosed.

Average Unit Bid Prices:
They are included in the table detailing the pavement section.

Typical Service Life for Standard Section:
The average service life is 10 to 12 years. Typically, rutting and ride quality dictate the rehabilitation. "Shave and Pave" is typically used, unless distress is due to deep failures, where reclamation and paving become necessary.

Adjacent State Treatments:
The Yukon Territory mainly uses high-float surface treatment.

If you have questions or need further clarifications, please call or e-mail me.

Sincerely,

Steve Sabaundjian, P.E.
Research Engineer
steve_saboundjian@dot.state.ak.us
Ph: (907) 451-5322

Typical flexible pavement for Alaska; Rural Primary (two lanes); 5M ESALs.
See drawing.

Pavement Course	Mainline and Shoulder	Item	Price
Wearing Course	50 mm (2 inch) HMA, Type II, Class B*	401 (1)	$27.56/metric ton ($25/ton)
Binder Course	75 mm (3 inch) HMA, Type II, Class B*	401 (1)	$27.56/metric ton ($25/ton)
Aggregate Base Course	180 mm (7 inch), Grading D-1**	301 (1)	$12.13/metric ton ($11/ton)
Subbase	305 mm (12 inch), Grading B	304 (1)	$9.92/metric ton ($9/ton)
Borrow	915 mm (36 inch), Selected Material Type A	203 (6)	$4.41/metric ton ($4/ton)
Total Depth:	**1525 mm (60 inch)**	**NA**	**NA**

Notes:
* Asphalt, PG 58-28, $371.55/metric ton ($337/ton)
** MC-30 liquid asphalt prime coat, $385.89/metric ton ($350/ton)
See Section 703 for Aggregates Specs.

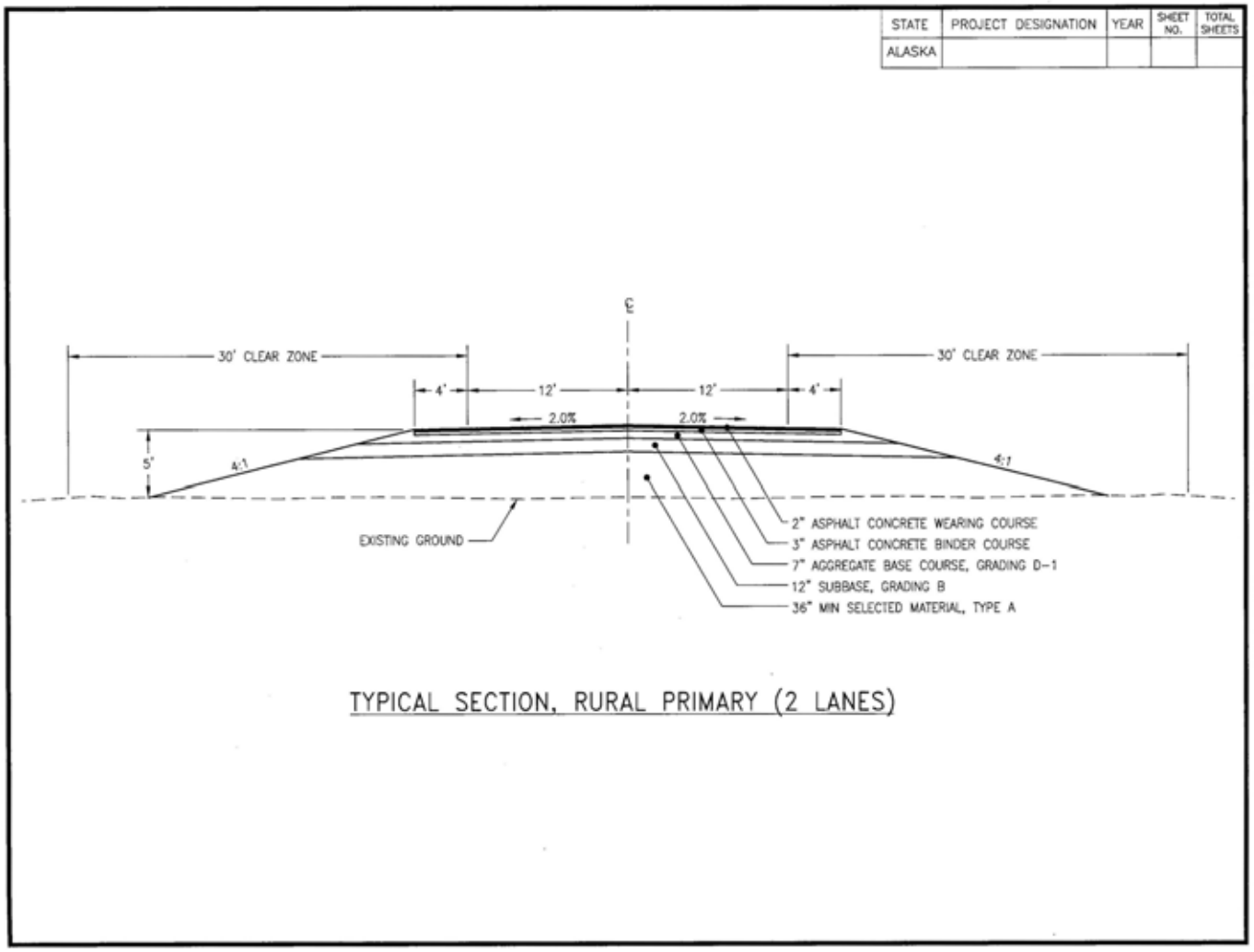

1 inch = 2.54 cm; 1 ft = 0.3 m

Figure 92. Diagram. Typical section for rural primary (2 lanes) in Alaska.

STATE OF IDAHO
Transportation Department
P.O. Box 7129
Boise, ID 83707-1129

December 20, 2004

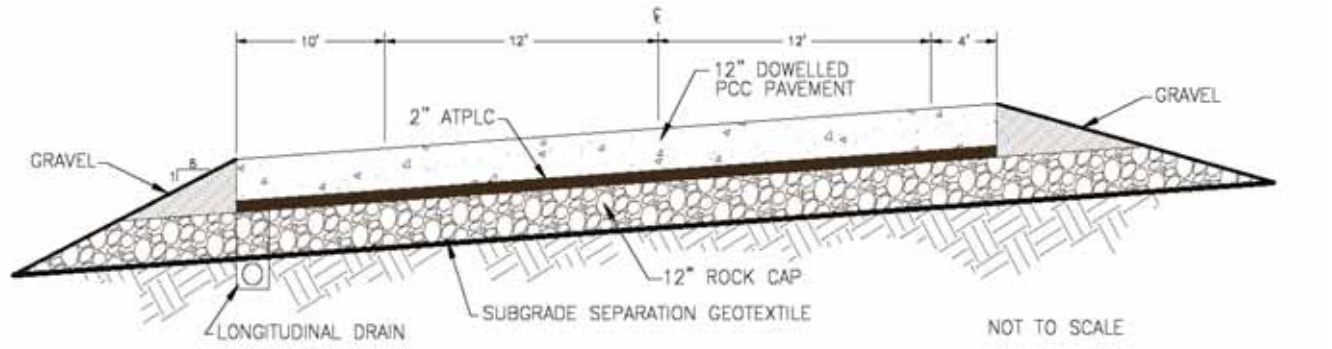

1 inch = 2.54 cm; 1 ft = 0.3 m

Figure 93. Diagram. Rigid pavement rural interstate typical section for Idaho.

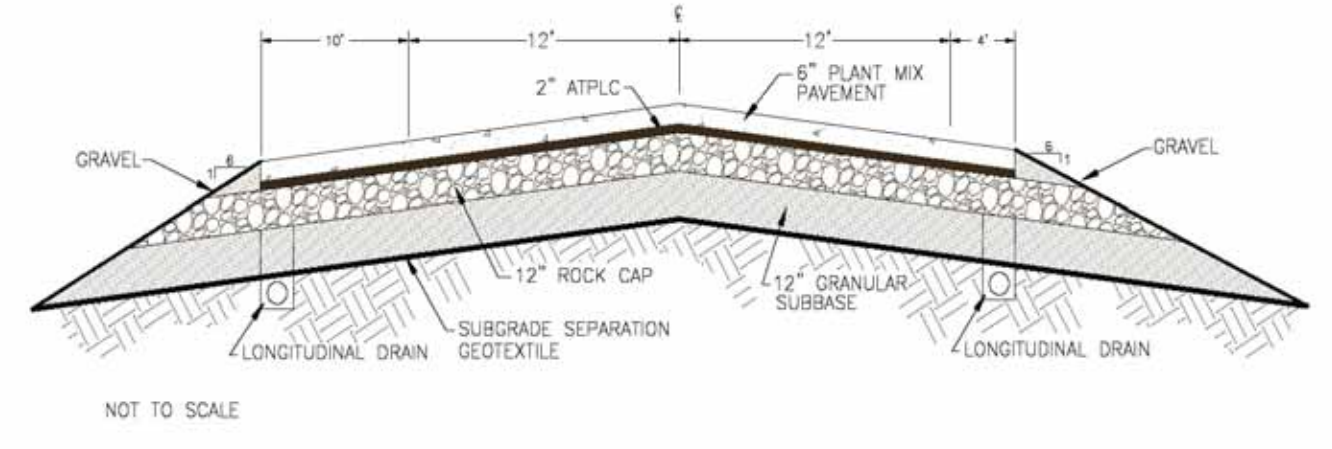

1 inch = 2.54 cm; 1 ft = 0.3 m

Figure 94. Diagram. Flexible pavement rural interstate typical section for Idaho.

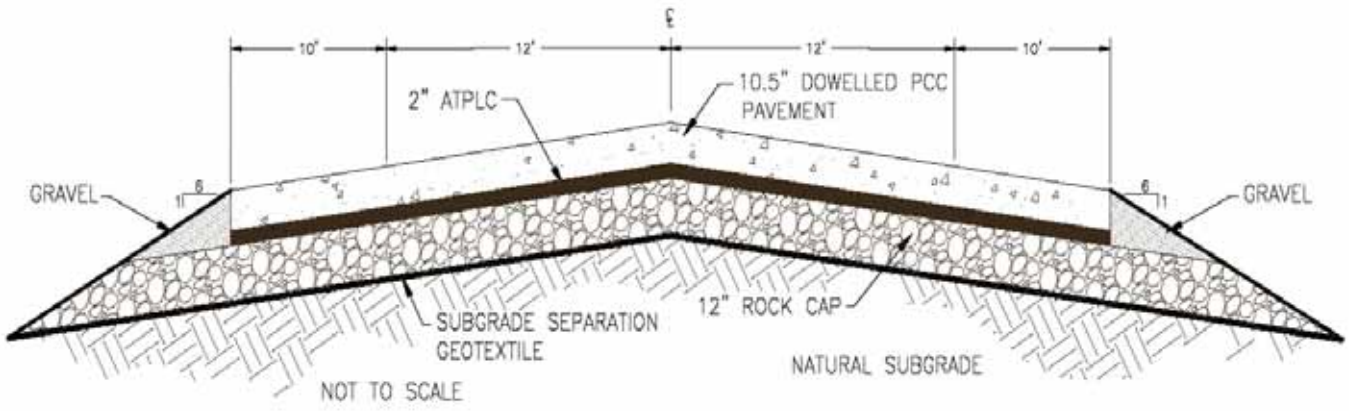

1 inch = 2.54 cm; 1 ft = 0.3 m

Figure 95. Diagram. Rigid pavement rural primary typical section for Idaho.

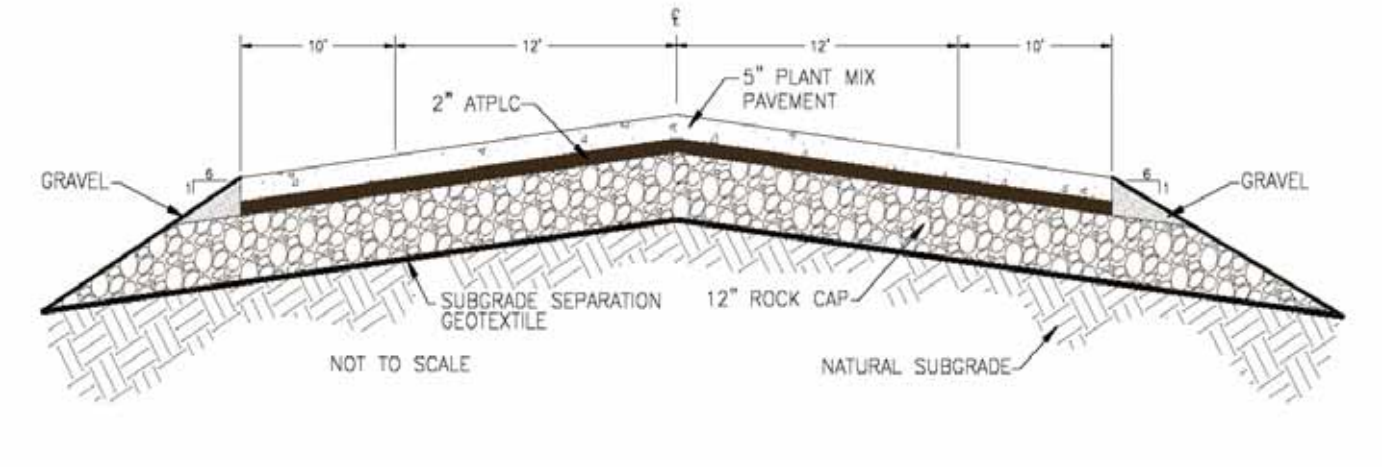

1 inch = 2.54 cm; 1 ft = 0.3 m

Figure 96. Flexible pavement rural primary typical section for Idaho.

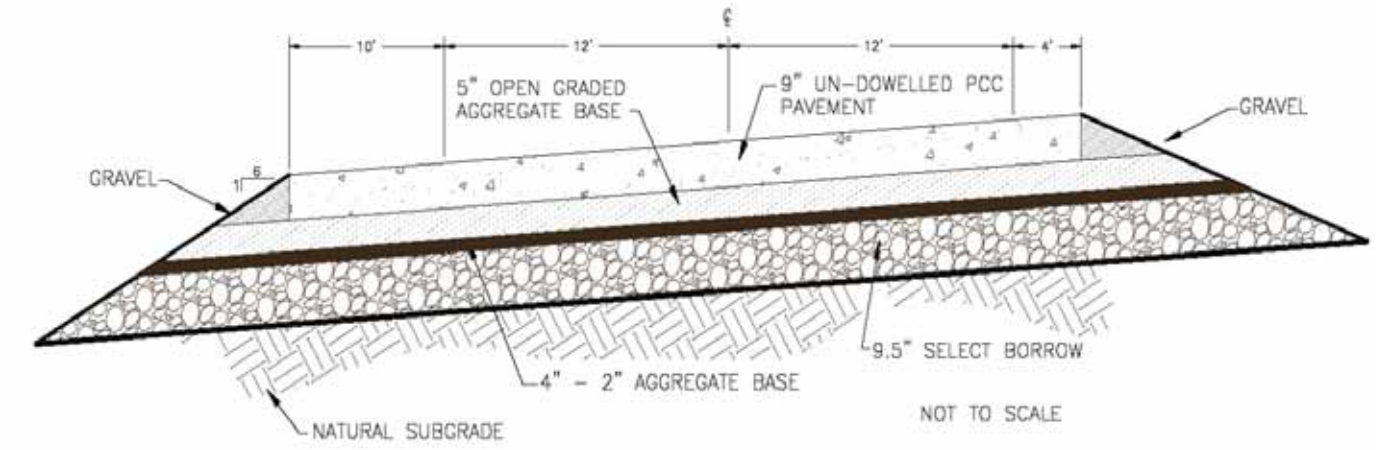

1 inch = 2.54 cm; 1 ft = 0.3 m

Figure 97. Diagram. Rigid pavement at LTPP site 163023 in Idaho.

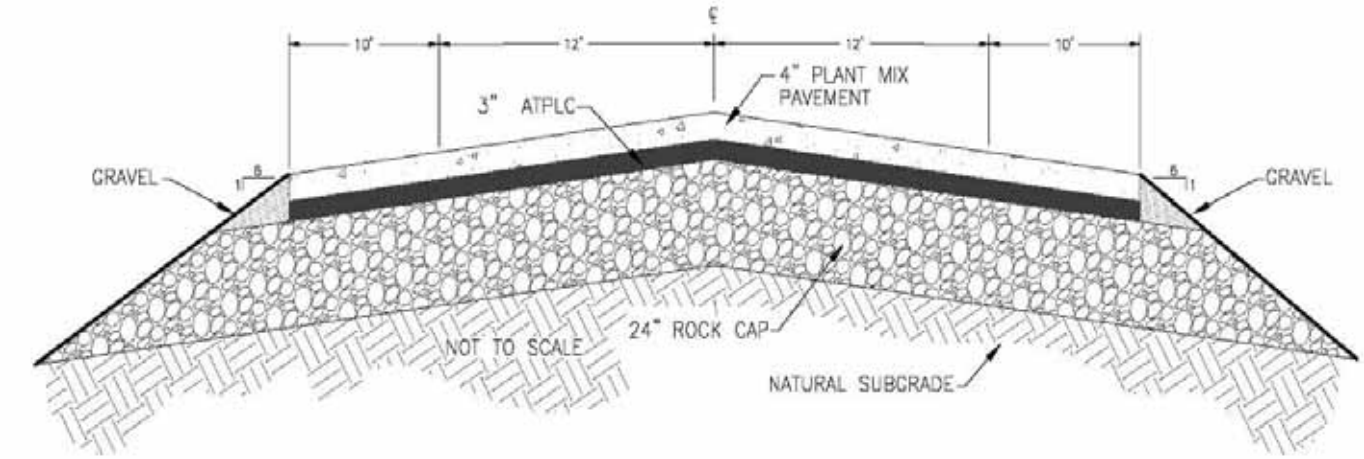

1 inch = 2.54 cm; 1 ft = 0.3 m

Figure 98. Diagram. Flexible pavement at LTPP site 169032 in Idaho.

STATE OF ILLINOIS
Department of Transportation
126 East Ash Street
Springfield, IL 62704-4766

Standard Roadway Sections

Rural Interstate Rigid

Pavement Course	Main Line	Shoulder
Jointed Plain Concrete: 4.6 m (15 ft) joints	265 mm (10.5 inch)	150 mm (6 inch)
Stabilized Subbase (CAM or BAM)	100 mm (4 inch)	
Subbase Granular Material, Type C		215 mm (8.5 inch)
Pipe Underdrains: 100 mm (4 inch)		
Aggregate Shoulder Wedge, Type B		
Lime Modified Subgrade	305 mm (12 inch)	305 mm (12 inch)
Total Depth	675 mm (26.5 inch)	675 mm (26.5 inch)

Note: Tied Shoulder

Rural Interstate Flexible

Pavement Course	Main Line	Shoulder
SuperPave HMA Surface Course	50 mm (2 inch)	50 mm (2 inch)
SuperPave HMA Binder Course	465 mm (18.25 inch)	150 mm (6 inch)
Subbase Granular Material, Type C		310 mm (12.25 inch)
Pipe Underdrains: 100 mm (4 inch)		
Aggregate Shoulder Wedge, Type B		
Lime Modified Subgrade	305 mm (12 inch)	305 mm(12 inch)
Total Depth	820 mm (32.25 inch)	820 mm (32.25 inch)

Rural Primary Rigid

Pavement Course	Main Line	Shoulder
Jointed Plain Concrete (15-ft Joints)	250 mm (9.75 inch)	
Stabilized Subbase (CAM or BAM)	100 mm (4 inch)	
SuperPave HMA Surface Course		50 mm (2 inch)
SuperPave HMA Binder Course		150 mm (6 inch)
Subbase Granular Material, Type C		145 mm (5.75 inch)
Aggregate Shoulder Wedge, Type B		
Lime Modified Subgrade	305 mm (12 inch)	305 mm (12 inch)
Total Depth	655 mm (25.75 inch)	655 mm (25.75 inch)

Note: Untied Shoulder

Rural Primary Flexible

Pavement Course	Main Line	Shoulder
SuperPave HMA Surface Course	50 mm (2 inch)	50 mm (2 inch)
SuperPave HMA Binder Course	305 mm (12 inch)	150 mm (6 inch)
Subbase Granular Material, Type C		150 mm (6 inch)
Aggregate Shoulder Wedge, Type B		
Lime Modified Subgrade	305 mm (12 inch)	305 mm (12 inch)
Total Depth	660 mm (26 inch)	660 mm (26 inch)

Standard drawings of the typical pavement cross sections may be found on the IDOT Internet site by following these directions.

Go to www.dot.il.gov
Under IDOT Links, click on Doing Business
Under Construction Guides, click on Specifications/Special Provisions/Highway Standards
Next, click on Highway Standards
Next, click on Index of Highway Standards
Next, click on Section 400
The appropriate drawings are: 420101, 482001, 482006, and 483001

Also, you will find two design drawings at:

Go to www.dot.il.gov
Under IDOT Links, click on Doing Business
Under Manuals – Memorandums – Rules, click on Bureau of Design & Environment Manual
Next, click on Chapter 54—Pavement Design
Select page 43 of 114 (Figure 54-4(9))
Select page 65 of 114 (Figure 54-5(13))

Standard Specifications

Standard specifications that apply to rigid and flexible pavement construction may be found on the IDOT internet site by following these directions.

Go to www.dot.il.gov
Under IDOT Links, click on Doing Business
Under Construction Guides, click on Specifications/Special Provisions/Highway Standards
Next, click on Standard Specifications for Road and Bridge Construction
Next, click on Section 400
The appropriate sections are: Section 406 (Starting on page 25 of 134)
Section 407 (Starting on page 47 of 134)
Section 420 (Starting on page 57 of 134)
Section 482 (Starting on page 129 of 134)
Section 483 (Starting on page 132 of 134)

Test Procedures

References to test procedures other than AASHTO or ASTM standard test procedures may be found in the IDOT Manual of Test Procedures for Materials. This manual is not available on the

internet; however, the order form to receive a copy of the manual may be found on the IDOT internet site by following these directions. The cost of the manual is $50.00.

Go to www.dot.il.gov
Under IDOT Links, click on Doing Business
Under Manuals – Memorandums – Rules, click on Highways Manuals Order Form
The item is number: ID 034 Manual of Test Procedures for Materials

Average Unit Bid Prices

The following are average bid prices for the bid items listed under the Standard Roadway Sections. These prices assume large quantities.

Table 66. Average unit prices for Illinois.

Item	Unit	Unit Price
Lime	Metric ton (ton)	$55.13 ($50.00)
Processing Lime Modified Soils: 305 mm (12 inch)	Square meter (square yard)	$1.67 ($1.40)
Subbase Granular Material, Type C	Metric ton (ton)	$16.54 ($15.00)
Stabilized Subbase: 100 mm (4 inch)	Square meter (square yard)	$10.77 ($9.00)
Pipe Underdrains: 100 mm (4 inch)	Meter (foot)	$9.84 ($3.00)
Dowel Bars: 40 mm (1.5-inch diameter)	Square meter (square yard)	$14.35 ($12.00)
PCC Pavement (Jointed): 250 mm (9.75 inch)	Square meter (square yard)	$35.89 ($30.00)
PCC Pavement (Jointed): 265 mm (10.5 inch)	Square meter (square yard)	$38.88 ($32.50)
Bituminous Concrete Pavement (Full-Depth): 515 mm (20.25 inch)	Square meter (square yard)	$47.85 ($40.00)
Bituminous Concrete Pavement (Full-Depth): 355 mm (14.0 inch)	Square meter (square yard)	$39.48 ($33.00)
Bituminous Shoulders: 205 mm (8 inch)	Square meter (square yard)	$21.53 ($18.00)
PCC Shoulders: 150 mm (6 inch)	Square meter (square yard)	$17.94 ($15.00)
Aggregate Shoulders, Type B	Metric ton (ton)	$14.33 ($13.00)

Typical Service Life for Standard Section

A description of the typical service life and the "planned" repair methods throughout the life of the pavement may be found on the IDOT internet site by following these directions.

Go to www.dot.il.gov

Under IDOT Links, click on Doing Business
Under Manuals—Memorandums—Rules, click on Bureau of Design & Environment Manual
Next, click on Chapter 54—Pavement Design
For jointed PCC pavement, select page 88 of 114 (Figure 54-7(A))
For HMA pavement (TF = 5), select page 89 of 114 (Figure 54-7(B))
For HMA pavement (TF = 30), select page 92 and 93 of 114 (Figure 54-7(D))

STATE OF MICHIGAN
Department of Transportation
8885 Ricks Road
P.O. Box 30049

Michigan's Typical Designs

Response for pooled fund study "Effects of Multiple Freeze Cycles and Deep Frost Penetration on Pavement Performance and Cost"

Note: We use a design life of 20 years, and an M_R of 69,000 kPa (10,000 psi) is much higher than anything we would typically encounter in Michigan.

Designs

Rural Interstate (four lanes) Rigid and Flexible
30-year design
30,000,000 ESALs
Frost susceptible fine grained soil M_R 69,000 kPa (10,000 psi)

HMA Cross-Section

Layer	Mainline	Shoulder
Wearing Course	40 mm (1.5 inch) Gap Graded Superpave	40 mm (1.5 inch) 4C
Leveling Course	50 mm (2.0 inch) 4E50	50 mm (2.0 inch) 3C
Base Course	95 mm (3.75 inch) 3E50	95 mm (3.75 inch) 2C
Base	150 mm (6.0 inch) 21AA	150 mm (6.0 inch) 21AA
Subbase	450 mm (18.0 inch) class IIA sand	450 mm(18.0 inch) class IIA sand
Drainage		150 mm (6.0 inch) subbase underdrains

Concrete Cross-Section

Layer	Mainline	Shoulder
Concrete	290 mm (11.5 inch) JPCP	230 mm (9.0 inch) JPCP
Base	150 mm (6.0 inch) 4G modified	215 mm (8.5 inch) 4G modified Geotextile Separator
Subbase	255 mm (10 inch) class IIA sand	255 mm (10.0 inch) class IIA sand
Drainage		150 mm (6.0 inch) base underdrains

Rural Primary (Two Lanes) Rigid and Flexible
30-year design
5,000,000 ESALs
Frost susceptible fine grained soil M_R 69,000 kPa (10,000 psi)

HMA Cross-Section

Layer	Mainline	Shoulder
Wearing Course	40 mm (1.5 inch) 5E10	40 mm (1.5 inch) 4C
Leveling Course	50 mm (2.0 inch) 4E10	50 mm (2.0 inch) 3C
Base Course	75 mm (3.0 inch) 3E10	75 mm (3.0 inch) 2C
Base	150 mm (6.0 inch) 21AA	150 mm (6.0 inch) 21AA
Subbase	450 mm (18.0 inch) class II sand	450 mm (18.0 inch) class II sand
Drainage		150 mm (6.0 inch) subbase underdrains

Concrete Cross-Section

Layer	Mainline	Shoulder
Concrete	215 mm (8.5 inch) JPCP	100 mm (4.0 inch) HMA (4C,3C)
Base	150 mm (6.0 inch) 4G modified	150 mm (6.0 inch) 4G modified
		Geotextile Separator
Subbase	255 mm (10.0 inch) class II sand	255 mm (10.0 inch) class II sand
Drainage		150 mm (6.0 in) base underdrains

If this were a freeway, it would be 230 mm (9.0 in), which is our minimum concrete thickness for freeways.

For equivalent designs (same traffic makeup) the ESALs would be different for asphalt and concrete. So, a 30 million ESAL design for HMA is not equivalent (structurally) to a 30 million ESAL design for concrete.

Specifications

Gap Graded Superpave—see attached special provision

4E50, 3E50, 5E10, 4E10, 3E10—Superpave mainline mixes. Covered by Division 5 of Standard Specifications for Construction which can be found at:

http://www.mdot.state.mi.us/specbook/

Materials for the mixes are covered in Division 9 of the Standard Specifications.

Also see the special provision for superpave mixes (03SP501F) and the HMA Mixture Selection Guidelines which are attached.

4C, 3C, 2C—Marshall mixes used for shoulders. Covered by Division 5 and Division 9 of the Standard Specifications. Also see the special provision for Marshall mixes (03SP501H) and HMA Mixture Selection Guidelines which are attached.

Jointed Plain Concrete Pavement—Covered by Division 6

21AA—Base layer under HMA pavements. Covered by Sections 302 and 902 of the Standard Specifications.

4G modified—Base layer under concrete pavements. Covered by Sections 303 and 902 of the Standard Specifications. The special provision for open graded drainage course, modified (03SP303A) covers the modifications to the Standard Specifications.

Class II—Subbase layer. Covered by Sections 301 and 902 of the Standard Specifications.

Geotextile Separator—Used between open graded bases and sand subbases. Covered by Section 910 of the Standard Specifications.

Underdrains – Covered by Section 404 and 909 of the Standard Specifications.

State Specific Test Methods

Any test methods specific to Michigan will be listed as MTM-xxx where 'xxx' will be a number. The Manual for the Michigan Test Methods (MTM's) can be found at:

http://www.michigan.gov/documents/mdot_MTM_CombinedManual_83501_7.pdf

Also, years ago Michigan developed its own "One Point" tests for determining maximum density for granular and cohesive soils. ("One Point" refers to compacting the density mold at only one moisture content, instead of doing an optimum moisture content curve.) T-99 molds are used for cohesive soils and an inverted cone shaped mold is used for granular soils and unbound base courses. Detailed procedures are outlined in the Density Control Handbook, which can be accessed at:

http://www.michigan.gov/mdot/0,1607,7-151-9622_11044_11367---,00.html

Average Unit Bid Prices

These are prices we use in life-cycle costing:

Item	Average Price
Gap Graded Superpave	$53.77/metric ton ($48.77/ton)
4E50	$44.71/metric ton ($40.55/ton)
3E50	$44.71/metric ton ($40.55/ton)
5E10	$40.62/metric ton ($36.84/ton)*
4E10	$39.25/metric ton ($35.60/ton)*
3E10	$38.04/metric ton ($34.50/ton)*
4C	$37.85/metric ton ($34.33/ton)
3C	$41.07/metric ton ($37.25/ton)*
2C	$38.26/metric ton ($34.70/ton)*
JPCP, 29.21 cm (11.5 inch)	$23.99/square meter ($20.06/square yd)*
21AA	$5.13/square meter ($4.29/square yd)*
4G, modified	$4.70/square meter ($3.93/square yd)*
Geotextile Separator	$0.93/square meter ($0.78/square yd)*
Class II sand	$5.63/cubic meter ($4.31/cubic yd)*
15.24-cm (6-inch) base underdrains	$10.73/meter ($3.27/ft)*
15.24-cm (6-inch) subbase underdrains	$11.75/meter ($3.58/ft)*

We divide the State into three zones and obtain average unit prices for each of the zones. Prices with an * are chosen from one of the zones (zone 2); otherwise it is a statewide average price.

Typical Service Life

In Michigan, we use a 20-year design life. Our service life for design 1 above (rural interstate) would be 26 years for both HMA and JPCP. Both would typically receive two cycles of preventive maintenance during that time. For the HMA, it would be a crack seal that averages about year 10 and a Distress Index of 29 and a mill and resurface that averages about year 13 and a Distress Index of 18. For the JPCP, it would be a joint reseal that averages about year 9 and a Distress Index of 6 and a CPR (full-depth repairs, spall repair, etc.) that averages about year 15 and a Distress Index of 18.

The service life for design 2 (rural two-lane) would be 30 years. Again, two cycles of the same preventive maintenance fixes for both pavement types. For HMA, the first cycle would be at an average age of 11 and Distress Index of 27 and the second cycle would be at an average age of 15 and Distress Index of 20. For JPCP, the first cycle would average age 8 and Distress Index of 6 for cycle one and age 16 and Distress Index of 20 for cycle two.

The Distress Index is Michigan's measure of the pavement condition. The pavement is visually surveyed and distresses are logged. Each distress has a point value assigned to it depending on its severity. The points are accumulated into 0.16 km (0.1 mile) segments that are called the Distress Index. When a pavement reaches a Distress Index of 50, it is considered to have 0 life left and needs to be rehabilitated/reconstructed. The amount and type of distresses can vary significantly for the same Distress Index. For that reason, typical distress values at which preventive maintenance fixes are applied, are not given here.

Michael Eacker
Pavement Design Engineer
eackerm@michigan.gov
517-322-3474
3-1-05

STATE OF NEW YORK
Department of Transportation
50 Wolf Road
Albany, NY 12232

MEMO via e-mail

Subject: Response to Pooled Fund Study
Date: June 15, 2004
From: RMORGAN@dot.state.ny.us
To: newt@nce.reno.nv.us
CC: WYANG@dot.state.ny.us

Newton,

In response to your questionnaire for the Pooled Fund Study, "Effect of Multiple Freeze Cycles & Deep Frost Penetration on Pavement, Phase 2," attached are NYSDOT standard pavement sections from our 2000 Comprehensive Design Manual.

For your information, NYS does not use rigid pavement for highways with less than 10,000,000 ESALs. Also MR (MPa in NYS) is used for HMA pavement only, and our typical allowed maximum is 62 MPa (9,000 psi). For rigid pavement, NYSDOT uses the Modulus of Subgrade Reaction (k-value).

You may obtain copies of NYSDOT's 2002 Standard Specifications and our Weighted Average Bid Price Book on NYDOT's website at: www.dot.state.ny.us/pubs/publist.html.

If you need additional information or have questions concerning this information, please feel free to contact me or Wes Yang.

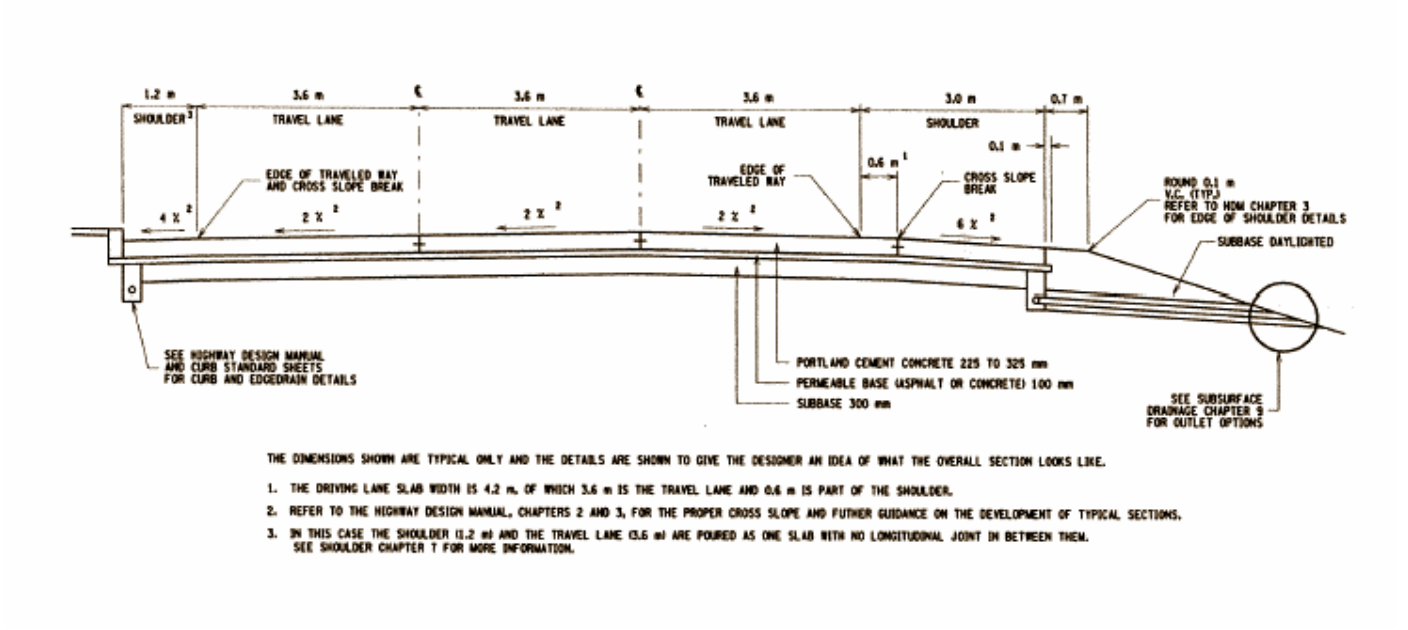

1 inch = 2.54 cm; 1 ft = 0.3 m

Figure 99. Diagram. Typical portland cement concrete pavement section for New York.

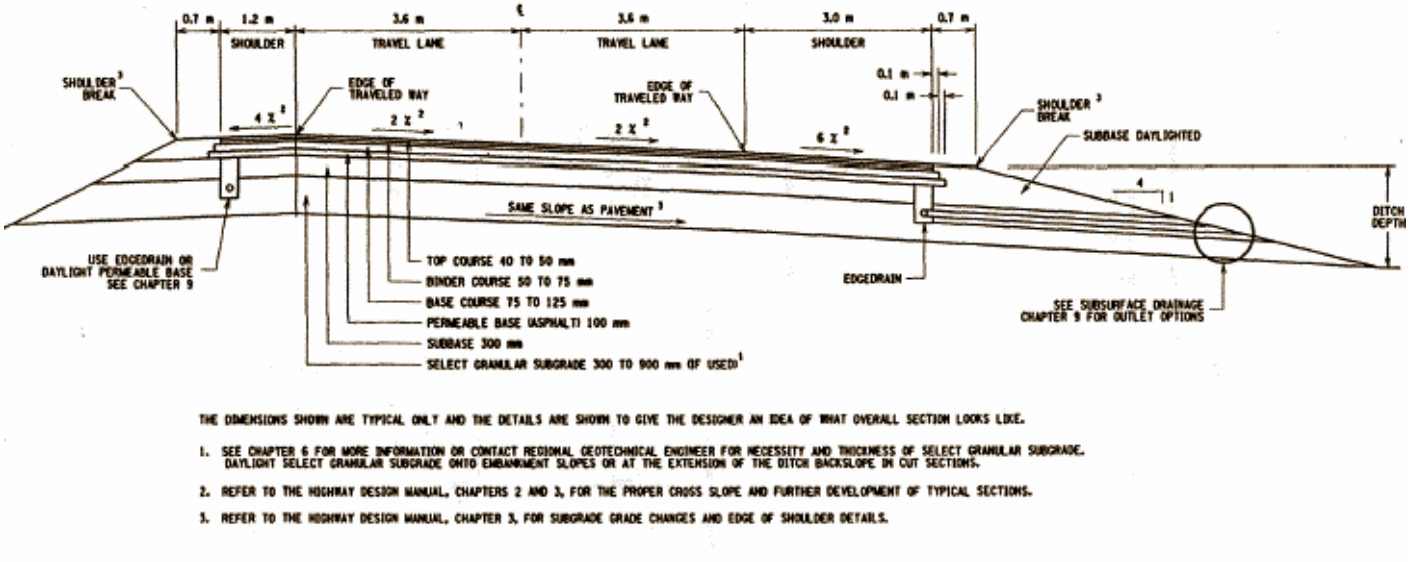

1 inch = 2.54 cm; 1 ft = 0.3 m

Figure 100. Diagram. Typical hot-mix asphalt pavement section for New York.

Table 67. PCC thickness table for New York.

80-kN ESALs	PCC Slab Thickness 4.2 m driving lane slab width	PCC Slab Thickness 3.6 m driving lane slab width
millions	mm	mm
≤ 22	225 (9 inch)	225 (9 inch)
> 22 ≤ 36	225 (9 inch)	250 (10 inch)
> 36 ≤ 65	225 (9 inch)	275 (11 inch)
> 65 – 100	250 (10 inch)	300 (12 inch)
> 100 – 165	275 (11 inch)	325 (12.75 inch)
> 165 – 250	300 (12 inch)	325[1] (12.75 inch)
> 250 – 400	325 (12.75 inch)	325[1] (12.75 inch)

[1] For ESALs over 165 million, 3.6 million, 3.6 m untied slabs may not be used for the right hand driving lane. Use either 3.6 m tied slabs, 4.2 m untied slabs, or 4.2 m tied slabs.

Table 68. HMA thickness table for New York (M_r=28 MPa).

M_r = 28 MPa		
80 kN ESALs Over Design Life	Total HMA Thickness	Select Granular Subgrade Thickness
millions	mm	mm
< 2	155 (6 inches)	0
2 – 4	175 (7 inches)	0
> 4 – 8	200 (8 inches)	0
> 8 – 13	225 (9 inches	0
> 13 – 23	250 (10 inches)	0
> 23 – 45	250 (10 inches)	150 (6 inches)
> 45 – 80	250 (10 inches)	300 (12 inches)
> 80 – 140	250 (10 inches)	450 (18 inches)
> 140 – 300	250 (10 inches	600 (24 inches)

Table 69. HMA thickness table for New York (M_r=34 MPa).

M_r = 34 MPa		
80 kN ESALs Over Design Life	**Total HMA Thickness**	**Select Granular Subgrade Thickness**
millions	mm	mm
< 4	155 (6 inches)	0
4 – 7	175 (7 inches)	0
> 7 – 13	200 (8 inches)	0
> 13 – 23	225 (9 inches)	0
> 23 – 40	250 (10 inches)	0
> 40 – 70	250 (10 inches)	150 (6 inches)
> 70 – 130	250 (10 inches)	300 (12 inches)
> 130 – 235	250 (10 inches)	450 (18 inches)
> 235 – 300	250 (10 inches)	600 (24 inches)

Table 70. HMA thickness table for New York (M_r=41 MPa).

M_r = 41 MPa		
80 kN ESALs Over Design Life	**Total HMA Thickness**	**Select Granular Subgrade Thickness**
millions	mm	mm
< 6	155 (6 inches)	0
6 – 11	175 (7 inches)	0
> 11 – 20	200 (8 inches)	0
> 20 – 35	225 (9 inches)	0
> 35 – 60	250 (10 inches)	0
> 60 – 110	250 (10 inches)	150 (6 inches)
> 110 – 200	250 (10 inches)	300 (12 inches)
> 200 – 300	250 (10 inches)	450 (18 inches)

Table 71. HMA thickness table for New York (M_r=48 MPa).

M_r = 48 MPa		
80 kN ESALs Over Design Life	**Total HMA Thickness**	**Select Granular Subgrade Thickness**
millions	mm	mm
< 8	155 (6 inches)	0
8 – 16	175 (7 inches)	0
> 16 – 30	200 (8 inches)	0
> 30 – 50	225 (9 inches)	0
> 50 – 85	250 (10 inches)	0
> 85 – 160	250 (10 inches)	150 (6 inches)
> 160 – 300	250 (10 inches)	300 (12 inches)

Table 72. HMA thickness table for New York (M_r=55 MPa).

M_r = 55 MPa		
80 kN ESALs Over Design Life	**Total HMA Thickness**	**Select Granular Subgrade Thickness**
millions	mm	mm
< 12	155 (6 inches)	0
12 – 20	175 (7 inches)	0
> 20 – 40	200 (8 inches)	0
> 40 – 65	225 (9 inches)	0
> 65 – 115	250 (10 inches)	0
> 115 – 215	250 (10 inches)	150 (6 inches)
> 215 – 300	250 (10 inches)	300 (12 inches)

Table 73. HMA thickness table for New York (M_r=62 MPa).

M_r = 62 MPa		
80 kN ESALs Over Design Life	**Total HMA Thickness**	**Select Granular Subgrade Thickness**
millions	mm	mm
< 15	155 (6 inches)	0
15 – 30	175 (7 inches)	0
> 30 – 50	200 (8 inches)	0
> 50 – 90	225 (9 inches)	0
> 90 – 150	250 (10 inches)	0
> 150 – 300	250 (10 inches)	150 (6 inches)

STATE OF NORTH CAROLINA
Department of Transportation
P.O. Box 25201
Raleigh, NC 27611

July 20, 2004

MEMO TO: Newton Jackson, P.E.
Principal Engineer
Nichols Consulting Engineers, Chtd.
1885 S. Arlington, Suite 111
Reno, NV 89509

FROM: Clark S. Morrison, P.E.
State Pavement Design Engineer
Pavement Management Unit, NCDOT

RE: Frost Penetration Pooled Fund Study Survey

Attached are the pavement designs you requested. Our Standard Specifications and Average Unit Bid Prices are available online at:

http://www.doh.state.nc.us/preconstruct/highway/dsn_srvc/contracts/

Please let me know if you have any difficulty with this site. This part of NCDOT is reorganizing, and their website address and the content may be changing in the near future. If you need help, please call me at 919-250-4094.

RURAL INTERSTATE (four lanes)
30-year design
30,000,000 ESALs
Frost-susceptible fine grained soil, M_R 69,000 kPa (10,000 PSI)
Use S = 3.0, R = 1.5 (Typical values used in North Carolina Western Divisions)

Recommended flexible pavements:

	<1A>	**<1B>**	**Shoulder**
Surface Course	100 mm (4 inches) S12.5 C	100 mm (4 inches) S12.5 C	100 mm (4 inches) S12.5 C
Intermediate Course	75 mm (3 inches) I19.0 C	75 mm (3 inches) I19.0 C	NA
Base Course	230 mm (9 inches) B25.0 C	140 mm (5.5 inches) B25.0 C	NA

Granular Base Course	250 mm (10 inches) ABC	250 mm (10 inches) ABC	Variable Depth
Stabilized Subgrade	NA	200 mm (8 inches) Lime or 175 mm (7 inches) Cement	NA
Total Depth	**660 mm (26 inches)**	**570 mm (22.5 inches)**	**Variable**

Recommended rigid pavement:

		Shoulders
	280 mm (11 inches) Jointed Concrete	280 mm (11 inches) adjacent to mainline
	75 mm (3 inches) B25.0 B	115 mm (4.5 inches) ABC
	40 mm (1.5 inches) S9.5 B	NA
	Lime/Cement Stabilization	NA
Total Depth	**395 mm (15.5 inches)**	**Variable**

RURAL PRIMARY (two lanes)
30-year design
5,000,000 ESALs
Frost-susceptible fine grained soil, M_R 69,000 kPa (10,000 psi)
Use S = 3.0, R = 1.5 (Typical values used in North Carolina Western Divisions)

Recommended flexible pavements:

	<1A>	**<1B>**	**Shoulder**
Surface Course	75 mm (3 inches) S9.5 C	75 mm (3 inches) S9.5 C	75 mm (3 inches) S9.5 C
Intermediate Course	75 mm (3 inches) I19.0 C	100 mm (4 inches) I19.0 C	NA
Base Course	105 mm (4.5 inches) B25.0 C	NA	NA
Granular Base Course	255 mm (10 inches) ABC	255 mm (10 inches) ABC	Variable Depth
Stabilized Subgrade	**NA**	205 mm (8 inches) Lime or 180 mm (7 inches) Cement	NA
Total Depth	**NA**	**430 mm (17 inches)**	**Variable**

Recommended rigid pavement:

	205 mm (8 inches) Jointed Concrete
	75 mm (3 inches) B25.0 B
	40 mm (1.5 inches) S9.5 B
	Lime/Cement Stabilization
Total Depth	**320 mm (12.5 inches)**

STATE OF OHIO
Department of Transportation
P.O. Box 899
Columbus, OH 43216-0899

ODOT on line is found at:
http://www.dot.state.oh.us/default.htm

In general all ODOT standards, specifications and design policies are found at:
http://www.dot.state.oh.us/drrc/

ODOT specifications can be found at:
http://www.dot.state.oh.us/construction/OCA/Specs/2002CMS/Specbook2002/Specbook2002.htm

Supplemental Specifications and approved plan notes can be found at:
http://www.dot.state.oh.us/construction/OCA/Specs/SSandPN2002/default.htm

Warranty Policy can be found at:
http://www.dot.state.oh.us/construction/OCA/Warranty/WarrantyDocs/warpolicy.htm

Warranty Guidelines can be found at:
http://www.dot.state.oh.us/construction/OCA/Warranty/WarrantyDocs/Warranty%20App%20Guidelines%20Rev3.pdf

Under drain policy can be found at:
http://www.dot.state.oh.us/se/hy/LD2/Sec1000/sec1000bookmarked.pdf

ODOT Pavement Design & Rehabilitation Manual can be found at:
http://www.dot.state.oh.us/pavement/publications.htm

Regarding a pavement buildup, our design standards do not reference a standard pavement section. ODOT does not have a catalogue type design approach. Instead we put together a unique design buildup for every project. In general, all rigid pavements use tied concrete shoulders, and all pavement types require pipe underdrains.

Rural Interstate—Flexible (93 AASHTO)
30,000,000 flexible ESAL
Mr = 69,000 kPa (10,000 psi)
R= 90%; Overall Deviation = 0.49; Initial Serviceability = 4.50;
Terminal Serviceability = 2.5
SN=5.12

Final Design—Rural Interstate—Flexible:

290 mm (11.5 inches)	Item 880	Asphalt Concrete with Warranty
150 mm (6 inches)	Item 304	Aggregate Base
	Item 605	Underdrains

Rural Interstate—Rigid (93 AASHTO)

30,000,000 rigid ESAL
Mr = 69,000 kPa (10,000 psi)
R=90%; Overall Deviation = 0.39; Modulus of rupture = 4800 kPa (700 psi); Modulus of Elasticity = 34,500 MPa (5,000,000 psi); J=2.8; k = 38.5 N/cubic cm (142 pci) { Mr (subgrade) = 69,000 kPa (10,000 psi), Mr (subbase) = 207,000 kPa (30,000 psi), subbase = 150 mm (6 in) LOS=1}; Cd=1.0; Initial Serviceability = 4.2; Terminal Serviceability = 2.5
PCC thickness = 287 mm (11.3 inches) round to 290 mm (11.5 inches)
Final Design—Rural Interstate—Rigid:

290 mm (11.5 inches)	Item 884	Concrete Pavement With Warranty
150 mm (6 inches)	Item 304	Aggregate Base
	Item 605	Underdrains

Rural Primary—Flexible (93 AASHTO)

5,000,000 flexible Esal
Mr = 69,000 kPa (10,000 psi)
R= 85%; Overall Deviation = 0.49; Initial Serviceability = 4.50; Terminal Serviceability = 2.5
SN= 3.8

Final Design—Rural Interstate—Flexible:

205 mm (8 inches)	Item 880	Asphalt Concrete with Warranty
150 mm (6 inches)	Item 304	Aggregate Base
	Item 605	Underdrains

Rural Primary—Rigid (93 AASHTO)

5,000,000 rigid Esal
Mr = 69,000 kPa (10,000 psi)
R=85%; Overall Deviation = 0.39; Modulus of rupture = 4800 kPa (700 psi); Modulus of Elasticity = 34,500 MPa (5,000,000 psi); J=2.8; k = 38.5 N/cubic cm (142 pci) { Mr (subgrade) = 69,000 kPa (10,000 psi), Mr (subbase) = 207,000 kPa (30,000 psi), subbase = 150 mm (6 in) LOS=1}; Cd=1.0; Initial Serviceability = 4.2; Terminal Serviceability = 2.5

PCC thickness = 208 mm (8.2 in) round to 205 mm (8 in)
Final Design—Rural Interstate—Rigid:

205 mm (8 inches)	Item 884	Concrete Pavement with Warranty
150 mm (6 inches)	Item 304	Aggregate Base
	Item 605	Underdrains

The research objective mentions frost penetration. In Ohio, all A-4b (silts>50% of number 200 sieve) must be removed by specification. Soils work is done to make recommendations concerning both lime and cement stabilization, but current design policy does not figure this strength into the pavement design. This is going to change within the next few years. Furthermore, typical subgrade strengths used in design for ODOT projects are closer to 49,600 kPa (7,200 psi).

If you need any further information, please do not hesitate to contact myself or Aric Morse @ 614-995-5994.

STATE OF PENNSYLVANIA
Department of Transportation
400 North Street, 6th Floor
Harrisburg, Pa. 17120

Standard Roadway Section-Designed Section
Base drains are required on all interstate projects. For non-interstates, base drains should be installed on all projects where subsurface water is a problem.

Rural Interstate (four lanes) Rigid and Flexible
30-year design
30,000,000 ESALs
Frost susceptible fine grained soil M_R 69,000 kPa (10,000 psi)

Table 74. Pavement structure information for rural interstate in Pennsylvania.

PAVEMENT COURSE	MAIN LINE mm (inches)	SHLDRS mm (inches)
Flexible (minimum section):	NA	NA
Superpave Asphalt Mixture Design, HMA Wearing Course, RPS, pg 76-22, >/= 30 Million ESALs, 9.5 mm mix, 40-mm (1.5-inch) depth, SRL-E	40 (1.5)	20 (0.75)
Superpave asphalt mixture design, HMA binder course, RPS, pg 76-22, >/= 30 million ESALs, 19.0 mm mix, 50-mm (2-inch) depth	50 (2)	NA
Superpave asphalt mixture design, HMA base course, pg 64-22, 10 to < 30 million ESALs, 25.0 mm mix	330 (13)	100 (4)
Subbase 255-mm (10-inch) depth (number 2a)	255 (10)	NA
Total Depth:	675 (26.5)	120 (4.75)
Rigid (minimum section):	NA	NA
Plain Cement Concrete Pavement, 330-mm (13-inch) depth	330 (13)	Same as mainline
Asphalt Treated Permeable Base Course, 100-mm (4-inch) depth (CTPBC allowed, but rarely chosen by contractors)	100 (4)	Same as mainline
Subbase 100-mm (4-inch) depth (number 2a)	100 (4)	Same as mainline
Total Depth:	530 (21)	530 (21)

Rural Primary (two lanes) Rigid and Flexible
30-year design
5,000,000 ESALs
Frost susceptible fine grained soil M_R 69,000 kPa (10,000 psi)

Table 75. Pavement structure information for rural primary in Pennsylvania.

PAVEMENT COURSE	MAIN LINE mm (inches)	SHLDRS mm (inches)
Flexible (minimum section):	NA	NA
Superpave asphalt mixture design, HMA wearing course, pg 64-22, 3 to < 10 million ESALs, 9.5 mm mix, 40-mm (1.5-inch) depth, SRL-H	40 (1.5)	20 (0.75)
Superpave asphalt mixture design, HMA wearing course, pg 64-22, 3 to < 10 million ESALs, 9.5 mm mix, 40-mm (1.5-inch) depth, SRL-G	50 (2)	NA
Superpave asphalt mixture design, HMA binder course, pg 64-22, 3 to < 10 million ESALs, 19.0 mm mix	130 (5)	100 (4)
Superpave asphalt mixture design, HMA base course, pg 64-22, 0.3 to < 3 million ESALs, 25.0 mm mix, 130-mm (5-inch) depth	230 (9)	NA
Total Depth:	445 (17.5)	NA
Rigid (minimum section):	NA	NA
Plain Cement Concrete Pavement, 205-mm (8-inch) depth	205 (8)	Same as mainline
Subbase 100-mm (4-inch) depth (no OGS)	100 (4)	Same as mainline
Subbase 100-mm (4-inch) depth (number 2a)	100 (4)	Same as mainline
Total Depth:	405 (16)	535 (21)

Standard Specifications
http://www.dot2.state.pa.us/
Follow links for: References, Highway Related Pubs, Publication 408 (on page 4 of the list).

GPS and SPS test sites (hat represent the performance data included in the LTPP database) were built using ID-2 and ID-3 mixes.

Test Procedures
AASHTO test procedures

Average Unit Bid Prices

In addition to the specifications we will also need the average unit bid prices or the prices you would prefer we use in this study, for each of the bid items noted in your standard or design roadway section.

Table 76. Average unit prices for Pennsylvania.

Item	Average Bid Price
Superpave asphalt mixture design, HMA wearing course, RPS, pg 76-22, >/= 30 million ESALs, 9.5 mm mix, 40-mm (1.5-inch) depth, SRL-E	$5.04/square meter ($4.21/square yard)
Superpave asphalt mixture design, HMA binder course, RPS, pg 76-22, >/= 30 million ESALs, 19.0 mm mix, 50-mm (2-inch) depth	$5.56/square meter ($4.65/square yard)
Superpave asphalt mixture design, HMA base course, pg 64-22, 10 to < 30 million ESALs, 25.0 mm mix	$46.00/metric ton ($41.73/ton)
Subbase 255-mm (10-inch) depth (number 2a)	$14.39/square meter ($12.03/square yard)
Superpave asphalt mixture design, HMA wearing course, pg 64-22, 3 to < 10 million ESALs, 9.5 mm mix, 40-mm (1.5-inch) depth, SRL-H	$5.63/square meter ($4.71/square yard)
Superpave asphalt mixture design, HMA wearing course, pg 64-22, 3 to < 10 million ESALs, 9.5 mm mix, 40-mm (1.5-inch) depth, SRL-G	$5.98/square meter ($5.00/square yard)
Superpave asphalt mixture design, HMA binder course, pg 64-22, 3 to < 10 million ESALs, 19.0 mm mix	$5.55/square meter ($4.64/square yard)
Superpave asphalt mixture design, HMA base course, pg 64-22, 0.3 to < 3 million ESALs, 25.0 mm mix, 130-mm (5-inch) depth	$15.16/square meter ($12.67/square yard)
Subbase 230-mm (9-inch) depth (number 2a)	$20.28/square meter ($16.95/square yard)
Plain Cement Concrete Pavement, 330-mm (13-inch) depth	$82.06/square meter ($68.60/square yard)
Asphalt Treated Permeable Base Course, 100-mm (4-inch) depth	$9.44/square meter ($7.89/square yard)
Plain Cement Concrete Pavement, 255-mm (8-inch) depth	$61.05/square meter ($51.04/square yard)
Subbase 100 mm (4-inch) depth (No OGS)	$6.38/square meter ($5.33/square yard)
Subbase 100-mm (4-inch) depth (number 2a)	$6.09/square meter ($5.09/square yard)

Typical Service Life for Standard Section

The amount of fatigue cracking, ride value, etc. when treatment is applied varies by district depending upon variables such as funding availability. Applicable sections of typical pavement maintenance timeline from the Publication 242, Pavement Policy Manual are as follows:

New Bituminous, Bituminous Reconstruction and Bituminous Overlay

5 years	Seal coat shoulders if Type 1, 1S, 3, 4, 6 or 6S shoulders Do nothing if Type 1F, 1I, 6F, 6I, or 7 shoulders
10 years	40 or 50 mm (1.5 or 2.0 inch) cold milling (recycling) Full depth patch, 2% of pavement area 40 or 50 mm (1.5 or 2.0 inch) bituminous inlay Saw and seal joints, as necessary Seal coat shoulders Maintenance and protection of traffic User delay
15 years	Seal coat shoulders
20 years	Full depth patch, 2% of pavement area 60-psy leveling course 40 or 50 mm (1.5 or 2.0 inch) bituminous overlay Saw and seal joints, as necessary Type 7 paved shoulders Adjust guide rail and drainage structures, if necessary Maintenance and protection of traffic User delay
30 years	Same as 10 years
35 years	Seal coat shoulders

New Concrete, Concrete Reconstruction and Unbonded Concrete Overlay

10 years	Clean and seal 25% of longitudinal joints Clean and seal 5% of transverse joints, 0% if neoprene seals are used Seal coat shoulders, if Type 1 paved shoulders
20 years	Concrete patch 2% of pavement area Diamond grind 50% of pavement area Clean and seal all longitudinal joints, including shoulders Clean and seal all transverse joints, 7% if neoprene seals are used Maintenance and protection of traffic User delay

30 years	Concrete patch 5% of pavement area Clean and seal all joints 600-psy leveling course 90 or 100 mm (3.5 or 4.0 inch) bituminous overlay Saw and seal joints in overlay Type 7 paved shoulders Adjust all guide rail and drainage structures Maintenance and protection of traffic User delay
35 years	Seal coat shoulders

Adjacent State Treatments

PennDOT is not aware of any treatments utilized by adjacent States. PA overdesigns for frost heave. Publication 242, PennDOT's Pavement Policy Manual is available on line at ftp://ftp.dot.state.pa.us/public/pdf/pricelist.pdf. The link is towards the bottom of the third page. See the following section from Publication 242, Pavement Policy Manual for PennDOT design guidelines.

APPENDIX F. SPECIFICATION AND PAVEMENT DESIGN SUMMARIES

Appendix F provides overviews of specifications and standard pavement designs for principal and rural interstate highways. The information was obtained from surveying the participating PFS as well as reviewing literature available on each SHA Web site.

Table 77. AC wearing course specification summary.

Pooled Fund State	HMAC Reference	AC Grade	Mix Design	Compaction	Mix Voids (%)	VFA (%)	Min VMA (%)	Max Agg. Size
AK	HMA, Type II, Class B	PG 58 - 28	M	50 blow	3 to 5	65 to 78	12	19 mm (0.75 inch)
ID	Plant Mix Pavement	PG	Superpave	NA	NA	NA	NA	NA
IL	SP HMA Surface Course	PG 58/64 - 22	Superpave/M	75 blow	3.5 to 4.5	68 to 78	14/15	19mm (0.75 inch)
MI	Gap Graded SP	PG 70-22P	Superpave	NA	NA	NA	NA	NA
NY	12.5-mm Superpave HMA	PG 64-28 PG 70-22	Superpave	NA	3 to 5	65 to 80	14	12.5 mm (0.5 inch)
NC	S-12.5C	PG 70 - 22	Superpave	NA	3 to 5	65 to 75	14	19 mm (0.75 inch)
OH	Item 880 (7-yr warranty)	PG 64-22 PG 7022M	Superpave/M	75/50/35blow	3.5	NA	14	19 mm (0.75 inch)
PA	Superpave HMA Wearing Cr	PG 64-22 PG 58-22	Superpave/M	75/50 blow	3 to 5	NA	15	12.5 mm (0.5 inch)

Table 78. AC wearing course specification summary (continued).

Pooled Fund State	HMAC Reference	% Pass Number 4	% Pass Number 200	Fracture (%)	La Wear	Deg	SS Loss (%)	Antistrip (%)	Field Compaction (%)
AK	HMA, Type II, Class B	33 to 70	3 to 7	80 min	54 max	30 min	9 max	NA	NA
ID	Plant Mix Pavement	NA	2 to 10	90	30 Max	NA	12 max	NA	NA
IL	SP HMA Surface Course	24 to 65	2 to 6	NA	40 max	NA	15 max	<75 TSR	92 to 96
MI	Gap Graded SP	NA	NA	NA	NA	NA	NA	NA	NA
NY	12.5-mm Superpave HMA	NA	2 to 10	75 to 85	35 Max	NA	18 max	<80 TSR	92 to 97 (88 to 98 w/penalty)
NC	S-12.5C	NA	4 to 8	95/90	55 Max	NA	15 max	<85 TSR (no F/T)	92 days average (89 w/penalty)
OH	Item 880 (7-yr warranty)	38 to 50	2 to 6	75/70	40 Max	NA	15 max	<70/80 TSR	93 to 97 (90 to 98 w/penalty)
PA	Superpave HMA Wearing Cr	40 to 80/M	3 to 6	85/80	40 max	NA	NA	NA	92 to 97 (89 to 99 w/penalty)

Table 79. AC base course specification summary.

Pooled Fund State	HMAC Reference	AC Grade	Mix Design	Compaction	Voids (%)	VFA (%)	Min VMA (%)	Max Agg. Size
AK	HMA, Type II, Class B	PG 58 - 28	M	50 blow	3 to 5	65 to 78	12	19 mm (0.75 inch)
ID	Plant Mix Leveling Course	PG	Superpave	NA	NA	NA	NA	NA
IL	SP HMA Binder Course	PG 58/64 - 22	Superpave/M	75 blow	3.5 to 4.5	68 to 78	14/15	19 mm (0.75 inch)
MI	4E50	PG 64 - 28	Superpave	NA	NA	NA	NA	NA
NY	Binder and Base Course	PG 64-28 PG 70-22	Superpave	NA	3 to 5	65 to 80	14	19 mm (0.75 inch)
NC	B-25.0C	PG 64 - 22	Superpave	NA	3.0 to 5.0	65 to 75	12	38 mm (1.5 inches)
OH	Item 880 (7-yr warranty)	PG 64-22 PG 64-28	Superpave/M	75/50/35blow	4 to 3.5	NA	14/16	19 mm (0.75 inch)
PA	Superpave HMA Base Cr	PG 64-22 PG 58-22	Superpave/M	50 blow	3 to 5	NA	15	12.5 mm (0.5 inch)

Table 80. AC base course specification summary (continued).

Pooled Fund State	HMAC Reference	% Pass Number 4	% Pass Number 200	Fracture (%)	La Wear	Deg	SS Loss (%)	Antistrip	Field Compaction (%)
AK	HMA, Type II, Class B	33 to 70	3 to 7	80 min	54 max	30 min	9 max	NA	NA
ID	Plant Mix Leveling Course	NA	2 to 10	90	30 Max	NA	12 max	NA	NA
IL	SP HMA Binder Course	24 to 65	2 to 6	NA	40 max	NA	15 max	75% TSR	92 to 96
MI	4E50	NA	4 to 8	95	50 Max	NA	NA	NA	92 to 96
NY	Binder and Base Course	NA	2 to 8	75 to 85	35 Max	NA	18 max	<80% TSR	92 to 97 (88 to 98 w/penalty
NC	B-25.0C	NA	3 to 7	95/90	55 max	NA	15 max	<85% TSR (no F/T)	92 days average (−3 w/penalty)
OH	Item 880 (7-yr warranty)	38 to 50	2 to 6	75/70	40 Max	NA	15 max	<70/80 TSR	93 to 97 (90 to 98 w/penalty)
PA	Superpave HMA Base Cr	40 to 80/M	3 to 6	85/80	40 max	NA	NA	NA	92 to 97 (89 to 99 w/penalty)

Table 81. Asphalt-treated permeable base course specification summary.

Pooled Fund State	HMAC Reference	AC Grade	Max Agg. Size	% Pass Number 4	% Pass Number 200
AK	NA	NA	NA	NA	NA
ID	NA	NA	NA	NA	NA
IL	NA	NA	NA	NA	NA
MI	NA	NA	NA	NA	NA
NY	ATPB Type1/2	PG 64-28 PG 70-22	38 mm (1.5 inches)	3 TO 15	2 TO 4
NC	NA	NA	NA	NA	NA
OH	NA	NA	NA	NA	NA
PA	NA	NA	NA	NA	NA

Table 82. Unbound base course specification summary.

Pooled Fund State	Reference	Max Agg. Size	% Pass number 4	% Pass number 200	Fracture	La Wear	Deg	SS Loss
AK	Grading D - 1	25 mm (1inch)	35 to 65	0 to 6	70%	50 max	45 min	9 max
ID	Rock Cap	75 mm (3 inches)	0 to 5	(0 to 5)	Quarry	40	NA	NA
IL	NA	NA	NA	NA	NA	NA	NA	NA
MI	21AA	25 mm (1 inch)	35 to 50	4 to 8	95%	50 max	NA	NA
NY	See Sub-base	NA	NA	NA	NA	NA	NA	NA
NC	Aggregate Base Course	38 mm (1.5 inches)	35 to 55	4 to 10	none	55 Max	NA	15 max
OH	Aggregate Base	50 mm (2 inches)	30 to 60	0 to 15	NA	40 Max	NA	15 Max
PA	2A	50 mm (2 inches)	24 to 50	0 to 10	NA	45 Max	NA	10 Max

Table 83. Subbase course specification summary.

Pooled Fund State	Reference	Max Agg. Size mm (inches)	% Pass Number 4	% Pass Number200	La Wear	Deg	LL	PI	SE
AK	Grading B	50 (2)	20 to 55	0 to 6	50	40	25	6	NA
ID	Granular Subbase	100(4)	30 to 75	0 to 15	40	NA	NA	NA	30
IL	CAM / BAM	NA	NA	NA	NA	NA	NA	NA	NA
MI	Class II Sand	NA	NA	NA	NA	NA	NA	NA	NA
NY	Subbase	**NA**	NA	**NA**	NA	NA	NA	NA	NA
NC	NA	NA	NA	NA	NA	NA	NA	NA	NA
OH	NA	NA	NA	NA	NA	NA	NA	NA	NA
PA	NA	NA	NA	NA	NA	NA	NA	NA	NA

Table 84. Select subgrade specification summary.

Pooled Fund State	Reference	Max Agg. Size mm (inches)	% Pass 1"	% Pass #4	% Pass #200	PI
AK	SM Type A	NA	NA	20 to 55%	0 to 6	6
ID	NA	NA	NA	NA	NA	NA
IL	NA	NA	NA	NA	NA	NA
MI	Granular Material Type II	75 (3)	60 to 100	NA	0 to 7	NA
NY	NA	NA	NA	NA	NA	NA
NC	Lime stabilized	NA	NA	NA	NA	NA
OH	NA	NA	NA	NA	NA	NA
PA	NA	NA	NA	NA	NA	NA

Table 85. Overview of rural interstate flexible pavement design.

Layer	AK		ID		IL		MI		NY		NC			OH		PA	
	Mainline	**Shoulder**	**Mainline**	**Shoulder**	**Mainline**	**Shoulder**	**Mainline**	**Shoulder**	**Mainline**	**Shoulder**	**Mainline**	**Shoulder**	**Mainline**	**Shoulder**	**Mainline**	**Shoulder**	**Mainline**
HMA Surface Course	No pavements at 30 M-ESAL		6 in.	6 in.	2.0 in. SP	2 in. SP	1.5 in.	1.5 in.	2 in.	2 in.	4 in. S12.5C	4 in. S12.5C	4 in. S12.5C	3.0 in. It 880	3.0 in. It 880	1.5 in. SP 9.5	0.75 in.
HMA Binder Course			NA	NA	18.25 in. SP	6 in. SP	2 in.	2 in.	2 in.	2 in.	3 in. I19.0C	3 in. I19.0C	NA	8.5 It 880	8.5 It 880	2 in. SP 19	NA
HMA Base Course			1.8 in.	1.8 in.	NA	NA	3.75 in.	3.75 in.	3 in.	3 in.	9 in. B25.0C	5.5 in. B25.0C	NA	NA	NA	13 in. SP 25	NA
ATPB			NA	NA	NA	NA	NA	NA	4 in.	4 in.	NA	NA	**NA**	NA	NA	NA	**NA**
Total HMA			7.8 in.	7.8 in.	20.25 in.	8 in.	7.25 in.	7.25 in.	11 in.	11 in.	16.0 in.	12.5 in.	4.0 in.	11.5 in.	11.5 in.	16.5 in.	4.75 in.
UT Base Course			12 in. Rock Cap	12 in. Rock Cap	NA	12.25 in. to C	6 in. 21AA	6 in. 21AA	NA	NA	10 in. ABC	10 in.ABC	Variable	6.0 in. It 304	6.0 in. It 304	NA	NA
UT Subbase Course			12 in.	12 in.	NA	NA	18 in. sand	18 in. sand	12 in.	12 in.	NA	NA	NA	NA	NA	10 in.	
Total UTBC			24 in.	24 in.	**NA**	NA	24 in.	24 in.	12 in.	12 in.	10 in.	10 in.	Variable	6 in.	6 in.	10	0
Lime Treated Subgrade			NA	NA	12 in.	**NA**	NA	NA	NA	NA	NA	8 in.	NA	NA	NA	NA	NA
Other Subgrade Treatment			Separa-tion Geotex-tile	NA	NA	NA	NA	NA	NA	NA	NA	NA	NA	36 in. (note)	36 in. (note)	NA	NA
Total Roadway Depth			31.8 in.	31.8 in.	32.25 in.	32.25 in.	31.25 in.	31.25 in.	23 in.	23 in.	26.0 in.	30.5 in.	Variable	54.5 in.	54.5 in.	26.5 in.	4.75 in.
Underdrains			yes	NA	yes	4 in.	yes	6 in.	Yes or Daylight ATPB	NA	NA	NA	NA	yes	NA	yes	NA

Note: Grading specifications require replacement of A-4b silt within 0.9 m (3 ft) of SG.
Measurements in inches (in.) (1 inch = 25.4 mm)

Table 86. Overview of rural interstate rigid pavement design.

Layer	AK		ID		IL		MI		NY		NC		OH		PA	
	Mainline	Shoulder	Mainline	Shoulder	Mainline	Shoulder	Mainline	Shoulder	Mainline	Shoulder	Mainline	Shoulder	Mainline	Shoulder	Mainline	Shoulder
PCCP Depth	No Pavements at 30 M ESAL		12 in.	NA	10.5 in.	6 in.	11.5 in.	9 in.	10 in.	10 in.	11	11	11.5 in.	11.5 in.	13 in.	NA
Treated Base Course			2 in. ATPLC	2 in. ATPLC	4 in.	NA	NA	NA	4 in. ATPB	4 in. ATPB	3 in. B25.0B	NA	NA	NA	4 in. ATPB	4 in. ATPB
UT Base Course			12 in. Rock Cap	12 in. Rock Cap	NA	8.5 in.	6 in. 4GMod	8.5 in. 4GMod	NA	NA	1.5 in. S9.5B	4.5 in. ABC	6 in.	6 in.	NA	NA
UT Subbase Course			NA	NA	NA	NA	10 in. IIA Sand	10 in. IIA Sand	12 in.	12 in.	NA	NA	NA	NA	4 in.	4 in.
Total BC			14 in.	14 in.	4 in.	8.5 in.	16 in.	18.5 in.	16 in.	16 in.	4.5 in.	4.5 in.	6 in.	6 in.	8 in.	8 in.
Lime Treated Subgrade			NA	NA	12 in.	12 in.	NA	NA	NA	NA	8 in.	8 in.	NA	NA	NA	NA
Other Subgrade Treatment			NA	NA	NA	NA	Geotech fab.4G/sand	NA	NA	NA	NA	NA	36 in. (note)	36 in. (note)	NA	NA
Total Roadway Depth			26 in.	26 in.	26.5 in.	26.5 in.	27.5 in.	27.5 in.	26 in.	26 in.	23.5 in.	23.5 in.	53.5 in.	53.5 in.	21 in.	21 in.
Underdrains			yes	NA	yes	4 in.	yes	6 in.	yes	NA	NA	NA	yes	NA	yes	NA
Other Subgrade Treatment			Separation Geo-textile	NA	NA	NA	NA	NA	NA	NA	NA	NA	NA	NA	NA	NA

Note: Grading specifications require replacement of A-4b silt within 0.9 m (3 ft) of SG.
Measurements in inches (in.) (1 inch = 25.4 mm)

Table 87. Overview of principal flexible pavement design.

Layer	AK		ID		IL		MI		NY		NC			OH		PA	
	Mainline	Shoulder	Mainline	Shoulder	Mainline	Shoulder	Mainline	Shoulder	Mainline	Shoulder	Mainline	Mainline Alt	Shoulder	Mainline	Shoulder	Mainline	Shoulder
HMA Surface Course	2 in.	2 in.	4.8 in.	4.8'	2 in. SP SC	2 in. SP SC	1.5 in.	1.5 in.	2 in.	2 in.	3 in. S12.5C	3 in. S12.5C	3 in. S12.5C	3 in.	3 in.	3.5 in.	0.75
HMA Binder Course	3 in.	3 in.	1.8 in.	1.8 in.	12 in. SP BC	6 in SP BC	2.0 in.	2.0 in.	2 in.	2 in.	3 in. I19.0C	4 in. I19.0C	NA	NA	NA	5 in.	4 in.
HMA Base Course	NA	NA	NA	NA	NA	NA	3.0 in.	3.0 in.	2 in.	2 in.	4.5 in. B25.0C	NA	NA	5 in.	5 in.	9 in.	NA
ATPB	NA	NA	NA	NA	NA	NA	NA	NA	4 in.	4 in.	NA	NA	NA	NA	NA	NA	NA
Total HMA	5 in.	5 in.	6.6 in.	6.6 in.	14 in.	8 in.	6.5 in.	6.5 in.	10 in.	10 in.	10.5	7 in.	3.0 in.	8 in.	8 in.	17.5 in.	4.75 in.
UT Base Course	7 in.	7 in.	12 in. RC	12 in. RC	NA	6 in.	6 in. 4Gmod	6 in. 4Gmod	NA	NA	10 in. ABC	10 in. ACB	Variable	6 in.	6 in.		
UT Subbase Course	12 in.	12 in.	NA	NA	NA	NA	18 in. IIA Sand	18 in. IIA Sand	12 in.	12 in.	NA	NA	NA	NA	NA	NA	NA
Total UBC	19 in.	19 in.	12'	12'	0	6 in.	24 in.	24 in.	12 in.	12 in.	10 in.	10 in.	Variable	6 in.	6 in.	0	0
Lime Treated Subgrade	NA	NA	NA	NA	12 in.	12 in.	NA	NA	NA	NA	NA	8 in.	NA	NA	NA	NA	NA
Other Subgrade Treatment	36 in. Select	36 in. Select	NA	NA	NA	NA	NA	NA	NA	NA	NA	NA	NA	36 in. (note)	36 in. (note)	NA	NA
Total Roadway Depth	60 in.	60 in.	18.6 in.	18.6 in.	26 in.	26 in.	30.5 in.	30.5 in.	22 in.	22 in.	20.5 in.	25 in.	Variable	50 in.	50 in.	17.5 in.	4.75 in.
Underdrain	NA	NA	no	NA	no	NA	yes	6 in. u-drain	yes or daylight ATPB	NA	NA	NA	NA	yes	NA	if required by	NA

Note: Grading specifications require replacement of A-4b silt within 0.9 m (3 ft) of SG.
Measurements in inches (in.) (1 inch = 25.4 mm)

Table 88. Overview of principal rigid pavement design.

Layer	AK		ID		IL		MI		NY		NC		OH		PA	
	Mainline	Shoulder	Mainline	Shoulder	Mainline	Shoulder	Mainline	Shoulder	Mainline	Shoulder	Mainline	Shoulder	Mainline	Shoulder	Mainline	Shoulder
PCCP Depth	No PCC Pavement		10.5	10.5	9.75 in.	2 in. SP SC	8.5	4 in. HMA	9 in.	9 in.	8 in.	8 in.	8 in.	8 in.	8 in.	8 in.
T Base Course			2 in. ATPLC	2 in. ATPLC	4 in. CAM/ BAM	6 in. SP BC	NA	NA	4 in. ATPB	4 in. ATPB	3 in. B25.0B/ 1.5 in. S9.5B	3 in. B25.0B/ 1.5 in. S9.5B	NA	NA	NA	NA
UT Base Course			12 in. Rock Cap	12 in. Rock Cap	NA	5.75 Type C	6 in. 4Gmod	6 in. 4Gmod	NA	NA	NA	NA	6 in.	6 in.	4 in. OGS	4 in. OGS
UT Subbase Course			NA	NA	NA	NA	10 in.	10 in.	12 in.	12 in.	NA	NA	NA	NA	4 in.	4 in.
Total BC			14 in.	14 in.	4 in.	5.75 in.	16 in.	16 in.	16 in.	16 in.	4.5 in.	4.5 in.	6 in.	6 in.	8 in.	8 in.
Lime Treated Subgrade			NA	NA	12 in.	12 in.	NA	NA	NA	NA	8 in.	8 in.	NA	NA	NA	NA
Other Subgrade Treatment			NA	NA	NA	NA	Geotech fab. 4G/sand	NA	NA	NA	NA	NA	36 in. (note)	36 in. (note)	NA	NA
Total Roadway Depth			24.5 in.	24.5 in.	25.75 in.	25.75 in.	26.5 in.	20 in.	26 in.	26 in.	20.5 in.	20.5 in.	50 in.	50 in.	16 in.	16 in.
Underdrains			no	NA	no	NA	yes	6 in.	yes	yes	NA	NA	yes	yes	if required by	NA

Note: Grading specifications require replacement of A-4b silt within 0.9 m (3 ft) of SG.
Measurements in inches (in.) (1 inch = 25.4 mm)

APPENDIX G: NCHRP 1-37A CALIBRATION FLOWCHART SAMPLE

This appendix provides an example of a calibration methodology flowchart for the NCHRP 1-37A pavement design procedures.

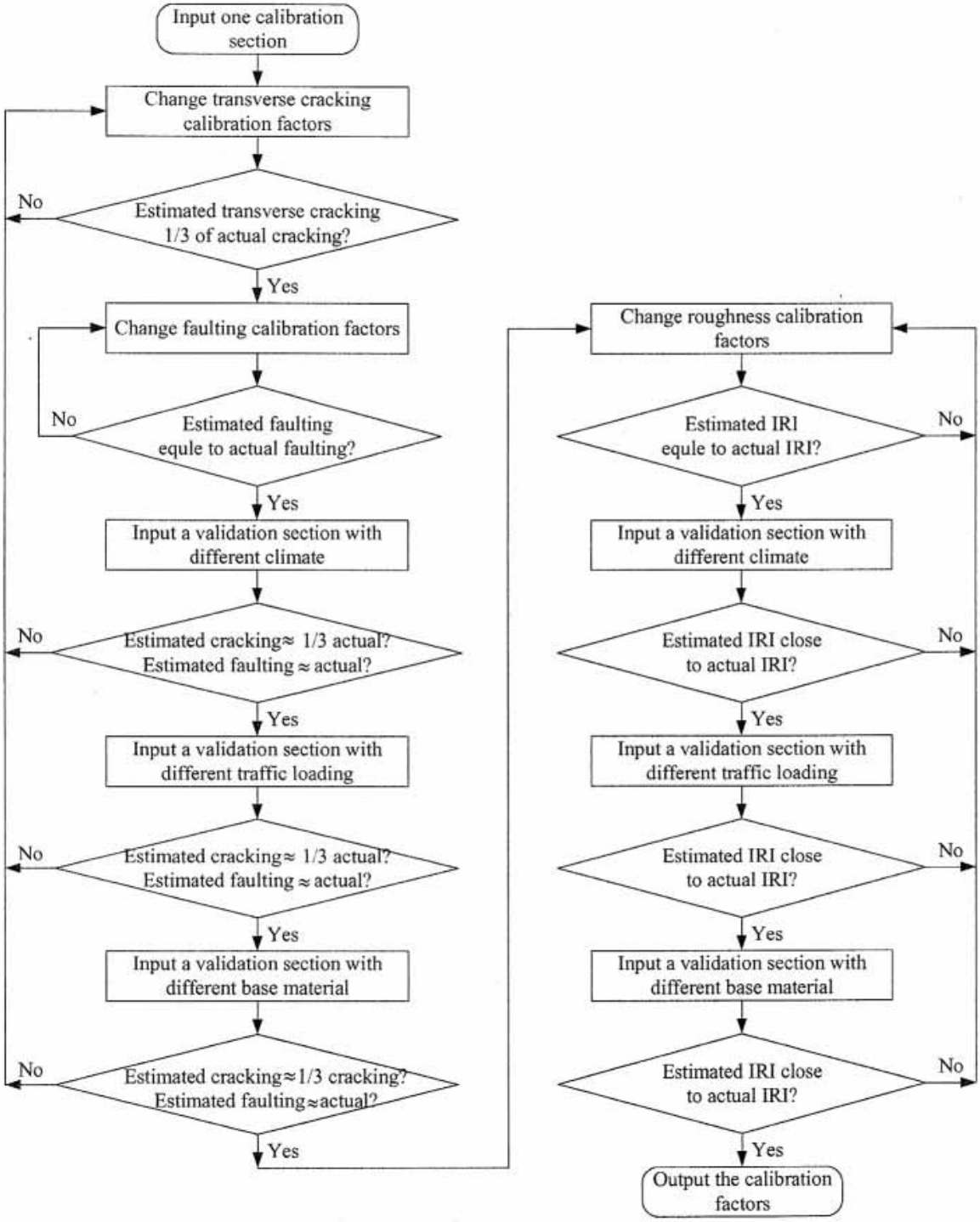

Source: J. Li et al., "PCCP Models for Rehabilitation/Reconstruction Decision Making," Washington State Department of Transportation, Report No. WA-RD 588.2, Olympia, WA, August 2005.

Figure 101. Flowchart. Example of NCHRP 1-37A calibration methodology flowchart.

REFERENCES

1. American Association of State Highway and Transportation Officials. 1993. *AASHTO Guide for Design of Pavement Structures*.

2. NCHRP. March 2004. *Guide for Mechanistic-Empirical Design of New and Rehabilitated Pavement Structures*, Project 1-37A final report. Washington, DC. Accessed at http://www.trb.org/mepdg/Part3PChapter3_Flexible%20Design.pdf.

3. Federal Highway Administration, Turner-Fairbank Highway Research Center-Research, Development, and Technology. January 2003. *Long Term Pavement Performance Information Management System Pavement Performance Database User Guide*. McLean, VA.

4. Washington State Department of Transportation. February 1995. *WSDOT Pavement Guide, Volume 2, Pavement Notes.*

5. Berg, R.L. 1997. "Calculating Maximum Frost Depths at Mn/ROAD Winters 1993–94, 1994–95, 1995–96." Minnesota Department of Transportation, St. Paul, MN.

6. Rada, G.R., G.E. Elkins, B. Henderson, R.J. Sambeek, and A. Lopez. January 1995. *LTPP Seasonal Monitoring Program: Instrumentation Installation and Data Collection Guidelines*. Report No. FHWA-RD-94-110, Federal Highway Administration. McLean, VA.

7. Marshal, T. 1965. "Pavement Condition Survey Procedures." Internal Report, Materials Laboratory, Washington State Department of Transportation. Olympia, WA.

8. Shahin, M.Y. 1998. "Pavement Management for Airports, Roads, and Parking Lots." Kluwer Academic Publishers.

9. Federal Highway Administration. 1998. "Pavement Management Systems." NHI Course No. 13135. Washington, DC.

10. Jackson, N., et al. 1996. "Development of Pavement Performance Curves for Individual Distress Indexes in South Dakota Based on Expert Opinion." *Transportation Research Record*.

11. Federal Highway Administration, LTPP Division. July 1993. "SHRP-LTPP Interim Guide for Laboratory Material Handling and Testing (PCC, Bituminous Materials, Aggregates and Soils). Operational Guide No. SHRP-LTPP-OG-004. McLean, VA.

12. SHRP-LTPP Technical Memorandum AU-167. November 1990. TDRF. Austin, TX.

13. American Association of State Highway and Transportation Officials. 1986. *AASHTO Guide for Design of Pavement Structures*, *Volume 2.*

14. SAS Institute, Inc. 2002. SAS online documentation, Version 8. Accessed at http://v8doc.sas.com/sashtml/stat/chap55/sect37.htm.

15. Fernandez, G. 2002. *Data Mining Using SAS Applications.* ISBN NO: 1584883456 CRC/Chapman-Hall UK/USA. Accessed at http://www.ag.unr.edu/gf/dm.html.

16. Kameyama S., M. Kato, A. Kawamura, K. Himeno, and A. Kasahara. 2002. "Effects of Frost Heave on the Longitudinal Profile of Asphalt Pavements in Cold Regions." pp. 1–14. *Ninth International Conference on Asphalt Pavements*. International Society for Asphalt Pavements, St. Paul, MN.

17. Personal observations and discussions with personnel from the Swedish National Road Administration, Borlange, Sweden, 1995.

18. Jackson, N., S. Gibson, and J. Mactutis. August 1998. "Pavement Design Technical Report I-15 Reconstruction." Prepared for Sverdrup/DeLeuw, Salt Lake City, UT.

19. Washington State Department of Transportation. February 2002. "Washington State Highway System Plan 2003 to 2022." Olympia, WA. Accessed at http://www.wsdot.wa.gov/NR/rdonlyres/9D14B579-134E-4456-B76C-94D5C4295AD8/0/HSP20032022.pdf

20. Chou, E., J. Tack, J. Yu, J. Wielinski. September 2004. "Evaluation of the Variation in Pavement Performance Between ODOT Districts." Ohio Department of Transportation.

21. Kulkarni, R., C. Saraf, F. Finn, J. Hilliard, and C.Van Til. June 1982. *Life Cycle Costing of Paved Alaskan Highways, Volume I.* Alaska Department of Transportation.

22. Esch, D., R. McHattie, and B. Connor. "Rost Susceptibility Ratings and Pavement Structure Performance." Alaska Department of Transportation.

23. Jackson, N.C. March 1986. "Controlling Frost Heaving and Thaw Weakening in Washington State Roads." *Proceedings 37th Annual Road Builders Clinic*. Pullman, WA.

24. Burnett, R.A. and D.R. Dwlyer. August 1999. "Fighting Frost Problems in New York State Pavements." *Proceedings of the Tenth International Conference on Cold Regions Engineering*. American Society of Civil Engineers. Lincoln, NH.

25. Ardani, A. August 1987. "Frost Heave Control with Buried Insulation Interim Report." Colorado Department of Highways. Denver, CO.

26. Wilson, J. and D. Bohnsack. October 2001. "Investigation of Shoulder Heave Problems on I-90, Monroe County." Wisconsin Department of Transportation.

27. Deighton, R., N. Jackson, G. Ruck, and J. Zavitski, July 14, 1995. "Development of Vermont Agency of Transportation's Pavement Management System," Final Report. Vermont Agency of Transportation.

28. Federal Highway Administration. September 1997. United States Department of Transportation Strategic Plan, 1997–2002. "Federal Highway Administration 1998 National Strategic Plan." pp. 57–71. Washington, DC. Accessed at http://www.fhwa.dot.gov/policy/fhplan.html#mobility.

29. Li, J., et al. July 2006. *PCCP Models for Rehabilitation and Reconstruction Decision-Making*. Report No. WA-RD 588.2. Washington State Department of Transportation. Olympia, WA.

30. American Association for State Highway and Transportation Officials. 1978. *Standard Specifications for Transportation Materials and Methods of Sampling and Testing*, 12th Ed., Part I, Specifications, 828 pp.; Part II, Tests, 998 pp. Washington, DC.

31. Zhang,W. and R.A. Macdonald 2002. "The Effects of Freeze-Thaw Periods on a Test Pavement in the Danish Road Testing Machine." *Ninth International Conference on Asphalt Pavements*. International Society for Asphalt Pavements. St. Paul, MN.

32. Doré, G., J.M. Konrad, and M. Roy. 1999. "A Deterioration Model for Pavements in Frost Conditions." *Transportation Research Record 1655I*. pp. 110–117. Transportation Research Board. Washington, DC.

33. Doré, G. and Y. Savard. 1998. "Analysis of Seasonal Pavement Deterioration." *77th Annual Meeting*. Transportation Research Board. Washington, DC.

34. Senn, K., D. Frith, M.T. Yapp, L. Scofield. 1997. "Development of Performance Prediction Models for Dry-No Freeze and Dry-Freeze Zones Using LTPP Data." pp. 997–1011. *Eighth International Conference on Asphalt Pavements*. Seattle, WA.

35. McBane, J.A. and G. Hanek. 1986. "Determination of the Critical Thaw-Weakened Period in Asphalt Pavement Structures." *Transportation Research Record 1089*. pp. 138–146. Transportation Research Board. Washington, DC.

36. Berg, R.L. 1997. "Calculating Maximum Frost Depths at Mn/ROAD Winters 1993–94, 1994–95, 1995–96." pp. 1–54. Minnesota Department of Transportation, St. Paul, MN

37. Raad, L., E. Johnson, D. Bush, and S. Saboundjian. 1998. "Parks Highway Load Restriction Field Data Analysis: A Case Study." *Transportation Research Record 1615*. pp. 32–40. Transportation Research Board. Washington, DC.

38. Khazanovich, L., M. Darter, R. Bartlett, and T. McPeak. January 1998. “Common Characteristics of Good and Poorly Performing PCC Pavements.” Report No. FHWA-RD-97-131, Federal Highway Administration, Washington, DC.

39. Hesham, A.A. and S.D. Tayabji. September 1999. “Determination of Frost Penetration in LTPP Sections, Final Report.” Report No. FHWA-RD-99-088. Federal Highway Administration. Washington, DC.

40. Archilla, A.R. and S. Madanat. July/August 2000. “Development of a Pavement Rutting Model from Experimental Data.” *Journal of Transportation Engineering*, Vol. 126, No. 4. pp. 291–299.

41. Prozzi, J.A. and S.M. Madanat. 2000. “Analysis of experimental pavement failure data using duration models.” *Transportation Research Record 1699*. pp. 87–94. Transportation Research Board. Washington, DC.

42. Janoo, V.C. and L. Barna. 2002. “Pavement Performance During Thaw Weakening.” *Ninth International Conference on Asphalt Pavements*. pp. 1–17.International Society for Asphalt Pavements. St. Paul, MN.

43. Boutonnet, M., P. Lerat, D. Saint-Laurent, and Y. Savard. 2003. “Thermal Aspect of Frost-Thaw Pavement Dimensioning: In Situ Measurement and Numerical Modeling.” Paper No. 03-2657, pp. 1–23. *82nd Annual Meeting.* Transportation Research Board. Washington, DC.

44. Gharaibeh, N.G. and M.I. Darter. 2003. “Probabilistic Analysis of Highway Pavement Life for Illinois.” Paper No. 03-4294, pp. 1–27. *82nd Annual Meeting.* Transportation Research Board. Washington, DC.

45. Mladenovic, G., Y. Jiang, and M. Darter. 2003. “Effects of Environmental Factors on Pavement Performance—Initial Evaluation of the LTPP SPS-8 Experiment.” Paper No. 03-3920, pp. 1–22. *82nd Annual Meeting*. Transportation Research Board. Washington, DC.

46. Chatti, K., et al., June 2005. “LTPP Data Analysis: Influence of Design and Construction Features on the Response and Performance of New Flexible and Rigid Pavements.” NCHRP-TRB.

Recycled
Recycled

HRDI-13/11-06(500)E